NTNU
Norwegian University of
Science and Technology

Design of Suspension Towers for Transmission Lines

Katrine Engebrethsen

Civil and Environmental Engineering
Submission date: January 2017
Supervisor: Arild Holm Clausen, KT
Co-supervisor: Árni Björn Jónasson, ARA Engineering

Norwegian University of Science and Technology
Department of Structural Engineering

Department of Structural Engineering
Faculty of Engineering Science and Technology
NTNU- Norwegian University of Science and Technology

ACCESSIBILITY
OPEN

MASTER THESIS 2017

SUBJECT AREA:	DATE:	NO. OF PAGES:
Design of Structures	22. January 2017	20+146+98

TITLE:

Design of Suspension Towers for Transmission Lines

Prosjektering av Bæremaster for Kraftlinjer

BY:

Katrine Engebrethsen

SUMMARY:
This thesis is concerned with the design and analysis of suspension towers for transmission lines. Three different portal tower designs are considered; one steel lattice tower, one steel tubular tower and one less conventional made of tubular elements using glass fibre reinforced polymer.

A literature study is conducted on tower design, dynamic response of tower structures and composites used in load-bearing structures.

The three alternative designs are modelled in PLS-POLE and PLS-TOWER and the 4.5 km long transmission line is modelled in PLS-CADD where the towers are applied climatic loading and analysed. The towers are then optimised and checked by hand-calculations.

A life cycle cost analysis on net present value, including a sensitivity analysis, and an environmental life cycle assessment on CO_2-emissions are conducted.

The three towers are then compared based on material preference and the analysis results. This results in the two tubular towers being the most economical alternatives, while the two steel towers are the most environmentally friendly.

RESPONSIBLE TEACHER: Arild Holm Clausen

SUPERVISOR(S): Árni Björn Jónasson (ARA Engineering), Janos Toth (ARA Engineering) and Rolv Geir Knutsen (ARA Engineering)

CARRIED OUT AT: Department of Structural Engineering (NTNU)

Preface

This master thesis represent the final part of a 5 year M.Sc Degree at the Department of Structural Engineering, with a specialisation in Design of Structures, at the Norwegian University of Science and Technology (NTNU). The master thesis was initiated in collaboration with ARA Engineering and was carried out over a time period of 21 weeks from September 2016 to January 2017. ARA Engineering has provided the relevant software and design standards for the different parts of the study.

First of all, I would like to thank ARA Engineering for giving me this opportunity and creating an interesting problem to be addressed, and for hosting me in Reykjavik for one month in September 2017. I would especially like to thank my supervisors Árni Björn Jónasson, Janos Toth and Rolv Geir Knutsen for all their advice, guidance and interesting discussions.

I would also like to thank professor Arild Holm Clausen at NTNU for his help and guidance.

Furthermore, I would like to thank everybody else at ARA Engineering who helped me, a special thanks to Thorgeir Holm Olafsson for all his help with the PLS-modelling and to both Katarzyna Mazur-Pytlowany and Thorgeir Holm Olafsson for advising the PLS-courses I was allowed to attend in September 2017.

Finally, I would like to thank my family for all their help during the past few months and all their insightful input.

Trondheim, 22. January 2017

Katrine Engebrethsen

Katrine Engebrethsen

Abstract

This thesis is concerned with the design and analysis of guyed suspension towers for transmission lines. The line is thought located somewhere in Norway and the design requirements are therefore based on European and Norwegian standards and national normative aspects.

Three different designs are considered for these 420 kV guyed portal towers. Two are designed using steel; one latticed and one made of tubular elements. The third tower is of a less conventional design made of tubular elements using glass fibre reinforced polymer. All the tower designs are 25 m high to the cross arm, with three triplex phases and two ground wires. The three phases are attached to the tower using V-insulator chains with a centre distance of 9 m between the conductors.

A literature study is conducted on tower design, dynamic response of tower structures and composites and their use in load-carrying structures.

The three alternative designs are modelled in PLS-POLE and PLS-TOWER and the 4.5 km long transmission line is modelled in PLS-CADD where the towers are applied climatic loading according to the standards, and analysed. Hand calculations are done to find preliminary cross sections and to verify the loads applied in the program. The cross sections are then optimised in the programs based on the load cases.

The deflections of the towers are then checked and the structures are found to be adequate. The natural frequencies of conductors and towers are determined for two wind load cases and are found to not coincide, meaning they will not excite each other. The steel poles are checked against buckling.

A life cycle cost analysis determining the net present value of the three tower designs is conducted, including a sensitivity analysis. In addition, an environmental life cycle assessment is conducted to determine the environmental impact based emissions of CO_2-equivalents. The design using FRP is found to be the most economic, but highest in regard to emissions. The two steel towers score fairly similarly when it comes to emissions, but the lattice design comes out last in regard to net present value.

A comparison of the three tower designs is also done based on material performance. Both steel and FRP offer good material properties, but the FRP has some advantages because of its non-conductivity and low weight that increases the safety of workers.

The material costs are found to be 165740 NOK for the steel lattice tower, 195500 NOK for the steel tubular tower and 233800 NOK for the FRP tubular tower.

Sammendrag

Denne masteroppgaven tar for seg design og analyse av bardunerte bæremaster for kraftlinjer. Linjen er tenkt plassert et sted i Norge og kravene til utforming er derfor stilt i henhold til europeiske og norske standarder og nasjonale tillegg.

Tre ulike utforminger er vurdert for disse 420 kV bardunerte portalmastene. To er designet ved bruk av stål; en gittermast og en rørmast. Den tredje masten er også en rørmast, men tar i bruk det mindre konvensjonelle materialet glassfiberforsterket polymer. Alle mastene er 25 m høye til traversen, med tre triplex faser og to toppliner. De tre fasene er opphengt ved bruk av V-isolatorkjeder med en senteravstand på 9 m mellom fasene.

En litteraturstudie er gjennomført for å se på masteutforming, dynamisk respons av master og kompositter og deres anvendelse i lastbærende konstruksjoner.

De tre alternative utformingene er modellert i PLS-POLE og PLS-TOWER og den 4,5 km lange kraftlinjen er modellert i PLS-CADD hvor mastene blir påført klimatisk belasting i henhold til standardene, og analysert. Håndberegninger gjøres for å finne foreløpige tverrsnitt og for å kontrollere lastene som påføres i programmene. Tverrsnittene blir deretter optimalisert i programmene basert på de ulike lasttilfellene.

Utbøyinger av mastene blir så kontrollert og konstruksjonene er funnet til å være tilstrekkelige. Egenfrekvensene til kablene og mastene er fastsatt for to vindlasttilfeller og er funnet til å ikke sammenfalle. Det skapes altså ikke resonans. Stålrørene i beina av rørmasten er kontrollert mot knekking.

En livssykluskostnadsanalyse (LCC) for å bestemme nåverdien av de tre utformingene er gjennomført, inkludert en sensitivitetsanalyse. I tillegg er en miljølivssyklusanalyse (LCA) utført for å bestemme miljøbelastningen basert på utslipp av CO_2-ekvivalenter. Utformingen i FRP er funnet til å være den mest økonomiske, men gir størst utslipp. De to stålmastene scorer ganske likt når det gjelder utslipp, men gittermasten kommer dårligst ut med tanke på nåverdi.

De tre utformingene blir også sammenlignet på bakgrunn av materialegenskaper. Både stål og FRP tilbyr gode materialegenskaper, men FRP har noen fordeler grunnet sine isolerende egenskaper og lav vekt som øker sikkerheten for arbeiderne.

Materialkostnadene er funnet til å være 165740 NOK for gittermasten i stål, 195500 NOK for rørmasten i stål og 233800 NOK for rørmasten i kompositt.

Contents

Nomenclature

k	=	Harmonic coefficient
a	=	Span
H	=	Tension in conductor
M_c	=	Unit weight of conductor
E	=	Modulus of elasticity for conductor
I	=	Second moment of inertia for conductor
k	=	Stiffness of structure
F	=	Force applied
δ	=	Deflection of structure
f	=	Natural frequency of structure
M	=	Mass of structure
g_T/g_{50}	=	Conversion factor for wind
V_h	=	mean wind velocity at reference height
$V_{b.0}$	=	basic wind velocity at reference height
c_{dir}	=	wind directional factor
c_o	=	orography factor
k_r	=	terrain factor
h	=	reference height above ground
z_0	=	roughness length
q_h	=	mean wind pressure
ρ	=	air density
V_h	=	mean wind velocity at reference height
I_v	=	turbulence intensity
q_p	=	peak wind pressure
Q_{Wx}	=	wind force on component
q_p	=	peak wind pressure at reference height
G_x	=	structural factor for component
C_x	=	drag factor for component
A_x	=	area of component projected onto a plane perpendicular to wind direction
Q_{Wc}	=	wind force

q_p	=	peak wind pressure at reference height
G_c	=	structural factor for conductor
C_c	=	drag factor for conductor
d	=	diameter of conductor
L_1	=	length of span 1
L_2	=	length of span 2
ϕ	=	angle between wind direction and the longitudinal axis of the cross arm
I	=	ice load per length of the conductor [N/m]
L_{w1}	=	weight span of span 1 of adjacent spans
L_{w2}	=	weight span of span 2 of adjacent spans
I_3	=	nominal ice load with return period of 3 years
Ψ_I	=	combination factor for ice load
I_{50}	=	structural factor for conductor
V_{IL}	=	wind velocity of low probability
V_T	=	wind velocity with given return period
B_I	=	reduction factor for wet snow
D	=	equivalent diameter of ice-covered conductor
d	=	diameter of bare conductor
I	=	ice load per length
ρ_I	=	ice density
Q_{WIc}	=	wind force
q_{Ip}	=	peak wind pressure at reference height
G_c	=	structural factor for conductor
C_{Ic}	=	drag factor for ice-covered conductor
D	=	equivalent diameter of ice-covered conductor
L_1	=	length of span 1
L_2	=	length of span 2
ϕ	=	angle between wind direction and the longitudinal axis of the cross-arm
$D_{el} = 2.8m$	=	Required electrical clearance
$h_{snow} = 0.5m$	=	Height of snow
NPV	=	net present value
C_t	=	cost in year t
r	=	discount rate
t	=	year

Abbreviations

FRP	=	Fibre Reinforced Polymer
GFRP	=	Glass Fibre Reinforced Polymer
ACSR	=	Aluminium conductor steel reinforced
ACAR	=	Aluminium conductor alloy reinforced
SSAC	=	Steel Supported Aluminium Conductor
CRS-tower	=	cross-rope suspension tower
V-, M-, Y-, H-tower	=	tower where legs make the shape of a V, M, Y, H
PLS	=	Power Line Systems
LCC	=	Life Cycle Cost
LCCA	=	Life Cycle Cost Analysis
LCA	=	Life Cycle Assessment
NPV	=	Net present value

Chapter 1

Introduction

Electricity is perhaps one of the most important infrastructures in today's world and our society relies heavily on reliable distribution of electrical power. Overhead transmission lines are the first link in a long chain to distribute the electrical power from the source to the user. It is of great importance that the towers used in transmission lines are able to withstand both static and dynamic loading from climatic actions such as ice and wind while still maintaining their function.

In the Norwegian transmission network, most of the towers used are self-supporting steel lattice towers. In other countries, particularly in North America, glass fibre reinforced polymer has in later years increased in use in tower design, and it has also found its way into the Norwegian distribution network. Glass fibre reinforced polymers consist of long glass fibres coated in a polymer matrix. The combination of strong fibres and a ductile matrix results in a material of low weight and high strength.

In collaboration with ARA Engineering it was decided to investigate three different outside guyed transmission line towers; two in steel and one in FRP. This thesis aims to compare the three tower types and determine whether FRP can make a good alternative to steel for use in transmission towers. The different designs are thought to be compared based on performance, cost and environmental impact.

A common way to determine the costs of long term investments is by conducting a life cycle cost analysis where the present values of all future costs are determined. The environmental impact is similarly determined by an environmental life cycle assessment, where the towers' global warming potential is considered based on their emissions of CO_2-equivalents.

The transmission line and towers are modelled according to the requirements and common specifications given in FprEN 50341-1 - Overhead electrical lines exceeding AC 1 kV, and the specifications given in the Norwegian National Normative Aspects. This is done using software from Power Line Systems Inc.: PLS-CADD, PLS-POLE and PLS-TOWER.

Chapter 2

Literature Review

2.1 Transmission lines and structures

The Norwegian electrical power network is divided into three levels. The transmission network (main grid) is mostly used for voltages of 420 kV and 300 kV, but there are lines with voltages down to 132 kV. The regional distribution network is used for voltages between 36 and 132 kV. And the local distribution network is used for voltages from 0.23 to 36 kV. In Norway, the main grid is operated by Statnett SF. They are responsible for the operation of about 11000 km of high-voltage power lines (Statnett SF, (2016)). In much of Europe there are only two levels: the transmission network and distribution network. Much indicates that this will soon be applied in Norway as well.

Transmission lines are thus used for transmitting electrical power from generating stations to substations to be distributed further or by interconnecting or adding to existing networks (Kiessling et al., (2003)).

As discussed by Kiessling et al. ((2003)) the use of overhead transmission lines is a preferred alternative to underground cables, especially for higher transmission voltages. This is much based on an economic aspect as underground cables can be 5 to 15 times more expensive than overhead transmission lines. Also the fact that maintenance and repair is a lot easier and less costly can affect this decision. Not all locations are however appropriate for overhead transmission lines, such as in near proximity to airports, substation getaways or ocean crossings. Also, when crossing nature conservation areas underground cables are used more and more. Factors such as environmental impact are difficult to assess, and while the construction of a line might be justified, it might still create public reactions (Kiessling et al., (2003)). Thus, planning is key when considering the construction of a new line.

Designing and construction of transmission lines requires good cooperation between many disciplines. Civil engineers, structural engineers, electrical engineers, mechanical engineers, foresters, environmental sciences, public relations, regulatory bodies etc. must all collaborate to create the best possible solution (Catchpole and Fife, (2014)). The selection of the conductor material and insulators, as well as the calculation of clearances and other electric requirements are done by the electrical engineer. Based on these requirements, the structural engineer then decides the structural aspects of the line.

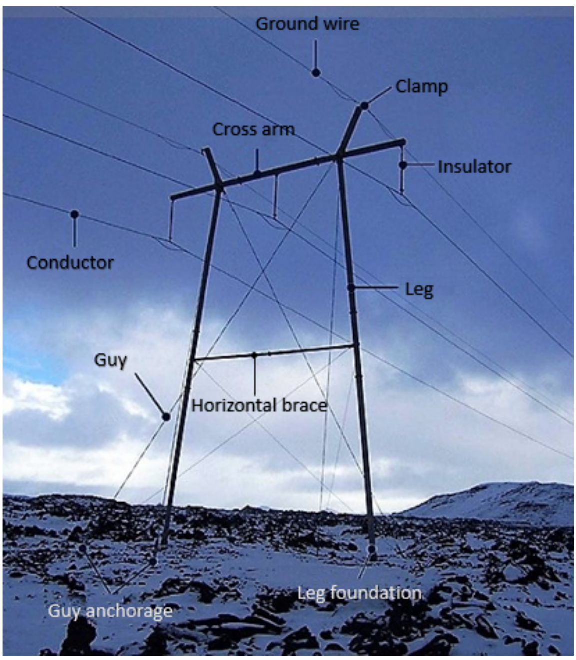

Figure 2.1: Definitions of tower parts

Figure 2.1 illustrates different parts of a transmission line, particularly concerning the transmission tower.

In regard to the structural part, the first thing to consider when designing a new line is what type of structures to use. This will depend a lot on the terrain beneath the line and how the structure should help distributing forces throughout the line. Kiessling et al. ((2003) divides structures into several categories based on their structural purpose.

Suspension structures carry the conductor in a straight line and do not transfer conductor tensile forces. Relatively light-weight and economic. An example is shown in Figure 2.2a.

Angle suspension structures are used when lines change direction with less than 20 degrees. They do not transfer conductor tensile forces.

Angle structures are used when lines change direction with more than 20 degrees. They carry the resulting conductor tensile forces and are equipped with tension insulator sets.

Strain and angle-strain structures carry conductor tensile forces in line direction or resultant direction respectively. They can withstand differing tensile forces on either side and therefore serve as rigid points in the line. To limit cascading they should be arranged regularly along the line (every 5-10 km). An example of an angle-strained structure is shown in Figure 2.2b.

Dead-end structures carry the total conductor load. They are used where the line ends and the conductors are transferred to substation portals.

Special structures are used when a structure has several functions. For example, for a T-off structure, where some circuits pass through and others branch off.

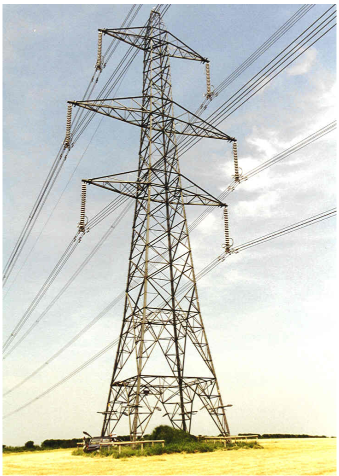

(a) Suspension steel lattice tower.

(b) Angle-strain lattice steel tower.

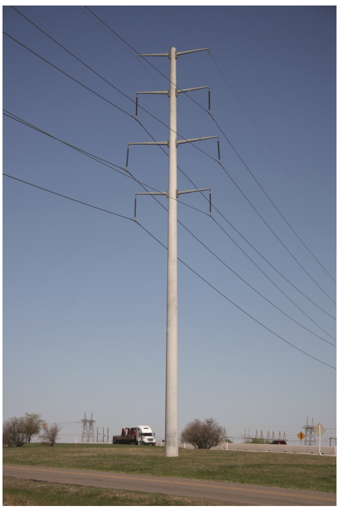

(c) Steel-reinforced concrete pole.

(d) V-guyed suspension tower.

Figure 2.2: Different types of structures and designs of transmission towers.

The selection of structure design for an overhead transmission line depends on several parameters. The impact of these will vary from line to line and will need to be considered for each new line being designed. The following parameters are given as the most important ones by Kiessling et al. ((2003).

- land used
- environmental impact
- capability to transfer necessary power
- life time
- location and importance
- terrain and access
- number of circuits
- loads
- necessary height
- the use of nearby land
- right-of-way and compensations
- keraunic level and arrangement of ground wires
- construction method and maintenance
- investment

The main categories of structure designs to be considered according to Kiessling et al. ((2003) are self-supporting lattice steel towers, self-supporting steel poles, steel-reinforced concrete poles, wooden poles, guyed structures and cross-armless structures. A brief description of these follows.

Self-supporting lattice steel towers are the most traditional tower type. They can be used where it is called for narrow towers and can accommodate several circuits and all conductor configurations. They are easy to transport and relatively economic, also for high towers. Updating and maintenance is easy. They are corrosion protected resulting in a long life cycle. The towers require a lower amount of steel than similar self-supporting tubular towers. Two examples are shown in Figure 2.2a and Figure 2.2b.

Self-supporting steel poles are used in urban or suburban areas, where limited right of way is available. To some they offer a more aesthetic option. These poles can be either suspension poles made of H-beam sections, seamless tubular steel poles with section by section differing diameters or continuously conical shape or conical steel poles with six, eight or more sides. The suspension poles are generally of higher cost than lattice towers due to the increased weight. The seamless tubular poles require expensive equipment for production. Conical sided poles can be adjusted to fit the loads.

Steel-reinforced concrete poles are used in residential areas due to aesthetics. They require a lower amount of steel, leading to lower costs than steel towers. Due to the high weight, brittle material and special equipment needed the transport and erection is more difficult and costly. They are only available for shorter towers. The concrete surface can cause long service life if maintained, but may be reduced by freeze and thaw and in coastal areas by corrosion due to salt. Spun concrete poles are used for low- and medium-voltage installations. Vibrated concrete poles are used where spun concrete poles are not available. Today no concrete poles are erected in Norway and those that exist are old ones. An example is shown in Figure 2.2c.

Wooden poles are common in countries where good quality and large quantities of timber can be found. As for example in Norway where they are much used in the regional and local distribution networks (0.23 - 132 kV).

Guyed structures are used for single-circuit lines. Guys are installed to support the structure. H-types and portal (M-) types have long been used. In later years, also V-types and Y-types have been used. They are aesthetically and economically favourable and often used in flat terrain. They generally yield lower weight, and by that cost, than self-supporting towers. An example of a V-guyed tower is shown in Figure 2.2d.

Cross rope structures (CRS) , also called Chainets, use tensioned ropes instead of a cross arm, thus reducing the amount of steel needed for the structure. They are commonly used for single-circuit lines and require wide site areas.

Guyed towers are based on the principles that a guy wire and a column are very effective structural components in regard to tension and compression respectively (White, (1993)). Because of the loads taken by the guys, the amount of steel can be reduced compared to self-supporting towers, resulting in lighter towers and a more economical and aesthetically pleasing design choice. The guyed towers, however, take up more site area than self-supporting towers due to the guy anchorages and are therefore only preferable where space is not a determinative factor, such as in remote areas (White, (1993)).

Figure 2.3: Guyed M-tower

As mentioned, many different designs for guyed structures are available. White ((1993) divides basic types of guyed structures into guyed single poles/masts, guyed rigid frames and guyed and hinged/pinned masted structures. Single masts normally use a pinned connection to the foundation and the guys are often attached close to each other at the pole. Thus, they rely on the mast and guys being designed so that the lines of action of the different loads are close to centric to prevent rotations. They are effective as angle towers and dead end towers. Guyed rigid frames are often designed with one leg and four guys, and a top structure similar to unsupported rigid frames. Y-towers are examples of this type of guyed structure. Pairs of guys are normally attached at separated points to ensure torsional stability.

The dimensions of the leg might get quite large to account for moments and shear in the leg if non-centric loads are induced. M-, V- and CRS-towers are examples of guyed and hinged/pinned masted structures. They often consist of two legs and two pairs of guys, attached at each side of a cross arm or tensioned wire rope. Due to the guy locations V-towers and CRS-towers are better suited than M-towers if affected by torsional loads. V-towers are more suitable in uneven terrain since the use of only one footing ensures equal leg lengths. CRS-towers can be preferred at higher voltages as large clearance is required and the towers easily can become top heavy. M-towers take up less space in regard to area than V-towers and CRS-towers, due to the use of only two guy attachment points. However, higher towers need four points as the guys need to be crossed to take up the loads, and thus this advantage is sometimes lost. An M-tower is illustrated in Figure 2.3. The conceptual design of these guyed towers are illustrated in Figure 2.4.

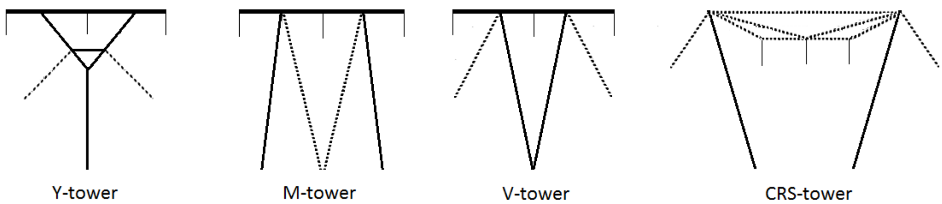

Figure 2.4: Conceptual design of guyed towers.

2.2 Dynamic response of tower structures

Structures are often affected by dynamic loads. Dynamic loads are loads that are time dependent, whether it be that they only last a small period of time or that they change greatly with time. A commonly known load such as this is wind load, which is applied to almost every structure unless built indoors. For transmission lines wind loading is very common and often governing in design (Gani and Légeron, (2010)). Other dynamic loads can be earthquake forces and loads from machinery and people.

The dynamic loads that affect structures can excite their natural frequency if they are of similar size. This can result in either fatigue problems or structural failure (Vinson and Sierakowski, (2012)). Much theory is available on vibration analysis, which is based on calculus and applied physics (Blevins, (2016)). Names like Euler, Bernoulli, Rayleigh and Timoshenko have all contributed to the development of the methods used today by including more parameters.

”The natural frequency of an object is the frequency at which the objects tends to vibrate when disturbed” (The Physics Classroom ((1996-2016)). Adjacent structural parts with similar natural frequencies can excite each other. Meaning that the conductors excited by the wind can in turn excite the tower structure if the natural frequencies are similar. The resulting resonances can lead to failure (Vinson and Sierakowski, (2012)).

Conductors have many different modes of vibrations of different frequencies. Wind load applied to them in a transverse fashion very often result in vertical excitations of the conductor since there almost always is a frequency that is similar. According to Kiessling et al. ((2003)) the main vibration modes of cables are called aeolian vibrations, subspan oscillations and conductor galloping.

Aeolian vibrations are of high frequency (5-50 Hz) and are so called vortex-induced vibrations. They usually occur at wind speeds of 5-10 m/s and the amplitudes can be around the size of the conductor diameter (Kiessling et al., (2003)).

Aeolian vibrations can cause fatigue failure to conductor strands because of bending at the suspension clamps or clamps of spacers, spacer dampers, dampers or other devices installed on the conductor. Optical- and conventional ground wires can experience vibration frequencies up to 150 Hz because of lower external diameter. These wires can also aggregate a thicker layer of ice and snow which will increase their apparent diameter and generate vibrations of higher amplitudes (Lilien, (2013)).

In order to control the conductor vibration amplitude so that the stress in the conductor strands is below the fatigue endurance limit, one has to introduce additional damping if the wires self-dampening effect is too low. OPGW has lower self-dampening effect since they have fewer layers and thereby less strands that take up energy as they are gliding relative to one another.

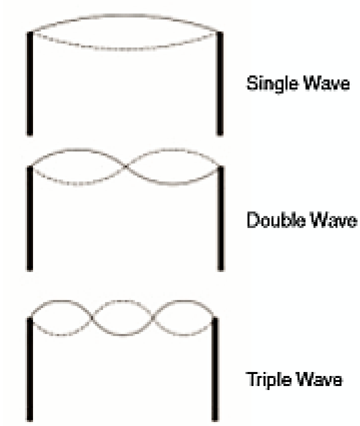

Figure 2.5: Standing waves of 1, 2 and 3 loops (Preformed Line Products, (2016)).

Where bundle conductors are arranged after one another in the direction of the wind subspan oscillations might occur. They are flow-induced vibrations and of low frequency, appearing at wind speeds of 4-18 m/s. Different wind speeds can yield different oscillation modes (Kiessling et al., (2003)).

Conductor galloping usually occurs at wind speeds of 6-25 m/s in both single or bundle conductors. These vibrations are common when wind is applied to ice covered conductors as the asymmetry of the cables leads to an aerodynamically unstable profile. The transverse force from the wind excites the oscillations further. The amplitude can be as large as the sag of the conductor, which can result in clashing and flash overs (Kiessling et al., (2003)). Galloping can occur as single, double and triple standing waves as illustrated in Figure 2.5 (Preformed Line Products, (2016)). It is thus for these number of loops the frequencies of the cables should be assessed.

If the natural frequencies of the towers and conductors coincide, the frequency must be altered to avoid negative effects. This can be done in many ways, as discussed by Preformed Line Products ((2016)). Possibly the most common one is to add dampers to the conductors. Others include air flow spoilers and detuning pendulums. Altering the cable span will also have an impact, but might not be the best solution.

The natural frequency of a conductor can be found using Equation 2.2 or 2.1 depending on whether the bending stiffness of the conductor should be included or not.

$$f = \frac{k}{2*a} * \sqrt{\frac{H}{M_c}} * \sqrt{1 + \frac{(k*\pi*a)^2 * E * I}{H}} \tag{2.1}$$

$$f = \frac{k}{2*a} * \sqrt{\frac{H}{M_c}} \tag{2.2}$$

Where:

k	=	Harmonic coefficient
a	=	Span
H	=	Tension in conductor
M_c	=	Unit weight of conductor
E	=	Modulus of elasticity for conductor
I	=	Second moment of inertia for conductor

(Kiessling et al., (2003))

The natural frequency of a structure is based on the stiffness of the system. When assuming a linear system, the stiffness and frequency of a tower structure can be found using Equations 2.3 and 2.4.

$$k = \frac{F}{\delta} \tag{2.3}$$

$$f = \frac{1}{2*\pi} * \sqrt{\frac{k}{M}} \tag{2.4}$$

Where:

k	=	Stiffness of structure
F	=	Force applied
δ	=	Deflection of structure
f	=	Natural frequency of structure
M	=	Mass of structure

(Blevins, (2016))

Gani and Légeron ((2010)) discuss that a nonlinear analysis is necessary as the system is not linear due to the behaviour of conductors, guys and towers. The simplification of an assumed linear system is however used here.

2.3 Steel

Steel has been used as a material for many years, both as a building material and for other uses. Its high strength and ductility, as well as its good formability and weldability makes it a preferred material in many settings. In later years, the development of the material has allowed it to become one of the most used construction materials.

Steel is an alloy based on iron with up to 2.1% carbon. Structural steel however, has a considerably lower amount of carbon and is also added several other alloying elements. These elements greatly affect the material properties of the steel. Structural steel can be divided into normal structural steel, stainless steel and cast steel, but is better classified by its strength class and by its quality. The strength class specifies the steel's yield stress while the quality specifies the chemical composition, thermal and mechanical processing and the impact strength of the steel (Larsen, (2015)).

The manufacturing process for steel has stayed more or less the same for 100 years. This process can be divided into five steps; reduction, oxidation, deoxidation, casting and rolling.

In the reduction step, pellets from the iron ore, coke and lime stone are added to the top of a blast furnace, where heated air is applied through the bottom. This turns it into pig iron and slag. The pig iron has a carbon concentration of 3-5% and contains unwanted elements, such as phosphorus and sulphur.

In the oxidation step the carbon concentration is lowered by adding oxygen so that CO_2 is produced. This increases the concentration of oxygen which can create pores in the material. This is called rimmed steel.

To reduce the pore formation, alloying elements that react with oxygen are added in the deoxidation step. Especially ferrosilicon and ferromanganese are used for this process. Depending on the amount of deoxidation done one can be left with killed or half-killed steel, where killed steel has been completely deoxidized.

The steel will now have the desired properties and is transferred to rolling mills for further processing. An alternative to this last step is to produce casting blocks that are cooled and then sent to the rolling mills where it can be reheated and processed further (Larsen, (2015)). For use in electrical utility fully killed steel should be used for angles and plates to ensure the material can withstand not only the static loading, but also alternating loads and possible vibrations (Kiessling et al., (2003)).

2.3.1 Material properties

The material properties of the steel are determined by the amount of different elements in the steel. These elements include aluminium, phosphorus, hydrogen, copper, chromium, manganese, nickel, nitrogen, oxygen, silicon and sulphur. The effect of these elements is discussed by many, for example by Larsen ((2015)). As the chemical composition of the steel is so important to determine the properties, it is regulated by international rules and regulations. In addition to this, the micro structure of the steel has a big impact on the mechanical properties. The micro structure is a function of the carbon content and temperature.

2.4 Composite materials

A composite material can be defined as ”a combination of two or more components differing in form or composition on a macro scale, with two or more distinct phases having recognisable interfaces between them” (Akovali et al. ((2001)), pg. 3). This process of combining materials is done to achieve new or improved properties; mainly in regard to physical, mechanical or chemical properties (Vinson and Sierakowski, (1993)). Opinions on the definition differ, especially on whether it should include the level of scaling.

The art of combining materials to achieve a new material with better properties has been around for many years. It has been used to develop stronger materials, more ductile materials or just to provide a smoother finish on surfaces. A much used and well known composite in the construction industry today is steel reinforced concrete that combines the high tensile strength of the steel with the compressive strength and lighter weight of concrete (Vinson and Sierakowski, (2012)). The use of composites today can be found everywhere from households to aerospace (Vinson and Sierakowski, (1993)). Some uses are discussed by Sinha and Vinay ((2010)).

Composites usually consist of a reinforcing material incorporated in a matrix. The matrix, which is generally of low modulus, is strengthened by the considerably stronger and stiffer reinforcement. On a basic level composites can be divided into three structural levels: elemental, micro-structural and macrostructural. Depending on the properties needed (e.g. application temperature or conductivity), different matrices can be used. The most common ones are of metal, ceramics, polymer, carbon or a hybrid of these (Vinson and Sierakowski, (2012)). The composite system acts differently according to how much and what kind of reinforcement is added. In particle strengthened composites, the reinforcing particles only prevent dislocations in the matrix while the matrix itself bears the load. In fibre reinforced composites, the reinforcing fibres bear the load while the matrix acts as a load distributor. Laminar composites are another group, where sheets of reinforcing agents are bonded together. To get the mechanical properties needed one of the most important features concerning composites is the adhesion between fibres and matrix (Akovali et al., (2001)).

2.4.1 Fibre Reinforced Polymers

In the last decade, the use of polymer matrix composites as an engineering material has become common. When produced using reinforcing fibres the elements can sport good mechanical properties, such as high strength and stiffness, low weight, non-conductivity, high durability and corrosion resistance. In addition fibre reinforced polymers can easily be shaped according to will (Sinha and Vinay, (2010)).

The fibres can be either continuous or discontinuous and are usually made of carbon/graphite, glass or aramid. Other fibres used include boron fibres, ceramic fibres and metallic fibres (Akovali et al., (2001)). Carbon fibres are produced by burning a precursor fibre at high temperatures such that only the carbon is left. By increasing the temperature graphite fibres are produced (Sinha and Vinay, (2010)). These fibres based on carbon are strong and light, but also very expensive. Due to this composites based on carbon fibres are often used in aerospace applications (Akovali et al., (2001)). Aramid fibres are produced by spinning a basic polymer into a fibre. These fibres are strong, flexible and can be produced into textile, but they are also quite expensive and UV-degradable. A known use for aramid fibres are in Kevlar vests. Depending on the manufacturing process used the fibres can come in different forms. These include woven mats and fabric, rovings, yarns and chopped strands (Sinha and Vinay, (2010)). Due to the high cost and electrical conductivity neither carbon fibres or other metallic fibres are used for electrical utility applications. As glass fibres are cheaper and still offer good material properties these are preferred for electrical utility applications.

The matrix comprises of about 30-40 % of the composite and its main function is to serve as a bond between reinforcing components while distributing loads, providing shear, compressive and transverse strength and protecting the reinforcement agents from wear (Akovali et al., (2001)). It is usually either consisting of thermoplastic or thermoset resins. The thermoplastic resin is the least used in the composite industry today. During the processing of thermoplastics, no chemical reaction occurs and only heat and pressure is required to form the parts. It can be reheated and reshaped, and is therefore often used in for example plastic bottles. The thermoset resin, on the other hand, sets permanently after curing as the polymer chains become crosslinked resulting in a final rigid matrix (Vinson and Sierakowski, (2012)). In the production of thermosets, a curing agent (catalyst) will be added and the resin will be applied to a reinforcing material. Due to heat and pressure a chemical reaction will then harden the resin and the parts will be shaped using the desired manufacturing method (Sinha and Vinay, (2010)). The most common thermosets are unsaturated polyesters, epoxies and polyimides (Akovali et al., (2001)). A more extensive research on the polymers used in FRPs can be found in Sinha and Vinay ((2010)). To get the desired properties, colour and filler can be added to the matrix, and sometimes a solvent is also added.

2.4.2 Manufacturing processes of FRPs

The two most used manufacturing processes to make electrical utility applications of FRP are filament winding and pultrusion. In addition to these, several open mould processes (wet lay-up, bag moulding and curing and autoclave moulding) and closed mould processes (transfer moulding, compression moulding and injection moulding) are available for manufacturing FRP elements for other uses (Akovali et al., (2001)). Laminar elements are also possible to create by bonding fibre layers together using a matrix as glue (Vinson and Sierakowski, (2012)).

The filament winding process can be done with either wet or pre-impregnated fibres. The process is illustrated in Figure 2.6. In the wet winding process, which is the most common one, continuous fibre reinforcement, on rovings is passed through a resin bath. A shuttle will then spin the resin soaked fibres onto a rotating mandrel in a pattern to ensure an even distribution. The angle with which the fibres are spun onto the mandrel is calculated beforehand for optimum usage according to the external loads. This method of spinning ensures the element has strength in several directions. The process is done until the desired thickness is achieved. Finally, the spun element is cured in an oven. It is possible to shape the spun elements into non-circular shapes before curing. Due to limitations of the size of the machine and oven, only elements up to a certain length can be produced by this method. The structural elements manufactured in this way are usually conical. To get longer elements these can later be stacked. The filament winding process is also possible to do using pre-impregnated fibre tows (Sinha and Vinay, (2010)). Over the years, the filament winding process has become highly automated. This and the progress in analysis programs has made the process from calculations to product both shorter and easier (Peters, (2011)). More information on the filament winding process can be found in Peters ((2011)) and Akovali et al. ((2001)).

Positive aspects with this production method is the automatic process and that both resin and fibre is used in its lowest cost form. Also, the process results in members with high mechanical performance. However, costs are high due to the investment needed for machines and equipment needed. In addition to this, the production series is limited and the use is limited to convex shaped structures (Huntsman International LLC_1, (2013)).

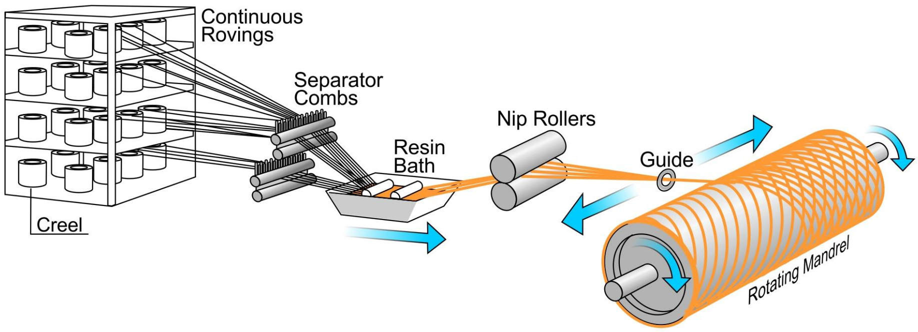

Figure 2.6: Filament winding process.

The pultrusion process is used to manufacture elements of continuous length with a constant cross section. The process is illustrated in Figure 2.7. Like with the filament winding process, the reinforcing fibres are passed through a device that tension the strands and a resin bath, often consisting of polyester or vinylester. The continuous roving strands only provide longitudinal tensile strength in this case. To ensure sufficient transverse properties, woven continuous reinforcing filament mats are added. Finishing is controlled by a surface veil. The soaked strands are then passed through a heated pultrusion die where the thermosetting reaction is begun and the composite is cured. A cut-off saw then cut the continuous cured part into elements of desired length (Sinha and Vinay, (2010)). More information on the filament winding process can be found in Akovali et al. ((2001)).

Due to the continuous production of elements, this process is fast and yields low labour costs. It is therefore a good choice, but it is limited to constant cross sections (Huntsman International LLC$_2$, (2016)).

2.4.3 Properties of Fibre Reinforced Polymers

Depending on materials used for the resin and fibres and the structural composition of the FRPs, different properties for a finished element can be obtained. As mentioned FRP is an anisotropic material. Thus the material properties will also depend on how the element is loaded. For FRPs imperfections are of overwhelming importance as a small flaw in a particular

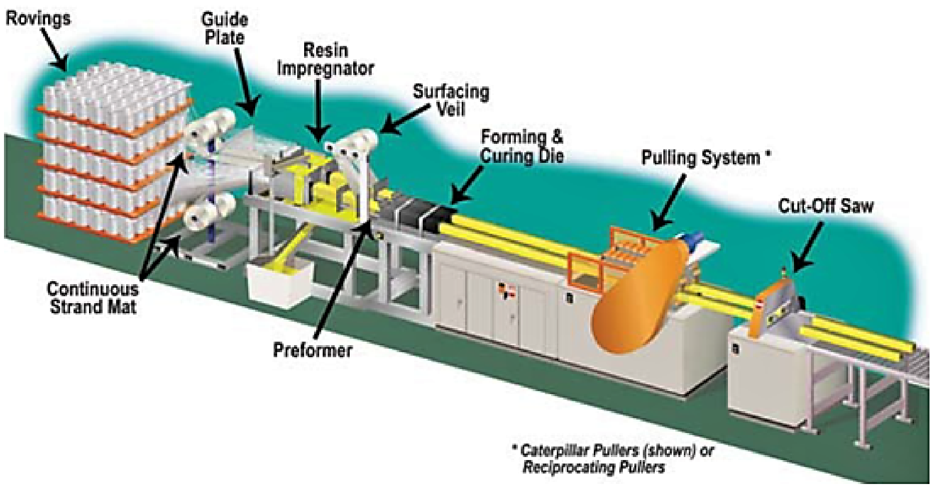

Figure 2.7: Pultrusion process.

place can have a major effect on the element's structural performance.

FRP-materials need other testing than steel. Both fibres and resin should have documented testing to ensure properties are adequate. The most common tests for finished FRP elements are tests concerning tensile, compressive and shear strength and moduluses as well as interlaminar strength. Also Possion's ratio, damage impact, density, fatigue and creep factor has to be tested (Vinson and Sierakowski, (2012)). More information on testing can be found in (Brown, (2002)) and Peters ((2011)).

2.5 Application of composites in load-carrying structures

Load carrying structures have historically been built using timber and rocks. In later years, steel and concrete has greatly taken over this task as the materials are strong, ductile and durable. Especially the combination of steel and concrete has greatly influenced the construction industry and has allowed for great structures to have been built.

The use of FRP in structures has mostly been limited to small components of buildings, such as window and door details. However, the use has expanded to include larger components like roofs, and cladding. Particularly when constructing curved roofs or other special structures FRPs can be used to great success. Some expect FRPs to revolutionise the construction industry by offering suitable and cost efficient alternatives to traditional structures (Kendall, unknown)).

Load carrying parts of structures are important not only for carrying load, but also to ensure the whole structure performs its task in a safe and reliable way. Most of a structure's weight is often represented by the load carrying part. FRPs are therefore a good option to use in these parts as they offer a high strength to weight ratio. They can also withstand large deflections which can open doors that have previously been closed in regard to material use.

FRP offers many advantages for use in load-carrying structures. The low weight can lead to less heavy lifts and use less heavy equipment, resulting in saved time and cost, which are critical factors in any project. They are very durable and easy to repair and strengthen in-situ (Halliwell, (2002)). Another major advantage is the possibility to tailor-make the material and its properties to best suit a project, whether it be shape, reinforcement direction or colour. The anisotropic nature of FRP, allows for the reinforcement to be adjusted to follow stress patterns and lead to economic designs (Kendall, unknown)).

Recently, particularly in North America, FRP has been successfully used in transmission towers. Another advantage to FRP that directly affects this section is its insulating properties. By being non-conductive it leads to safer installation and maintenance of the transmission lines. Also here, the very good durability is a great factor.

Chapter 3

Design

3.1 Basis for Design

Standards:

FprEN 50341-1:2012 E: Overhead electrical lines exceeding AC 1 kV - Part 1: General requirements - Common specifications (CENELEC, (2012)) define the basic requirements for design of overhead power lines. It gives requirements for the reliability, security and safety of the structure.

NO NNA based on EN 50341-3-16:2008 and EN 50423-3-16:2008: National Normative Aspects for Norway (The Norwegian National Committee, (2008)) defines factors and the like for use in Norway.

NS-EN 1993-1-1:2005+NA:2008: Prosjektering av stålkonstruksjoner - Del 1-1: Allmenne regler og regler for bygninger (CEN, (2005)) is the basis for steel calculations.

Computer programs:

PLS-CADD (Power Line Systems - Computer Aided Design and Drafting) is a design program for overhead power lines from Power Line Systems Inc. It combines terrain modelling, engineering, tower spotting and drafting

(Power Line Systems Inc_1, (Updated 2016)). This is used to do the tower spotting of the line.

PLS-TOWER is a program from Power Line Systems Inc for analysing and designing steel latticed towers used in power lines and communication facilities. It can perform design checks of the structure under specified load cases and calculate wind and weight spans (Power Line SystemsI nc_2, (Updated 2016)). PLS-TOWER is used to model the lattice tower.

PLS-POLE is a program from Power Line Systems Inc for analysing and designing structures made up of wood, laminated wood, steel, concrete and Fibre Reinforced Polymer (FRP) poles or modular aluminium masts. Like Tower it can perform design checks of the structure under specified load cases and calculate wind and weight spans (Power Line Systems Inc_3, (Updated 2016)). PLS-POLE is used to model the two towers with tubular legs.

3.2 Limit states

All structures should be checked in the ultimate limit state and the serviceability limit state. These limit states are the states where the design requirements of the overhead line no longer are met (CENELEC, (2012)).

The ultimate limit state is concerned with the structural failure or collapse of a structure due to deformation, stability loss, buckling and so on (CENELEC, (2012)). In the ultimate limit state the structure's capacity is controlled by using the material's strength parameters and tensile properties to determine the various elements' strength and stability due to loading conditions based on requirements for safety and reliability (Larsen, (2015)).

In the serviceability limit state, it is checked whether the construction meets the requirements set for its purpose and use over its lifetime (Larsen, (2015)). Examples of aspects to check are vibrations, deformations that do not lead to collapse, electrical flashovers and durability (CENELEC, (2012)).

3.3 Line location

A 4-5 km long line consisting of 13 intermediate suspension towers has been modelled and analysed. Thus, the towers are spaced approximately 350 m apart. This thesis focuses on suspension towers and the stretch of terrain used for the alignment is therefore chosen to avoid the use of tension and angle towers.

The line is assumed to be located in Norway in regard to standards, national annexes and requirements used. However, the data used for the modelling in PLS-CADD describes a terrain located in Iceland. As this thesis is more of a conceptual study, this is not a problem. Also, having some terrain data is essential to get a lifelike model in PLS-CADD as terrain seldom is flat in Norway. The terrain profile is shown in Figure 3.1.

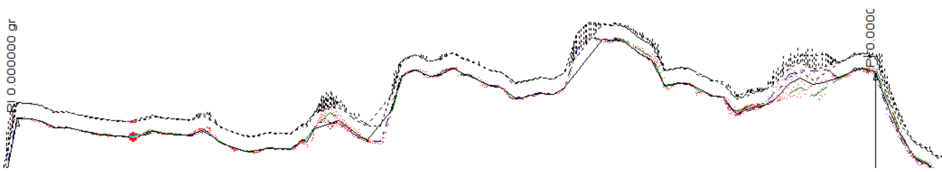

Figure 3.1: Terrain profile.

3.4 Tower structure and geometry

The towers designed in this thesis are guyed portal suspension towers for three 420 kV conductors and two ground wires. The outline of the tower as shown in Figure 3.2 was given by ARA Engineering as a basis for design. This incorporates normal requirements concerning the slope of the legs and guys, 1:8 and 1:2 respectively.

To account for ground clearance requirements, it was found that the towers needed to be approximately 25 m high. This was based on the max ice load and max temperature weather cases, that were assumed to induce the largest sag in the conductors, including electrical clearance requirements.

Insulators used are composite suspension V-strings. Composite insulators

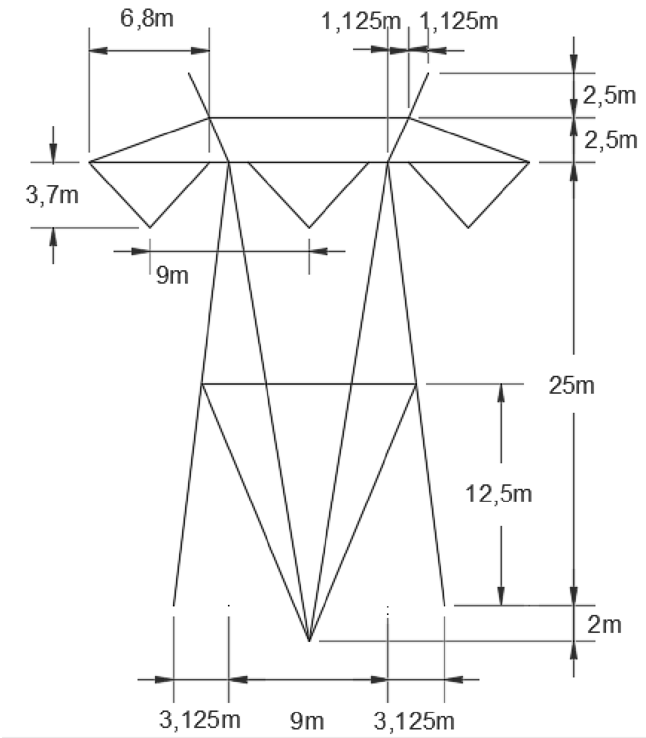

Figure 3.2: General dimensions of tower structure.

are more light weight and more durable than ceramic or glass ones. Figures 3.3 and 3.4 illustrate maximum allowed insulator swings and geometry of the composite V-string insulator. These, as well as requirements for insulator lengths and number of discs for a 420 kV system to prevent creepage and flash overs, were given by ARA Engineering. In addition to Figure 3.4, Figure D.19 of Appendix D.2 gives information about the insulators used. Based on the given data, the distance between phases was set to 9.0 m.

The conductor used is a Triplex Grackle. See Figure D.5 of Appendix D.1 for more information. There will be three phases installed in a parallel manner. The three phases are all consisting of three wires that are separated by spacers. An illustration of a similar configuration of conductors and ground wires can be seen in Figure 3.5.

The chosen ground wire is a F 69 Sveid. More information can be found in Figure D.7 of Appendix D.1. The main purpose of ground wires is to

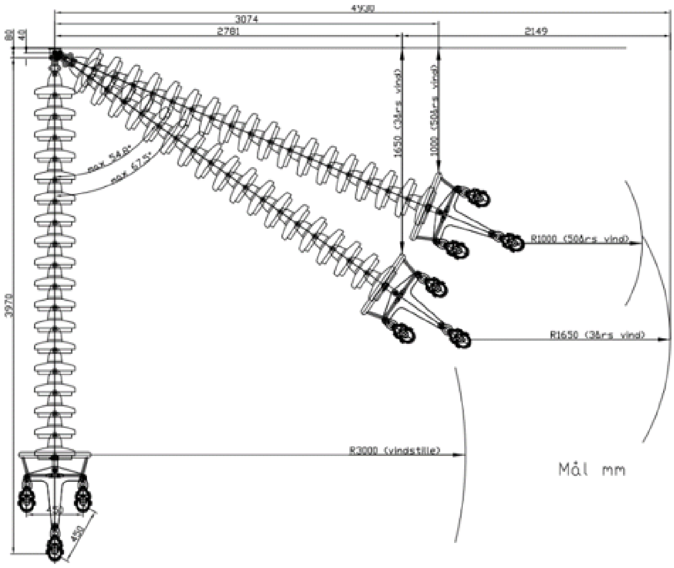

Figure 3.3: Allowed insulator angles.

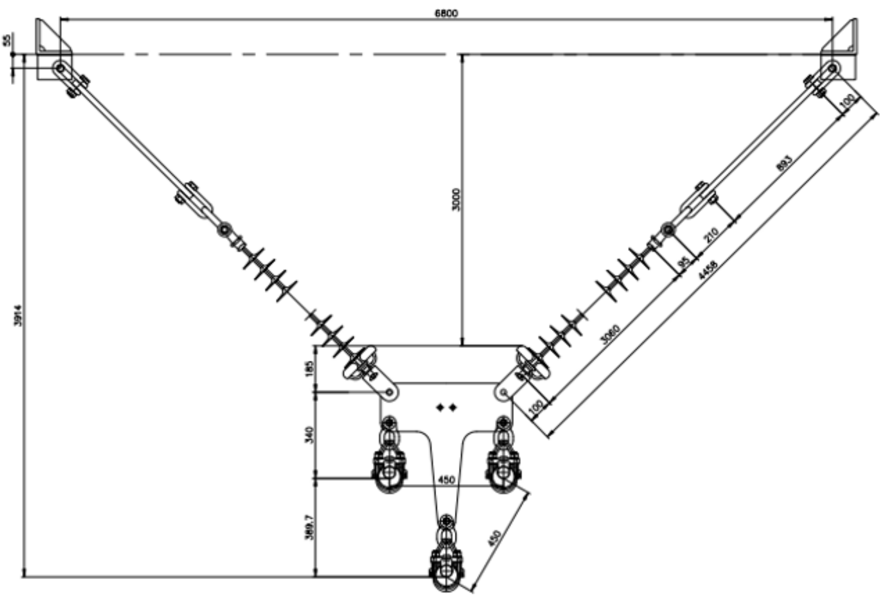

Figure 3.4: V-suspension composite insulators.

Figure 3.5: Configuration of three conductors and two ground wires. The left line with duplex conductors and the right line with triplex conductors (Statnett).

protect the conductors from direct effects of lightning strikes. As seen in Figure 3.6 the conductors are protected as long as they lie within an angle of 26° from the vertical plane of the ground wire. By having one of the ground wires being an optical ground wire (OPGW) data can be transferred through the wire. This enables transfer of large amounts of data which can be used for relay and protection purposes, operation of the power system or for commercial purposes. Figure 3.7 illustrates how the ground wire connection can look.

The guys used should be of galvanised extra high strength steel wire strands according to FprEN 50341-1 (CENELEC, (2012)). They should be designed as tension components in accordance with NS-EN 1993-1-1 (CEN, (2005)) and thus be pre-tensioned after instalment. According to NS-EN 1993-1-1 the pre-tension should be less than 15 % of capacity to minimise the possibility of vibrations. It is set to 5 %. Examples of anchoring of guys in bedrock or soil are shown in Figure 3.8.

Cables, like guys, should be designed as tension components in accordance with NS-EN 1993-1-1. The pretension is decided so that the deflection of the cross arm is as close to zero as possible under everyday stress.

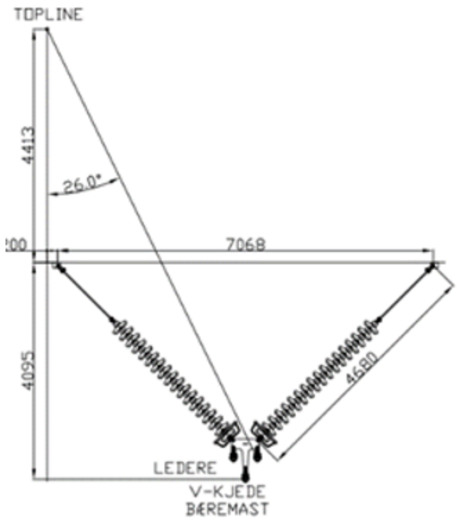

Figure 3.6: Shield angles of ground wires.

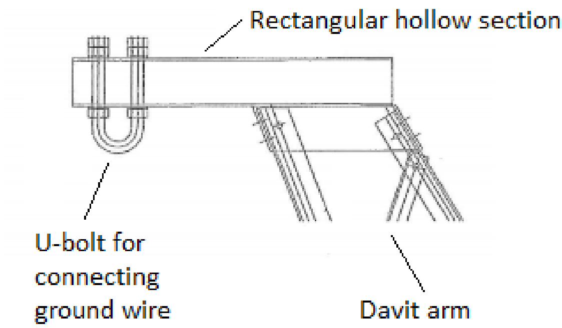

Figure 3.7: Ground wire connection.

Foundations are assumed designed in accordance with (CENELEC, (2012)) and (The Norwegian National Committee, (2008)).

All steel connections use bolt of grade 8.8 and are assumed designed in accordance with NS-EN 1993-1-1 (CEN, (2005)). When designing new towers connections are designed so that members fail before the connections. This is for safety reasons. All steel connections should be galvanised for protection (CEN, (2005)). Refurbishment of coating should be done when necessary.

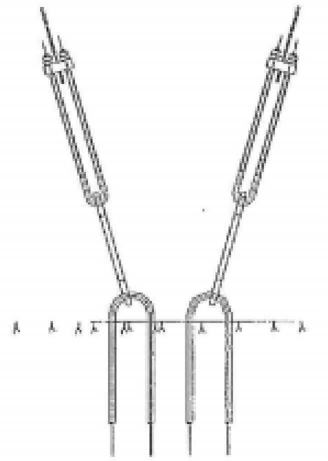

(a) Guy anchor in bedrock.

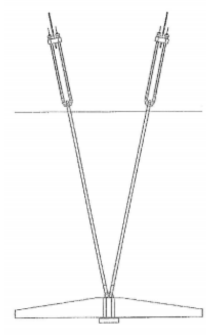

(b) Guy anchor with anchor plate.

Figure 3.8: Guy anchoring.

For maintenance purposes towers must be designed to give access to personnel. According to FprEN 50341-1 a removable device should give access to pole cross arms (CENELEC, (2012)). Inserting step bolts to assist personnel is also possible. These should be removed in the lowest section to ensure no unauthorised personnel gets access. To prevent climbing on the tower, protection could be added at the lower parts of the tower (CENELEC, (2012)).

3.4.1 Steel lattice tower

The steel lattice tower shown in Figure 3.9 is designed as an Icelandic type tower. It is a single guyed tower, meaning the guys are attached at one level: at the cross arm. The legs are at a slope of 1:8 and has a 3D latticed structure. This differs from the transmission towers typically used by Statnett today, which are self supporting with vertical legs where the lattice structure is only in one direction.

The lattice tower is designed using angle members. Angle members should not be thinner than 4 mm according to the NO NNA (The Norwegian Na-

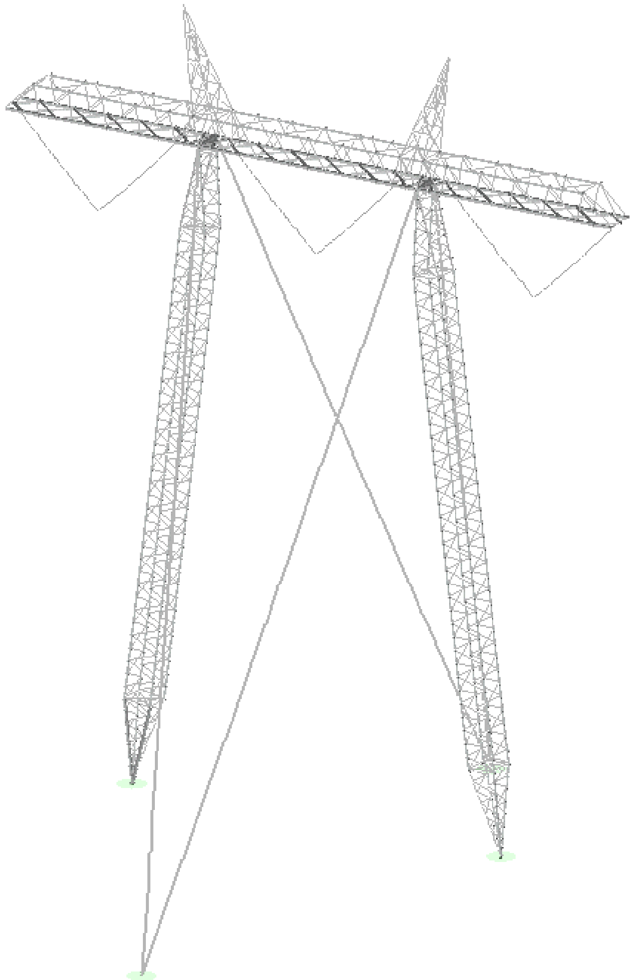

Figure 3.9: Steel lattice tower from PLS-TOWER.

tional Committee, (2008)). It is also recommended to use members no thinner than 5 mm for main members. The different types of members used are given in Table 3.1. In accordance with EN 10056 and EN 10029 angle profiles and plates should be hot rolled. The steel elements used are of S355 type steel.

Connections are to be done using bolts and steel plates as specified. According to the NO NNA bolts should minimum be of size M12 (The Norwegian National Committee, (2008)), thus M12 and M16 bolts are used.

Table 3.1: Elements used in steel lattice tower.

Member	Angle size (mm)
Main leg members	70x70x7
Crossing diagonals in leg	40x40x4
Leg braces	50x50x5
Lower cross arm main members	100x100x10
Upper cross arm main members	90x90x9
Crossing diagonals in cross arm top	50x50x5
Crossing diagonals in cross arm bottom	90x90x9
Crossing diagonals in cross arm side	70x70x7
Main davit arm members	60x60x6
Crossing diagonals in davit arm	40x40x4
Bracing members	UNP 120

The connections used are listed in Table 3.2.

Examples of connections are illustrated in Figure 3.10. These are seen from one side only. For main members, angles will be fastened at both flanges. The diagonal members will be fastened at one flange only. Where possible in regard to strength, only one bolt should be used at each end of the diagonal members to reduce the need for extra plates. The side crossing members below the davit arm need 2xM16 bolts and plates. Both the main members of the legs and lower and upper cross arm will need to be spliced, like illustrated in Figure 3.10d.

According to FprEN 50341-1 (CENELEC, (2012)) overall maximum slenderness for lattice steel legs is 150, which is maintained.

Table 3.2: Connections used in steel lattice tower.

Connection	Description
Leg base	plates and 6xM16 bolts each member
Leg top	plates and 4xM16 bolts each member
Leg splice	plates and 4xM16 bolts each member
Leg diagonals	1xM16 bolt each end
Cross arm main members end	plates and 4xM16 bolts each member
Cross arm splice	plates and 4xM16 bolts each member
Crossing diagonals in cross arm top	1xM12 bolt each end
Crossing diagonals in cross arm bottom	1xM16 bolt each end
Crossing diagonals in cross arm side	1xM16 bolt each end
Main davit arm members	plates and 4xM12 bolts each member
Crossing diagonals in davit arm	1xM12 bolt each end
Bracing members	1xM12 bolt each end

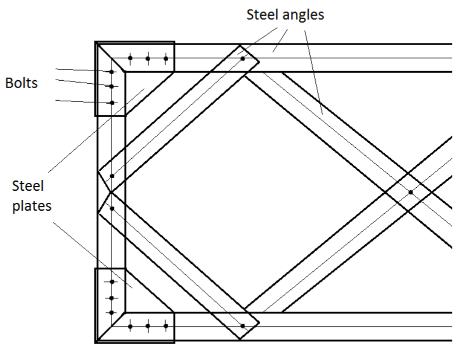

(a) Connection of bottom part of cross arm end.

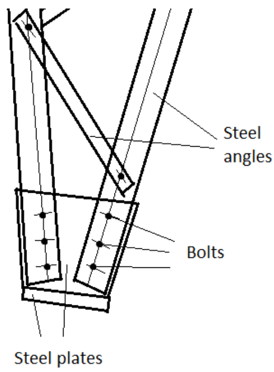

(b) Connection at bottom of leg.

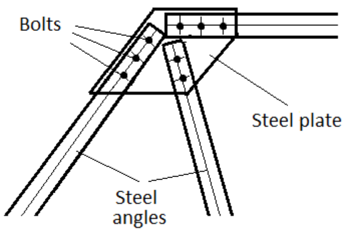

(c) Connection at upper part of cross arm.

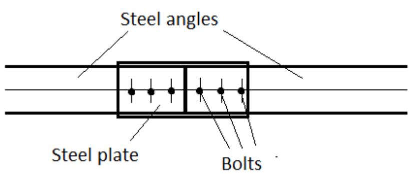

(d) Spliced connection.

Figure 3.10: Examples of connections of steel lattice tower.

3.4.2 Steel tubular tower

The steel tubular tower shown in Figure 3.11 has two guy levels: one connected by the horizontal brace and one connected to the cross arm.

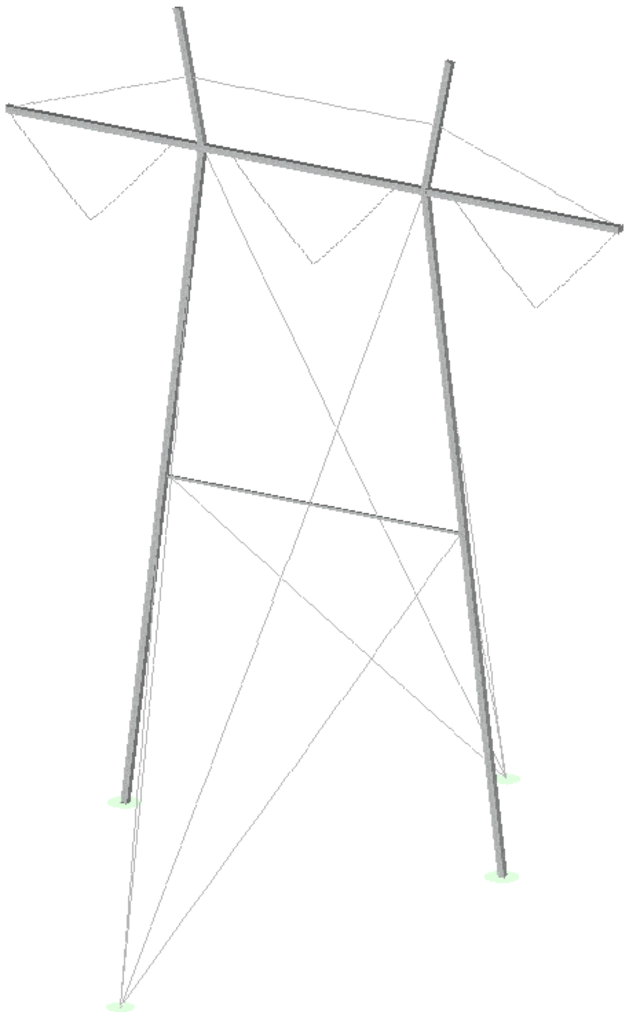

Figure 3.11: Steel tubular tower from PLS-POLE.

The tubular steel legs are designed to be 25.2 m. Due to limitations in transport and the galvanising process, maximum length of elements is 15 m. The poles will therefore need to be spliced. Common ways to do this is using either a slip joint or flange joint (Kiessling et al., (2003)) like shown in Figure 3.12.

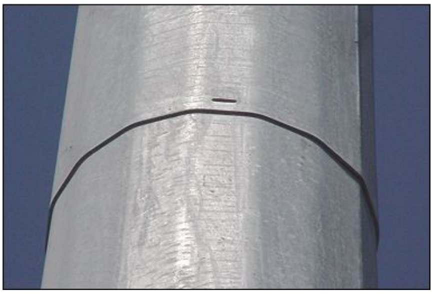

(a) Slip joint.

(b) Flange joint.

Figure 3.12: Examples of how to splice steel poles.

The different elements used in the steel tubular tower are given in Table 3.3. Square cross section were chosen in stead of round ones to make the connections easier and also because square cross sections have larger moment capacity than round ones of same diameter.

Table 3.3: Members used in tubular steel tower.

Member	Size (mm)
Leg	250x250x10
Cross arm	250x250x10
Davit arm	250x250x12.5
Horizontal brace	100x100x10

Figure 3.13 illustrates how the elements can be connected and thus how they interact. Most of the connections will be similar to those of the FRP tubular tower in Figure 3.15, except for the steel caps.

According to FprEN 50341-1 (CENELEC, (2012)) overall maximum slenderness for tubular steel legs is 150. The legs have a slenderness of 50, which is within the requirements. Maximum slenderness for horizontal beams between legs in multi-guyed portal supports is 250. The horizontal brace has a slenderness of 121, which is within the requirements.

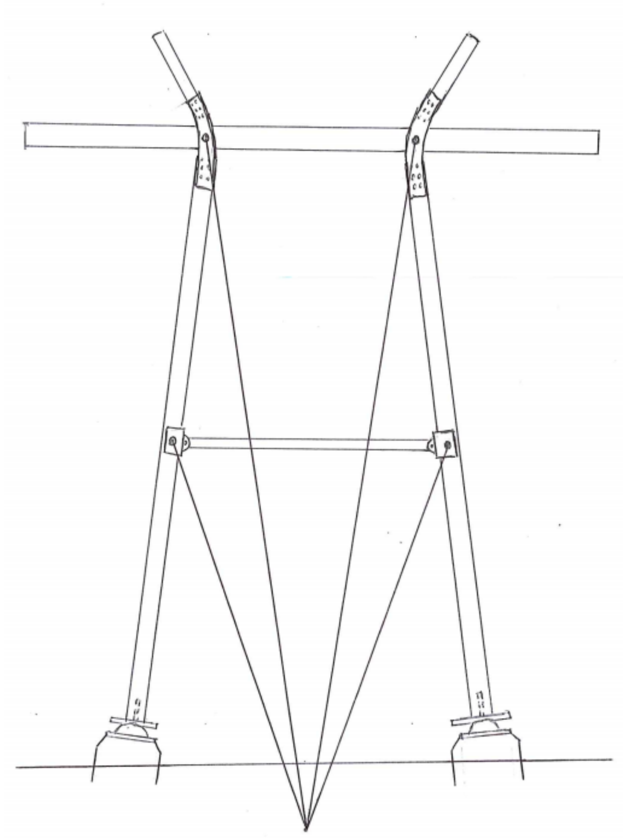

Figure 3.13: Conceptual sketch of connections for tubular steel tower. Dimensions are given on Figure 3.2.

3.4.3 FRP tubular tower

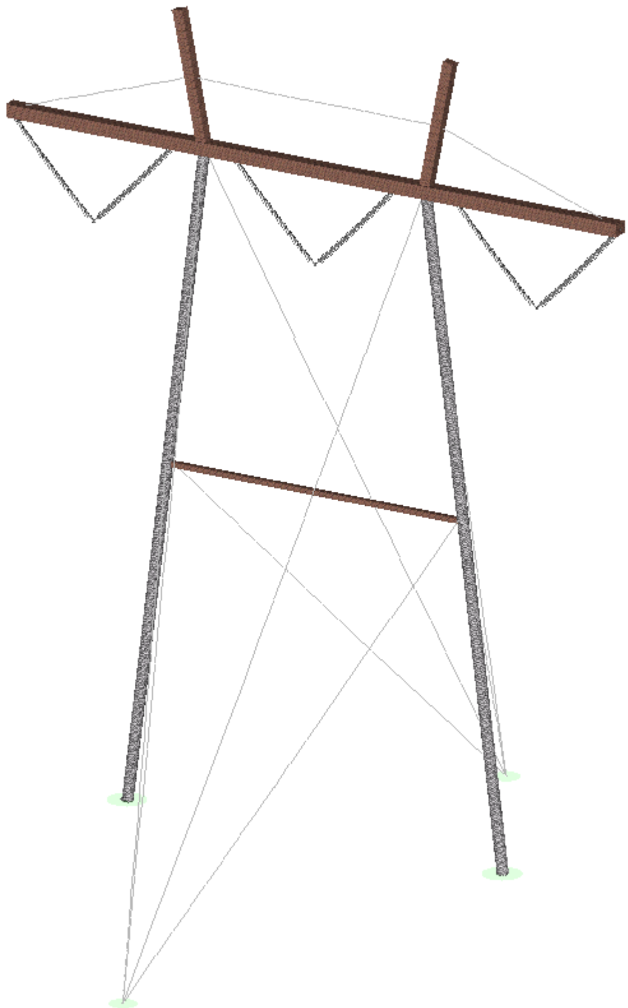

Figure 3.14: FRP tubular tower from PLS-POLE.

Similar to the steel tubular tower, the FRP tubular tower has two guy levels: one connected by the horizontal brace and one connected to the cross arm. The tower is shown in Figure 3.14.

FprEN 50341-1 makes requirements for the performance of materials not specified, like FRP, to be designed so as to provide both sufficient strength and serviceability (CENELEC, (2012)). As no particular

The FRP Tower will be compiled of tubular elements. Due to the use of pultrusion, the elements will be of constant shape and thickness throughout its length. Due to modelling reasons the legs are circular. In real life it would also be possible to use octagonal poles, which might make connections easier (Toth, (2016)). The horizontal brace and davit arms are square, and the cross arm consist of one square section at either side of the pole.

Table 3.4: Members used in tubular FRP tower.

Member	Size (mm)
Leg	ϕ450x15.9
Cross arm	2 à 300x300x9.5
Davit arm	400x400x15.9
Horizontal brace	200x200x9.5

The connections will be fairly similar to the tubular steel tower, the only difference being the steel caps that connects the poles. Connections are illustrated in Figure 3.15.

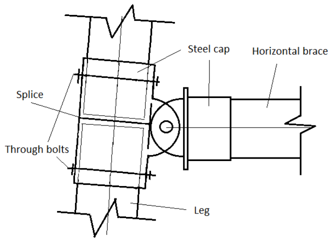

(a) Pinned connection of horizontal brace.

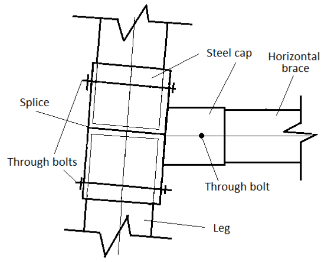

(b) Rigid connection of horizontal brace.

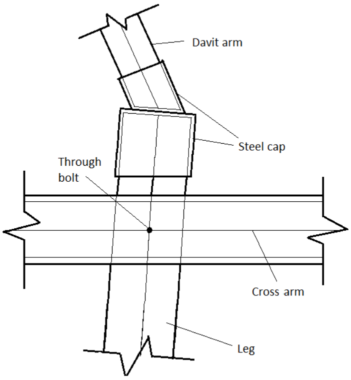

(c) Cross arm and davit arm connection.

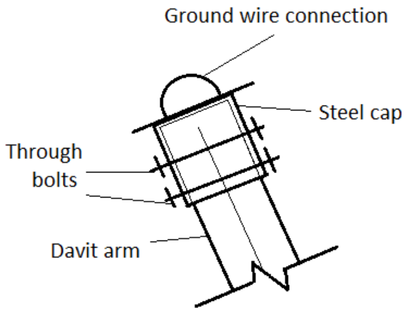

(d) Top of davit arm.

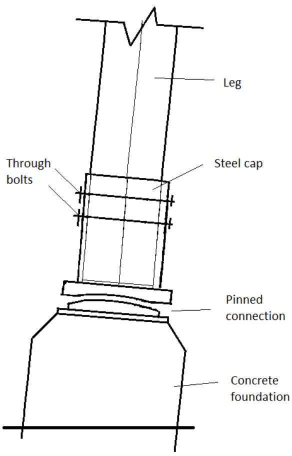

(e) Base connection.

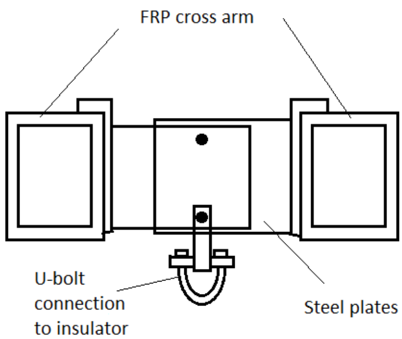

(f) Insulator connection.

Figure 3.15: Examples of connections of FRP tubular tower.

Chapter 4

Actions on Lines

The standard FprEN 50341-1:2012 (CENELEC, (2012)) given by the European Committee for Electrotechnical Standardization give guidance on how to calculate the loads on the lines and their components; such as insulator sets, conductors, poles and lattice towers.

The loads affecting the transmission lines come from several sources and are in the design process given different amount of attention. The most critical ones are the ones due to environmental effects. Such as wind loads, ice loads and the effect of temperature on loads. Then come the loads due to our actions, such as the construction or maintenance of the structure. Last there are the discrete events. These can be from natural sources, such as earthquakes, landslides and avalanches, or from internal sources, like failed components (Catchpole and Fife, (2014)).

These actions can also be classified by their duration where they are either permanent or variable. Permanent actions include the dead loads of all components of the structure. Variable actions are often caused by climatic actions such as wind, ice or temperature changes. These are often referred to as live loads. Accidental actions happen seldom and can refer to avalanches or component failures (CENELEC, (2012)).

Data used in these calculations can either be provided in standards, it can be determined based on statistical data and field observations or it can be based on data calibrated from previous successful designs.

4.1 Dead load

The dead load is represented by the tower structure itself. All components of the structure are taken into account when calculating this action; the supports, insulators, conductors and ground wires of adjacent spans and other installations or fixed equipment on the supports or cables (CENELEC, (2012)). The self weight of the different components found in this thesis are shown in Table 4.1.

The weight of the conductors and ground wires are here calculated for half a span on either side of the support with a ruling span of 350 m (weight given in the table is for a pair). The weight of spacers used between the conductors is not included in the calculation. For the steel lattice tower, weight of members, plates and other connectors not in the model is accounted for with an assumption of this being 15 % of the weight in the model. For the steel tubular tower and FRP tubular tower these weights are also included assumed weights of connections: 5 kN for the steel tubular tower, and due to the extra weight of the steel caps 8 kN for the FRP tubular tower. The weight of insulators, guys and cables are included in the tower weights.

Table 4.1: Calculated dead loads.

Item	Load (N)
Steel lattice tower	81298
Steel tubular tower	76800
FRP tubular tower	48154
Insulators	10596
Conductors	3 à 23491
Ground wires	2 à 4935

4.2 Temperature load

Fpr EN 50341-1 (CENELEC, (2012)) gives five events where temperature effect should be taken into account. These are presented in Table 4.2 which also include variables from the NNA (The Norwegian National Committee, (2008)).

Table 4.2: Temperatures for climatic situations.

No.	Climatic action	Temperature
1	Minimum temperature and no other actions	-20°C or lower
2	Extreme wind pressure	0°C
3	Nominal wind velocity	Not relevant
4	Icing	Not relevant
5	Combined wind and ice	0°C

4.3 Wind load

The wind loads can be found in clause 4.3 and the wind load on overhead line components and be found by looking at clause 4.4 of FprEN 50341-1:2012 (CENELEC, (2012)). The reference height above ground used in the calculations should be correct for the component being considered.

The basic wind velocity has a return period of 50 years. This value can be given in the NO NNA (CENELEC, (2012)). To get other return periods the conversion factors from the NO NNA which are presented in Table 4.3 should be used.

The mean wind velocity at the reference height is found by Equation 4.1. It is affected by terrain and the height above ground (CENELEC, (2012)).

Table 4.3: Conversion factors for wind, given in Table B.1 of EN 50341-1 (CENELEC, (2012)).

Return period (T)	Conversion factor (g_T/g_{50})
3	0,76
50	1,00
150	1,09
500	1,18

$$V_h = V_{b.0} * c_{dir} * c_o * k_r * ln\left(\frac{h}{z_0}\right) \tag{4.1}$$

Where:

V_h	=	mean wind velocity at reference height
$V_{b.0}$	=	basic wind velocity at reference height
c_{dir}	=	wind directional factor
c_o	=	orography factor
k_r	=	terrain factor from table 4.1 of FprEN 50341-1
h	=	reference height above ground
z_0	=	roughness length from table 4.1 of FprEN 50341-1

From the mean wind velocity, the mean wind pressure can be found using Equation 4.2. The effects of gusts is accounted for by the turbulence intensity, which is found using Equation 4.3. From these two values the peak wind pressure can be found using Equation 4.4 (CENELEC, (2012)).

$$q_h = \frac{1}{2} * \rho * V_h^2 \tag{4.2}$$

$$I_v = \frac{1}{c_o * ln\left(\frac{h}{z_0}\right)} \tag{4.3}$$

$$q_p = (1 + 7 * I_v) * q_h \tag{4.4}$$

Where:

q_h	=	mean wind pressure
ρ	=	air density
V_h	=	mean wind velocity at reference height
I_v	=	turbulence intensity
q_p	=	peak wind pressure

The wind force on any overhead line component can then be found using Equation 4.5 with the correct factors and areas for that component. This is for example used for insulator sets and poles of steel, concrete, wood or composites.

$$Q_{Wx} = q_p * G_x * C_x * A_x \tag{4.5}$$

Where:

Q_{Wx}	=	wind force on component
q_p	=	peak wind pressure at reference height
G_x	=	structural factor for component
C_x	=	drag factor for component
A_x	=	area of component projected onto a plane perpendicular to wind direction

The wind pressure on bare conductors and ground wires results in both transverse (in direction of cross-arm) and longitudinal (perpendicular to cross-arm) forces on the supports (CENELEC, (2012)). For suspension towers where the angle of line direction change, θ, is equal to 0, these are given by Equations 4.6 and 4.7 respectively. The reference height used can be determined by many methods. The most conservative one assumes the height as the mean arithmetic height of the attachment point of the insulator at the support.

$$Q_{Wc\_V} = q_p * G_c * C_c * d * cos^2\phi * \left(\frac{L_1 + L_2}{2}\right) \tag{4.6}$$

$$Q_{Wc\_U} = 0 \tag{4.7}$$

Where:

Q_{Wc}	=	wind force
q_p	=	peak wind pressure at reference height
G_c	=	structural factor for conductor
C_c	=	drag factor for conductor
d	=	diameter of conductor
L_1	=	length of span 1
L_2	=	length of span 2
ϕ	=	angle between wind direction and the longitudinal axis of the cross arm

The wind force on lattice towers can be found using one of two methods. Either dividing the tower into sections or by considering each element individually. The NNA should define which method to use, however the NO NNA does not seem to choose one over the other. Equation 4.5 is then applied using factors relevant to the members of the lattice tower.

The wind load acting on the support calculated is presented in Table 4.4. See calculations in Appendix C. A ruling span of 350 m has been used and the reference heights for each component has been used.

Table 4.4: Calculated wind loads acting on structure

Item	Force (N)
From conductors	3 à 23909
From ground wires	2 à 5240
From insulator sets	269
On steel lattice tower	36539
On steel tubular tower	16403
On FRP tubular tower	22461

4.4 Ice load

Ice on conductors will cause vertical forces on the structures and tension in the conductors. The ice load on conductors, and as far as applicable on guy wires, can be calculated by looking at clause 4.5 of FprEN 50341-1:2012 (CENELEC, (2012)).

FprEN 50341-1 divides atmospheric ice into two main types based on the formation process; precipitation ice and in-cloud ice (CENELEC, (2012). Precipitation ice can be either wet snow or glaze ice and is formed when large drops of water (or wet snow) hit the surface then freeze. This type is usually colourless and tends to twist the conductor so that the drops hit the other side of it and a cylindrical shape around the conductor occurs. In-cloud ice is soft or hard rime and occurs when smaller and nearly frozen droplets hit the conductor, often when clouds pass by (Catchpole and Fife, (2014)). This gives the ice a whiter colour. These two can be difficult to distinguish, particularly in mountainous regions where a combination of the two is often found. An example of ice on a transmission line can be seen in Figure 4.1. The methods for the calculations can be used independently for the two types (CENELEC, (2012)).

Figure 4.1: Ice on transmission line

The influence of the terrain on the ice load shall be taken into account if necessary. Guidance on the effect of topography and the height above terrain can be found in IEC 61774 and ISO 12494 (CENELEC, (2012)).

In places where the atmospheric and climatic conditions are varying along the overhead line, the line shall be divided into zones. This is done to get the most accurate results possible (CENELEC, (2012)).

In many countries, the statistical data for ice is often poor. When that is the case, the ice load must be based on experience (CENELEC, (2012)). For Norway, data for some regions is given in clause 4.2.3.2 of the National Annex (NA) (The Norwegian National Committee, (2008)). The values given in the NA are presented in Table 4.5. For data concerning other regions, a meteorologist should be consulted.

Table 4.5: Design ice loads, given in Table 4.2.3.2/NO.1 of the NA (The Norwegian National Committee, (2008)).

No.	Region	Height above sea level (m)	Design ice load (N/m) 50 year return period
1	Main areas of the South East region*	0 - 200	30
2	Main areas of the South East region*	200 - 400	40
3	Main areas of the South East region	400 - 600	50
4	østfold and Vestfold	0 - 200	20
5	Telemark and Agder	0 - 200	35
6	Telemark and Agder	200 - 400	50
7	The coast Rogaland - Stad	0 - 200	35
8	The fjords Rogaland - Stad	0 - 400	40
9	The coast Stad - Namdalen	0 - 200	40
10	The fjords Stad - Namdalen	0 - 400	40
11	The coast Namdalen - Lofoten	0 - 200	40
12	The inland of Nordland	0 - 200	30
13	The coast Vesterålen - Nordkapp	0 - 100	35
14	The inland Troms - Vest-Finnmark	0 - 200	30
15	The coast of Aust-Finnmark	0 - 100	30
16	The inland of Aust-Finnmark	0 - 200	20

*Except areas mentioned in no 3 and 4.

To get the correct return period for the design loads, the conversion factors presented in Table 4.6 found in the NO NNA, is used.

Table 4.6: Conversion factors for ice, given in Table 4.2.3.2/NO.2 of the NA (The Norwegian National Committee, (2008)).

Return period (T)	Conversion factor (g_T/g_{50})
3	0,35
50	1,00
150	1,25
500	1,50

The vertical force on a support from each sub-conductor due to ice load is found by Equation 4.8 (clause 4.5.2 of FprEN 50341-1:2012 (CENELEC, (2012)). The weight length of the conductor is dependent on the horizontal and vertical length between its attached points, including the effect of sagging due to the ice load.

$$Q_I = I * (L_{w1} + L_{w2}) \tag{4.8}$$

Where:

I	=	ice load per length of the conductor [N/m]
L_{w1} and L_{w2}	=	weight span of two adjacent spans

The calculated ice loads acting on a support is presented in Table 4.7. See calculations in Appendix C. A ruling span of 350 m has been used.

Table 4.7: Calculated ice loads acting on structure

Item	Force (N)
From conductors	3 à 52500
From ground wires	2 à 17500

4.5 Combined wind and ice load

As ice accumulates on the conductors and ground wires, the area on which the wind is applied increases. Wind force on ice covered conductors are determined by the velocity of the wind and the mass and shape of the ice layer. The combined load is based on an ice load with high probability to occur, that is a return period of 3 years, and a wind pressure with low probability to occur, that is a return period of 50, 150 or 500 years (The Norwegian National Committee, (2008)). This supposes that the two actions are independent. Clause 4.6.6.2 of FprEN 50341-1:2012 (CENELEC, (2012)) gives the ice load and wind velocity with the return periods of this combination to be given by Equations 4.9 and 4.10 respectively. FprEN 50431-1:2012 does not consider wind and ice load on lattice towers or steel poles (CENELEC, (2012)).

$$I_3 = \Psi_I * I_{50} \tag{4.9}$$

$$V_{IL} = V_T * B_I \tag{4.10}$$

Where:

I_3	=	nominal ice load with return period of 3 years
Ψ_I	=	combination factor for ice load
I_{50}	=	structural factor for conductor
V_{IL}	=	wind velocity of low probability
V_T	=	wind velocity with given return period
B_I	=	reduction factor for wet snow

The mean wind pressure and peak wind pressure associated with icing is calculated as in Equation 4.2 and 4.4.

$$q_{IL} = \frac{1}{2} * \rho * V_{IL}^2$$

$$q_{Ip} = (1 + 7 * I_v) * q_{IL}$$

The equivalent diameter of the ice-covered conductor is calculated using Equation 4.11.

$$D = \sqrt{d^2 + \frac{4 * I}{9.81 * \pi * \rho_I}} \tag{4.11}$$

Where:

D	=	equivalent diameter of ice-covered conductor
d	=	diameter of bare conductor
I	=	ice load per length
ρ_I	=	ice density

The transverse (in direction of cross-arm) and longitudinal (perpendicular to cross-arm) forces on a suspension towers where the angle of line direction change, θ, is equal to 0, due to wind on ice covered conductors (CENELEC, (2012)) are given by Equations 4.12 and 4.13 respectively. The reference height can be found in the same way as for bare conductors.

$$Q_{WI\_V} = q_{Ip} * G_c * C_{Ic} * D * cos^2\phi * \left(\frac{L_1 + L_2}{2}\right) \tag{4.12}$$

$$Q_{Wc\_U} = 0 \tag{4.13}$$

Where:

Q_{WIc}	=	wind force
q_{Ip}	=	peak wind pressure at reference height
G_c	=	structural factor for conductor
C_{Ic}	=	drag factor for ice-covered conductor
D	=	equivalent diameter of ice-covered conductor
L_1	=	length of span 1
L_2	=	length of span 2
ϕ	=	angle between wind direction and the longitudinal axis of the cross-arm

The combined wind and ice loads acting on a support calculated are presented in Table 4.8. See calculations in Appendix C.3.

Table 4.8: Calculated combined wind and ice loads acting on structure

Item	Force (N)
Vertical from conductors	3 à 14700
Transverse from conductors	3 à 13037
Vertical from ground wires	2 à 4900
Transverse from ground wires	2 à 6627

4.6 Security loads

Security loads take into account torsional or longitudinal stress on a structure. The torsional loads on a structure can be induced when a release of the tension from a cable is experienced, for example due to a line break of a conductor or ground wire (CENELEC, (2012)). The unbalanced tension in the rest of the conductors is not required to be checked (The Norwegian National Committee, (2008)). Longitudinal security loads on the structure are unbalanced overloads due to higher loads on all cables of one of the adjacent spans or a release in tension of all cables of one of the adjacent spans (CENELEC, (2012)). As suspension supports with insulators sets of typical length allow for some swing in the string, the tension forces from these loads are normally low (CENELEC, (2012)).

Both relaxations of the load due to a swing in the insulator sets and deflections or rotations of the support may be taken into account when calculating security loads. It can also be taken as a fraction of the tension force in the conductor (CENELEC, (2012)).

4.7 Safety loads

Tower erection and the stringing and maintenance of cables may cause unbalanced and/or higher loads in a structure. These loads should be checked for as required by the NO NNA (The Norwegian National Committee, (2008)).

- Construction: Lifting points and stressed members shall withstand double (or lower until 1.45 times) of load implied by construction method.

- Stringing and sagging: Structure should withstand double (or lower until 1.45 times) of sagging tension in all conductors being pulled out. Vertical (e.g. high ground), transverse (angle towers and wind) and longitudinal (tension and dead end towers and stringing tension).

- Maintenance: Attachment points shall withstand double (or lower until 1.45 times) of vertical load due to sagging.

- Maintenance: A concentrated load of 1.5 kN should also be applied to all parts of a structure that acts as steps to account for the weight of linemen (The Norwegian National Committee, (2008)).

4.8 Other loads

Short circuits in addition to large swinging of conductors can lead to conductor clashes that can result in permanent circuit isolation in spans close to a substation. The use of interphase spacers can reduce these movements (CENELEC, (2012)). The effect of short-circuit loads should be included if specified in the project (The Norwegian National Committee, (2008)).

If a line is routed through mountainous areas, the possible loads due to avalanches or creeping snow should be accounted for. Both the direct effect of the avalanche and aftereffects due to an excess of powdered snow should be assessed. The additional forces on foundations and lower parts of the towers due to creeping snow should also be considered (CENELEC, (2012)). The NO NNA (The Norwegian National Committee, (2008)) states that this should be done if deemed necessary for each project.

Additional loads due to earthquakes are not considered in Norway (The Norwegian National Committee, (2008)), but may be of great importance in seismically active areas.

4.9 Load cases

To account for all the situations described in the previous chapters, several load cases need to be checked. The load cases consist of one or a combination of temperature, ice load and wind load, as well as stating the desired effect each load case is to induce, thereby how the loads should be applied to the line. For overhead lines where the nominal system voltage is between AC 1 kV and AC 45 kV regulations are specified in the NNAs or for each project, whereas for lines exceeding AC 45 kV regulations are specified in FprEN 50341-1:2012 (CENELEC, (2012)). Based on the general load cases given by FprEN 50341-1:2012 and the NO NNA (The Norwegian National Committee, (2008)), specific load cases are developed by Statnett to check suspension towers. These load cases are presented in Table 4.9. A more thorough description can be found in Table A.1.

As described in the table some load cases are meant to induce longitudinal, transverse or torsional loads. By applying the loads as shown in Figures 4.2a, 4.2b and 4.2c this is acquired.

The design working life of overhead lines is considered to be 50 years, resulting in reliability level 1 (CENELEC, (2012)). The partial and combination factors for combined actions as given in FprEN 50341-1 (CENELEC, (2012)) and the NO NNA (The Norwegian National Committee, (2008)) for reliability level 1 are presented in Table 4.10. These factors should be combined with partial factors for material properties.

Table 4.9: Load cases used in model

No.	Description
0	EDS
1	Full ice load
2	Uneven ice load - Transverse bending towards the right
3	Uneven ice load - Transverse bending towards the left
4	Uneven ice load previous span
5	Uneven ice load next span
6	Uneven ice load previous span - Transverse bending towards the right
7	Uneven ice load previous span - Transverse bending towards the left
8	Uneven ice load next span - Transverse bending towards the right
9	Uneven ice load next span - Transverse bending towards the left
10	Wind on line towards the right
11	Wind on line towards the left
12	Wind on ice loaded line towards the right
13	Wind on ice loaded line towards the left
14	Minimum temperature
15	Line break left phase of next span
16	Line break left phase of previous span
17	Line break middle phase of next span
18	Line break middle phase of previous span
19	Line break right phase of next span
20	Line break right phase of previous span
21	Line break left ground wire of next span
22	Line break left ground wire of previous span
23	Line break right ground wire of next span
24	Line break right ground wire of previous span

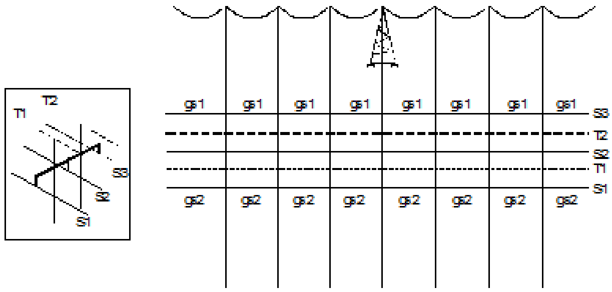

(a) Ice loads leading to transverse bending, Figure 4.2.10/NO1 of the NO NNA (The Norwegian National Committee, (2008))

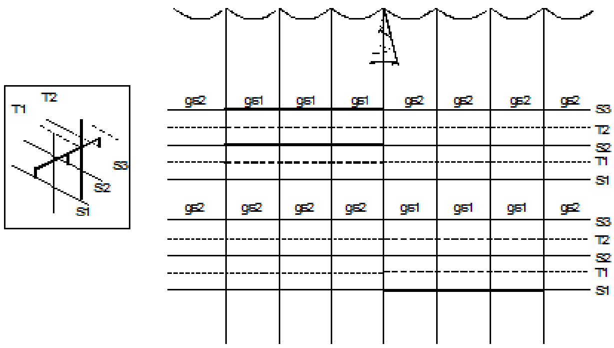

(b) Ice loads leading to longitudinal bending, Figure 4.2.10/NO2 of the NO NNA (The Norwegian National Committee, (2008))

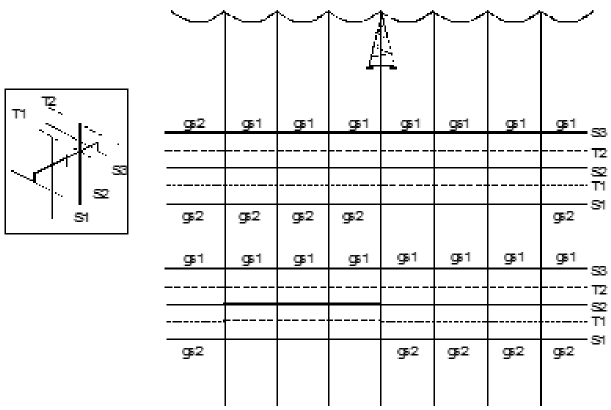

(c) Ice loads leading to torsional bending, Figure 4.2.10/NO3 of the NO NNA (The Norwegian National Committee, (2008))

Figure 4.2: Effect of unbalanced ice loads.

Table 4.10: Partial factors for actions.

Action	Symbol	Value
Extreme wind load	γ_W	1.0
Nominal wind load	Ψ_W	0.25
Extreme ice load	γ_I	1.0
Nominal ice load	Ψ_I	0.35
Self-weight	γ_G	1.0
Torsional loads due to conductor tension	γ_{A1}	1.0
Longitudinal loads due to conductor tension	γ_{A2}	1.0
Construction and maintenance loads	γ_P	2 (or 1.45)

Chapter 5

Modelling

All modelling is done according to FprEN 50341-1 and the NO NNA and by help of the user's manuals for the different programs.

The modelling of the line is done in PLS-CADD. This program enables the user to route and design the line as well as conduct structure checks and tension and sag calculations based on criteria input to account for all loading situations described in Chapter 4 (Power Line Systems Inc_4, (2016).

The steel lattice tower is modelled using PLS-TOWER, while the steel tubular tower and FRP tubular tower are modelled using PLS-POLE.

By connecting the detailed models to PLS-CADD, the calculated loads are applied to the structures and several outputs depicting for example stresses and usage are attained. Optimisation of the structures by reducing or increasing sizes where needed is then easily visualised.

Before modelling, some preliminary calculations were done to find some cross sections to begin with. This is explained further in 6.1.

After the modelling was done, the cross sections were optimised so that their strength was utilised as much as possible.

5.1 Modelling of Line in PLS-CADD

The modelled line can be viewed in three different ways; plan view, profile view and 3D view. Examples of the different views can be seen in Figure 5.1, Figure 5.2 and Figure 5.3. These different views make for easier execution of various actions and good visualisation of the different aspects of the line.

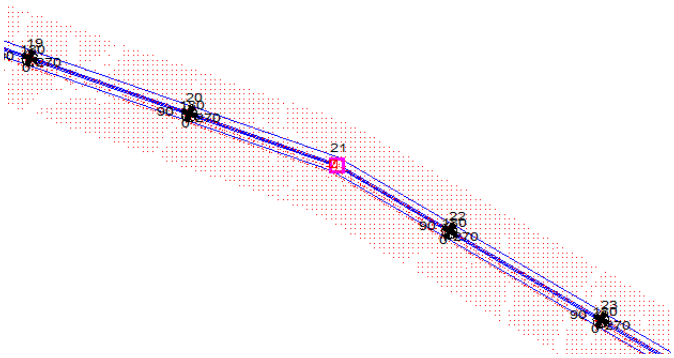

Figure 5.1: Example of a line shown in plan view.

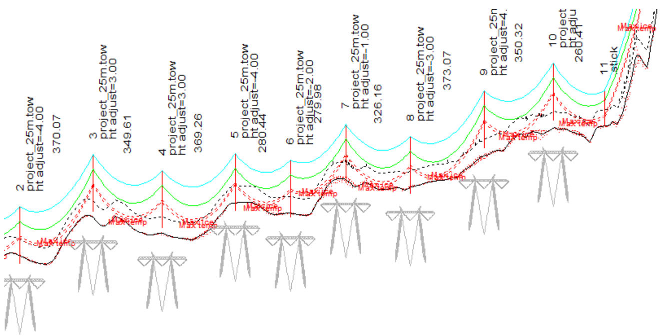

Figure 5.2: Example of a line shown in profile view.

5.1.1 Terrain

PLS-CADD uses a three-dimensional Geographic Information System type terrain model. Terrain data is collected electronically and transformed into

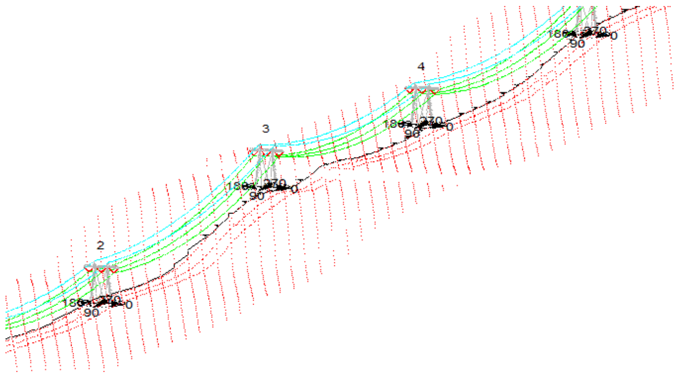

Figure 5.3: Example of a line shown in 3D view.

ASCII terrain files which can be opened in the program. These files contain several terrain or above-terrain points and may also include information about the location. If desired, a TIN (Triangulated Irregular Network) model can be made. This model shows a surface that is created by triangles with the terrain points at their apexes and can be rendered to show contour lines, colour by height or colour by bitmap (Power Line Systems Inc$_4$, (2016). See Figure 5.4. The terrain file used in this thesis was provided by ARA Engineering and includes 35493 points describing the terrain somewhere in Iceland.

When the terrain file has been loaded, the alignment needs to be defined. This is done by adding points of intersection (PI points) that will in the plan view create straight line segments between them. The points will automatically snap to the closest terrain point and thus gain the correct height. By adding several of these stretches one can model angled lines, branches or loops. If desired, multiple alignments can be made in the same model to ensure crossing lines have the required clearances. When the alignment is created, the terrain profile can be observed in the profile view. The profile visible consists of all terrain points within the maximum offset for centreline ground profile, which value can be edited in the *Terrain Widths* menu. Here one can also define the maximum offset for profile view, that should be large enough to incorporate the entire width of the line including offsets (Power Line Systems Inc$_4$, (2016). The maximum offset for profile view is here set to 20.0m while the maximum offset for centreline ground profile is set to 1.0m. A too large value for the last one will result in a jagged line.

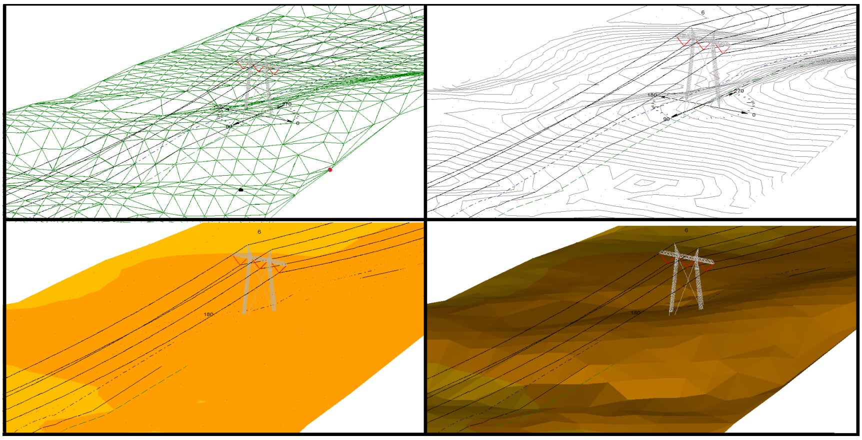

Figure 5.4: Various renderings of a TIN model for the lattice tower line, showing unrendered triangle outlines (upper left corner), contour lines (upper right corner), rendered triangles-coloured by elevation (bottom left corner) and rendered triangles-colour by bitmap). From Figure 6.4-3 of (Power Line Systems Inc$_4$, (2016)

In the terrain file given, it would be natural to create an angled line, as can be seen in the plan view of Figure 5.1. However, as this thesis focuses on suspension towers only one stretch is modelled.

After the line is modelled clearance violations between the wires and the ground can be identified by PLS-CADD automatically if the required vertical and horizontal clearances are input in the *Feature Code Data Edit* table for the voltages used. Depending on the input PLS-CADD will check either a rectangular or radial zone around each terrain point (Power Line Systems Inc$_4$, (2016). The required vertical and horizontal clearances for this 420kV line is set to 8.3m and 3.0m respectively.

Terrain points on the sides of the ground centreline may have a higher altitude. To ensure the side wires are not violating the clearance requirements, side profiles can be added in the *Side Profiles* table. An offset from the centreline, an offset tolerance (as for the ground centreline) and a distance of max separation tell PLS-CADD which terrain points to include. The side profile is shown as a dotted line either above or below the centreline profile (Power Line Systems Inc$_4$, (2016). This model has three phases, and thus two side profiles with offsets of -9.0m and 9.0m are used in this model.

They both have an offset tolerance set to 1.0m and a max separation set to 90.0m. Figure 5.5 illustrates the side profiles at one point along the line, represented by the dark blue and dark green dotted lines. Here the side profiles show considerable sloping ground and on one side the side profile represent higher ground and will be limiting.

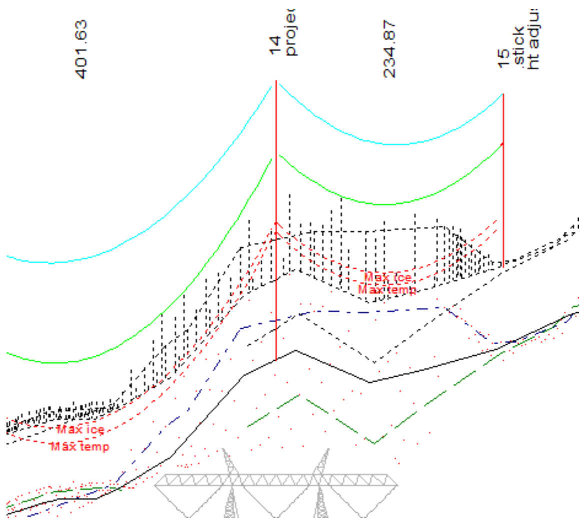

Figure 5.5: Examples of side profiles, ground clearance lines and wire clearance lines

Wire clearance lines are added in the *Clearance Lines* menu to visualise the actual positions of the wires under selected weather cases (see 5.1.3). In addition to choice of weather case, the clearance line type, wire condition and vertical shift (clearance) can be specified. The user can also choose to display the line for some wires or voltages only (Power Line Systems Inc$_4$, (2016). The value for vertical shift can be found in the standard or specified in the NNA. According to Table 5.4.4/NO of the NNA for Norway (The Norwegian National Committee, (2008) clearance for maximum temperature and full ice load should for a class B protection system and normal ground profile be 8.3 m and 7.3 m respectively. See Equations 5.1 and 5.2 for calculations. The electrical clearance requirement should be confirmed by an electrical engineer. The clearance lines for these two weather cases; maximum temperature and full ice load, are illustrated as the two red dotted lines below the green wires in Figure 5.5.

$$c_{max.temp} = 5.5m + D_{el} = 5.5m + 2.8m = 8.3m \tag{5.1}$$

$$c_{ice} = 4.0m + D_{el} + h_{snow} = 4.0m + 2.8m + 0.5 = 7.3m \tag{5.2}$$

Where:

$D_{el} = 2.8m$	=	Required electrical clearance
$h_{snow} = 0.5m$	=	Height of snow

The wire clearance lines have to be updated manually every time a change is made. Therefore, to make visualisation easier without having to update them, ground clearance lines can also be added in the *Clearance Line* table. They will be displayed as dotted lines and dotted spikes shifted a certain height above the centre profile and side profiles. The spikes represent terrain points outside the offsets of the three profile lines, but still within the maximum offset for terrain profile that require a larger clearance (Power Line Systems Inc$_4$, (2016). This can be a very helpful tool as the clearance lines has to be updated manually every time a change is made. This is illustrated in Figure 5.5, where the ground clearance line is shifted 8.3m up from the ground centreline profile and side profile lines. 8.3m is chosen because this is the highest required clearance. In this figure one can clearly see the spikes.

5.1.2 Basis for Criteria

PLS-CADD has implemented a range of international design techniques for overhead power lines, and has built-in design checks that are general enough to apply to many of them (Power Line Systems Inc$_4$, (2016). The CENELEC EN 50341-1 (CENELEC, (2012) mostly used in this thesis is one of them. Design criteria input gives PLS-CADD a basis to implement these standards.

The first thing to decide is what modelling level to be used. There are four levels, differing in complexity. Level 1 is the simplest one and is based on the ruling span method. This level should be used in preliminary design. Level 2 is based on the real span method and uses finite element modelling. Level 3 takes into account the interaction between the wires. Level 4 is the most complex one and gives a full structural analysis of the tension section (from one dead end support to the next). This is time intensive and is only used in special situations. When using level 1, 2 or 3, complex calculations are done by PLS-CADD (Power Line Systems Inc_4, (2016). Multi-guyed steel supports should according to EN 50341-1 be analysed using the finite element method (CENELEC, (2012). Thus level 2 is used in this thesis.

Wind and ice loads are the most important design loads when working with overhead power lines. Different standards have different ways of distributing and calculating the loads. In the user's manual (Power Line Systems Inc_4, (2016) many of these are described.

The wind pressures reported by PLS-CADD are at the reference height, usually 10m. PLS-TOWER and PLS-POLE will then increase the pressure above this height.

PLS-CADD uses Equation 5.3 (formula 7-3 from (Power Line Systems Inc_4, (2016)) to calculate the wind load per unit length of wire.

$$UH = WLF * Q * W_z^2 * GRF_c * CD_c * \cos^2(W_a) * (D + 2 * t_z) \quad (5.3)$$

Where:

WLF	=	Weather load factor
Q	=	Air density factor
W_z	=	Wind velocity at height z
GRF_c	=	Gust response factor for wire
CD_c	=	Drag coefficient factor
WA	=	Incidence angle between the wind direction and perpendicular to the span
D	=	Diameter of wire
t_z	=	Ice thickness at height z

The design wind force on a structure located at height z is calculated using Equation 5.4 (formula 7-4 from (Power Line Systems Inc_4, (2016)).

$$WF = LFW * WLF * Q * W_z^2 * GRF_s * CD_s * A \tag{5.4}$$

Where:

LFW	=	Load factor for wind
WLF	=	Weather load factor
Q	=	Air density factor
W_z	=	Wind velocity at height z
GRF_s	=	Gust response factor for structure
CD_s	=	Drag coefficient factor for structure
A	=	Exposed area of part of structure

Some of these parameters are included in the program, some need to be chosen and others again can be added in PLS-TOWER or PLS-POLE. This varies for the different standards (Power Line Systems Inc$_4$, (2016).

The vertical ice load per unit length is calculated using Equation 5.5 (formula 7-6 from (Power Line Systems Inc$_4$, (2016)).

$$UI = WLF * \pi * (D + t_z) * t_z * DENS + W_{ICE} \tag{5.5}$$

Where:

WLF	=	Weather load factor
D	=	Cable diameter
t_z	=	Ice thickness at height z
$DENS$	=	Ice density
W_{ICE}	=	Ice load per unit length

Where the ice thickness is to be increased with height, PLS-CADD does it automatically.

Some standards require ice on structures to be calculated. If this is the case, PLS-TOWER and PLS-POLE will do this automatically for the specified ice thickness and ice density input in the *Structure Loads Criteria* table.

5.1.3 Detailed Criteria

CENELEC EN 50341-1 (CENELEC, (2012) and the NNA for Norway (The Norwegian National Committee, (2008) give guidance on what conditions to use for the different weather cases. The directives laid down by Statnett Norway are also taken into account, due to the line being located in Norway where Statnett is responsible for most of the overhead power line system. Here follows a brief description of the criteria input used in this thesis. The complete input can be found in Appendix II.

The level of modelling as described in the Basis for Criteria is input in the *SAPS Finite Element Sag-Tension* menu. As previously stated L2 is used, which means the sections have no interaction (Power Line Systems Inc_4, (2016).

All calculations done in PLS-CADD, whether it be for checking the strength of structures, tensions in the wires or geometric clearances, are based on a combination of wind, ice and temperature conditions, and their probability. These are called weather cases and can be specified in the *Weather Cases* table. The weather cases used by Statnett, and in this thesis are listed below. A complete description of the input for the weather cases can be found in Figure D.4 of the appendix.

- EDS: Everyday stress, should not be affected by ice or wind load.
- Assembly: Should not be affected by ice load or wind load (CENELEC, (2012).
- Full ice load: Full ice load, no wind load.
- 100% ice load: Full ice load, no wind load.
- 70% ice load: Reduced wire ice load by a factor of 0,7, no wind load.
- 30 % ice load: Reduced wire ice load by a factor of 0,3, no wind load.
- Uneven ice load: No wind load, only ice load. Will be edited to account for uneven loading.
- Uneven ice load previous span: No wind load, only ice load. Will be edited to account for uneven loading.
- Uneven ice load next span: No wind load, only ice load. Will be edited to account for uneven loading.
- Temperature: Temperature is set to 80°C. Will induce larger sag.
- Minimum temperature: Temperature is set to -20°C. Will induce less sag.
- Wind 500 year: Only wind load. Conversion factor based on the return period.

- Wind on ice: Both wind and ice load. Conversion factor and a combination factor.
- Wind 50 year: Only wind load. Conversion factor based on the return period.
- Wind on ice 50 year: Both wind and ice load. Conversion factor and a combination factor.
- Wind 3 year: Only wind load. Conversion factor based on the return period.

A wire temperature of 0°C is used for most of the weather cases. By inputting an air density and a wind velocity, the program automatically calculates the wind pressure by Equation 5.6. One can also input the wind pressure and get the wind velocity (Power Line Systems Inc$_4$, (2016).

$$P = Q * W^2 \tag{5.6}$$

Where:

W	=	Wind velocity
P	=	Wind pressure at the reference height
Q	=	air density factor

A 50 year return period is used as a basis for wind load calculations. To get values for the other return periods, conversion factors are given in Table 4.3. The air density factor is calculated as in Equation 5.7.

The 150 year return period is used as a basis for calculations with ice loads. The conversion factors used to get values for the other return periods are given in Table 4.6. The wire ice density is given by Equation 5.8.

$$Q = \rho * 0,5 * \frac{g}{10} = 1.25kg/m^3 * 0.5 * \frac{9.81m/s^2}{10} = 0.613kg/m^3 \quad (5.7)$$

$$Q_I = \rho_I * g = 600kg/m^3 * 9.81m/s^2 = 5886N/m^3 \quad (5.8)$$

Where:

Q	=	Air density factor
$\rho = 1.25kg/m^3$	=	Air density used in Norway (The Norwegian National Committee, (2008)
$g = 9.81m/s^2$	=	Gravitational acceleration
Q_I	=	Wire Ice density
$\rho_I = 600kg/m^3$	=	Ice density for wet snow used in Norway (The Norwegian National Committee, (2008)

PLS-CADD calculates the wind effects based on what standard is chosen. By choosing the STATNETT model, the wind velocity/pressure and wire ice load is to contain only the conversion factors and combination factors. The value of the design wind velocity and design wire ice load is then taken into account by input as a Structure comment in the *Staking Table* under *Structures* and then applied in *Code Specific Wind and Terrain Parameters/Span Specific Wind and Ice Adjustments*. This method allows for user input adjustments on a span by span or structure by structure basis. The values given by ARA Engineering are presented in Table 5.1.

Table 5.1: Design values given by ARA Engineering.

Load	Value
Design wire ice load	50 N/m
Design wind load, normal component	35 m/s
Design wind load, max wind gust	38 m/s

For the three ”uneven ice load” weather cases, a load train is to be applied. This is input under *Code Specific Wind and Terrain Parameters/ Statnett Norway*. The load train will induce an uneven loading in the line. The number of spans in the train is set to three, the ice load factor inside the train is set to 0.7 and the ice load factor outside the train is set to 0.3. PLS-CADD will then perform calculations for each possible position of the load train, either obtaining the largest sag or the largest longitudinal load on the structure depending on the load train type chosen. For the weather case

”uneven ice load” the type ”max sag load train” is used, and for weather cases ”uneven ice load previous span” and ”uneven ice load next span” the ”structure loads load train” type is used with ”max positive longitudinal load” and ”max negative longitudinal load” respectively.

PLS-CADD calculates the tension and sag of a cable for three conditions; initial, final after creep and final after load. The final after creep condition originates in everyday stress in the cable over long time, thus inducing creep. Short exposure to extreme load may lead to permanent stretches of the cable, thus the final after load condition is used. The weather cases used for these two conditions are specified in the *Weather Cases for Permanent Stretch Due to Creep and Load* table (Power Line Systems Inc$_4$, (2016). For final after creep the EDS weather case is used, and for the final after load the full ice load weather case is used.

PLS-CADD also offers a choice for the aluminium outer part of the cable, whether it can take compression at high temperature or not. Due to aluminium having a higher thermal expansion factor than steel it will at some temperature no longer be under tension. This choice can be made in the *Bimetallic Conductor Model* menu (Power Line Systems Inc$_4$, (2016). In this thesis it is chosen to not have aluminium take compression.

Design limits for the ground wires and conductors are specified in the *Cable Tensions* table for different weather cases. In addition to weather case, the cable condition and a maximum tension either as a percentage or as a max value for tension or catenary has to be input. It is also possible to choose which wires to apply these limits to (Power Line Systems Inc$_4$, (2016). In this thesis the limits for all cables are set to 80% of ultimate tension for all weather cases chosen. The actual geometry of the wires are used to calculate the maximum tension. Another option is to calculate the maximum tension of the ruling span with equal and elevations. This is chosen in the *Maximum Tension Criteria* table (Power Line Systems Inc$_4$, (2016).

There are four ways PLS-CADD checks the strength of structures, see 5.1.4. Method 1 is defined in the *Weight Span Model* and *Weight Span Criteria (Method 1)* menus. The interaction diagrams for method 2 can be edited in the *Interaction Diagram Criteria (Method 2)* table. Methods 3 and 4 are based on load cases defined in the *Structure Loads (Method 3,4)* table. Method 4 structures are used in this thesis. To define the structure load cases, input is needed for weather case, cable condition, wind direction (only relevant for wind cases), load factors for different parts of the structures and how the load is applied to the different conductors and ground wires. This will induce either transverse loads, longitudinal loads, torsional loads or a combination of these (Power Line Systems Inc$_4$, (2016). The load cases are presented in Table 4.9 and the complete input in Figures D.9, D.10 and D.11 in Appendix D.1.

In Norway it is normal to use a material factor for steel of 1.1, a partial strength factor on ultimate strength for guys of 1.6 and a strength factor for insulators of 2. However, some of these factors may be taken into account in the PLS-TOWER and PLS-POLE models instead as has been done for steel in the lattice tower model and for the guys in all models. As this thesis focuses on suspension towers, the ”No DE (dead end)” structure group is chosen. The first load case specified will automatically be checked for the safety load caused by the weight of linesmen. By adding a load to the first load case specified, the PLS-programs automatically check relevant members for the safety load caused by the weight of linesmen.

PLS-CADD can check clearance violations for the clearances specified in 5.1.1. To do this, some more criteria needs to be input. Weather cases and cable conditions to check for must be specified in the *Survey Point Clearance Criteria* menu. PLS-CADD can then use this for survey point clearances, danger tree locator, isoclearance lines and clearance to TIN options, see 5.1.6. The case inducing the largest sag will also be used for optimum spotting clearance checks. Any clearance violations found will be reported and displayed graphically (Power Line Systems Inc$_4$, (2016), see Figure 5.6. Clearances between sets of phases, for example with crossing spans, can also be calculated where applicable. The criteria for this is input in the *Phase Clearance Criteria* table, where weather cases and cable conditions needs to be specified. This is not applicable in our case.

Choice of weather cases and cable conditions are also the input needed for PLS-CADD to calculate lateral swings or load inclinations for 2-part insulators. Maximum and minimum allowable swing or load angles for the specified conditions should be given in the structure file (Power Line

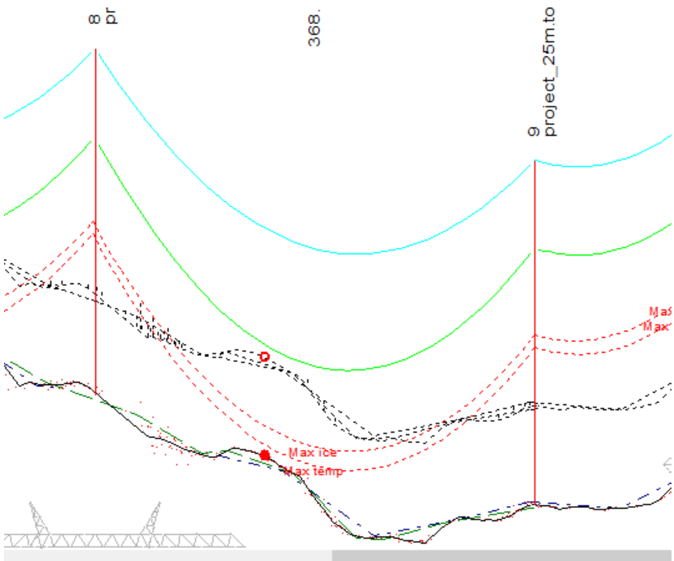

Figure 5.6: Clearance violations from PLS-CADD.

Systems Inc4, (2016). The input is done in the *Insulator Swing Criteria* table.

PLS-CADD is able to draw single and double loop galloping ellipses for the conductors according to one of the built-in guidelines, and check if the ellipses cross each other. The criteria needed for these calculations can be input in the *Galloping Ellipse Criteria* menu.

In the *Default Wire Temperature and Condition, Section Sort Order* default criteria used when stringing new sections are defined. Conditions for structure attachment coordinates and section numbering are also defined here (Power Line Systems Inc4, (2016).

5.1.4 Basis for Calculating Structure Strength

PLS-CADD can check structure strength by one of four methods. For method 1, 2, and 3 one has to describe the positions of structure attachment points in a local coordinate system and define geometric properties of the attachments, such as insulators. Method 4 structures that are created in either PLS-TOWER or PLS-POLE has this data automatically included in their structure files. The level of modelling will also influence the calculations. For level 1 the ruling span is used and the horizontal tension component is assumed constant for all spans in one tension section (between two dead end towers), whereas for level 2, 3 and 4 the finite element method is used so that each span can have different horizontal tension (Power Line Systems Inc$_4$, (2016).

Method 1 for checking structure strength is based on actual and allowable wind and weight spans. The actual wind span, or horizontal span, at a structure is the average length of the cables on either side of the structure. The actual weight span, or vertical span, is the vertical distance between the lowest points of the two adjacent spans. It is important to remember that the geometry of the cable can make the lowest point appear outside of the span in question. As the geometry of the cables varies with what load cases are applied, the weight span is calculated for three specified weather cases and cable conditions. Different cases are used to take into account the fact that weight spans for conductors with ice are shorter than without ice and thus need other allowed values. Common cases to check for include extreme wind, extreme cold and extreme ice. For each of these cases allowable weight spans are calculated, in addition to the wind span and minimum weight span so that no strength or serviceability violations occur for a range of line angles. Figure 5.7 illustrates this. If the calculated values fall inside the marked areas, the strength of the structure is sufficient (Power Line Systems Inc$_4$, (2016).

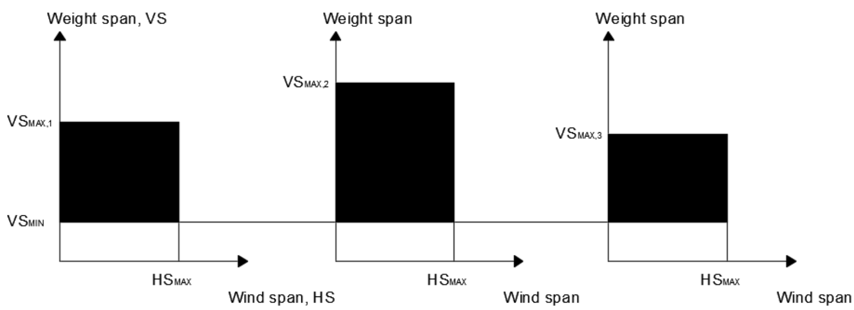

Figure 5.7: Method 1. Figure 8.3-1 of (Power Line Systems Inc$_4$, (2016))

With method 2 interaction between separate spans are taken into account.

This is done by creating interaction diagrams between allowable wind and weight spans for several weather cases and cable conditions. The curve 1-9 in Figure 5.8 shows an example of such an interaction diagram for a specified load case and line angle. If the calculated wind and weight span combination falls inside the interaction curve, the strength of the structure is sufficient. PLS-TOWER and PLS-POLE can establish these interaction diagrams for the structures automatically (Power Line Systems Inc$_4$, (2016).

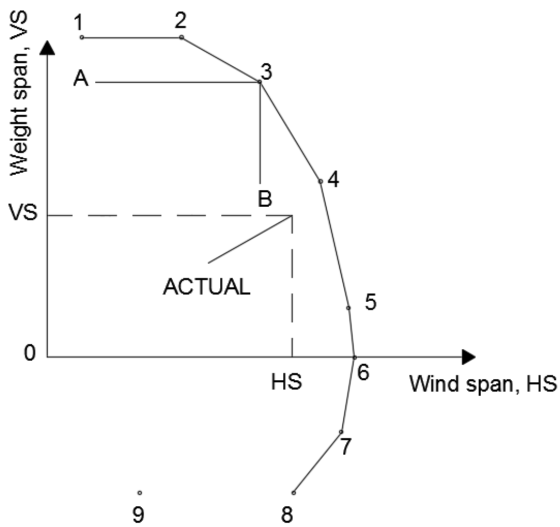

Figure 5.8: Method 2. Figure 8.3-2 of (Power Line Systems Inc$_4$, (2016))

Method 3 structures are checked by unit loads at the structure attachment points. These loads are obtained by looking at forces and moments in critical components and relating them by a matrix of influence coefficients. This requires manual input of these components' design strength. It was previously used where method 4 required too much time and memory, but due to technological progress it is no longer recommended to use.

By using method 4, PLS-CADD checks the strength of the structures through PLS-TOWER and PLS-POLE. Structure loads describing actual events, such as line breakage and uneven loading and, are defined based on weather cases, cable conditions and a range of other factors, see 5.1.3. PLS-CADD will then generate loading trees as those in Figure 5.9, that are sent to the structural program used. The loading trees can be determined at the point where the cable is connected to the insulator or where the insulator is connected to the structure (as in the figure), and includes components in the vertical, transverse and longitudinal directions as well as transverse and longitudinal pressure on the structure. Depending on which of these is being used the weight of the insulators and wind on them is either added afterwards or included in the load tree. PLS-TOWER and PLS-POLE will then analyse the structure and return reports and graphical summaries to PLS-CADD (Power Line Systems Inc_4, (2016).

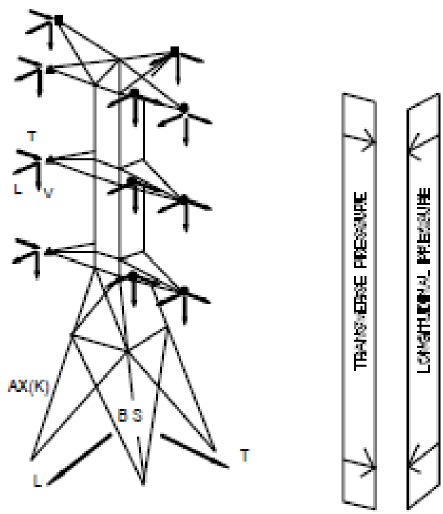

Figure 5.9: Loading trees and pressure on tower, method 4. Figure 8.3-4 of (Power Line Systems Inc_4, (2016))

5.1.5 Basis for Calculating Tension and Sag in Cables

PLS-CADD can calculate sags and tensions of cables according to three different mechanical models. One used in most European countries, where the cables are assumed to be elastic and creep is taken into account by an equivalent increase in temperature, the North American method, where the cables are assumed to be nonlinear, and a third method, where creep is accounted for by a shift in temperature at a certain tension (Power Line Systems Inc_4, (2016). As mentioned in 5.1.3 PLS-CADD calculates sag and tension for three different states: initial, final after creep and final after load.

Initial Behaviour

The difference between the elastic and nonlinear models for the initial behaviour of cables is presented in Figure 5.10 depicting the stress-strain relationship. The elastic behaviour is shown by line O-A where the modulus of elasticity, E, or final modulus of elasticity, EF, describes the slope. Loading and unloading will lead to movement along this line, and the elongation is only temporary. Most cables will behave in an nonlinear way, as shown by line O-I, where a tensile stress, σ_1, leads to elongation, point ε_1, and unloading causes the stress-strain curve to follow a straight line with the slope EF, to point P_1 which gives the permanent elongation. Increasing the stress further will lead to linear behaviour up to point 1 before the stress-strain curve again follows the nonlinear curve to point 2. Unloading will then again cause movement along a line with the slope EF, and result in permanent elongation as seen in point P_2.

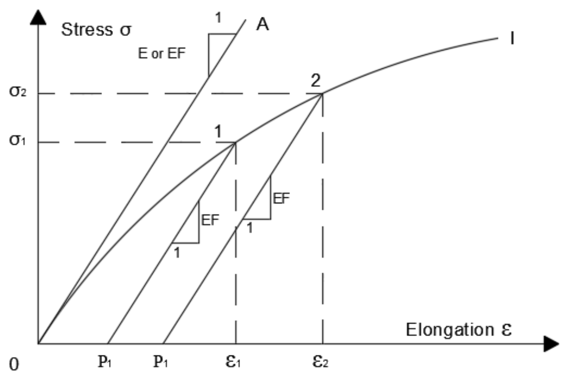

Figure 5.10: Elastic and nonlinear initial behaviour of cables. Figure 9.1-1 of (Power Line Systems Inc$_4$, (2016))

The stress-elongation relationship of a nonlinear cable, curve O-I of Figure 5.10, is in PLS-CADD described by a fourth degree polynomial as shown in Equation 5.9 (formula 9-1 from (Power Line Systems Inc$_4$, (2016)) (Power Line Systems Inc$_4$, (2016).

$$\sigma = k_0 + k_1 * \varepsilon + k_2 * \varepsilon^2 + k_3 * \varepsilon^3 + k_4 * \varepsilon^4 \tag{5.9}$$

Where:

σ	=	tensile stress in cable
$k_{0,1,2,3,4}$	=	coefficients found by curve fitting of experimental data
ε	=	elongation expressed in percent of the cable reference unstressed length

By setting k_0, k_2, k_3 and k_4 equal to zero and k_1 equal to E, Equation 5.9 can be used for a linear elastic cable as well (Power Line Systems Inc$_4$, (2016).

When using composite cables, such as ACSR- (used in this thesis), ACAR- or SSAC-conductors, the stress-strain curve is obtained by combining the two materials' stress-strain curves. This is illustrated in Figure 5.11. Equation 5.10 (formula 9-2 from (Power Line Systems Inc$_4$, (2016)) shows how to combine the two curves. The stresses in the outer and core materials can be found using Equation 5.9, where the coefficients model the stress adjusted by the ratio of that material's area to the total cable area as in Equation 5.11 and 5.12 (Power Line Systems Inc$_4$, (2016).

$$\sigma = \sigma_O * (\frac{AR_O}{AT}) + \sigma_C * (\frac{AR_C}{AT}) \tag{5.10}$$

$$\sigma_O * (\frac{AR_O}{AT}) = a_0 + a_1 * \varepsilon + a_2 * \varepsilon^2 + a_3 * \varepsilon^3 + a_4 * \varepsilon^4 \tag{5.11}$$

$$\sigma_C * (\frac{AR_C}{AT}) = b_0 + b_1 * \varepsilon + b_2 * \varepsilon^2 + b_3 * \varepsilon^3 + b_4 * \varepsilon^4 \tag{5.12}$$

Where:

σ	=	combined tensile stress in cable
σ_O	=	stress in outer material
σ_C	=	stress in core material
AR_O	=	area of outer material
AR_C	=	area of core material
AT	=	$AR_O + AR_C$ (total cable area)
$a_{0,1,2,3,4}$	=	coefficients for outer material adjusted accordingly
$b_{0,1,2,3,4}$	=	coefficients for core material adjusted accordingly

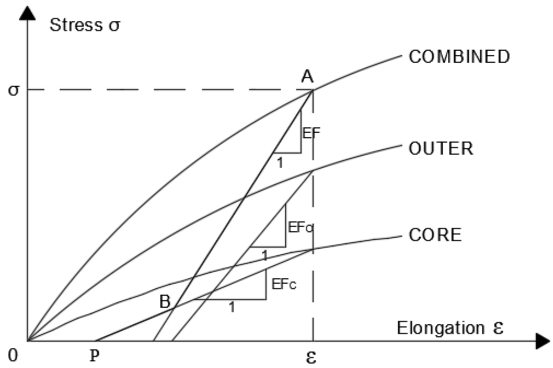

Figure 5.11: Behaviour of composite cable. Figure 9.1-2 of (Power Line Systems Inc_4, (2016))

As the composite cable is loaded it will follow the combined curve to point A with an elongation of ε. Unloading the cable will due to superposition of each material's path lead to movement first to point B and then to point P. As for the stress in Equations 5.11 and 5.12, the slopes of the unloading paths for the different materials need to be adjusted by the ratio of that material's area to the total cable area (Power Line Systems Inc_4, (2016). See Equation 5.13 (formula 9-3 from (Power Line Systems Inc_4, (2016)) and 5.14 (formula 9-4 from (Power Line Systems Inc_4, (2016)).

$$EF_O = \left(\frac{AR_O}{AT}\right) * E_O \tag{5.13}$$

$$EF_C = \left(\frac{AR_O}{AT}\right) * E_C \tag{5.14}$$

Where:

EF_O	=	slope of unloading paths for outer material
EF_C	=	slope of unloading paths for core material
E_O	=	final modulus of elasticity for outer material
E_C	=	final modulus of elasticity for core material

Creep behaviour

The estimate of creep elongation for transmission lines is very uncertain as steel creeps little while aluminium creeps considerably more and due to the fact that creep is significantly higher the first days after the cables are strung than the rest of their life span (Power Line Systems Inc$_4$, (2016).

The different mechanical models include the effect of creep in different ways.

Figure 5.12 illustrates the behaviour for nonlinear cables affected by creep. The curve O-I is the same as in Figure 5.10. Curve O-C represent the long term creep curve, where the relationship between constant stress and expected elongation is shown. Thus by keeping constant tensile stress at σ_C over a period of time, the state of the cable has moved from point 1 to point 2 due to creep elongation. The final elongation is then ε_C. The unloading curve is the same as in Figure 5.10, with a slope of EF. Thus, if a stress of σ_3 is applied, a permanent stretch represented by P_C will have been obtained if the cable is unloaded. If the cable is loaded again after creeping to the state of point 2 and then loaded again, the cable will follow path P_C-2-3-I (Power Line Systems Inc$_4$, (2016).

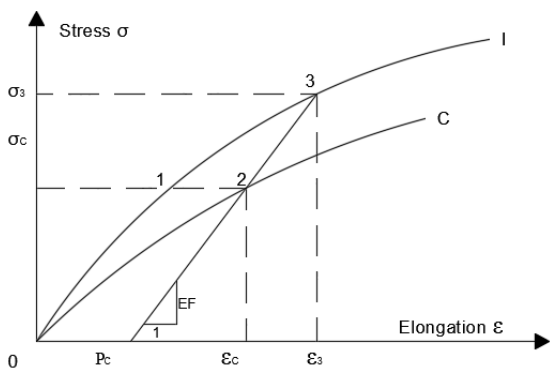

Figure 5.12: Behaviour of nonlinear cables after creep. Figure 9.1-3 of (Power Line Systems Inc$_4$, (2016))

PLS-CADD uses the weather case specified for ”Final after creep” cable condition, see 5.1.3, to calculate σ_C for the cable which then gives a value for the permanent creep elongation, P_C, for that stress according to the O-C curve. Similar to the initial curve O-I, the creep curve O-C can be described by a fourth degree polynomial as in Equation 5.15 (Power Line Systems Inc$_4$, (2016).

$$\sigma = c_0 + c_1 * \varepsilon + c_2 * \varepsilon^2 + c_3 * \varepsilon^3 + c_4 * \varepsilon^4 \tag{5.15}$$

Where:

$c_{0,1,2,3,4}$	=	coefficients for creep

In the case of a composite cable the combined curve is found by using Equations 5.16, 5.17 and 5.18. If the outer material does not creep, the d-coefficients in Equation 5.17 are equal to the a-coefficients in Equation 5.11. The same is the case if the core material does not creep, where the e-coefficients in Equation 5.18 are equal to the b-coefficients in Equation 5.12 (Power Line Systems Inc$_4$, (2016).

$$\sigma = \sigma_O * \left(\frac{AR_O}{AT}\right) + \sigma_C * \left(\frac{AR_C}{AT}\right) \tag{5.16}$$

$$\sigma_O * \left(\frac{AR_O}{AT}\right) = d_0 + d_1 * \varepsilon + d_2 * \varepsilon^2 + d_3 * \varepsilon^3 + d_4 * \varepsilon^4 \tag{5.17}$$

$$\sigma_C * \left(\frac{AR_C}{AT}\right) = e_0 + e_1 * \varepsilon + e_2 * \varepsilon^2 + e_3 * \varepsilon^3 + e_4 * \varepsilon^4 \tag{5.18}$$

Where:

$d_{0,1,2,3,4}$	=	coefficients for creep in outer material adjusted accordingly
$e_{0,1,2,3,4}$	=	coefficients for creep in core material adjusted accordingly

To account for the elongation due to creep when using the elastic model and assuming the material is homogeneous, two different methods are used. In the first one the elongation due to creep is assumed equal to the elongation due to a temperature rise, see Figure 5.13. This temperature is called the ”creep compensation temperature”. By assuming homogeneous elastic behaviour and creep elongation due to a temperature rise the stresses for initial and after creep conditions are given by Equation 5.19 and 5.20. This method can be used by PLS-CADD by choosing *Linear elastic with permanent stretch due to creep specified as a user input temperature increase* in the cable data file (Power Line Systems Inc_4, (2016).

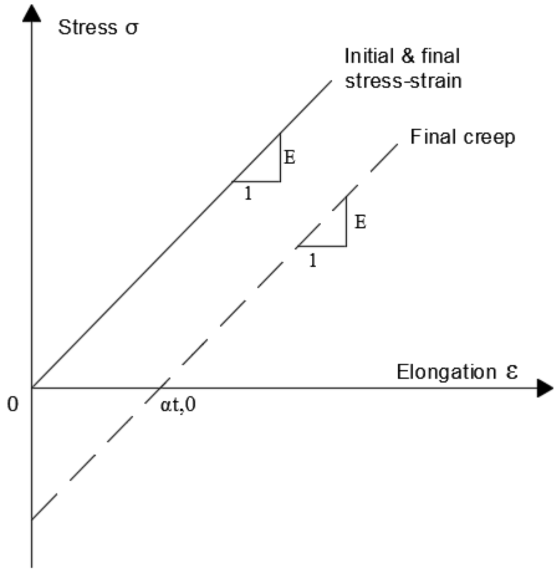

Figure 5.13: Elastic cable with creep due to temperature rise. Figure 9.1-3a of (Power Line Systems Inc_4, (2016))

$$\sigma = E * \varepsilon \tag{5.19}$$

$$\sigma = -E * P_C + E * \varepsilon = -E * \alpha t + E * \varepsilon \tag{5.20}$$

Where:

E	=	elastic modulus
ε	=	elongation expressed in percent of the cable reference unstressed length
P_C	=	creep elongation due to temperature rise
α	=	thermal expansion coefficient for cable
t	=	temperature shift used to model long term creep

The second method assumes that the creep varies proportionally with tension as illustrated in Figure 5.14. Thus the initial stress is still calculated by Equation 5.19, while after creep the stress can be calculated by Equation 5.21. This method can be used by PLS-CADD by choosing *Linear elastic with permanent stretch due to creep proportional to tension* in the cable data file (Power Line Systems Inc_4, (2016).

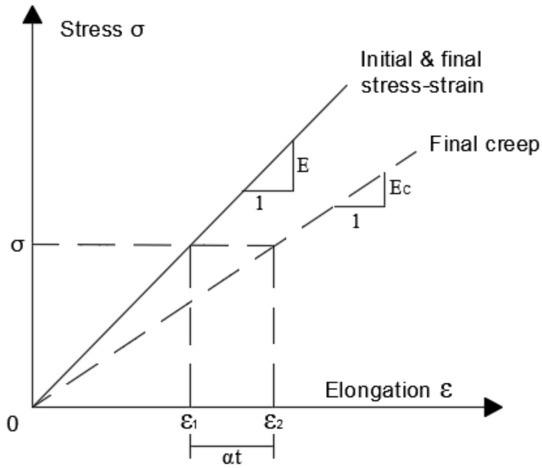

Figure 5.14: Elastic cable with creep proportional to tension. Figure 9.1-3b of (Power Line Systems Inc$_4$, (2016))

$$\sigma = \frac{\varepsilon}{\left(\dfrac{1}{E} + \dfrac{\alpha t}{\sigma_1}\right)} \tag{5.21}$$

Where:

E	=	elastic modulus
ε	=	elongation expressed in percent of the cable reference unstressed length
P_C	=	creep elongation due to temperature rise
α	=	thermal expansion coefficient for cable
t	=	temperature shift used to model long term creep
σ_1	=	stress at which temperature shift t applies

Heavy Loading

Figure 5.15 illustrates how the cable behaves after being subject to a severe load. The high stress $\sigma_C P$ induced by the high load leads to an elongation of $\varepsilon_C P$ that after unloading results in a permanent stretch of $P_C P$. Curve $P_C P$-CP-I describes the behaviour if the cable is loaded again. PLS-CADD calculates $\sigma_C P$ based on the weather case specified for the "Final after loading" cable condition, see 5.1.3 (Power Line Systems Inc$_4$, (2016).

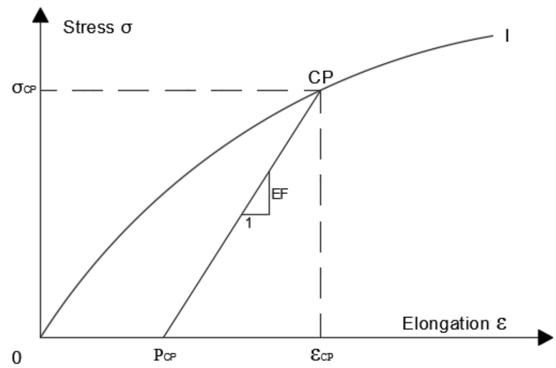

Figure 5.15: Behaviour of cables after heavy loading. Figure 9.1-4 of (Power Line Systems Inc$_4$, (2016))

Thus the final sag in the cable will be calculated as the largest of the three cable conditions. Due to the permanent stretch after loading and creep, this will be either $P_C P$ in Figure 5.15 or P_C in Figure 5.12 as they are larger or equal to the elongation for the initial condition (Power Line Systems Inc$_4$, (2016).

Temperature Effects on Sag

When the cable temperature changes from the reference value to a new value, be it lower or higher, the elongation of the cable or each cable material is also changed. This effect is illustrated in Figure 5.16 where the stress-strain curve and elongation value is shifted right due to an increase in temperature. The shift is equal to the value $ET_{MAT}()$ The change in unit elongation is given by Equation 5.22 (Power Line Systems Inc$_4$, (2016).

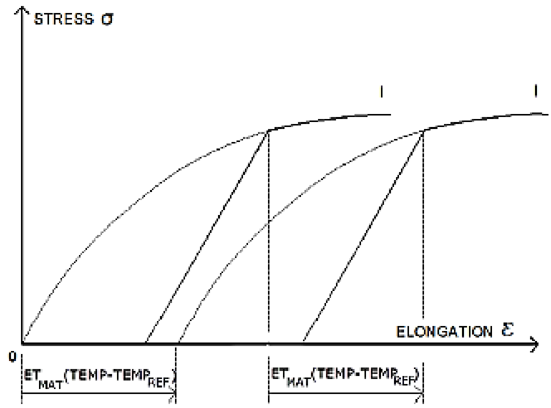

Figure 5.16: Effect of change in temperature. Figure 9.1-5 of (Power Line Systems Inc$_4$, (2016))

$$\left(\frac{\Delta L}{L_{REF}}\right)_{MAT} = ET_{MAT}(TEMP - TEMP_{REF}) \tag{5.22}$$

Where:

ΔL	=	change in length
L_{REF}	=	unstressed cable reference length
ET_{MAT}	=	thermal expansion coefficient of material MAT
$TEMP$	=	new temperature
$TEMP_{REF}$	=	reference temperature

5.1.6 Reports

In the *Lines* menu, PLS-CADD offers a range of checks and reports. The *structure usage report* provides structure strength usage, insulator swing usage, joint support reactions, loads at insulator attachments and angle member checks (for latticed tower). The *sections usage report* gives the tension forces in all spans. PLS-CADD can make reports on survey point clearances, clearance to TIN, danger tree locator, structure clearances and wire clearances.

5.1.7 Structure and Section Modelling

In the *Structures* menu, structures can be added, edited, moved or deleted. If the structures are modelled already, for example in PLS-TOWER or PLS-POLE, these structures can be used or edited. If not, then this menu also offers the possibility of creating new structures, like stick figures. They can be either dead end structures or not, of a specified height, with specified sets and phases, all with a chosen insulator type, see Figure D.13.

As for the structures, PLS-CADD offers options for adding, editing and deleting cables. This is done in the *Sections* menu. It is also possible to edit existing cable files or create new ones, as well as checking the sag and tension of the different cables.

Minimum two dead end towers need to be placed along the alignment before a wire can be strung. It is less work to string the wire before adding intermediate structures, but it does not have to be done in this order. When modelling this line, dead end stick figures of 18m height were created and placed approximately 4.5km apart along the alignment. The input for these structures can be seen in Figure D.12. Three triplex Grackle conductors, see Figure D.5, were then strung between the dead end towers from phases 1:1, 2:1 and 3:1 to 11:1, 22:1 and 33:1 respectively, 1 and 11 being on one side and 3 and 33 on the other. It is important to make sure the conductors are strung correctly so that they do not cross. This can easily be checked in the plan view or 3D-view. Two ground wires, of the type F 69 Sveid, see Figure D.7, were also strung, from phases 4:1 to 4:1 and 5:1 to 5:1.

The initial tension of the conductors was set to $39651N$ and the initial tension of the ground wires was calculated to $25050N$ so that the sag of the ground wires would not exceed that of the conductors, thus maintaining the required clearance between them. See Appendix C.4 for this calculation.

Then the tower spotting of the intermediate structures was done. Thirteen towers were added at approximately 350m intervals and adjusted to maintain the clearances specified in 5.1.3. Three separate PLS-CADD models were made; one with lattice towers, one with tubular steel and the last using FRP structures. To simplify the production and erection processes and minimize the costs it was decided to keep the structures to as similar heights as possible when tower spotting.

Instead of doing the tower spotting manually, PLS-CADD is able to do automatic tower spotting based on the criteria input and limitations like spotting constraints for prohibited and extra cost zones along the alignment. This was not used in the model, but can be selected in the *Automatic Spotting* menu.

An illustrating selection of input from PLS-CADD is shown in Appendix D.1.

5.2 Modelling in PLS-TOWER

5.2.1 Basis for Modelling

Like for PLS-CADD several standards can be used for the design checks. EN 50341-1 (CENELEC, (2012) is used here.

PLS-TOWER is organised so that the user can import component data bases or libraries for the different elements; such as steel angles, bolts, guys, insulators, cables and so on, in the *Preferences* menu. The elements can also be defined manually under the *Components* menu if desired. From the elements defined the model can be built in the *Geometry* menu. From this model the computer will generate a finite element model (Power Line Systems Inc$_6$, (2016).

The finite element model can either be linear or nonlinear. The linear model ignores P-Δ effects and models guys and cables as tension only members. The nonlinear model takes P-Δ effects into account, which enables PLS-TOWER to detect buckling and gives a better cable representation by modelling cables and guys as exact cable members. It is therefore recommended to use the nonlinear model for finite analysis of guyed towers (Power Line Systems Inc$_6$, (2016).

The analysis of the finite element model is done by PLS-TOWER using solution algorithms implemented in the program. Two modes are available:

design check mode and allowable spans mode. The one used here is the design check mode. It is based on loading trees describing longitudinal, vertical and transverse loads in the conductors and ground wires and wind pressure on the structure. The vector loads files can be coming from the connected PLS-CADD file or be created manually. When using this mode, the analysis gives deformed shapes and usage of the elements. The allowable span mode is based on loads per unit length in the longitudinal and vertical direction from the conductor and ground wire and the wind pressure on the structure and determines allowable wind and weight spans for specified line angles. The wire loads files can be coming from the connected PLS-CADD file or be created manually (Power Line Systems Inc_6, (2016). From the analysis, interaction diagrams for allowable spans are made, see method 2 of 5.1.4 for an example. To get the loads directly from PLS-CADD an insulator link has to be made, defining what sets and phases are connected at what insulator attachment point. See Figure D.23 for an example.

The tower model is created by defining the location of joints in a 3-dimensional coordinate system and connecting them by members. Latticed towers should be modelled so that no high moments occur, as this is not specifically calculated by PLS-TOWER. Redundant members does not need to be included in the model, unless to check them, but if so the weight and wind area of them will need to be included by other means later. Joints should not be included where there is no need for them, for example if redundant members are excluded, as this causes stiffness problems (Power Line Systems Inc_6, (2016). The members are either angled, as seen in Figure 5.17 or round.

The angle members used in lattice towers are normally modelled with trusses or beams, both of which are able to take tension and compression. In addition the beam elements can take shear and moments. To provide adequate stiffness and avoid stiffness problems due to planar joints, most members should be modelled with beams, except diagonals and single horizontal struts that should be modelled with trusses. However, if these members have intermediate joints, they should be modelled with beams as well. Trusses behave as bolted connections, whereas beams behave as welded joints. Thus, using too many beam elements results in a model that is stiffer than it should be.

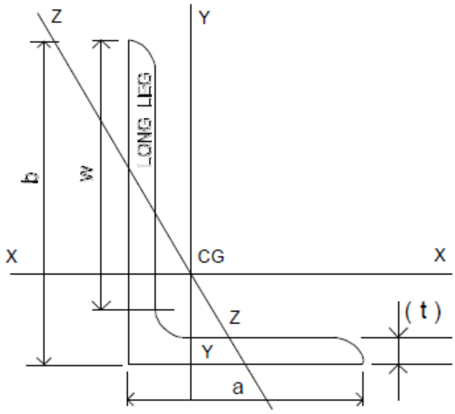

Figure 5.17: Angle member. Figure 3.1-3 of (Power Line Systems Inc$_6$, (2016).

The capacity of an angle subjected to compression is taken as the minimum of the compression capacity based on slenderness, the connection shear capacity and the connection bearing capacity. The capacity of an angle subjected to tension is taken as the minimum of the tension capacity based on net section, the tension capacity based on connection rupture, the connection shear capacity and the connection bearing capacity. The minimum of these values is then timed by the safety factor and compared to the force in the member.

PLS-TOWER determines the capacity of angled member according to the chosen standard. For EN 50341-1 these calculations are based on the loading eccentricity, the end restraint, the member slenderness ratios for the three angle axes and the connection properties which is determined in the *Angle Member Connectivity* table, see Figure D.17. Figure 5.18 illustrates the different eccentricity codes and restrain codes and the three axes can be seen in Figure 5.17. The modelled members are assigned to a group and a section that can be adjusted by certain variables. This is done in the *Angle Groups* and *Sections* tables.

Pairs of crossing diagonals influence the forces in each other. This is illustrated in Figure 5.19 where the solid lines represent out of plane buckling for different loading situations. To account for this effect pairs of diagonals should be modelled as crossing diagonals. PLS-TOWER will then include the effect one has on the other in the analysis.

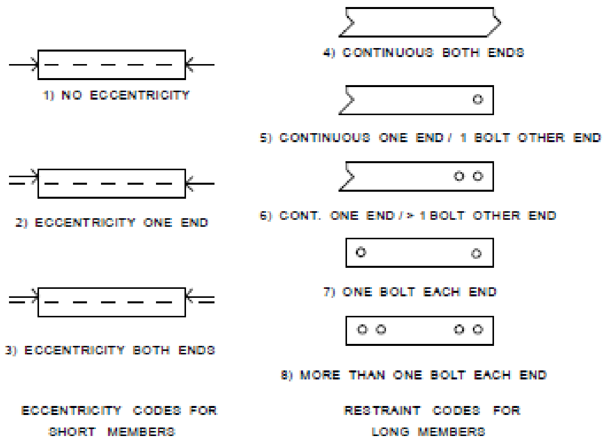

Figure 5.18: End conditions for members. Figure 3.1-10 of (Power Line Systems Inc$_6$, (2016).

In addition to checking tension and compression in the members, PLS-TOWER checks all members within 30° from horizontal for a climbing load of 1 kN as stated by EN 50341-1 (CENELEC, (2012), and controls the angle between members to ensure bracing members can provide full support. The minimum angle is set to 15° by EN 50341-1 (Power Line Systems Inc$_6$, (2016).

PLS-TOWER is able to model and check five different types of insulators: clamps, strain insulators, suspension insulators, 2-parts insulators (such as V-strings) and post insulators (Power Line Systems Inc$_6$, (2016). A strength factor of 0.5 is used for checking the capacity of the insulators.

Guys must be strung between a joint on one side and a fixed anchor on the other. When using a nonlinear analysis, they are modelled as exact cable elements. The cable usage is found by Equation 5.23.

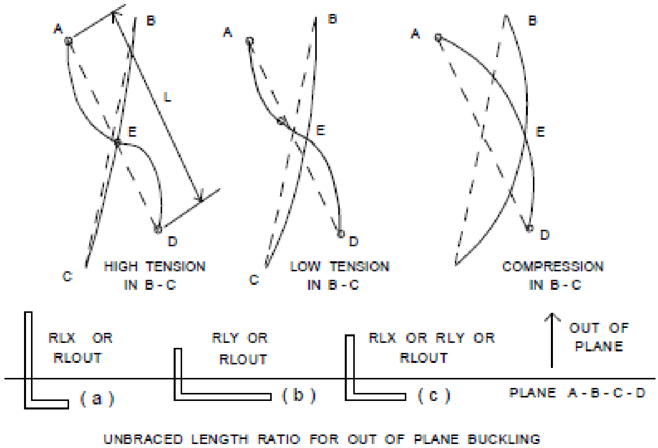

Figure 5.19: Crossing diagonals. Figure 3.1-12 of (Power Line Systems Inc$_6$, (2016)

$$Usage = \frac{T}{TCAPxPCTx100xSF)} \tag{5.23}$$

Where:

T	=	Tension force in cable
$TCAP$	=	Tension capacity of cable
PCT	=	Allowed percent of ultimate tension
SF	=	Safety factor

The loads affecting the tower are wire loads, dead loads and wind loads on the tower structure. Some standards also include ice load on members. The wire loads are the results of ice and wind loads on the conductors and ground wires. The dead load is calculated automatically by PLS-TOWER (Power Line Systems Inc$_6$, (2016).

As mentioned in 5.1.2 PLS-TOWER will use the input from PLS-CADD to calculate the wind load on the structure. There are three models on how to apply wind loads on the structures: standard wind on face, standard wind on all and SAPS. The last one applies wind load to all members and assumes no shielding. It is thus a conservative model and is used here. Figure 5.20 illustrates how the model works. A wind pressure is defined for a given reference height. Above this the wind velocity increases with height (Power Line Systems Inc$_6$, (2016).

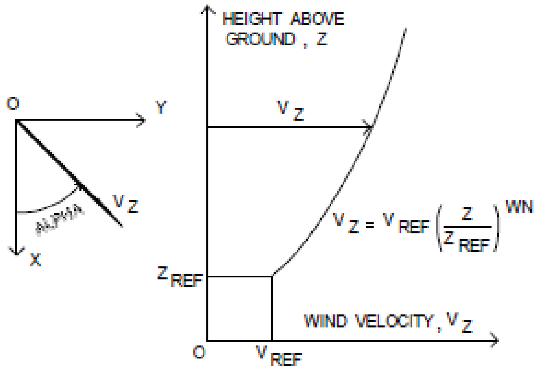

Figure 5.20: SAPS wind model. Fig. 5.1-3 of (Power Line Systems Inc$_6$, (2016)

The wind load on a member is calculated using Equation 5.24. The load acts perpendicular to the member.

$$F_n = P_0 * K_z * G * C_D * (U_n)^2 * WA_F * W_W * L \tag{5.24}$$

$$P_0 = \gamma * 0.5 * \rho * (V_0)^2$$

Where:

F_n	=	Factored wind load on structure member
P_0	=	Basic factored design pressure
γ	=	load factor for wind load
ρ	=	mass density of air
V_0	=	basic design wind velocity at reference height. EN 50341-1 bases this on the 50 year return period wind averaged over 2 seconds
K_z	=	height adjustment factor
G	=	structure gust response factor
C_D	=	member drag coefficient
U_n	=	projection of a unit wind velocity vector blowing in the same direction as V0 onto the direction normal to the member
WA_F	=	wind area adjustment factor
W_W	=	bare member wind width
L	=	member length

Wind load on guys are neglected for guyed transmission towers (Power Line Systems Inc$_6$, (2016). The SAPS wind model will however take it into account.

According to the PLS-TOWER user's manual (Power Line Systems Inc_6, (2016) ice load on tower members is uncertain. It is therefore recommended to either ignore it, include it by approximation, by adjusting dead load and/or wind area, or include it by choosing a value for ice thickness and density and letting PLS-TOWER do the calculation.

5.2.2 Steel Lattice Tower Model

The steel lattice tower is modelled based on the geometry given in 3.4.

Primary joints are added to define the main outline of the structure, for example at the structure base, top and connection between the legs and cross arm. Secondary joints are then added by interpolation or extrapolation of the positions of the primary joints. The joints can have up to three translational degrees of freedom and three rotational degrees of freedom. For example, joints at the base of the tower have no translational degrees of freedom and depending on the tower being fixed or pinned, either zero or three rotational degrees of freedom. In this model, the base is pinned. Other joints are usually modelled with three translational and three rotational degrees of freedom.

Members are then placed between the joints as described in 5.2.1, see Figure D.17. The groups and sections are defined as shown in Figures D.16 and D.15. It is here assumed that approximately 15 $\%$ of the structure weight is not modelled, for example redundant members, bolts and plates. Thus the *Dead Load Adjustment Factor* is set to 1.15. The SAPS wind model is used to calculate wind loads on the tower. As most members are modelled it is assumed that the area not included is 5 $\%$ of the area of the section. The angle drag factor is assumed to be 1.6. Thus the *SAPS Angle Drag x Area Factor* is set to $1.6 * 1.05 = 1.68$.

By using symmetry about the x-axis (longitudinal) and/or y-axis (transverse) when modelling joints and/or members the process is a lot quicker. PLS-TOWER also offers the options of copying and rotating parts of the structure to simplify the modelling process.

Guys and insulators are then attached as specified in Figure 3.2. The insulators used are clamps for attaching ground wires and 2-parts (V-string) insulators for conductors. The dimensions for the V-strings are given in Figure 3.4. PLS-TOWER can then find allowable swing angles for the insulators so that they do not go into compression for the four weather cases specified in PLS-CADD. An insulator link to PLS-CADD is created, where the three V-strings are attached to phases 1:1, 2:1 and 3:1 and the clamps are attached to phases 4:1 and 5:1. The conductor and ground wire vector loads as well as the wind pressure on the structure is thus collected from PLS-CADD and applied to the structure. EN 50341-1 (CENELEC, (2012) does not define any ice load on lattice tower members, thus it is ignored.

The finished model can be found in Figure 3.9.

An illustrating selection of input from PLS-TOWER is shown in Appendix D.2.

The result of the structural analysis in PLS-CADD is given in Figure 5.21.

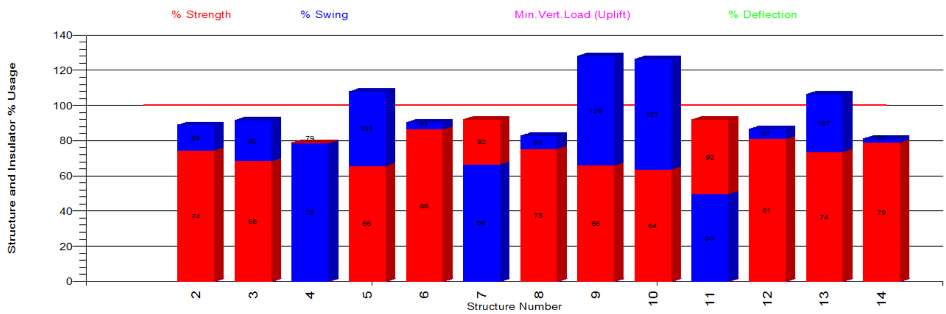

Figure 5.21: Structure usage of steel lattice towers.

The resulting models depicting the tower usage are shown in Figures 5.22 and 5.23. The usage is shown in % where red colour means 100 %, yellow is down to 75 %, green is down to 50 %, light blue is down to 25 % and dark blue down to 0 % of max usage.

A close up of one of the towers is shown in Figure 5.24. Here the undeformed geometry of the tower is shown illustrating the max % usage in the various members for all the load cases.

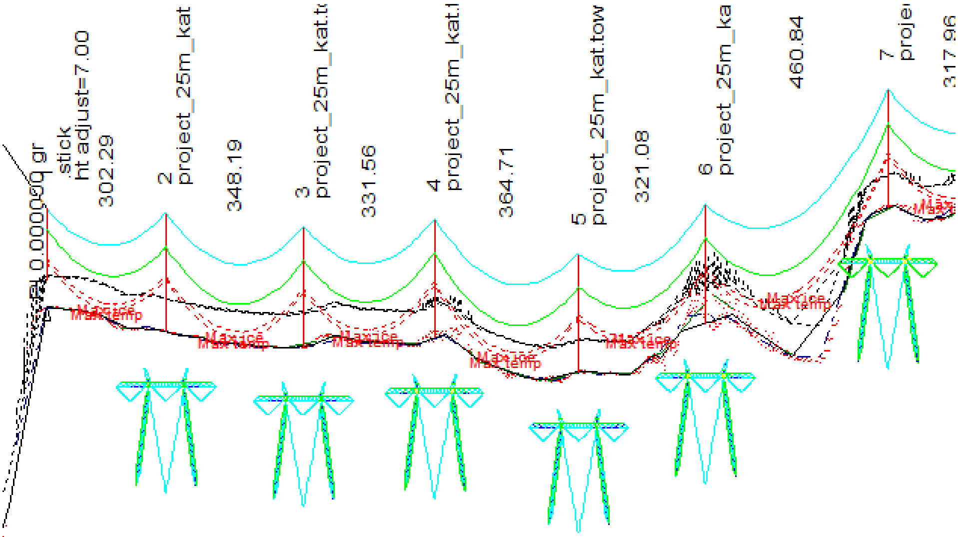

Figure 5.22: Structure usage of tower 2-7.

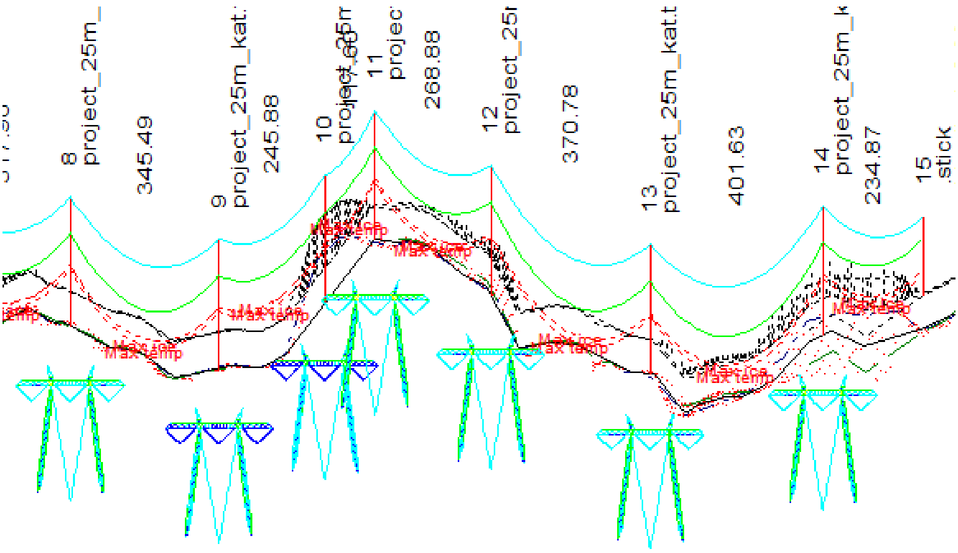

Figure 5.23: Structure usage of tower 8-14.

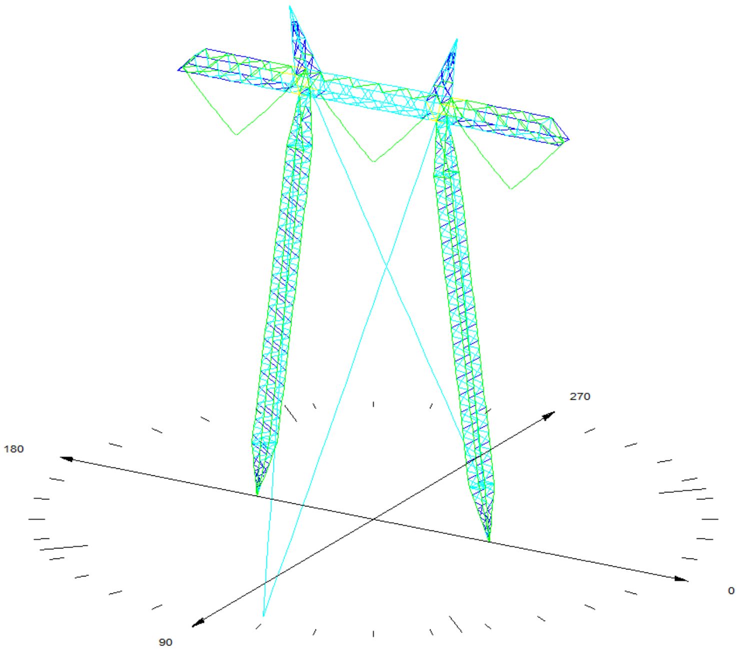

Figure 5.24: Max % usage in steel lattice tower.

5.3 Modelling in PLS-POLE

5.3.1 Basis for Modelling

PLS-POLE is a program made for the design and analysis of single pole structures or frames (multipole structures). The structures can be made of steel, concrete, wood, fibre reinforced polymer or a combination of elements of different materials.

Like PLS-TOWER and PLS-CADD, PLS-POLE has implemented design checks according to several standards. It also shares the same analysis engine as PLS-TOWER and therefore operates in a similar way when it comes to the analysis. It can be linear or nonlinear and it can be based on the design check mode or the allowable spans mode. See 5.2.1 for more information on this. The PLS-POLE user's manual recommends using a nonlinear analysis for guyed pole structures. For this tower the design check mode is used. Loads are dealt with in a similar fashion as in PLS-TOWER (Power Line Systems Inc$_5$, (2016). The wind load on elements is generally taken as the perpendicular design force times the depth of the member times the member's drag coefficient.

Like for PLS-TOWER components libraries containing elements to build the structure from can be imported or the elements can be defined manually in the *Components* menu. There are options for defining poles, davit arms, cross arms, braces, guys, cables, insulators and other equipment (Power Line Systems Inc$_5$, (2016).

The poles can be modelled in several materials: steel, wood, concrete and FRP, and can be defined by both material and dimensional properties under the *Components* menu. In the model they are defined by a shape, diameter, taper and length. They can be modelled as embedded or not, and either with a fixed, pinned or "PinFrm" base connection. A joint where PinFrm is chosen will also be allowed to rotate about the z-axis, removing any torsional moment at the base. When using tapered poles of steel or FRP it is possible to define several elements that are stacked to form a longer pole. A fixed joint cannot have any lateral or rotational movement, whereas a pinned joint allows for rotational movement about the x- and y-axes. Different approaches are used when checking the different materials. The ASCE approach for tubular steel poles and FRP poles checks the quadrant with the highest stress at each end for points along the outer face of the element. The strength usage at each of these points for tubular steel poles in transmission towers is found by looking at the combined effect of several loads as seen in Equation 5.25 (Power Line Systems Inc$_5$, (2016).

$$Usage = \frac{\sqrt{(f_a + f_b)^2 + 3 * (f_v + f_t)^2}}{f_{all} * SF} \tag{5.25}$$

Where:

f_a	=	normal stress due to axial load
f_b	=	normal stress due to bending
f_v	=	shear stress due to shear force
f_t	=	shear stress due to torsion
f_{all}	=	allowable combined stress defined in ASCE Standard
SF	=	strength factor for steel poles

PLS-POLE applies the steel strength factor when checking the strength of FRP poles as well. At the moment, PLS-POLE has only been tested with round poles, but it is possible to define other cross section shapes. FRP poles properties varies with temperature. Therefore PLS pole accounts for the temperature effect when calculating the modulus of elasticity and failure stress. This is done using quadratic equations, as shown in Equations 5.26 and 5.27 respectively (Power Line Systems Inc$_5$, (2016).

$$E_{FRP} = AT^2 + BT + C \tag{5.26}$$

$$f_{all} = AT^2 + BT + C \tag{5.27}$$

Where:

E_{FRP}	=	Modulus of elasticity
f_{all}	=	Failure stress
A	=	Input
B	=	Input
C	=	Input at 0°C
T	=	Temperature of current load case

Cross arms are straight prismatic elements with constant cross section that are defined by length, diameter and shape. They can be attached to one or more poles, either as a rigid or pinned connection. Davit arms are assumed rigidly connected where they are attached. If designed in steel it is possible to model them as tapered elements, if not they must have a constant cross section. Both types however can be modelled as curved elements by defining intermediate points. In Figure 5.25 are illustrated some different ways to model the attachments between pole, cross arm and davit arm according to design preference.

Both for cross arms and davit arms PLS-POLE separates between generic ones and tubular steel ones. The nominal strength check does not work well for the cross arm element between poles as it is meant for elements with loading applied at the tips. Thus the calculated strength check is a better option. For generic arms the strength is checked by using Equation 5.28. Tubular steel ones are checked similarly to the tubular steel poles, as in Equation 5.25.

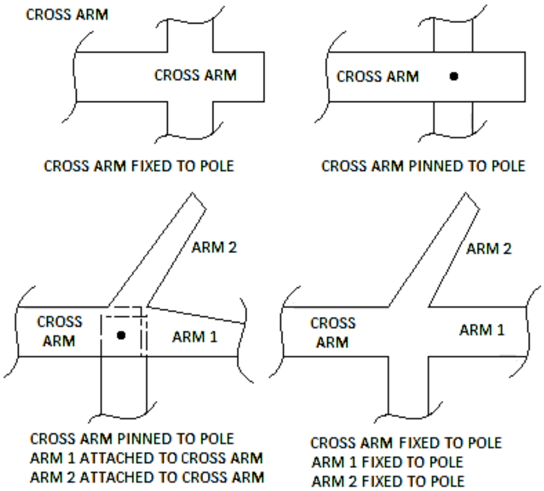

Figure 5.25: Connection of cross arms and davit arms. Fig. 4.6-3 of (Power Line Systems Inc$_5$, (2016)

$$Usage = \frac{\frac{N}{A} + \frac{M_x}{S_x} + \frac{M_z}{S_z}}{FNxSF} \tag{5.28}$$

Where:

N	=	Axial load
A	=	Area
M_x	=	Moment about x-axis
S_x	=	First moment of area about x-axis
M_z	=	Moment about z-axis
S_z	=	First moment of area about z-axis
FN	=	Capacity of element
SF	=	Safety factor

Braces are defined as prismatic elements of uniform cross section. They can be modelled either as truss members or fuse members based on them having unlimited or limited axial capacity.

Modelling and calculation of guys and insulators are approached in the same way as in PLS-TOWER. The use of cables is similar to that of guys. The only difference is that cables must be strung between two joints.

5.3.2 Steel Tubular Tower Model

The steel tubular tower is modelled in PLS-TOWER based on the geometry given in 3.4.

All elements used are square tubular steel members with constant cross section throughout the length of the pole. The cross arms and davit arms are modelled after section sizes available by Ruukki. The legs are modelled as pinned at the bottom, connected to a base plate. The cross arm is modelled as one member that is pinned at the attachment points at the top of the poles. The davit arms are then modelled as rigidly connected to the pole/cross arm.

Guys, cables, braces and insulators are attached as specified in Figure 3.2. The insulator link as described in 5.2.2 is also created in this model.

The finished model can be found in Figure 3.11.

An illustrating selection of input from PLS-POLE is shown in Appendix D.3.

The result of the structural analysis in PLS-CADD is given in Figure 5.26.

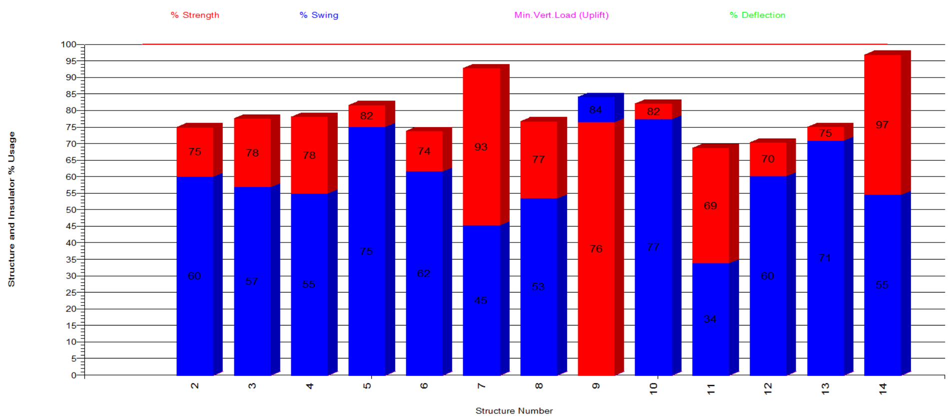

Figure 5.26: Structure usage of steel tubular towers.

The resulting models depicting the tower usage are shown in Figures 5.27 and 5.28. The usage is shown in % where red colour means 100 %, yellow is down to 75 %, green is down to 50 %, light blue is down to 25 % and dark blue down to 0 % of max usage.

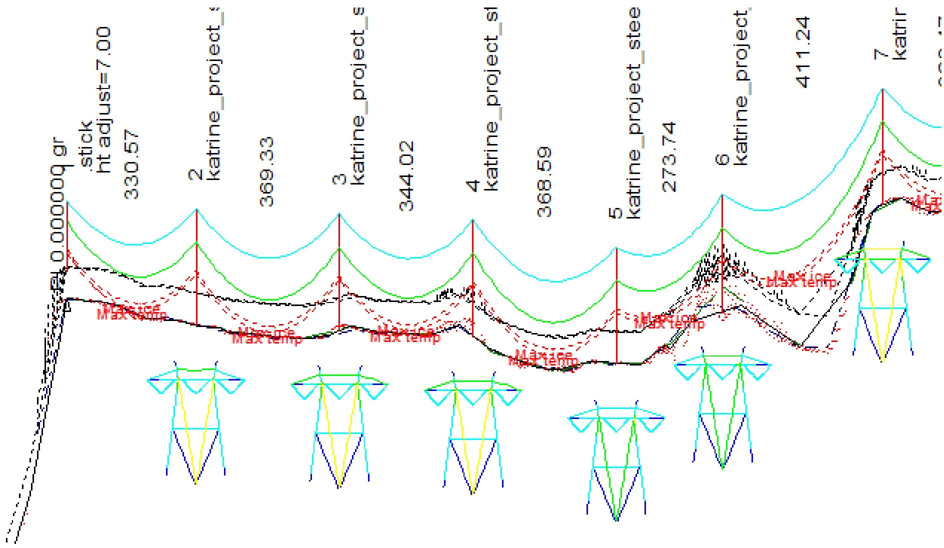

Figure 5.27: Structure usage of tower 2-7.

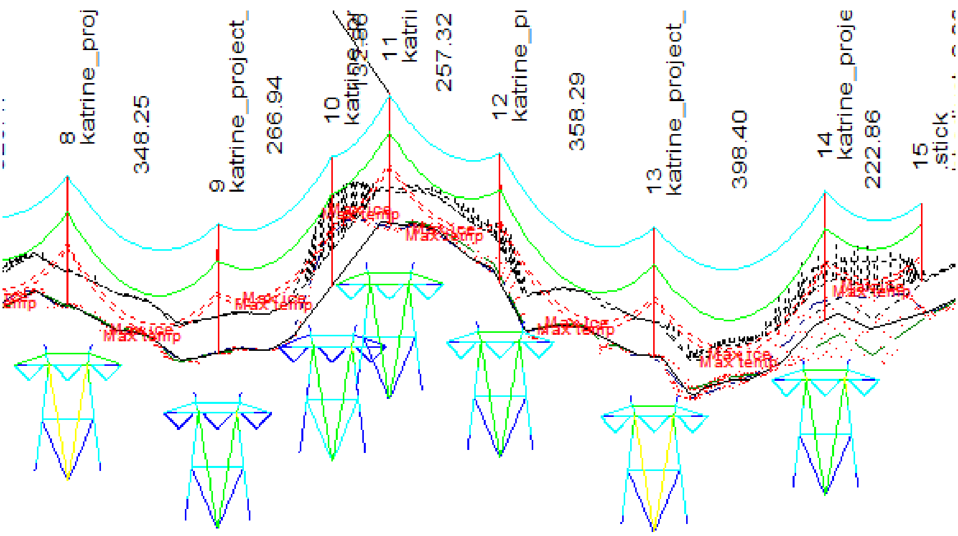

Figure 5.28: Structure usage of tower 8-14.

A close up of one of the towers is shown in Figure 5.29. Here the undeformed geometry of the tower is shown illustrating the max % usage in the various members for all the load cases.

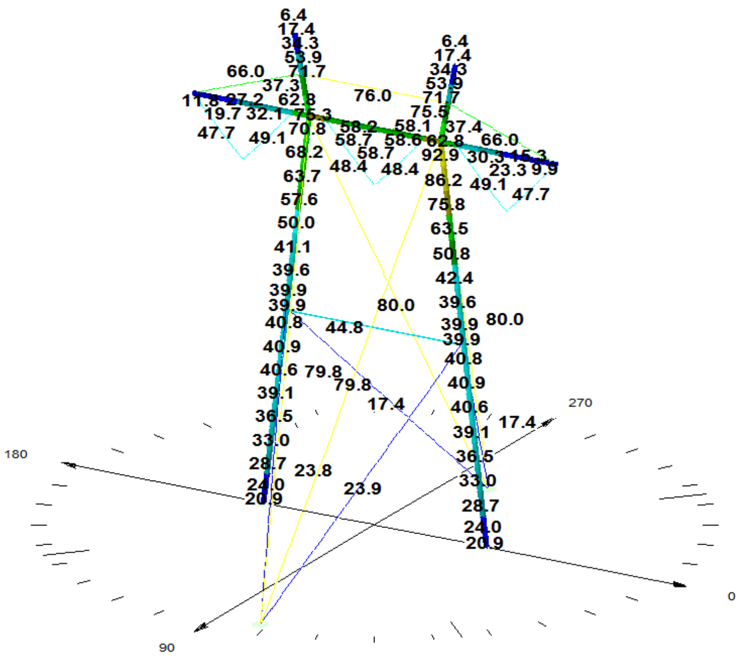

Figure 5.29: Max % usage in steel tubular tower.

5.3.3 FRP Tubular Tower Model

The FRP tubular tower is modelled in PLS-TOWER based on the geometry given in 3.4.

The FRP tubular legs are modelled as round poles as this is the only option offered by PLS at the moment. All other members are defined manually by geometric and material properties as FRP members. The FRP sizes are defined as advised by supervisors in regard to thicknesses (Toth, (2016). The cross arm is design to consist of two parallel elements, but the modelling was done of one member with the geometric properties of both incorporated.

Guys, cables, bracings and insulators are attached as specified in Figure

3.2. The insulator link as described in 5.2.2 is also created in this model.

The finished model can be found in Figure 3.14.

An illustrating selection of input from PLS-POLE is shown in Appendix D.4.

The result of the structural analysis in PLS-CADD is given in Figure 5.30.

Figure 5.30: Structure usage of FRP tubular towers.

The resulting models depicting the tower usage are shown in Figures 5.31 and 5.32. The usage is shown in % where red colour means 100 %, yellow is down to 75 %, green is down to 50 %, light blue is down to 25 % and dark blue down to 0 % of max usage.

A close up of one of the towers is shown in Figure 5.33. Here the undeformed geometry of the tower is shown illustrating the max % usage in the various members for all the load cases.

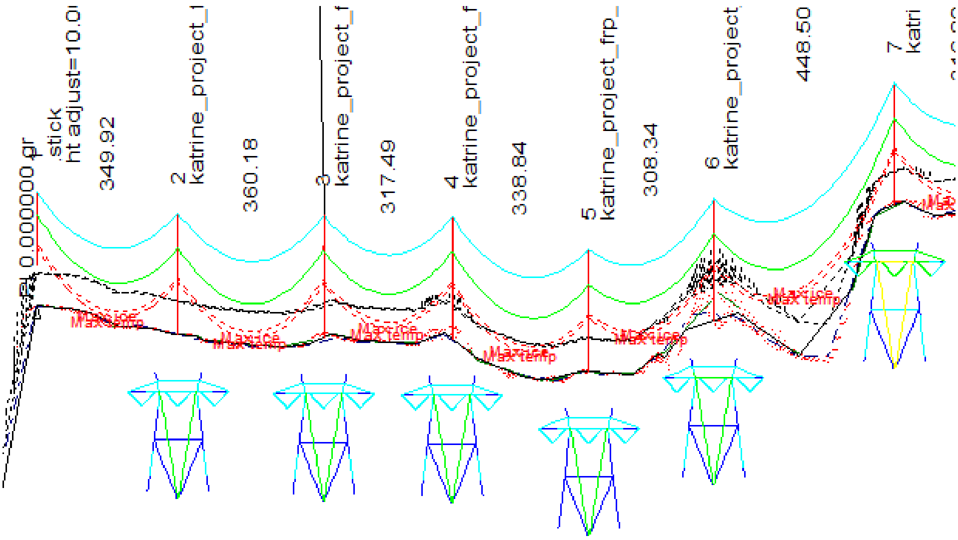

Figure 5.31: Structure usage of tower 2-7.

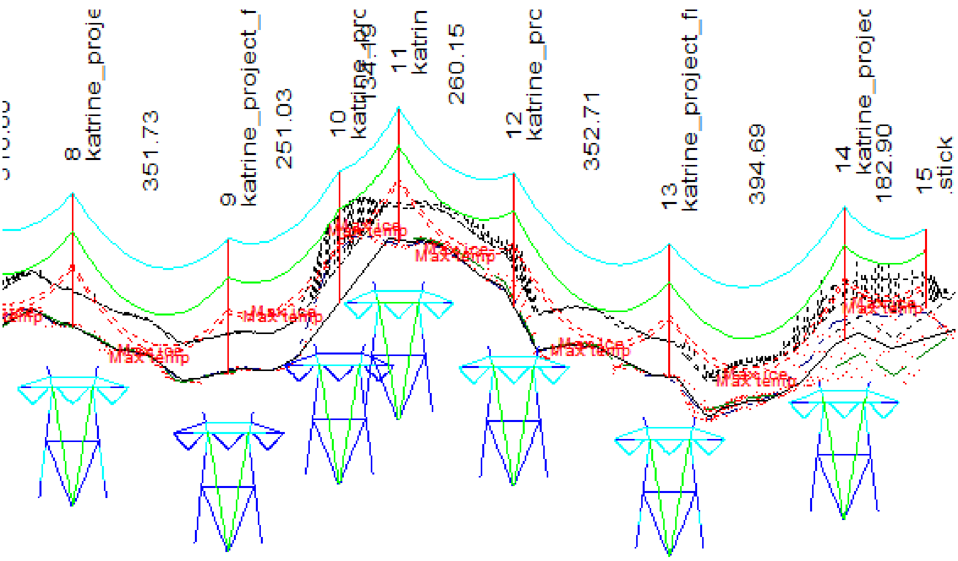

Figure 5.32: Structure usage of tower 8-14.

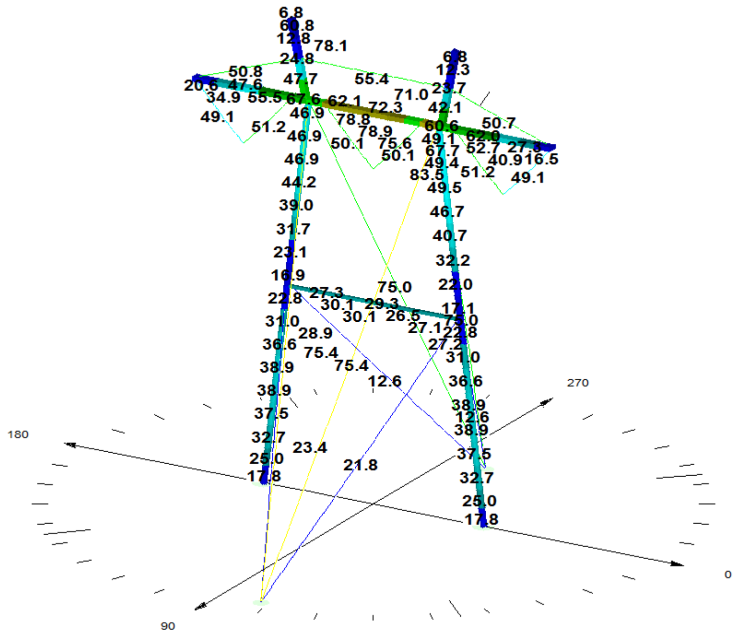

Figure 5.33: Max % usage in FRP tubular tower.

Chapter 6

Calculations and Checks

6.1 Preliminary Calculations

The dead loads, wind loads and ice loads were applied to the structure leading to forces in the vertical and transverse directions. From this, preliminary cross sections were obtained.

The preliminary calculations are done based on assumptions that the ruling span is 350 m and that the towers are located on a straight line horizontally unless specified otherwise. It was in these calculations assumed that the vertical components are taken as compression by the legs and the transverse components to be taken as tension in the guys, yielding extra compression in the legs and crossarm. Also, for the tubular towers, only the guys connected to the cross arm were assumed to take any load.

6.1.1 Vertical loads

Vertical loads on the structures come from the dead load and the ice load on conductors and ground wires. When assuming a weight span of 350 m (assumes flat terrain) the vertical load on a support from ice load was found to be 52.5 kN for a conductor and 17.5 kN for a ground wire. See

Appendix C.2 for calculations. The dead load is the same as in 4.1, now including conductors and ground wires.

Table 6.1: Vertical loads.

Tower	Dead load (kN)	Ice load (kN)	Dead + Ice load (kN)
Steel lattice tower	172.2	192.5	364.7
Steel tubular tower	167.7	192.5	360.2
FRP tubular tower	139.1	192.5	331.6

As mentioned, the vertical loads lead to compression forces in the legs and the middle part of the cross arm. See Appendix C.5 for calculations. These forces are given in Table 6.2

Table 6.2: Forces due to vertical loads.

Tower	Element	Compressive force Due to dead load (kN)	Compressive force Due to dead + ice load (kN)
Steel lattice	Leg	86.8	183.8
Steel lattice	Cross arm	10.8	22.8
Steel tubular	Leg	84.5	181.5
Steel tubular	Cross arm	10.5	22.5
FRP tubular	Leg	70.1	167.1
FRP tubular	Cross arm	8.7	20.7

6.1.2 Transverse loads

Wind on the cables lead to forces in attachment points of conductors and ground wires. When applied parallel to the cross arm only two of the guys will be in tension and take loads. The resulting forces will be divided into tension in the guys and compression in the legs. See Appendix B.1 for derivation of this.

In addition the wind load on the structure itself will affect the forces. For simplification all transverse loads are added at the top. The wind load calculated are presented in Table 4.4.

The forces in guys and legs found are presented in Table 6.3. See Appendix C.6 for calculations.

Table 6.3: Forces due to transverse loads.

Tower	Element	Force (kN)
Steel lattice	Leg	284
Steel lattice	Guy	158
Steel tubular	Leg	236
Steel tubular	Guy	131
FRP tubular	Leg	250
FRP tubular	Guy	139

6.1.3 Longitudinal loads

Ice load and wind load on the conductors and ground wires lead to increased tension in the cables. These loads will be taken by tension towers throughout the line and the dead-end towers at each end. For suspension towers the longitudinal loads from the adjacent spans will more or less cancel each other out if the spans and heights are of similar size. This will of course rarely happen in real life, but for the simplicity of the preliminary calculations, it is assumed that they do. Only when stringing the cables and at conductor breaks will these towers experience any longitudinal loading.

When loaded in the longitudinal direction, tension forces are taken by the guys resulting in compressive forces in the leg and cross arm. Derivation of the forces affecting the towers can be found in Appendix B.2.

6.1.4 Combined Forces

The combined forces from vertical, transverse and longitudinal loads are given in Table 6.4

Table 6.4: Combined forces due to loading.

Tower	Element	Force (kN)
Steel lattice	Leg	431.8
Steel lattice	Cross arm	22.8
Steel lattice	Guy	158
Steel tubular	Leg	417.5
Steel tubular	Cross arm	22.5
Steel tubular	Guy	131
FRP tubular	Leg	417.1
FRP tubular	Cross arm	20.7
FRP tubular	Guy	139

6.1.5 Cross Sections

Preliminary cross sections were found based on the compressive forces in the legs calculated in 6.1.4. These are presented in Table 6.5. The calculations used can be found in Appendix C.7.

Table 6.5: Cross sections of members.

Tower	Element	Cross section (mm)
Steel lattice	Leg main member	50x50x5
Steel lattice	Leg diagonal	20x20x3
Steel lattice	Cross arm main member	35x35x4
Steel lattice	Guy	ϕ21 (tension capacity 220 kN)
Steel tubular	Leg	70x70x5
Steel tubular	Cross arm	25x25x2
Steel tubular	Guy	ϕ21 (tension capacity 220 kN)
FRP tubular	Leg	ϕ100x9.5
FRP tubular	Cross arm	25x25x2
FRP tubular	Guy	ϕ21 (tension capacity 220 kN)

6.2 PLS-checks

6.2.1 Load calculation

Load case 10: wind on clear line (wind 500 year) on a conductor yields a transverse load applied to the structure of 30119 N in PLS. The calculated transverse wind load on a structure is 23909 N. This is not exactly the same, but may be a result of the wind model chosen in PLS. One can assume that the input is being correctly processed.

Load case 01: full ice load on a conductor yields a vertical load applied to the structure of 52630 N in PLS. The calculated ice load for a weight span of 350 m is 52500 N which is almost similar.

6.2.2 Deflections

The stiffness of a structure can be more critical than the strength, as a structure that is too flexible might not be able to do its intended task of supporting the hardware (Vinson and Sierakowski, (2012)). This might lead to line failure.

The maximum deflection of a composite utility tower structure is 12 % of the height according to REN (Ren Elektrisk Nettvirksomhet AS). This equals a deflection at the top of 3.6 m, and for the cross arm ends 1.1 m. This requirement is checked against deflections for the tower top and cross arm acquired from PLS for all load cases. Both are within the requirement.

Maximum deflection of a steel utility tower structure is for suspension poles 4 % of the pole length (Kiessling et al., (2003)). This equals a deflection at the top of 1.2 m, and for the cross arm ends 0.3 m. This requirement is checked against deflections for the tower top and cross arm acquired from PLS for all load cases. Both are within the requirement.

For both towers the load cases yielding the largest deflections are in the transverse direction 500 year wind on clear line and in the longitudinal direction line breaks and uneven ice loading.

According to (CENELEC, (2012)) it is normally unnecessary to consider deflection of a lattice tower.

6.2.3 Dynamic Response

When assessing the dynamic response of the conductors and towers a simplified model is used where the structural system is assumed linear and the stiffness of the conductors are neglected. Two load cases were used in the calculations: 10 - Wind on clear line and 12 - Wind on ice.

The natural frequencies of the conductors and ground wires are found for standing waves of one, two and three loops. These are presented in Table 6.6. The natural frequencies for the different tower designs found are presented in Table 6.7. See Appendix C.8 for calculations used.

Table 6.6: Natural frequencies of cables.

Load case	Numbers of loops	Natural frequency conductor (Hz)	Natural frequency ground wire (Hz)
Wind on clear line	1	0.124	0.101
	2	0.248	0.202
	3	0.372	0.304
Wind on iced line	1	0.110	0.090
	2	0.220	0.180
	3	0.329	0.270

6.2.4 Buckling of Steel Poles

Elements in compression or subject to shear loading are prone to buckle due to instabilities. This can in the worst case lead to structural collapse. The load required to induce buckling might be a fraction of the material strength for a slender section (Vinson and Sierakowski, (2012)).

Table 6.7: Natural frequencies of towers.

Load case	Tower	Natural frequency (Hz)
Wind on clear line	Steel lattice	0.651
	Steel tubular	0.552
	FRP tubular	0.472
Wind on iced line	Steel lattice	1.009
	Steel tubular	0.575
	FRP tubular	0.525

Based on the moment distributions in the longitudinal and transverse directions and the axial compression load, the buckling is checked according to NS-EN 1993-1-1:2005 (CEN, (2005)) by Clause 6.3.3 and Annex B. Load cases 01: Full ice load and 10: 500 year wind on clear line were found to induce the largest moments and axial loads and were thus the ones checked. It is assumed that the guys provide lateral stability, making the length of the elements 12.1 m.

The steel poles analysed do not buckle. See calculations in Appendix C.9.

Chapter 7

Life Cycle Analyses

Life cycle analyses are done to evaluate a product based on all of its life phases by summarising potential benefits and costs throughout its life span. Results of such analyses can be used for example to compare different designs or material usages, as is done here.

Both monetary cost and environmental impact is evaluated in this thesis.

These analyses are performed to give an additional basis for comparing the three different designs defined in Chapter 3. All the towers are assumed to have fairly similar foundations and equal insulators, conductors and ground wires. Thus the difference will mainly lie in the design of the tower itself.

For both the life cycle cost analysis and the environmental assessment the life span of the tower is divided into several phases to describe the life from raw material to decommissioning. The production phase is thought to include raw materials, transport of raw materials and manufacturing of elements. The assembly phase consists of transport of finished elements either by ship, truck or both, and the assembly of the structure on site. The use phase is determined as the time span from when the tower is commissioned until it is taken out of service, thus including checks, any maintenance required and possible repairs. The end-of-life phase consists of deconstruction, transport, waste processing and disposal. Any recycling potential the materials have will also be added here.

7.1 Theory

7.1.1 Life Cycle Cost

Life cycle cost (LCC), also called life cycle cost analysis (LCCA), takes into account all costs of a product during its life span by discounting them to their present value to give a holistic look of the system (Wübbenhorst, (1986)). This is done with a goal of optimising value for money to result in a cost efficient solution (Woodward, (1997)). By considering the costs of all life phases of the product it is easier to assess where in a project cuts in costs can be made. This is particularly important in a society where cost often is the most important aspect. LCC also offers a way to compare alternatives based on both CapEx (Capital Expenditure) and OpEx (Operational Expenditure).

An LCCA can be done in many ways. A general way is to first determine the cost elements, then define the cost structure, for so to establish the cost estimating relationship and finally establishing the method of LCC formulation. Other approaches might divide these phases further, like Kaufman's formulation as mentioned by Woodward ((1997)). This divides the process into eight steps.

On of the aspects to influence the LCC most is the discount rate used to get present values. A high discount rate favours options where the capital cost is low and the life span short. A low one will then do the opposite (Woodward, (1997)). If this is not assessed correctly the LCC may wrongly favour one alternative if costs and life span differ greatly. This can thus be a problem when trying to show long term investments as more desirable than short term ones. The discount rate will be influenced by the inflation rate and base rate (Woodward, (1997)). The discount rate is set to 5% in this thesis based on recommendations from supervisors.

A common tool for cost estimating is the net present value (NPV) method. By moving all future cash flows to the present, this tool enables us to evaluate costs happening at different times in the future at a common principal level by determining their present value. This is based on the interest rate, or discount rate (Remer and Nieto, (1995)). The net present value can be found using Equation 7.1.

$$NPV = \frac{C_t}{(1+r)^t} \tag{7.1}$$

Where:

NPV	=	net present value
C_t	=	cost in year t
r	=	discount rate
t	=	year

7.1.2 Life Cycle Assessment

In later years we as a society have begun to understand the importance of preserving our planet. The effects on the environment has greater impact on the choices we make and the environmental impact has become a key factor when evaluating projects and choosing alternatives also in the construction industry (Alfredsen et al., (2012)).

The purpose of the life cycle assessment (LCA), also called environmental life cycle assessment, is to evaluate the effect a product has on the environment throughout its life span (The Environmental Literacy Council, (2015)) and to find ways to reduce these effects while still maintaining its functionality and quality. Some products might be composed of many elements that will all need to be taken into account to get a correct look at the problem.

To ensure the environmental aspect of a problem is given the correct amount of consideration and is used in a correct way the LCA should be conducted according to international guidelines given by ISO 14040: Environmental management - Life cycle assessment - Principles and framework (Alfredsen et al., (2012)).

ISO 14040 states that an LCA should be conducted in four phases: definition of goal and scope, inventory analysis, impact assessment and interpretation. Figure 7.1 illustrates how these phases influence each other (Alfredsen et al., (2012)).

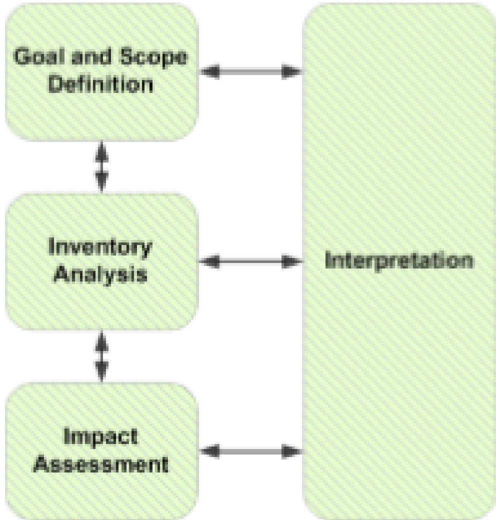

Figure 7.1: LCA structure (Alfredsen et al., (2012))

Defining the goal and scope is important to be able to conduct the assessment in an effective way. If the goal is to compare alternatives, the aspects that are similar between them can be omitted. Similarly, if the goal is to reduce the environmental impact one makes there is little point in assessing the aspects that cannot be changed (Alfredsen et al., (2012)).

The inventory analysis is possibly the most comprehensive part of the LCA. In this phase all inputs and outputs throughout the product's life span need to be examined and quantified. Everything from material extraction, product manufacturing and assembly to distribution, use and disposal should be included (The Environmental Literacy Council, (2015)). By assessing elements based on their life span and functional unit, comparative numbers can be acquired for products of different life spans.

In the impact assessment the values found in the inventory analysis are enumerated (The Environmental Literacy Council, (2015)). This is done by converting the various emissions to equivalents so they can be combined to find the total environmental impact. Different types of impacts can be considered, such as climate change, acidification or ozone depletion (Alfredsen et al., (2012)).

In the interpretation phase several factors should be taken into account concerning the sensitivity of the analysis and what aspects are most critical. From this an improvement analysis can be done to find ways to decrease the environmental impact (The Environmental Literacy Council, (2015)).

Environmental product declarations (EPDs) are registered documents communicating the environmental impact of a component, a finished product or service in a standardized and objective way (The Norwegian EPD Foundation, (2016)). They can therefore be used as parts of LCAs. The stages illustrated in Figure 7.2 are those The Norwegian EPD Foundation recommends to use for the LCA. This is based on NS-EN 15804:2012+A1:2013. These stages have been the basis for the division of the life span mentioned previously.

Product stage			Assemby stage		Use stage							End of life stage				Beyond the system boundaries
Raw materials	Transport	Manufacturing	Transport	Assembly	Use	Maintenance	Repair	Replacement	Refurbishment	Operational energy use	Operational water use	De-construction demolition	Transport	Waste processing	Disposal	Reuse-Recovery-Recycling-potential
A1	A2	A3	A4	A5	B1	B2	B3	B4	B5	B6	B7	C1	C2	C3	C4	D
X	X	X	X	MND	MND	MND	MND	MND	MND	MND	MND	MND	MND	MND	MND	X

Figure 7.2: Stages of EPD life cycle assessment.

A common way to find the environmental impact is by assessing the product's global warming potential (GWP), which is determined by evaluating greenhouse gas emissions by their CO_2-equivalents. The relationship between one gas and CO_2 is based on how long they persist in the atmosphere (Solomon et al., (2007)). The most important greenhouse gases; CO_2, CH_4, NO_x, HFC's, PFC's and SF_6 (Dudok van Heel et al., (2011)). Examples of some of these gases GWP for 100 years is shown in Table 7.1.

Other ways to assess the environmental impact can be by looking at cumulative energy demand, ecopoints and power usage. Some of this is discussed further by Duflou et al. ((2012)). The GWP is what will be considered in this assessment.

Table 7.1: Global warming potential (GWP_100) of greenhouse gases (Solomon et al., (2007)).

Greenhouse gas	kg CO_2-equivalents per kg gas
CO_2	1
CH_4	21
NO_x	310

7.2 Conducted Analyses

7.2.1 Assumptions

The assumptions done in order to complete the assessments are given here. These are based on data found online, contact with businesses and discussions with supervisors.

As the goal of the analyses is to give a basis for comparison of the three different designs, only the factors that are different are assessed. By doing so the process is simplified.

Similarities that are omitted in the analyses:

- Space needed for work and area prepping
- Foundation work and material
- Storage
- Insulator material and installation
- Conductor and ground wire materials, transport and stringing
- Other hardware installations
- Inspections done every 1, 5 and 10 years
- Insulators and corona ring often the first to need repair regardless of tower, thus hardware maintenance and repair is assumed similar.

- life span of hardware 40 years, same for all towers so omitted

General assumptions:

- Same life span of 80 years for tower structures (Knutsen, (2017))
- Inflation at 2 %
- Discount rate at 5 %

Acquisition:

- Import tax at 0 % in Norway (Norwegian Customs)
- Cost of FRP at 2528 NOK/m (Rempro AS, (2017))
- Cost of angle steel members at 20 NOK/kg steel (Knutsen, (2017))
- Cost of tubular steel members at 25 NOK/kg steel (Knutsen, (2017))
- Emissions of FRP based on Jerol EPD (Jerol Industri AB, (2015))
- Emissions of steel based on Ruukki EPD (Ruukki Construction Oy, (2015))

Installation:

- FRP imported from Creative Pultrusions in USA
- Shipping emission is 31.99 g CO_2 per t km (Wallenius Wilhelmsen Logistics, (2016))
- Steel imported from Dalekovod in Croatia
- Truck data based on EUR5 60t
- Truck emissions are 5 times that of shipping the same weight and distance (Haram, (2017))

- Hourly rate of workers is 680 NOK/h
- Assembly time of guyed lattice steel tower (81298) 20 h/t (Knutsen, (2017))
- Assembly time of guyed tubular steel tower (76800) 10 h/t (Knutsen, (2017))
- Assembly time of guyed tubular FRP tower (48154) 9 h/t (Knutsen, (2017))
- Helicopter data based on Airbus H135 can lift 1000-1200 kg (Airbus Helicopters Inc, (2017))
- Hourly helicopter rate at 15000 NOK/h (Knutsen, (2017))
- Helicopter emissions are 3 kg CO_2 per l fuel (Triple Pundit: Pablo, (2007))
- Helicopter use for lattice steel tower is 8 lifts of 10 min
- Helicopter use for tubular steel tower is 8 lifts of 10 min
- Helicopter use for tubular FRP tower is 5 lifts of 10 min

Use:

- Galvanized coating does not need refurbishment
- Repainting of steel every 20 years
- Cost of repainting is 3000 NOK/t (Knutsen, (2017))
- Transport is done by helicopter
- No refurbishment needed for FRP tower

Decommissioning:

- Deconstruction uses the same amount of time as assembly

- All waste is transported 360 km or 6 hours.
- Steel is recycled as in Ruukki EPD (Ruukki Construction Oy, (2015))
- FRP is used as landfill
- Price for landfill is 1567 NOK/t (Renovasjonsselskapet for Drammensregionen IKS, (2017))
- Price for steel recycling is -1250 NOK/t (Hellik Teigen, (2017))

7.2.2 Life Cycle Cost Analysis

The LCCA is done based on the assumptions stated previously. The resulting net present values (NPV), given in NOK, of the three tower designs are presented in Table 7.2.

Table 7.2: Result of LCCA

	Steel lattice	Steel tubular	FRP tubular
NPV (NOK)	377181	340145	363854

The total LCC of the towers for a life span of 40 years can be found in Tables 7.3, 7.4 and 7.5 for the steel lattice tower, steel tubular tower and FRP tubular tower respectively. A more detailed description of the LCC can be found in E.1.

Table 7.3: Total LCC of steel lattice tower for life span of 40 years

Year	Event	Cost	Inflated cost	NPV
0	Manufacture	165740	165740	165740
0	Import tax	0	0	0
0	Transport	35200	35200	35200
0	Installation	132743	132743	132743
20	Refurbishment	29361	43629	16443
40	Refurbishment	29361	64830	9209
60	Refurbishment	29361	96334	5157
80	Deconstruction	132743	647180	13058
80	Transport	6600	32178	649
80	Recycle	-10359	-50505	-1019
	TOTAL	550750	1167330	377181

Table 7.4: Total LCC of steel tubular tower

Year	Event	Cost	Inflated cost	NPV
0	Manufacture	195500	195500	195500
0	Import tax	0	0	0
0	Transport	35200	35200	35200
0	Installation	73216	73216	73216
20	Refurbishment	27960	41547	15659
40	Refurbishment	27960	61737	8769
60	Refurbishment	27960	91738	4911
80	Deconstruction	73216	356960	7202
80	Transport	6600	32178	649
80	Recycle	-9775	-47657	-962
	TOTAL	457837	840418	340145

Table 7.5: Total LCC of FRP tubular tower

Year	Event	Cost	Inflated cost	NPV
0	Manufacture	233800	233800	233800
0	Import tax	0	0	0
0	Transport	82000	82000	82000
0	Installation	42562	42562	42562
20	Refurbishment	NA	NA	NA
40	Refurbishment	NA	NA	NA
60	Refurbishment	NA	NA	NA
80	Deconstruction	42562	207508	4187
80	Transport	6600	32178	649
80	Landfill and recycle	6672	32529	656
	TOTAL	414196	630577	363854

7.2.3 Life Cycle Assessment

The LCA is done based on the assumptions stated previously. The resulting equivalent CO_2-emission, given in kg, of the three tower designs are presented in Table 7.6.

Table 7.6: Result of LCA

	Steel lattice	Steel tubular	FRP tubular
Emission (kg CO_2)	17139	16321	37670

The total LCA of the towers for a life span of 40 years can be found in Tables 7.7, 7.8 and 7.9 for the steel lattice tower, steel tubular tower and FRP tubular tower respectively. A more detailed description of the LCA can be found in E.2.

Table 7.7: Total LCA of steel lattice tower for life span of 40 years

Year	Event	kg CO2
0	Manufacture	22375
0	Transport	2916
0	Installation	802
20	Refurbishment	180
40	Refurbishment	180
60	Refurbishment	180
80	Deconstruction	802
80	Transport	477
80	Recycle	-10773
	TOTAL	17139

Table 7.8: Total LCA of steel tubular tower for life span of 40 years

Year	Event	kg CO2
0	Manufacture	21114
0	Transport	2752
0	Installation	802
20	Refurbishment	180
40	Refurbishment	180
60	Refurbishment	180
80	Deconstruction	802
80	Transport	477
80	Recycle	-10166
	TOTAL	16321

Table 7.9: Total LCA of FRP tubular tower for life span of 40 years

Year	Event	kg CO2
0	Manufacture	35231
0	Transport	2168
0	Installation	501
20	Refurbishment	NA
40	Refurbishment	NA
60	Refurbishment	NA
80	Deconstruction	501
80	Transport	330
80	Landfill and recycle	-1060
	TOTAL	37670

Chapter 8

Discussion

8.1 Material Properties

The material properties for glass fibre reinforced polymers as given by Sinha and Vinay ((2010)) are presented in Table 8.1, where they are also compared to concrete, steel and wood.

Table 8.1: Material properties of FRP, concrete, steel and wood.

Material	FRP	Steel	Concrete	Timber
Glass fibre %	40-80	-	-	-
Specific gravity	1.66-2.05	7.85	2.4	0.42-0.52
Tensile strength (MPa)	200-1200	470-630	-	-
Tensile modulus (GPa)	19-32	210	-	-
Flexural strength (MPa)	200-1240	415-550	-	80
Flexural modulus (GPa)	12-20	210	-	11-12
Compressive strength (MPa)	200-480	220-250	20-60	17-50
Thermal conductivity (W/mK)	0.27-4	45-55	0.4-1.8	0.8-0.19
Coefficient of thermal expansion	7-10	6-12	10-15	1.7-2.5

Source: IPI (Indian Plastics Institute) Journal. 1998. p.21.

In Table 8.2 some key characteristics of the different materials are presented.

Table 8.2: Characteristics of FRP, steel, concrete and wood

Material	FRP	Steel	Concrete	Timber
Conductive	No	Yes	Steel reinf. can be	Moisture dependant
Durability	Very	Need corrosion protection	Quite	Need treatment
Environmental impact	No leaching Less energy	Rust, zinc. More energy	No leaching More energy	Creosote Low energy
Disposal	No problem with landfill	Special treatment	Usually no problem	If treated need special
Recycling	Limited	Yes	Some	Limited

8.1.1 Use in Electrical Utility Applications

Concrete is not used much in transmission towers in Norway. It is however common in other parts of the world, usually then as single reinforced poles. In regard to foundation work on the other hand, concrete is used much for its good moulding properties, durability and compressive strength.

Timber is more commonly used in Norway than concrete for self supporting poles in the regional and local distribution network (up to 132 kV). Since timber is a relatively ample resource in Norway using it yield low emissions in regard to transport. It offers good strength to weight properties, but is limited to smaller towers. When treated with creosote or similar substances, it is quite durable.

For transmission line sized towers steel is the most used material in Norway. Steel has a high strength to weight ratio which makes it ideal for use in construction. It is also quite durable when galvanised and can be painted if desired. Compared to for example concrete it can save much in regard to resources used and emissions for building the same structures, and it also offers more options in design.

Table 8.3: Comparison of steel and FRP in electrical utility application

Item	Steel	FRP
Durability	Needs corrosion protection, e.g. hot dipped galvanising.	Corrosion resistant. UV-degradable unless counteracted. Likely longer life span.
Conductivity	Electrically conductive. - Extra grounding not needed.	Electrically insulating. - Extra grounding needed. - Safer for workers.
Temperature	Brittle in cold conditions. Properties constant.	Remains ductile in cold conditions. Increased strength. Properties dependent on temperature.
Environment	Galvanised coating might leach into environment. Much is recycled and reused.	Does not leach into environment. Can be recycled, but not reused. Lower weight lead to less emissions from transport.
Assembly		Less lifts and hours needed.
Deflections	Smaller. Stiffer structure.	Larger. Can be overloaded.
Maintenance	No need for re-coating, but need repainting if used.	No need for coating, Can be coloured.
Replacements	Easy to replace and repair, both bolts and welds used. Cut surface must be coated.	Bolts are easy to replace. No need for coating.
Access	Lattice easily climbed - good for maintenance - need block for people Poles need stepping bolts.	Poles need stepping bolts. Safer as non-conductive. More vandalise resistant.
Experience	Much used and well known. Normal utilities used.	Less known to many. Might need special tools.

FRP, and in particular GFRP (glass fibre reinforced polymer), have recently become more and more common to use in transmission tower design, particularly in USA and Canada. It has in recent years also made its appearance in the Norwegian market, albeit for lower voltages. The low structural weight of the composite material is a great advantage for use in construction as it allows for lighter structures, and the high strength to weight ratio ensures strength is maintained.

Steel and GFRP are thus the best alternatives for design of transmission towers. Table 8.3 describes some of the advantages and disadvantages of using steel and GFRP in electrical utility applications.

Both steel and FRP have good material properties and offer durable solutions (as long as the steel is galvanised). No maintenance is needed for FRP and very little for steel. They can both be assumed to be durable in normal Norwegian weather conditions, but FRP absorbs more elastic energy than steel making it a better fit for storms and especially rough conditions. This can mean that some parts of the steel tower might need repair more often than the FRP.

As can be found from Table 8.1 FRP has a greater strength to weight ratio than steel. This is one of the best advantages FRP has. The low weight means lower costs and emissions in transport and assembly and safer installation for workers compared to using steel.

Another advantage of FRP is the insulating properties, which allows for maintenance to be done on an operational line with lower risk to the workers. It also decreases the risk of injury if unauthorised personnel should appear where they are not supposed to.

FRP can be manufactured to be any colour desired. Steel will need to be painted if the grey steel colour is unwanted. It is relatively normal to paint the towers so that they blend in with the environment. This can be for either camouflage or aesthetic reasons. This means the steel towers will need to be repainted every 20 years or so.

Unlike steel, which in cold weather steel can become brittle, FRP will stay ductile and actually increase in strength. This can be a great advantage since Norwegian winters can experience very low temperatures in many places.

In regard to toxicity zinc from the galvanised coating and rust if the coating is damaged can leach out into the environment from steel material (Toth, (2016)). This does not happen often, though it is a risk to consider. FRP is an inert material and does not pose a risk in regard to leaching or other environmental issues. It is therefore safe to landfill FRP without any treatment being conducted first. Steel is normally not used as landfill as most of it is recycled. What is not will need to be treated before it can be disposed.

FRP is not that common to use in load-bearing structures in Norway, both in terms of design and use. There are standards, like the Eurocode, that determines many aspects of steel design and can give help and guidance. For FRP there are no such standards to follow and there are no established requirements for manufacturers. This makes testing of the products vital to ensure material properties are as stated. It also makes the design process more difficult. As steel is more known and more workers are familiar with it, maintenance and assembly might be easier. New standards and measures may need to be developed to properly take advantage of FRPs differing qualities.

8.2 Tower Designs

For self supporting steel towers, lattice structures are often lighter because the truss structure works in tension and compression which is more efficient than pole structures that acts like a cantilever when loaded at the top. By using guyed towers, the cantilever effect is removed as the guys and legs then work in tension and compression respectively like in a truss structure. The weight of guyed towers can therefore be reduced by up to 50 % compared to self supporting ones. However, due to the uneven terrain often found in Norway, guyed structures might be difficult to place. This will need to be assessed further as it is assumed in this thesis that the legs are of even length and the guys fastened at the same point which might not be applicable in the real world.

The preliminary cross sections found are very small considering this is a

25 m high tower with much dead load, ice load and wind load. This may result from a mistake in the load calculations or too many simplifications. It may be that it is not enough to predetermine the cross sections based on compressive axial force only. The preliminary guy calculations are however not so off compared to what the analysis in PLS leads to. The wind load and ice load calculated are relatively similar to what PLS calculates. This should indicate that it is correct.

PLS checks the structures against all the load cases given in Table 4.9. These induce much stress in the different elements of the structures so that their cross sections will need to be changed from the preliminarily determined sizes. Figures 5.24, 5.29 and 5.33 show the maximum usage of the different tower structures for all load cases. From this it is easy to determine which elements can be changed up or down in order to optimise the cross sections.

Figures 5.21, 5.26 and 5.30 illustrate how all the towers along the lines are loaded. As one can see, some are more exposed to high stresses due to their location along the line, particularly when located on top of steep hills as the weight span of that tower then increases. For both the steel lattice tower line and the FRP tubular tower line, the insulator swing is larger than the maximum allowed value. This can be corrected by adding tension structures at these points, and generally throughout the line to take up the longitudinal loads.

Based on the figures showing the usage of the structures, the steel lattice structure looks as if it is utilised best. This might not however be for the entire structure, it can also mean that just one member is induced with high stresses. All the structures are analysed like this using the PLS programs and their cross sections have been determined as given in Tables 3.1, 3.3 and 3.4.

For some structures the stiffness is more important than strength. Even if the capacity is far from reached, the intended task of a structure may be dependant on deflections. The structures were therefore checked against the requirements stated in 6.2.2. The FRP tubular tower yields more deflections than the steel tubular tower, but both are within their requirements. The high ductility of FRP is very positive when considering cascade resistance.

FRP will actually be able to withstand up to two times overload (Toth, (2016)).

In addition to checking the deflection of the structures, the location and magnitude of maximum stresses should be considered. Especially for FRP this is important, to be able to determine the strength in each direction.

PLS calculates stresses based on the von Mises criteria both for steel and FRP. This might be fine also for FRP since the maximum shear stresses usually appear where the axial and bending stresses are minimum. This leads to the largest stresses appearing where shear stresses are close to zero. Since PLS only has been tested with FRP poles, it would be of great importance to check the stress in the structure. The maximum stresses should be checked both for steel and FRP and it is recommended to include this in any further work.

The steel poles were also checked against buckling based on load cases 01: Full ice load and 10: 500 year wind on clear line, as they were found to induce the largest moments and axial loads. It is assumed that the guys provide lateral stability, making the length of the elements 12.1 m. The poles were found to withstand the buckling load.

The wind load acting on the towers will excite the conductors and ground wires and induce vibrations. If the tower structures have similar natural frequencies as the cables, the cables might excite the tower structures and create resonance. This is undesirable and can harm the towers and hardware. As a rule of thumb, if the natural frequencies of the adjacent elements are more than 20 % of the value apart, there is no risk for them to coincide.

From Table 6.7 it is found that the steel lattice tower structure's 20 % limits based on 500 year wind loading and wind on ice loading are 0.520 Hz and 0.807 Hz respectively. From Table 6.6 we can see that both the conductor and ground wire have frequencies outside of this for all loop numbers and both wind load cases. From Table 6.7 it is found that the steel tubular tower structure's 20 % limits based on 500 year wind loading and wind on ice loading are 0.442 Hz and 0.460 Hz respectively. From Table 6.6 we can see that both the conductor and ground wire have frequencies outside of this for all loop numbers and both wind load cases. From Table 6.7 it is found that the FRP tubular tower structure's 20 % limits based on 500 year wind loading and wind on ice loading are 0.378 Hz and 0.420 Hz respectively. From Table 6.6 we can see that both the conductor and ground wire have frequencies outside of this for all loop numbers and both wind load cases.

All towers are thus adequate when checked for these wind loads. It might be relevant to check vibrations other set up by other wind velocities to see if they induce resonance. For example for lower wind velocities to check against aeolian vibrations.

8.3 LCCA and LCA

LCAs and LCCAs are done based on many assumptions and uncertain factors. It can be a hard task to correctly judge the different aspects of the analyses and experience is therefore key.

Since not all tower elements and life phases are included in the analyses, the results are only applicable under the stated conditions and to the materials chosen. When assessing the results it is important to keep this in mind as the differences found will make a lower impact when looking at the system as a whole, both for the LCCA and the LCA.

The steel elements used in the analysis are assumed produced by Dalekovod, which is one of the manufacturers used by Statnett today. Another one is Mitas, located in Turkey. Choosing a different manufacturer will change some of the costs and emissions in regard to transport, unless the delivery cost to Norway is included in the material cost. There are other manufacturers in Norway or closer such as Skanska, Contiga and Ruukki, but these are normally not used for the transmission network. They may however be relevant for the regional or distribution network. Ruukki's EPD for hot rolled steel elements is used as a basis for the LCA calculations, as well as the ones from Skanska and Contiga.

The FRP elements also have some uncertainty in regard to the transport part. When assuming they are produced in the US, extra costs and emissions are added by requiring longer transport stretches. However, as technology advances new and better systems are being used resulting in lower emissions from ships than trucks for the same load and distance. An alternative is to use manufacturers closer to Norway such as Jerol, Melbye or Rempro. This will reduce the costs which are quite large due to the long way of transport. As of now, Jerol and Melbye use the filament winding process which is more expensive, and Rempro only produce smaller poles used in the distribution network. In time this might however be an option. Jerol offers an EPD for their FRP elements (Jerol Industri AB, (2015)) which is used as a basis when calculating the emission for the manufacturing process of FRP elements. The cost used for FRP is given by Rempro after a discussion. This is given in NOK/m and is thus timed by the total length of tubular elements.

In the analyses conducted the cost of transportation has not been scaled according to weight transported. Some more difference can be made by doing so in a positive way for the lighter composite poles. Melbye Skandinavia AS gives the numbers shown in Figure 8.1 for different materials for 18 m long towers. This is based on conical modules that can be stored inside each other, but also for pultruded elements the lower weight of FRPs give some advantage. By utilising the full potential of the trucks, more FRP can be transported than steel in one go. When designing an entire line this can make some impact, but it will not be too large compared to material costs.

From the results of the LCCA presented in Table 8.4 the three towers are fairly similar in NPV, with the steel tubular tower being the least expensive, then the FRP tubular tower and the most expensive design being the steel lattice tower. The tubular steel design is the most economic alternative based on this LCCA.

Table 8.4: Result of LCC analysis

	Steel lattice	Steel tubular	FRP tubular
NPV (NOK)	377181	340145	363854

The LCCA is based on the current economic situation and also the assumed life span of the structure. To assess the difference changes in the economy can make on future investments a sensitivity analysis should therefore be conducted. In this analysis, three different aspects have been considered: the life span, discount rate and inflation.

Figure 8.1: Load capacity of truck for different materials (Melbye Skandinavia Norge AS, (2014))

The life span was originally assumed to be 80 years, which is is common practice for investments of tower structures. Hardware and other technical equipment will have an assumed life span of 40 years, but is excluded as it will be similar for all towers. With proper maintenance, steel towers can easily reach 80 years, and for FRP producers disagree on whether it should be 80 years (Jerol AB) or 120 years (Melbye Skandinaia AS). Therefore, two other analyses with differing life spans were conducted: 120 years and 120 years with steel being replaced. It might not be possible to have the steel tower standing for 120 years without larger replacement, which is not included in the analysis, but it is done to see how great the difference will be.

The originally assumed discount rate was set to 5 % and the inflation rate to 2 %. One analysis was conducted with a discount rate increased to 7 % and one where it was lowered to 3 %. The change in inflation was assessed by conducting analyses with the inflation rate set to 1 % and 3 %.

The resulting NPVs from these analyses, given in NOK, can be found in Table 8.5. A more thorough description of the sensitivity analysis conducted can be found in E.3.

Table 8.5: NPV in NOK from sensitivity analysis

	LATTICE	TUBULAR	FRP
80 years life span	377118	340145	363854
120 years life span, steel replaced	412529	372445	360085
120 years life span, steel maintained	372978	339707	360085
80 years life span	377118	340145	363854
80 years life span, discount rate 7 %	353754	321881	359576
80 years life span, discount rate 3 %	453162	393508	383944
80 years life span, inflation 3 %	404228	359761	370350
80 years life span, inflation 1 %	362020	328539	360859

The increase in life span from 80 and to 120 years affects the NPV some. As long as the steel is maintained, all the designs get less expensive as the life span increase, with the steel tubular tower design staying the least expensive alternative. When assuming the steel needs to be replaced, the FRP based alternative is the least expensive. Due to the discounting of the costs, this does not make as much an impact on the NPV as one might think.

As can be seen in Table 8.5 using a high discount rate favours the steel designs, making the FRP design the most expensive. A decreased discount rate favours the FRP design, as it then becomes the most economical alternative. This is to be expected as FRP has higher initial costs and steel have more costs later in life. The difference between the two steel designs also increase with a low discount rate. The impact from changing inflation still maintains the steel tubular tower as the most economical. A higher inflation favours the FRP tubular alternative over the steel lattice one, while a ower inflation evens out the difference between them.

Table 8.6: Result of LCA

	Steel lattice	Steel tubular	FRP tubular
Emission (kg CO_2)	17139	16321	37670

As seen in the results from the life cycle assessment in Table 8.6 the global warming potential of the FRP tower is greater than that of steel ones. This is primarily due to the large emissions from the manufacturing phase as seen in Table 7.9. In addition to the recycling potential of the steel these constitute a great difference. The advantages the low weight give in transportation and assembly are not enough to close the gap. In regard to waste management of the decommissioned towers, it is assumed that most of the steel is recycled. FRPs are assumed to be land filled, and as there are no emissions from FRP to air or water this is a good solution.

However, since the emissions in the production phase are so large, it would be better to recycle the FRP. As discussed by Shuaib and Mativenga ((2016)) recovering products from waste uses much less energy than producing virgin materials. Thus by recycling the FRPs as well the carbon footprint can be reduced. This is based on a process where the materials are granulated which means they cannot be used in the same way as before as the fibres no longer are clean and long. Some research is being conducted on fungi and polymers to assess the possibility of recycling the glass fibres while keeping them intact. In the future this might be a possibility, which can greatly reduce the global warming potential as seen in Table 7.9. The expectation is that by the time of the commissioning of these towers, complete recycling of FRP will be possible (Toth, (2016)).

An assessment done by Erlandsson (2011)) also considers different materials used for utility poles, including both concrete and wood in addition to steel and FRP. This assessment considers more types of environmental impact than just CO_2-equivalents. It is found that FRP generally scores similarly or better than steel. Especially considering human toxicity it is better.

If the assumed life span was increased so that the steel would have to be replaced and not the FRP, the environmental impact of the steel towers would almost be similar to that of the FRP. This could likely happen if one is to trust manufacturers and if so these results should not make as great an impact on the decision.

Chapter 9

Conclusion

Both steel and FRP offer good material properties for use in transmission towers. Their properties are in many cases similar, but the insulating abilities and low weight of FRP does give it an advantage relative to steel.

All the three different tower designs with the chosen dimensions are found to be of sufficient strength.

Based on the life cycle cost analysis conducted the steel tubular tower offers the most economic design, with the FRP tubular tower as the second most economic. The most expensive tower design is the steel lattice tower.

From the environmental life cycle assessment conducted one can see that the designs using steel offers the most environmentally friendly alternatives, with the tubular design being the best one. The FRP tubular tower design scores lower when it comes to environmental impact as the emissions of CO_2-equivalents is the highest of the three by about the double of the others.

The sensitivity of the analyses in regard to inflation and life span is deemed quite low as the results stay mostly the same when these parameters are changed. Using a lower discount rate will however change the outcome and must be considered.

Based on this, the conclusion is that FRP can make a good alternative to the traditional use of steel in transmission towers, particularly when considering the life cycle costs. The initial cost however, is lower for the steel designs. Developing new and efficient recycling processes of FRP and routines and standardisations for its use and design, can lead to FRP becoming a better alternative in the future, particularly in regard to emissions.

For the time being, the steel tubular tower design is considered a better alternative when both life cycle cost and environmental impact are considered.

Some further work that can be assessed:
- detailed connection design
- optimising span length in regard to cost by comparing costs for different tower heights
- hand calculations of stresses in the tower members and buckling of FRP-poles

Bibliography

Airbus Helicopters Inc, (2017). *H135 (formerly known as EC135) specifications*. (Used: 20. December 2016).
URL http://airbushelicoptersinc.com/products/H135-specifications.asp

Akovali, G., Uyanik, N., Kaynak, C., Akgül, T., Kenig, S., Parnas, L., Ardiç, S., Giordano, M., Borzacchiello, A., Nicolais, L., Elaldi, F., (2001). *Handbook of Composite Fabrication*. Rapra Technology Limited, UK.

Alfredsen, K., Brattebø, H., Heie, A., Killingtveit, Å., Lia, L., Renaas, M., Sægrov, S., Thorolfsson, S. T., Østerhus, S. W., (2012). *Kompendium TVM4101 BM2 Vann- og miljøteknikk*. NTNU - IVT - IVM.

Blevins, R. D., (2016). *Formulas for Dynamics, Acoustics and Vibration*, 1st Edition. John Wiley & Sons, Ltd.

Brown, R., (2002). *Handbook of Polymer Testing*. Rapra Technology Ltd.

Catchpole, P., Fife, B., (2014). *Structural Engineering of Transmission Lines*. ICE Publishing.

CEN, (2005). *NS-EN 1993-1-1:2005+NA:2008: Prosjektering av stålkonstruksjoner - Del 1-1: Allmenne regler og regler for bygninger*. Standard Norge.

CENELEC, (2012). *FprEN 50341-1:2012 Overhead electrical lines exceeding AC 1 kV - Part 1: General requirements - Common specifications*. CENELEC - European Committee for Electrotechnical Standardization.

Dudok van Heel, D., Maas, T., De Gijt, J., Said, M., (2011). *Comparison of Infrastructure Designs for Quay Wall and Small Bridges in Concrete, Steel, Wood and Composites with Regard to the CO2-Emission and the Life Cycle Analysis*, the 3rd International Conference of EACEF.

Duflou, J. R., Deng, Y., Van Acker, K., Dewulf, W., (2012). *Do fiber-reinforced polymer composites provide environmentally benign alternatives? A life-cycle-assessment-based study*. MRS Bulletin 37 (4), 374–382.

Erlandsson, M., 2011. *Comparison of the environmental impacts from utility poles in different materials - a life cycle assessment*. Tech. rep., IVL Swedish Environmental Research Institute AB.

Gani, F., Légeron, F., (2010). *Dynamic response of transmission lines guyed towers under wind loading*. Canadian Journal of Civil Engineering 37, 450–464.

Halliwell, S., (2002). *Polymers in Buildings and Structures*. Rapra Technology Ltd.

Haram, H. K., (2017). *Mye mindre CO2 via sjø*. (Used: 20. December 2016).
URL http://old.shortseashipping.no/sitepages/News.aspx?t=Mye+mindre+CO2+via+sj%C3%B8

Hellik Teigen, January (2017). *Private communication*.

Huntsman International LLC_1, (2013). *Video - How it works: Filament Winding*. (Used: 10. October 2016).
URL https://www.youtube.com/watch?v=ign6W5ENJAA

Huntsman International LLC_2, (2016). *Video - Pultrusion*. (Used: 10. October 2016).
URL https://www.youtube.com/watch?v=YFyvCf322_g

Jerol Industri AB, (2015). *Kap. 11. Miljöaspekter – arbetsmiljö och markmiljö*. (Used: 23. November 2016).
URL http://jerol.se/wp-content/uploads/2014/11/Kap11_Miljoaspekter_2015-11-05.pdf

Kendall, D., unknown. *Fibre Reinforced Polymer (FRP) Composite Buildings - Future Opportunities*. National Composites Network.

Kiessling, F., Nefzger, P., Nolasco, J. F., Kaintzyk, U., (2003). *Overhead Power Lines*. Springer.

Knutsen, R. G., January (2017). *Private communication*.

Larsen, P. K., (2015). *Dimensjonering av stålkonstruksjoner*. Fagbokforlaget Vigmostad og Bjørke AS, Norway.

Lilien, J.-L., (2013). *Power Line Aeolian Vibrations*. Tech. rep., Department of Electronics, Electricity and Computer Sciences, University of Liège.

Melbye Skandinavia Norge AS, (2014). *Komposittmaster - Fremtidens løsning i dag*. (Used: 10. September 2016).
URL `http://www.melbye.com/melbye/frontend/mediabank/2294/Komposittmaster-web.pdf`

Peters, S. T., (2011). *Composite Filament Winding*. ASM International.

Power Line Systems Inc$_1$, (Updated 2016). *PLS-CADD (Power Line Systems - Computer Aided Design and Drafting)*. (Used: 16. September 2016).
URL `https://www.powline.com/products/pls_cadd.html`

Power Line Systems Inc$_3$, (Updated 2016). *PLS-POLE (Power Line Systems - Computer Aided Design and Drafting)*. (Used: 16. September 2016).
URL `https://www.powline.com/products/pls_pole.html`

Power Line Systems Inc$_4$, (2016). *PLS-CADD User's Manual, version 14.2*.

Power Line Systems Inc$_5$, (2016). *PLS-POLE User's Manual, version 14.2*.

Power Line Systems Inc$_6$, (2016). *PLS-TOWER User's Manual, version 14.2*.

Power Line SystemsI nc_2, (Updated 2016). *PLS-TOWER (Power Line Systems - Computer Aided Design and Drafting)*. (Used: 16. September 2016).
URL `https://www.powline.com/products/tower.html`

Preformed Line Products, (2016). *Conductor Galloping Basics*. (Used: 19. December 2016).
URL `http://www.preformed.com/images/pdfs/Energy/Transmission/Motion_Control/Detuning_Pendulum/Conductor_Galloping_Basics-EN-ML-1166.pdf`

Remer, D. S., Nieto, A. P., (1995). *A compendium and comparison of 25 project evaluation techniques. Part 1: Net present value and rate of return methods*. International Journal of Production Economics 42, 79–96.

Rempro AS, January (2017). *Private communication*.

Renovasjonsselskapet for Drammensregionen IKS, (2017). *Prisliste for levering av næringsavfall*. (Used: 20. December 2016).
URL `http://www.rfd.no/bedrift/bli-bedriftskunde/priser/prisliste`

Ruukki Construction Oy, (2015). *NEPD-324-204-EN Welded and coated sections, trusses and beams made of hot-rolled plate, sheet and coil*.

Shuaib, N. A., Mativenga, P. T., (2016). *Energy demand in mechanical recycling of glass fibre reinforced thermoset plastic composites*. Journal of Cleaner Production 120, 198–206.

Sinha, S., Vinay, K., (2010). *Polymeric Systems and Applications*. Studium Press (India) Pvt. Ltd.

Solomon, S., Qin, D., Manning, M., Alley, R. B., Berntsen, T., Bindoff, N. L., Chen, Z., Chidthaisong, A., Gregory, J. M., Hegerl, G. C., Heimann, M., Hewitson, B., Hoskins, B. J., Joos, F., Jouzel, J., Kattsov, V., Lohmann, U., Matsuno, T., Molina, M., Nicholls, N., Overpeck, J., Raga, G., Ramaswamy, V., Ren, J., Rusticucci, M., Somerville, R., Stocker, T. F., Whetton, P., Wood, R. A., Wratt, D., (2007). *Technical Summary*. Climate Change 2007: The Physical Science Basis. Contribution of Working Group I to the Fourth Assessment Report of the Intergovernmental Panel on Climate Change.

Statnett SF, (2016). *About us - Statnett*. (Used: 22. November 2016).
URL http://www.statnett.no/en/About-Statnett/

The Environmental Literacy Council, (2015). *Life Cycle Analysis*. (Used: 23. November 2016).
URL https://enviroliteracy.org/environment-society/life-cycle-analysis/

The Norwegian EPD Foundation, (2016). *Hva er en EPD?* (Used: 25. November 2016).
URL http://epd-norge.no/hva-er-en-epd/

The Norwegian National Committee, (2008). *NO NNA-EN 50341-3-16:2008: National Normative Aspects for Norway*. CENELEC - European Committee for Electrotechnical Standardization.

The Physics Classroom, (1996-2016). *Natural Frequency*. (Used: 19. December 2016).
URL http://www.physicsclassroom.com/class/sound/Lesson-4/Natural-Frequency

Toth, J., September (2016). *Private communication*.

Triple Pundit: Pablo, (2007). *AskPablo: Helicopter Emissions*. (Used: 20. December 2016).
URL http://www.triplepundit.com/2007/10/askpablo-helicopter-emissions/

Vinson, J. R., Sierakowski, R. L., (1993). *The behaviour of structures composed of composite materials*. Kluwer Academic Publishers.

Vinson, J. R., Sierakowski, R. L., (2012). *The Behaviour of Structures Composed of Composite Materials*, 2nd Edition. Kluwer Academic Publishers.

Wallenius Wilhelmsen Logistics, (2016). *Sustainability report 2015*. (Used: 20. December 2016).
URL http://www.2wglobal.com/news-and-insights/infographics/sustainability-report-2015/#.WH9juIWcHIU

White, H. B., (1993). *Guyed structures for transmission lines*. Engineering Structures 15 (4), 289–302.

Woodward, D. G., (1997). *Life cycle costing - theory, information acquisition and application*. International Journal of Project Management 15 (6), 335–344.

Wübbenhorst, K. L., (1986). *Life Cycle Costing for Construction Projects*. Long Range Planning 19 (4), 87–97.

Appendices

A Load cases

Table A.1 shows the different load cases used in the program in order to check all load situations as given by FprEN 50341-1 and the NO NNA. The description of how they should be applied to the line is also given.

Table A.1: Description of load cases for suspension towers

Description	**Weather case**	**Cable condition**	**Adjust cable loads**	**Adjustment explanation**
0 EDS	EDS	Initial FE	No	Applied to all phases and ground wires
1 Full ice load	Full ice load	Initial FE	No	Applied to all phases and ground wires
2 Uneven ice load - Transverse bending towards the right	100% ice load	Load FE	Yes	70% ice thickness on right phase and ground wire of both spans, 30% on rest
3 Uneven ice load - Transverse bending towards the left	100% ice load	Load FE	Yes	70% ice thickness on left phase and ground wire of both spans, 30% on rest
4 Uneven ice load previous span	Uneven ice load previous span	Load FE	No	-
5 Uneven ice load next span	Uneven ice load next span	Load FE	No	-
6 Uneven ice load previous span - Transverse bending towards the right	Uneven ice load previous span	Load FE	Yes	233% ice thickness on right phase and ground wire of previous span
7 Uneven ice load previous span - Transverse bending towards the left	Uneven ice load previous span	Load FE	Yes	233% ice thickness on left phase and ground wire of previous span
8 Uneven ice load next span - Transverse bending towards the right	Uneven ice load next span	Load FE	Yes	233% ice thickness on right phase and ground wire of next span
9 Uneven ice load next span - Transverse bending towards the left	Uneven ice load next span	Load FE	Yes	233% ice thickness on left phase and ground wire of next span
10 Wind on line towards the right	Wind 500 years	Load FE	No	(Wind direction NA+)
11 Wind on line towards the left	Wind 500 years	Load FE	No	(Wind direction NA-)
12 Wind on ice towards the right	Wind on ice	Load FE	No	(Wind direction NA+)
13 Wind on ice towards the left	Wind on ice	Load FE	No	(Wind direction NA-)
14 Minimum temperature	Min temp	Initial FE	Yes	145% on all loads of both spans
15 Line break left phase next span	Assembly	Initial FE	Yes	80% on all loads on left phase of next span
16 Line break left phase previous span	Assembly	Initial FE	Yes	80% on all loads on left phase of previous span
17 Line break middle phase next span	Assembly	Initial FE	Yes	80% on all loads on middle phase of next span
18 Line break middle phase previous span	Assembly	Initial FE	Yes	80% on all loads on middle phase of previous span
19 Line break right phase next span	Assembly	Initial FE	Yes	80% on all loads on right phase of next span
20 Line break right phase previous span	Assembly	Initial FE	Yes	80% on all loads on right phase of previous span
21 Line break left ground wire next span	Assembly	Initial FE	Yes	Broken subconductor left ground wire next span
22 Line break left ground wire previous span	Assembly	Initial FE	Yes	Broken subconductor left ground wire next span
23 Line break right ground wire next span	Assembly	Initial FE	Yes	Broken subconductor right ground wire next span
24 Line break right ground wire previous span	Assembly	Initial FE	Yes	Broken subconductor right ground wire previous span

B Derivations

B.1 Transverse Forces Derivation

TRANSVERSE FORCE DERIVATION

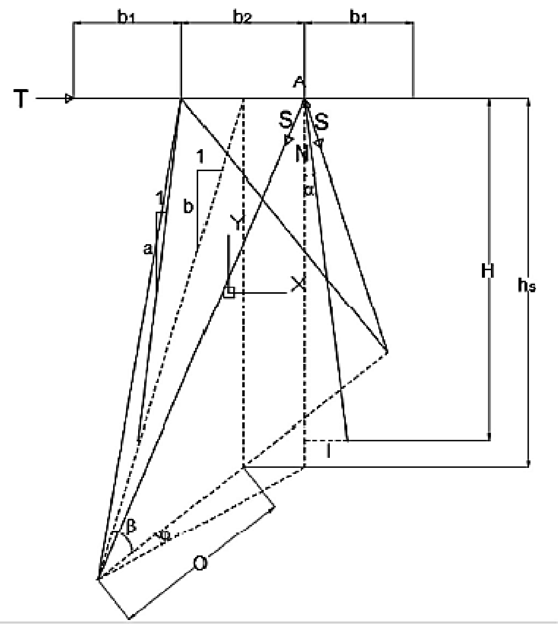

The sum of forces in point A:

$$\Sigma X = T - 2 \cdot S \cdot \sin(\phi_1) - \sin(\phi_2) \cdot N = 0 \tag{1}$$

$$\Sigma Y = N \cdot \cos(\phi_2) - 2 \cdot S \cdot \cos(\phi_1) \cdot \cos(\phi_3) = 0 \tag{2}$$

This leads to:

$$N = \frac{2 \cdot S \cdot \cos(\phi_1) \cdot \cos(\phi_3)}{\cos(\phi_2)} \tag{3}$$

Created with PTC Mathcad Express. See www.mathcad.com for more information.

Inserted (3) into (1) gives:

$$0 = T - 2 \cdot S \cdot sin\left(\phi_1\right) - \frac{2 \cdot S \cdot cos\left(\phi_1\right) \cdot cos\left(\phi_3\right)}{cos\left(\phi_2\right)} \cdot sin\left(\phi_2\right) \qquad (4)$$

$$0 = T - 2 \cdot S \cdot sin\left(\phi_1\right) - 2 \cdot S \cdot tan\left(\phi_2\right) \cdot cos\left(\phi_1\right) \cdot cos\left(\phi_3\right)$$

$$T = 2 \cdot S \cdot \left(sin\left(\phi_1\right) + tan\left(\phi_2\right) \cdot cos\left(\phi_1\right) \cdot cos\left(\phi_3\right)\right)$$

$$S = \frac{T}{2} \cdot \frac{1}{\left(sin\left(\phi_1\right) + tan\left(\phi_2\right) \cdot cos\left(\phi_1\right) \cdot cos\left(\phi_3\right)\right)} \qquad (5)$$

$$sin\left(\phi_1\right) = \frac{b_2}{L_1} \qquad (6)$$

$$cos\left(\phi_1\right) = \frac{L_2}{L_1} = \frac{\sqrt{1+b^2} \cdot \frac{h_s}{b}}{L_1} \qquad (7)$$

$$cos\left(\phi_3\right) = \frac{h_s}{L_2} = \frac{1}{\sqrt{1+b^2} \cdot \frac{1}{b}} = \frac{b}{\sqrt{1+b^2}} \qquad (8)$$

$$tan\left(\phi_2\right) = \frac{1}{a} \qquad (9)$$

Inserting (6), (7), (8) and (9) into (5):

$$S = \frac{T}{2} \cdot \frac{1}{\frac{b_2}{L_1} + \frac{1}{a} \cdot \frac{1}{L_1}} = \frac{T}{2} \cdot \frac{1}{\frac{b_2}{L_1} + \frac{h_s}{a \cdot L_1}} = \frac{T}{2} \cdot \frac{1}{\frac{1}{L_1} \cdot \left(b_2 + \frac{h_s}{a}\right)}$$

$$= \frac{T \cdot L_1}{2} \cdot \frac{1}{b_2 + \frac{h_s}{a}} = \frac{T \cdot L_1}{2} \cdot \frac{a}{b_2 \cdot a + h_s} \qquad (10)$$

Force in guy:

$$S = T \cdot \frac{L_1 \cdot a}{2 \cdot \left(h_s + a \cdot b_2\right)} \qquad (11)$$

$$cos\left(\phi_2\right) = \frac{a}{\sqrt{1+a^2}} \qquad (12)$$

Inserting (6), (7), (8), (9), (11) and (12) into (3):

$$N = \frac{2 \cdot \left(T \cdot \frac{L_1 \cdot a}{2 \cdot \left(h_s + a \cdot b_2\right)}\right) \cdot \left(\frac{\sqrt{1+b^2} \cdot \frac{h_s}{b}}{L_1}\right) \cdot \frac{b}{\sqrt{1+b^2}}}{\frac{a}{\sqrt{1+a^2}}}$$

$$= T \cdot \frac{1}{\left(h_s + a \cdot b_2\right)} \cdot h_s \cdot \sqrt{1+a^2} \qquad (13)$$

Force in leg:

$$N = T \cdot \frac{h_s \cdot \sqrt{1+a^2}}{\left(h_s + a \cdot b_2\right)} \qquad (14)$$

B.2 Longitudinal Forces Derivation

LONGITUDINAL FORCE DERIVATION

Symmetrical tower and guys. Assumed only the long guys take tension.

Superposition of two cases give the wanted case:

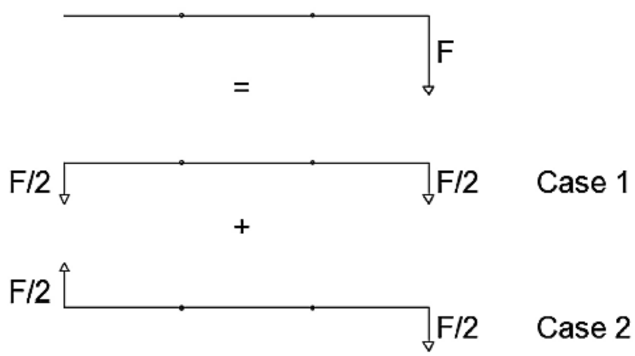

Case 1: Half force in same direction. Leads to a tensional force in guy 1 and guy 2.

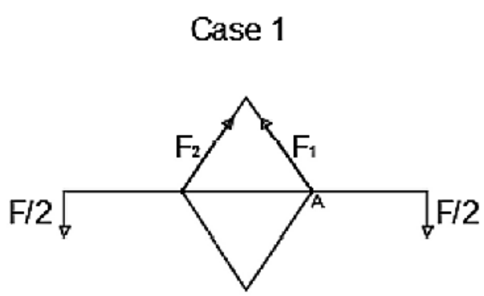

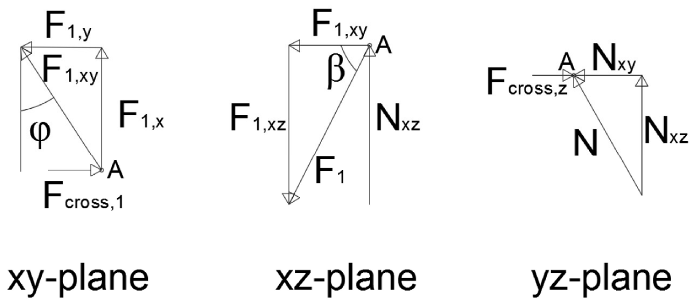

Due to symmetry and sum of forces in X-direction:

$$F_{1.X} = \frac{F}{2}$$

$$F_{1.XY} = F_{2.XY} = \frac{F_{1.X}}{cos(\phi)} = \frac{F}{2 \cdot cos(\phi)}$$ In the horizontal direction (XY-plane)

Leads to a compression force in the crossarm:

$$F_{cross.1} = F_{1.XY} \cdot tan(\phi) = \frac{F \cdot tan(\phi)}{2 \cdot cos(\phi)}$$

Force needs to be in 3D. Leads to compression force in the leg:

$$F_1 = F_2 = \frac{F_{1.XY}}{cos(\beta)} = \frac{F}{2 \cdot cos(\phi) \cdot cos(\beta)}$$ Tension force in guy 1 and 2, 3D

$$N_{XZ} = F_{1.XY} \cdot tan(\beta) = \frac{F \cdot tan(\beta)}{2 \cdot cos(\phi)}$$ Compression force in leg, xz-plane

$$N = \frac{N_{XZ}}{cos(\alpha)} = \frac{F \cdot tan(\beta)}{2 \cdot cos(\phi) \cdot cos(\alpha)}$$ Compression force in leg, 3D

Leads to additional compression force in the crossarm:

$$F_{cross.2} = N \cdot tan(\alpha) = \frac{F \cdot tan(\beta) \cdot tan(\alpha)}{2 \cdot cos(\phi) \cdot cos(\alpha)}$$

The total force in the crossarm will be:

$$F_{cross} = F_{cross.1} + F_{cross.2} = F_{cross.1} = \frac{F}{2} \cdot \frac{tan(\phi)}{cos(\phi)} + \frac{F \cdot tan(\beta) \cdot tan(\alpha)}{2 \cdot cos(\phi) \cdot cos(\alpha)}$$

$$F_{cross} = \frac{F}{2} \cdot \left(\frac{tan(\phi)}{cos(\phi)} + \frac{tan(\beta) \cdot tan(\alpha)}{cos(\phi) \cdot cos(\alpha)} \right)$$

Case 2: Half force in different direction. Leads to a tensional force in guy 1 and 4.

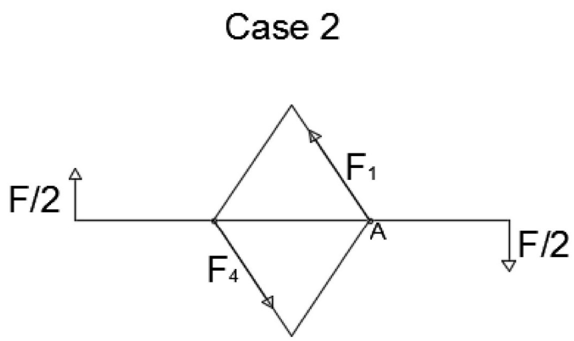

Due to symmetry and sum of forces in X-direction:

$$F_{1.X} = \frac{F}{2}$$

$$F_{1.XY} = F_{4.XY} = \frac{F_{1.X}}{cos(\phi)} = \frac{F}{2 \cdot cos(\phi)}$$ In the horizontal direction (XY-plane)

Leads to a compression force in the crossarm:

$$F_{cross.1} = F_{1.XY} \cdot tan(\phi) = \frac{F}{2} \cdot cos(\phi)$$

Force needs to be in 3D. Leads to compression force in the leg:

$$F_1 = F_4 = \frac{F_{1.XY}}{cos(\beta)} = \frac{F}{2 \cdot cos(\phi) \cdot cos(\beta)}$$ Tension force in guy 1 and 4, 3D

$$N_{XZ} = F_{1.XY} \cdot tan(\beta) = \frac{F \cdot tan(\beta)}{2 \cdot cos(\phi)}$$ Compression force in leg, xz-plane

$$N = \frac{N_{XZ}}{cos(\alpha)} = \frac{F \cdot tan(\beta)}{2 \cdot cos(\phi) \cdot cos(\alpha)}$$ Compression force in leg, 3D

Leads to additional compression force in the crossarm:

$$F_{cross.2} = N \cdot tan(\alpha) = \frac{F \cdot tan(\beta) \cdot tan(\alpha)}{2 \cdot cos(\phi) \cdot cos(\alpha)}$$

The total force in the crossarm will be:

$$F_{cross} = F_{cross.1} + F_{cross.2} = F_{cross.1} = \frac{F}{2} \cdot \frac{tan(\phi)}{cos(\phi)} + \frac{F \cdot tan(\beta) \cdot tan(\alpha)}{2 \cdot cos(\phi) \cdot cos(\alpha)}$$

$$F_{cross} = \frac{F}{2} \cdot \left(\frac{tan(\phi)}{cos(\phi)} + \frac{tan(\beta) \cdot tan(\alpha)}{cos(\phi) \cdot cos(\alpha)} \right)$$

Superposition: to determine final forces**.**

Force in crossarm:

$$F_{ca} = 2 \cdot \left(\frac{F}{2} \cdot \left(\frac{tan(\phi)}{cos(\phi)} + \frac{tan(\beta) \cdot tan(\alpha)}{cos(\phi) \cdot cos(\alpha)} \right) \right) = F \cdot \left(\frac{tan(\phi)}{cos(\phi)} + \frac{tan(\beta) \cdot tan(\alpha)}{cos(\phi) \cdot cos(\alpha)} \right)$$

Force in leg:

$$N = 2 \cdot \left(\frac{F \cdot tan(\beta)}{2 \cdot cos(\phi) \cdot cos(\alpha)} \right) = F \cdot \frac{tan(\beta)}{cos(\phi) \cdot cos(\alpha)}$$

Force in guy wire 1:

$$F_1 = 2 \cdot \left(\frac{F}{2 \cdot cos(\phi) \cdot cos(\beta)} \right) = F \cdot \frac{1}{cos(\phi) \cdot cos(\beta)}$$

Force in guy wire 2 and 4:

$$F_2 = F_4 = \frac{F}{2} \frac{1}{cos(\phi) \cdot cos(\beta)}$$

Force in guy wire 3:

$$F_3 = 0$$

When all cables are loaded:

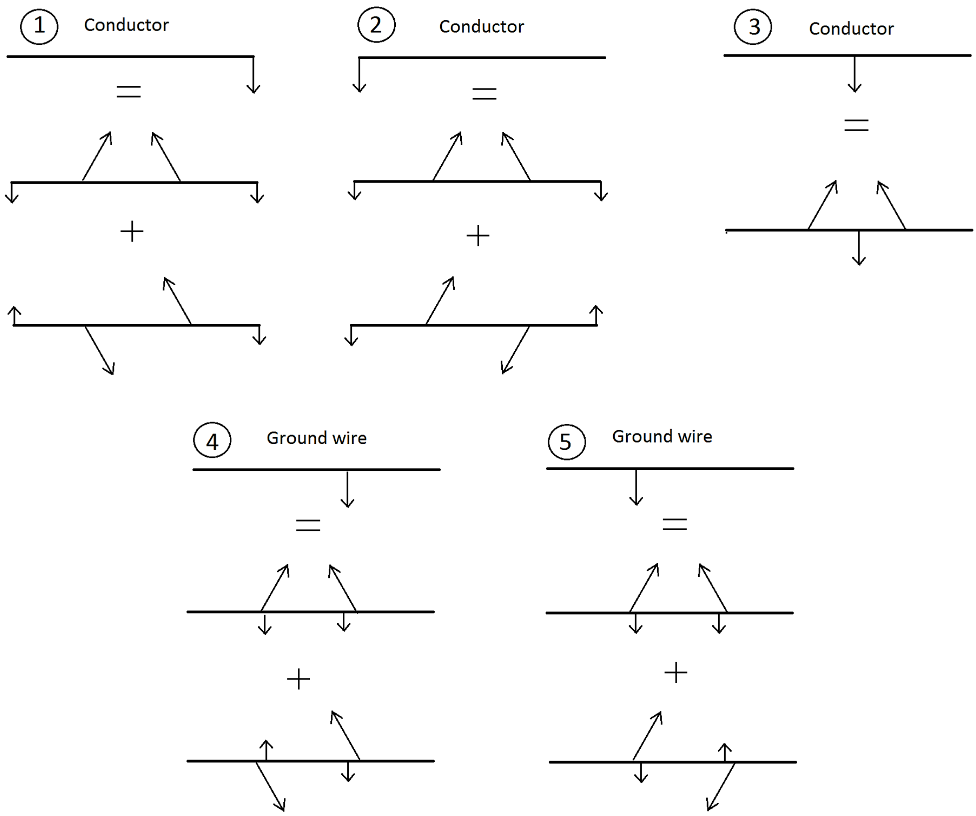

$G_1 = F_1 \cdot 3 + F_2 \cdot 2$	Force in guy 1
$G_2 = F_1 \cdot 3 + F_2 \cdot 2$	Force in guy 2
$G_3 = 2 \cdot F_4$	Force in guy 3
$G_4 = 2 \cdot F_4$	Force in guy 4
$L_1 = L_2 = N \cdot 5$	Force in leg
$CA = F_{ca} \cdot 5$	Force in cross arm

C Calculations and Checks

C.1 Wind Loads

$V_{b.0} := 35\ \frac{m}{s}$ — Design wind speed for 50 year return period given by ARA Engineering. Normal component. Max wind at 38 m/s.

Conversion factors:

$q_3 := 0.76$ — Conversion factor, 3 year return period.

$q_{50} := 1.0$ — Conversion factor, 50 year return period.

$q_{150} := 1.09$ — Conversion factor, 150 year return period.

$q_{500} := 1.18$ — Conversion factor, 500 year return period.

Assume terrain category II. Table 4.1 of 50341-1:2012:

$z_0 := 0.05$ — Roughness length.

$k_r := 0.189$ — Terrain factor.

Mean wind velocity. Clause 4.3.2 of 50341-1:2012:

$c_{dir} := 0.8$

$c_0 := 1$

Reference height for each component, conservative.

$h := 15 \qquad V_{h.15} := V_{b.0} \cdot q_{150} \cdot c_{dir} \cdot c_0 \cdot k_r \cdot \ln\left(\frac{h}{(z_0)}\right) = 32.901 \ \frac{m}{s}$

$h := 23 \qquad V_{h.23} := V_{b.0} \cdot q_{150} \cdot c_{dir} \cdot c_0 \cdot k_r \cdot \ln\left(\frac{h}{(z_0)}\right) = 35.367 \ \frac{m}{s}$

$h := 25 \qquad V_{h.25} := V_{b.0} \cdot q_{150} \cdot c_{dir} \cdot c_0 \cdot k_r \cdot \ln\left(\frac{h}{(z_0)}\right) = 35.848 \ \frac{m}{s}$

$h := 28 \qquad V_{h.28} := V_{b.0} \cdot q_{150} \cdot c_{dir} \cdot c_0 \cdot k_r \cdot \ln\left(\frac{h}{(z_0)}\right) = 36.501 \ \frac{m}{s}$

$h := 30 \qquad V_{h.30} := V_{b.0} \cdot q_{150} \cdot c_{dir} \cdot c_0 \cdot k_r \cdot \ln\left(\frac{h}{(z_0)}\right) = 36.899 \ \frac{m}{s}$

Mean wind pressure. Clause 4.3.3 of 50341-1:2012:

$\rho := 1.25 \ \frac{kg}{m^3}$ Air density factor.

Mean wind pressure.

$h := 15 \qquad q_{h.15} := \frac{1}{2} \cdot \rho \cdot V_{h.15}^{\ 2} = 676.548 \ Pa$

$h := 23 \qquad q_{h.23} := \frac{1}{2} \cdot \rho \cdot V_{h.23}^{\ 2} = 781.749 \ Pa$

$h := 25 \qquad q_{h.25} := \frac{1}{2} \cdot \rho \cdot V_{h.25}^{\ 2} = 803.156 \ Pa$

$h := 28 \qquad q_{h.28} := \frac{1}{2} \cdot \rho \cdot V_{h.28}^{\ 2} = 832.716 \ Pa$

$h := 30 \qquad q_{h.30} := \frac{1}{2} \cdot \rho \cdot V_{h.30}^{\ 2} = 850.973 \ Pa$

Turbulence intensity and peak wind pressure. Clause 4.3.4 of 50431-1:2012:

Turbulence intensity.

$h:=15 \qquad I_{V.15}:=\dfrac{1}{c_0 \cdot \ln\left(\dfrac{h}{z_0}\right)}=0.175$

$h:=23 \qquad I_{V.23}:=\dfrac{1}{c_0 \cdot \ln\left(\dfrac{h}{z_0}\right)}=0.163$

$h:=25 \qquad I_{V.25}:=\dfrac{1}{c_0 \cdot \ln\left(\dfrac{h}{z_0}\right)}=0.161$

$h:=28 \qquad I_{V.28}:=\dfrac{1}{c_0 \cdot \ln\left(\dfrac{h}{z_0}\right)}=0.158$

$h:=30 \qquad I_{V.30}:=\dfrac{1}{c_0 \cdot \ln\left(\dfrac{h}{z_0}\right)}=0.156$

Peak wind pressure.

$h:=15 \qquad q_{p.15}:=\left(1+7 \cdot I_{V.15}\right) \cdot q_{h.15}=\left(1.507 \cdot 10^{3}\right)\ \mathbf{Pa}$

$h:=23 \qquad q_{p.23}:=\left(1+7 \cdot I_{V.23}\right) \cdot q_{h.23}=\left(1.674 \cdot 10^{3}\right)\ \mathbf{Pa}$

$h:=25 \qquad q_{p.25}:=\left(1+7 \cdot I_{V.25}\right) \cdot q_{h.25}=\left(1.708 \cdot 10^{3}\right)\ \mathbf{Pa}$

$h:=28 \qquad q_{p.28}:=\left(1+7 \cdot I_{V.28}\right) \cdot q_{h.28}=\left(1.754 \cdot 10^{3}\right)\ \mathbf{Pa}$

$h:=30 \qquad q_{p.30}:=\left(1+7 \cdot I_{V.30}\right) \cdot q_{h.30}=\left(1.782 \cdot 10^{3}\right)\ \mathbf{Pa}$

Wind force on conductor, 50341-1:2012:

$q_{p.23} = \left(1.674 \cdot 10^3\right) \; Pa$ Peak wind pressure

$G_c := 0.4$ Structural factor for the conductor/span factor

N

$C_c := 1$ Drag factor for the conductor/force coefficient

$d := 34 \cdot 3 \; mm$ Diameter of conductor

$L_1 := 350 \; m$ Length of span 1

$L_2 := 350 \; m$ Length of span 2

$\phi := 0 \; deg$ Angle between wind direction and long. axis of crossarm

$\theta_1 := 0$ Change in angle of line

$\theta_2 := 0$ Change in angle of line

Wind coming in the direction of the crossarm:

$$Q_{wc.v1} := q_{p.23} \cdot G_c \cdot C_c \cdot d \cdot \cos(\phi)^2 \cdot \frac{L_1 + L_2}{2} = 23.909 \; kN$$

$$Q_{wc.v2} := 0 = 0 \; \frac{1}{N} \cdot kN$$

Wind force on ground wire:

$d_{gw} := 21 \; mm$ Diameter of conductor

$$Q_{gw} := q_{p.30} \cdot G_c \cdot C_c \cdot d_{gw} \cdot \cos(\phi)^2 \cdot \frac{L_1 + L_2}{2} = 5.24 \; kN$$

3 triplex conductors and two ground wires.

$Q_{T.c} := Q_{wc.v1} \cdot 3 = 71.726 \; kN$ Wind force from all subconductors

$Q_{T.gw} := Q_{gw} \cdot 2 = 10.479 \; kN$ Wind force from all subconductors

Wind on insulator sets, clause 4.4.2 of 50341-1:2012:

$q_{p.23} = \left(1.674 \cdot 10^{3}\right)\ \boldsymbol{Pa}$ Peak wind pressure

$G_{ins} := 1$ Structural factor, recommended value

$C_{ins} := 1.2$ Drag factor, recommended value

$A_{ins} := 4458\ \boldsymbol{mm} \cdot 30\ \boldsymbol{mm}$ Projected area of insulator set

$Q_{Wins} := q_{p.23} \cdot G_{ins} \cdot C_{ins} \cdot A_{ins} = 268.7\ \boldsymbol{N}$

Wind on steel poles, clause 4.4.4 of 50341-1:2012:

$h := 0.6 \cdot 25 = 15$ Reference height of pole, method 2

$q_{p.15} = \left(1.507 \cdot 10^{3}\right)\ \boldsymbol{Pa}$ Peak wind pressure

$G_{pol} := 1$ Structural factor, recommended value

$C_{pol} := 1.4$ Drag factor, boxed cross section

$d := 250\ \boldsymbol{mm}$ Diameter of pole

$A_{pol} := d \cdot 25\ \boldsymbol{m} = 6.25\ \boldsymbol{m}^{2}$ Projected area of pole.

$Q_{w.pol} := q_{p.15} \cdot G_{pol} \cdot C_{pol} \cdot A_{pol} = 13.185\ \boldsymbol{kN}$

Crossarm and davit arms. Same G as for poles.

$A_{ca} := 250\ \boldsymbol{mm} \cdot 250\ \boldsymbol{mm} = 0.063\ \boldsymbol{m}^{2}$ Projected area of cross arm.

$Q_{w.ca} := q_{p.25} \cdot G_{pol} \cdot C_{pol} \cdot A_{ca} = 0.149\ \boldsymbol{kN}$

$A_{da} := 250\ \boldsymbol{mm} \cdot 5\ \boldsymbol{m} = 1.25\ \boldsymbol{m}^{2}$ Projected area of davit arm.

$Q_{w.da} := q_{p.28} \cdot G_{pol} \cdot C_{pol} \cdot A_{da} = 3.069\ \boldsymbol{kN}$

Wind on FRP poles, clause 4.4.4 of 50341-1:2012:

$h := 0.6 \cdot 25 = 15$ Reference height of pole, method 2

$q_{p.15} = \left(1.507 \cdot 10^{3}\right)\ \mathbf{Pa}$ Peak wind pressure

$G_{pol} := 1$ Structural factor, recommended value

$C_{pol} := 1$ Drag factor, circular cross section

$d := 450\ \mathbf{mm}$ Diameter of pole

$A_{pol} := d \cdot 25\ \mathbf{m} = 11.25\ \mathbf{m}^2$ Projected area of pole.

$Q_{w.pol} := q_{p.15} \cdot G_{pol} \cdot C_{pol} \cdot A_{pol} = 16.952\ \mathbf{kN}$ Wind load on pole.

crossarm and davit arms. Same G as for poles.

$A_{ca} := 500\ \mathbf{mm} \cdot 500\ \mathbf{mm} = 0.25\ \mathbf{m}^2$ Projected area of cross arm.

$C_{ca} := 1.4$ Drag factor, boxed cross section

$Q_{w.ca} := q_{p.25} \cdot G_{pol} \cdot C_{ca} \cdot A_{ca} = 0.598\ \mathbf{kN}$ Wind load on cross arm.

$A_{da} := 400\ \mathbf{mm} \cdot 5\ \mathbf{m} = 2\ \mathbf{m}^2$ Projected area of davit arm.

$C_{da} := 1.4$ Drag factor, boxed cross section

$Q_{w.da} := q_{p.28} \cdot G_{pol} \cdot C_{da} \cdot A_{da} = 4.911\ \mathbf{kN}$ Wind load on davit arm.

Wind on lattice tower, clause 4.4.4 of 50341-1:2012:

$h := 0.6 \cdot 25 = 15$ Reference height of tower, method 2

$q_{p.15} = \left(1.507 \cdot 10^{3}\right) \ \boldsymbol{Pa}$ Peak wind pressure

$G_{leg} := 1$ Structural factor, recommended value

$C_{leg} := 2.8$ Drag factor, angle cross section (flat against the wind)

$A_{leg} := 7906000 \ \boldsymbol{mm}^{2}$ Projected area of leg.

$Q_{w.leg} := q_{p.15} \cdot G_{leg} \cdot C_{leg} \cdot A_{leg} = 33.357 \ \boldsymbol{kN}$ Wind load on leg.

crossarm and davit arms. Same G and D as for legs.

$A_{ca} := 533800 \cdot \boldsymbol{mm}^{2}$ Projected area of cross arm.

$Q_{w.ca} := q_{p.25} \cdot G_{pol} \cdot C_{ca} \cdot A_{ca} = 1.276 \ \boldsymbol{kN}$ Wind load on cross arm.

$A_{da} := 776320 \cdot \boldsymbol{mm}^{2}$ Projected area of davit arm.

$Q_{w.da} := q_{p.28} \cdot G_{pol} \cdot C_{da} \cdot A_{da} = 1.906 \ \boldsymbol{kN}$ Wind load on davit arm.

C.2 Ice Loads

$I_{150} := 50 \, \frac{N}{m}$ Design ice load for 150 year return period given by ARA Engineering.

Conversion factors for different return periods

$g_3 := \frac{0.35}{1.25} = 0.28$ Conversion factor, 3 year return period.

$g_{50} := \frac{1}{1.25} = 0.8$ Conversion factor, 50 year return period.

$g_{150} := \frac{1.25}{1.25} = 1$ Conversion factor, 150 year return period.

$g_{500} := \frac{1.5}{1.25} = 1.2$ Conversion factor, 500 year return period.

Design ice load for 150 year return period.

$I_{150} := I_{150} \cdot g_{150} = 50 \, \frac{N}{m}$ Design ice load, 150 year return period.

Span lengths

$L_w := 350 \; m$ Assumed weight span at support.

Vertical force on support:

$Q_{I.c} := I_{150} \cdot L_w \cdot 3 = 52.5 \; kN$ Vertical ice force on support from one conductor. 150 year return period.

$Q_{I.gw} := I_{150} \cdot L_w = 17.5 \; kN$ Vertical ice force on support from one ground wire. 150 year return period.

C.3 Combined Wind and Ice Loads

Ice load with 3 year return period:

$$I_{150} := 50\ \frac{N}{m}$$

$$\psi_3 := \frac{0.35}{1.25} = 0.28$$

$$I_3 := \psi_3 \cdot I_{150} = 14\ \frac{N}{m}$$

Wind load with 50 year return period:

$$V_{50} := 35\ \frac{m}{s}$$

$$B_I := 0.7$$

$$V_{IL} := V_{50} \cdot B_I = 24.5\ \frac{m}{s}$$

Equivalent diameter:

$$d := 3 \cdot 34\ mm \qquad d_{gw} := 21\ mm$$

$$g = 9.807\ \frac{m}{s^2}$$

$$\rho_I := 600\ \frac{kg}{m^3}$$

$$D := \sqrt{d^2 + \frac{4 \cdot I_3}{g \cdot \pi \cdot \rho_I}} = 115.903\ mm \qquad D_{gw} := \sqrt{{d_{gw}}^2 + \frac{4 \cdot I_3}{g \cdot \pi \cdot \rho_I}} = 58.911\ mm$$

$\rho_{air} := 1.25 \ \frac{kg}{m^3}$ — Density factor for air, conservative from EN 50341-1

$c_0 := 1.0$ — Orography factor. Set to 1.0 for preliminary calculations. (For steep slopes this must be calculated)

$z_0 := 0.05 \ m$ — Roughness length based on terrain category

$h := 23 \ m$ — Reference height

$$I_V := \frac{1}{c_0 \cdot \ln\left(\frac{h}{z_0}\right)} = 0.163$$

Turbulence intensity

$$q_{IL} := \frac{1}{2} \cdot \rho_{air} \cdot V_{IL}^{\ 2} = 375.156 \ Pa$$

$$q_{Ip} := \left(1 + 7 \cdot I_V\right) \cdot q_{IL} = 803.471 \ Pa$$

Wind forces on supports due to ice covered conductors:

$G_c := 0.4$ — Structure factor/span factor

$C_{Ic} := 1.0$ — Drag factor for ice-covered conductor (Tab 4.2.6/NO NNA)

$L_1 := 350 \ m$ — Length of span 1

$L_2 := 350 \ m$ — Length of span 2

$\theta_1 := 0$ — Change in angle of line

$\theta_2 := 0$ — Change in angle of line

For wind in direction of cross arm:

$\phi := 0$ Angle between wind direction and long. axis of crossarm

Transverse (in direction of cross-arm):

$$Q_{WIc\_V.1} := q_{Ip} \cdot G_c \cdot C_{Ic} \cdot D \cdot \cos(\phi)^2 \cdot \frac{L_1 + L_2}{2} = 13.037 \ kN$$

$$Q_{WIc\_V.2} := 0 \ kN$$

Ground wire:

$$Q_{WIc\_V.1} := q_{Ip} \cdot G_c \cdot C_{Ic} \cdot D_{gw} \cdot \cos(\phi)^2 \cdot \frac{L_1 + L_2}{2} = 6.627 \ kN$$

$$Q_{WIc\_V.2} := 0 \ kN$$

Ice load:

$$I_c := I_3 \cdot \frac{L_1 + L_2}{2} \cdot 3 = 14.7 \ kN$$

$$I_c := I_3 \cdot \frac{L_1 + L_2}{2} = 4.9 \ kN$$

C.4 Ground Wire Tension

Equation 14.25 from FprEN 50341-1:2012:

$$s=\frac{a^2 \cdot w}{8 \cdot H}$$

Where:

s = Maximum sag
a = Span length
w = Unit weight of conductor
H = Horizontal tensile force

Sag of the triplex grackle:

$a := 350\ m$	Span length
$H_1 := 39651\ N$	Horizontal tension
$w_1 := 22.3141\ \frac{N}{m}$	Unit weight of conductor
$c_1 := \frac{H_1}{w_1} = (1.777 \cdot 10^3)\ m$	Coefficient
$s_1 := \frac{a^2}{c_1 \cdot 8} = 8.617\ m$	Sag of conductor

Tension in the ground wire:

$s_2 := s_1 = 8.617\ m$	Initially sag of the ground wire is equal to the conductor.
$a = 350\ m$	Span length
$w_2 := 14.1\ \frac{N}{m}$	Unit weight of ground wire
$c_2 := \frac{a^2}{s_2 \cdot 8} = (1.777 \cdot 10^3)\ m$	Coefficient
$H_2 := c_2 \cdot w_2 = (2.505 \cdot 10^4)\ N$	Horizontal tension in the ground wire.

C.5 Vertical Loads

ONLY DEAD LOAD

LATTICE TOWER STRUCTURE:

Geometry:

$n := 8$ The slope of the leg

$\alpha := \operatorname{atan}\left(\frac{1}{n}\right) = 7.125\ \boldsymbol{deg}$ Angle between the leg force and the vertical plane.

From the tower structure:

$W_t := 91894\ \boldsymbol{N}$ Total weight of tower from PLS-TOWER

$F_t := W_t = 91.894\ \boldsymbol{kN}$ Load from self weight

From the conductors and ground wires (assumed half of each span on support):

$w_c := 22.3724 \cdot 3\ \frac{\boldsymbol{N}}{\boldsymbol{m}}$ Unit weight of conductor

$w_{gw} := 14.1\ \frac{\boldsymbol{N}}{\boldsymbol{m}}$ Unit weight of ground wire

$L_c := 350\ \boldsymbol{m}$ Span length

$W_c := w_c \cdot L_c = 23.491\ \boldsymbol{kN}$ Weight of triplex conductor

$W_{gw} := w_{gw} \cdot L_c = 4.935\ \boldsymbol{kN}$ Weight of ground wire

$F_c := 3 \cdot W_c + 2 \cdot W_{gw} = 80.343\ \boldsymbol{kN}$ Load from cables

Assuming all vertical forces are taken by the legs. Disregarding the initial tension in the guys that will lead to some extra compression in the legs.

$n_{legs} := 2$	Number of legs
$F_{L.V} := \dfrac{(F_t + F_c)}{n_{legs}} = 86.119\ kN$	Vertical load in leg
$F_L := \dfrac{F_{L.V}}{\cos(\alpha)} = 86.789\ kN$	Compression load in leg
$F_{crossarm} := F_{L.V} \cdot \tan(\alpha) = 10.765\ kN$	Compression load in crossarm

STEEL POLE TOWER STRUCTURE:

Geometry:

$n := 8$	The slope of the leg
$\alpha := \operatorname{atan}\left(\dfrac{1}{n}\right) = 7.125\ deg$	Angle between the leg force and the vertical plane.

Tower structure:

$W_t := 82396\ N$	Total weight of tower from PLS-POLE
$W_{t.c} := 5\ kN$	Assumed weight of connections
$F_t := W_t + W_{t.c} = 87.396\ kN$	Load from self weight

Conductors and ground wires:

$w_c := 22.3724 \cdot 3\ \dfrac{N}{m}$	Unit weight of conductor
$w_{gw} := 14.1\ \dfrac{N}{m}$	Unit weight of ground wire
$L_c := 350\ m$	Span length
$W_c := w_c \cdot L_c = 23.491\ kN$	Weight of triplex conductor
$W_{gw} := w_{gw} \cdot L_c = 4.935\ kN$	Weight of ground wire
$F_c := 3 \cdot W_c + 2 \cdot W_{gw} = 80.343\ kN$	Load from cables

Assuming all vertical forces are taken by the legs. Will be a bit wrong as initial tension in the guys will give some extra compression in the legs.

$n_{legs} := 2$	Number of legs
$F_{L.V} := \dfrac{(F_t + F_c)}{n_{legs}} = 83.87\ \boldsymbol{kN}$	Vertical load in leg
$F_L := \dfrac{F_{L.V}}{\cos(\alpha)} = 84.522\ \boldsymbol{kN}$	Compression load in leg
$F_{crossarm} := F_{L.V} \cdot \tan(\alpha) = 10.484\ \boldsymbol{kN}$	Compression load in crossarm

FRP TOWER STRUCTURE:

Geometry:

$n := 8$	The slope of the leg
$\alpha := \text{atan}\left(\dfrac{1}{n}\right) = 7.125\ \boldsymbol{deg}$	Angle between the leg force and the vertical plane.

Tower structure:

$W_t := 50750\ \boldsymbol{N}$	Total weight of tower from PLS-POLE
$W_{t.c} := 8\ \boldsymbol{kN}$	Assumed weight of connections
$F_t := W_t + W_{t.c} = 58.75\ \boldsymbol{kN}$	Load from self weight

Conductors and ground wires:

$w_c := 22.3724 \cdot 3\ \dfrac{\boldsymbol{N}}{\boldsymbol{m}}$	Unit weight of conductor
$w_{gw} := 14.1\ \dfrac{\boldsymbol{N}}{\boldsymbol{m}}$	Unit weight of ground wire
$L_c := 350\ \boldsymbol{m}$	Span length
$W_c := w_c \cdot L_c = 23.491\ \boldsymbol{kN}$	Weight of triplex conductor
$W_{gw} := w_{gw} \cdot L_c = 4.935\ \boldsymbol{kN}$	Weight of ground wire
$F_c := 3 \cdot W_c + 2 \cdot W_{gw} = 80.343\ \boldsymbol{kN}$	Load from cables

Assuming all vertical forces are taken by the legs. Will be a bit wrong as initial tension in the guys will give some extra compression in the legs.

$n_{legs} := 2$ Number of legs

$F_{L.V} := \frac{(F_t + F_c)}{n_{legs}} = 69.547\ kN$ Vertical load in leg

$F_L := \frac{F_{L.V}}{\cos(\alpha)} = 70.088\ kN$ Compression load in leg

$F_{crossarm} := F_{L.V} \cdot \tan(\alpha) = 8.693\ kN$ Compression load in crossarm

DEAD LOAD + ICE LOAD

LATTICE TOWER STRUCTURE:

Geometry:

$n := 8$ The slope of the leg

$\alpha := \operatorname{atan}\left(\frac{1}{n}\right) = 7.125\ deg$ Angle between the leg force and the vertical plane.

From the tower structure:

$W_t := 91894\ N$ Total weight of tower from PLS-TOWER

$F_t := W_t = 91.894\ kN$ Load from self weight

From the conductors and ground wires (assumed half of each span on support):

$w_c := 22.3724 \cdot 3\ \frac{N}{m}$ Unit weight of conductor

$w_{gw} := 14.1\ \frac{N}{m}$ Unit weight of ground wire

$L_c := 350\ m$ Span length

$W_c := w_c \cdot L_c = 23.491\ kN$ Weight of triplex conductor

$W_{gw} := w_{gw} \cdot L_c = 4.935\ kN$ Weight of ground wire

$F_c := 3 \cdot (W_c + 52.5\ kN) + 2 \cdot (W_{gw} + 17.5\ kN) = 272.843\ kN$ Load from cables

Assuming all vertical forces are taken by the legs. Disregarding the initial tension in the guys that will lead to some extra compression in the legs.

$n_{legs} := 2$ Number of legs

$F_{L.V} := \frac{(F_t + F_c)}{n_{legs}} = 182.369\ \mathbf{kN}$ Vertical load in leg

$F_L := \frac{F_{L.V}}{\cos(\alpha)} = 183.788\ \mathbf{kN}$ Compression load in leg

$F_{crossarm} := F_{L.V} \cdot \tan(\alpha) = 22.796\ \mathbf{kN}$ Compression load in crossarm

STEEL POLE TOWER STRUCTURE:

Geometry:

$n := 8$ The slope of the leg

$\alpha := \operatorname{atan}\left(\frac{1}{n}\right) = 7.125\ \mathbf{deg}$ Angle between the leg force and the vertical plane.

Tower structure:

$W_t := 82396\ \mathbf{N}$ Total weight of tower from PLS-POLE

$W_{t.c} := 5\ \mathbf{kN}$ Assumed weight of connections

$F_t := W_t + W_{t.c} = 87.396\ \mathbf{kN}$ Load from self weight

Conductors and ground wires:

$w_c := 22.3724 \cdot 3\ \frac{\mathbf{N}}{\mathbf{m}}$ Unit weight of conductor

$w_{gw} := 14.1\ \frac{\mathbf{N}}{\mathbf{m}}$ Unit weight of ground wire

$L_c := 350\ \mathbf{m}$ Span length

$W_c := w_c \cdot L_c = 23.491\ \mathbf{kN}$ Weight of triplex conductor

$W_{gw} := w_{gw} \cdot L_c = 4.935\ \mathbf{kN}$ Weight of ground wire

$F_c := 3 \cdot (W_c + 52.5\ \mathbf{kN}) + 2 \cdot (W_{gw} + 17.5\ \mathbf{kN}) = 272.843\ \mathbf{kN}$ Load from cables

Assuming all vertical forces are taken by the legs. Will be a bit wrong as initial tension in the guys will give some extra compression in the legs.

$n_{legs} := 2$	Number of legs
$F_{L.V} := \dfrac{(F_t + F_c)}{n_{legs}} = 180.12\ kN$	Vertical load in leg
$F_L := \dfrac{F_{L.V}}{\cos(\alpha)} = 181.521\ kN$	Compression load in leg
$F_{crossarm} := F_{L.V} \cdot \tan(\alpha) = 22.515\ kN$	Compression load in crossarm

FRP TOWER STRUCTURE:

Geometry:

$n := 8$	The slope of the leg
$\alpha := \operatorname{atan}\left(\dfrac{1}{n}\right) = 7.125\ deg$	Angle between the leg force and the vertical plane.

Tower structure:

$W_t := 50750\ N$	Total weight of tower from PLS-POLE
$W_{t.c} := 8\ kN$	Assumed weight of connections
$F_t := W_t + W_{t.c} = 58.75\ kN$	Load from self weight

Conductors and ground wires:

$w_c := 22.3724 \cdot 3\ \dfrac{N}{m}$	Unit weight of conductor
$w_{gw} := 14.1\ \dfrac{N}{m}$	Unit weight of ground wire
$L_c := 350\ m$	Span length
$W_c := w_c \cdot L_c = 23.491\ kN$	Weight of triplex conductor
$W_{gw} := w_{gw} \cdot L_c = 4.935\ kN$	Weight of ground wire
$F_c := 3 \cdot (W_c + 52.5\ kN) + 2 \cdot (W_{gw} + 17.5\ kN) = 272.843\ kN$	Load from cables

Assuming all vertical forces are taken by the legs. Will be a bit wrong as initial tension in the guys will give some extra compression in the legs.

$n_{legs} := 2$ Number of legs

$F_{L.V} := \dfrac{\left(F_t + F_c\right)}{n_{legs}} = 165.797\ kN$ Vertical load in leg

$F_L := \dfrac{F_{L.V}}{\cos(\alpha)} = 167.087\ kN$ Compression load in leg

$F_{crossarm} := F_{L.V} \cdot \tan(\alpha) = 20.725\ kN$ Compression load in crossarm

C.6 Transverse Loads

Geometry and given values:

$b_1 := 9000\ mm$	Distance from leg to centreline.
$b_2 := 8000\ mm$	Distance from leg to end of crossarm.
$T_c := 23.909\ kN \cdot 3 + 5.24\ kN \cdot 2 = 82.207\ kN$	Transversal force from wind load on cables.
$a := 8$	Assumed gradient of leg.
$b := 2$	Assumed gradient of guy.
$h := 25\ m$	Heigth of tower irt. leg.
$h_s := 27\ m$	Heigth of tower irt. guy.
$O := 13.5\ m$	Offset of guy.
$L_1 := \sqrt{O^2 + {h_s}^2} = 30.187\ m$	Length of guy.

Lattice:

$T_L := 36.539\ kN$

$T := T_c + T_L = 118.746\ kN$

$S := T \cdot \dfrac{L_1 \cdot a}{2 \cdot (h_s + a \cdot b_2)} = 157.564\ kN$ Tension force in guy.

$N := T \cdot \dfrac{h_s \cdot \sqrt{1 + a^2}}{(h_s + a \cdot b_2)} = 284.052\ kN$ Compression force force in leg.

Tubular steel:

$$T_T := 16.403 \cdot kN$$

$$T := T_c + T_T = 98.61 \ kN$$

$$S := T \cdot \frac{L_1 \cdot a}{2 \cdot (h_s + a \cdot b_2)} = 130.845 \ kN$$ Tension force in guy.

$$N := T \cdot \frac{h_s \cdot \sqrt{1 + a^2}}{(h_s + a \cdot b_2)} = 235.885 \ kN$$ Compression force force in leg.

FRP:

$$T_F := 22.461 \ kN$$

$$T := T_c + T_F = 104.668 \ kN$$

$$S := T \cdot \frac{L_1 \cdot a}{2 \cdot (h_s + a \cdot b_2)} = 138.884 \ kN$$ Tension force in guy.

$$N := T \cdot \frac{h_s \cdot \sqrt{1 + a^2}}{(h_s + a \cdot b_2)} = 250.376 \ kN$$ Compression force force in leg.

C.7 Cross Sections

Lattice tower:

Leg, main member:

$\gamma_{M0} := 1.10$ — Partial factor of safety from cenelec.

$f_y := 355\ \mathbf{MPa}$ — Yield stress of steel S355.

$c := 50\ \mathbf{mm}$ — Width of angle.

$t := 5\ \mathbf{mm}$ — Thickness of angle.

$A := c \cdot t + (c - t) \cdot t = 475\ \mathbf{mm}^2$ — Area of angle.

$N_{c.Rd} := A \cdot \frac{f_y}{\gamma_{M0}} = 153.295\ \mathbf{kN}$ — Eq. 6.10 of NS-EN 1993-1-1:2005

$N_{c.Ed} := 431.8\ \frac{\mathbf{kN}}{4} = 107.95\ \mathbf{kN}$ — Compression force from preliminary calculations.

Leg, diagonal:

$\gamma_{M0} := 1.10$ Partial factor of safety.

$f_y := 355\ MPa$ Yield stress of steel S355.

Applied 1.5 kN point load at midpoint. Check shear:

$c := 20\ mm$ Length of web parallel to load.

$t := 3\ mm$ Thickness of web parallel to load.

$\eta := 1.0$ Conservative value.

$A_V := c \cdot t \cdot \eta = 60\ mm^2$ Shear area of angle.

$$V_{Rd} := A_V \cdot \frac{\left(\frac{f_y}{\sqrt{3}}\right)}{\gamma_{M0}} = 11.18\ kN$$ Eq. 6.10 of NS-EN 1993-1-1:2005

$V_{Ed} := 0.75\ kN$ Shear force in angle due to point load.

Crossarm, main member:

$\gamma_{M0} := 1.05$ Partial factor of safety.

$f_y := 355\ MPa$ Yield stress of steel S355.

$c := 35\ mm$ Width of angle.

$t := 4\ mm$ Thickness of angle.

$A := c \cdot t + (c - t) \cdot t = 264\ mm^2$ Area of angle.

$$N_{c.Rd} := A \cdot \frac{f_y}{\gamma_{M0}} = 89.257\ kN$$ Eq. 6.10 of NS-EN 1993-1-1:2005

$$N_{c.Ed} := \frac{300}{4}\ kN = 75\ kN$$ Compression force from preliminary calculations.

Tubular steel due to compression force:

Leg due to compression force:

$\gamma_{M0} := 1.10$ Partial factor of safety.

$f_y := 355\ MPa$ Yield stress of steel S355.

$t := 5\ mm$ Thickness of wall

$a := 70\ mm$

$A := 2 \cdot a \cdot t + 2 \cdot (a - 2 \cdot t) \cdot t = \left(1.3 \cdot 10^3\right)\ mm^2$ Area of square tube.

$N_{c.Rd} := A \cdot \dfrac{f_y}{\gamma_{M0}} = 419.545\ kN$ Eq. 6.10 of NS-EN 1993-1-1:2005

$N_{c.Ed} := 417\ kN$ Compression force from preliminary calculations.

Crossarm due to compression force:

$\gamma_{M0} := 1.05$ Partial factor of safety.

$f_y := 355\ MPa$ Yield stress of steel S355.

$t := 2\ mm$ Thickness of wall

$a := 25\ mm$

$A := 2 \cdot a \cdot t + 2 \cdot (a - 2 \cdot t) \cdot t = 184\ mm^2$ Area of square tube.

$N_{c.Rd} := A \cdot \dfrac{f_y}{\gamma_{M0}} = 62.21\ kN$ Eq. 6.10 of NS-EN 1993-1-1:2005

$N_{c.Ed} := 22.5$ Compression force from preliminary calculations.

FRP:

Tensile strength 480-1600 MPa,

$f_{fu} := 480\ MPa$ Assumed tensile strength

$c := 0.2$ Creep rupture reduction factor

Elastic modulus 35-51 GPa

$E_{FRP} := 35\ GPa$ Assumed elastic modulus

$t := 9.5\ mm$ Thickness of wall

$N_{c.Rd} := 417\ kN$ Compression force from preliminary calculations.

$$N_{c.Rd} = A \cdot f_{fu} \cdot c$$

$A := \dfrac{N_{c.Rd}}{c \cdot f_{fu}} = \left(4.344 \cdot 10^3\right)\ mm^2$ Required area.

$A = \dfrac{\pi}{4} \cdot (D-d)^2$ Area of round tube, where $d = D - 2 \cdot t$.

$D := \dfrac{A}{2 \cdot t \cdot \pi} + \dfrac{t}{2} = 77.522\ mm$ Required diameter.

Cross arm:

$N_{ca.Rd} := 20.7\ kN$

$A := \dfrac{N_{ca.Rd}}{c \cdot f_{fu}} = 215.625\ mm^2$ Required area.

$t := 2\ mm$

$A = 2 \cdot (2 \cdot D \cdot t + 2 \cdot (D - 2 \cdot t) \cdot t) = 0$ Area of two square tubes.

$D := \dfrac{A}{4 \cdot t} - 2 \cdot t$ Required diameter.

C.8 Dynamic Response

LOAD CASE 1: Wind on clear line

CONDUCTORS:

$k_c := 3$	Harmonic coefficient
$a := 350\ \mathbf{m}$	Span
$H_c := 51584\ \mathbf{N}$	Horizontal tension in conductor
$M_c := 3 \cdot 2.28\ \frac{\mathbf{kg}}{\mathbf{m}}$	Unit weight of conductor

Natural frequency of conductor:

$$f_1 := \frac{k_c}{2 \cdot a} \cdot \sqrt{\frac{H_c}{M_c}} = 0.372\ \mathbf{Hz}$$

GROUND WIRES:

$k_{gw} := 3$	Harmonic coefficient
$a = 350\ \mathbf{m}$	Span
$H_{gw} := 34322\ \mathbf{N}$	Horizontal tension in ground wire
$M_{gw} := 1.437\ \frac{\mathbf{kg}}{\mathbf{m}}$	Unit weight of ground wire

Natural frequency of ground wire:

$$f := \frac{k_{gw}}{2 \cdot a} \cdot \sqrt{\frac{H_{gw}}{M_c}} = 0.304\ \mathbf{Hz}$$

LATTICE STEEL TOWER:

Stiffness of the structure:

$F := 93036\ N$ Force on structure

$\delta := 0.2384\ m$ Deflection of structure

$k := \dfrac{F}{\delta} = \left(3.903 \cdot 10^{5}\right) \dfrac{kg}{s^{2}}$ Stiffness of structure

Natural frequency of the structure:

$M := 23304\ kg$ Mass of structure

$f := \dfrac{1}{2 \cdot \pi} \cdot \sqrt{\dfrac{k}{M}} = 0.651\ Hz$ Natural frequence

TUBULAR STEEL TOWER:

Stiffness of the structure: Force on structure

$F := 93036\ N$ Deflection of structure

$\delta := 34\ cm$

Stiffness of structure

$k := \dfrac{F}{\delta} = \left(2.736 \cdot 10^{5}\right) \dfrac{kg}{s^{2}}$

Natural frequency of the structure: Mass of structure

$M := 22781\ kg$

Natural frequence

$f := \dfrac{1}{2 \cdot \pi} \cdot \sqrt{\dfrac{k}{M}} = 0.552\ Hz$

TUBULAR FRP TOWER:

Stiffness of the structure:

$F := 111841\ N$ Force on structure

$\delta := 60.36\ cm$ Deflection of structure

$k := \frac{F}{\delta} = \left(1.853 \cdot 10^{5}\right) \frac{kg}{s^{2}}$ Stiffness of structure

Natural frequency of the structure:

$M := 21108\ kg$ Mass of structure

$f := \frac{1}{2 \cdot \pi} \cdot \sqrt{\frac{k}{M}} = 0.472\ Hz$ Natural frequence

LOAD CASE 2: Wind on iced line

CONDUCTORS:

$k_c := 3$ Harmonic coefficient

$a := 350\ m$ Span

$H_c := 40405\ N$ Horizontal tension in conductor

$M_c := 3 \cdot 2.28\ \frac{kg}{m}$ Unit weight of conductor

Natural frequency of conductor:

$$f_1 := \frac{k_c}{2 \cdot a} \cdot \sqrt{\frac{H_c}{M_c}} = 0.329\ Hz$$

GROUND WIRES:

$k_{gw} := 3$ Harmonic coefficient

$a = 350\ m$ Span

$H_{gw} := 27159\ N$ Horizontal tension in ground wire

$M_{gw} := 1.437\ \dfrac{kg}{m}$ Unit weight of ground wire

Natural frequency of ground wire:

$$f := \frac{k_{gw}}{2 \cdot a} \cdot \sqrt{\frac{H_{gw}}{M_c}} = 0.27\ Hz$$

LATTICE STEEL TOWER:

Stiffness of the structure:

$F := 93036\ N$ Force on structure

$\delta := 0.1024\ m$ Deflection of structure

$k := \dfrac{F}{\delta} = \left(9.086 \cdot 10^{5}\right)\ \dfrac{kg}{s^2}$ Stiffness of structure

Natural frequency of the structure:

Mass of structure

$M := 22625\ kg$

Natural frequence

$$f := \frac{1}{2 \cdot \pi} \cdot \sqrt{\frac{k}{M}} = 1.009\ Hz$$

TUBULAR STEEL TOWER:

Stiffness of the structure:

$F := 45698\ N$ Force on structure

$\delta := 15.84\ cm$ Deflection of structure

$k := \dfrac{F}{\delta} = \left(2.885 \cdot 10^{5}\right)\ \dfrac{kg}{s^{2}}$ Stiffness of structure

Natural frequency of the structure:

$M := 22100\ kg$ Mass of structure

$f := \dfrac{1}{2 \cdot \pi} \cdot \sqrt{\dfrac{k}{M}} = 0.575\ Hz$ Natural frequence

TUBULAR FRP TOWER:

Stiffness of the structure:

$F := 53963\ N$ Force on structure

$\delta := 24.36\ cm$ Deflection of structure

$k := \dfrac{F}{\delta} = \left(2.215 \cdot 10^{5}\right)\ \dfrac{kg}{s^{2}}$ Stiffness of structure

Natural frequency of the structure:

$M := 20325\ kg$ Mass of structure

$f := \dfrac{1}{2 \cdot \pi} \cdot \sqrt{\dfrac{k}{M}} = 0.525\ Hz$ Natural frequence

C.9 Buckling check of steel poles

Figures C.1, C.2 and C.3 illustrate the moment distribution in the right and left legs for load cases 00 - EDS, 01 - Full ice load and 10 - Wind on line towards the right. The values are from the PLS-report.

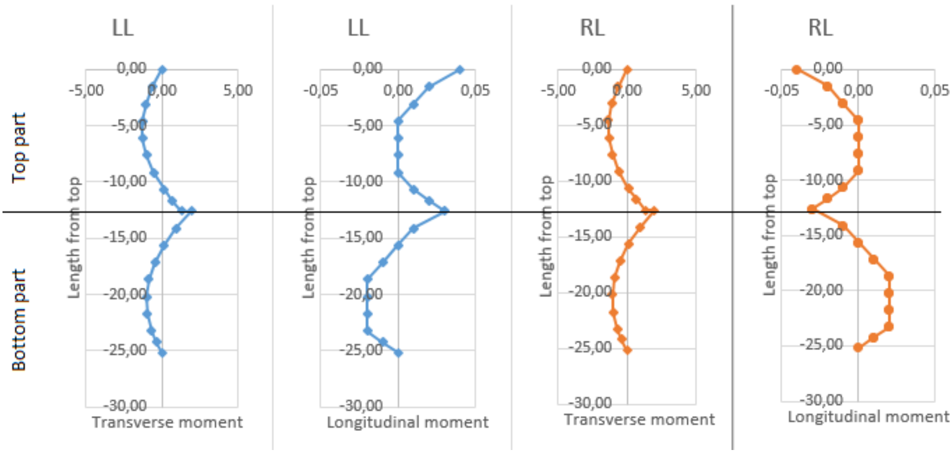

Figure C.1: Moment distribution in steel poles due to load case: EDS.

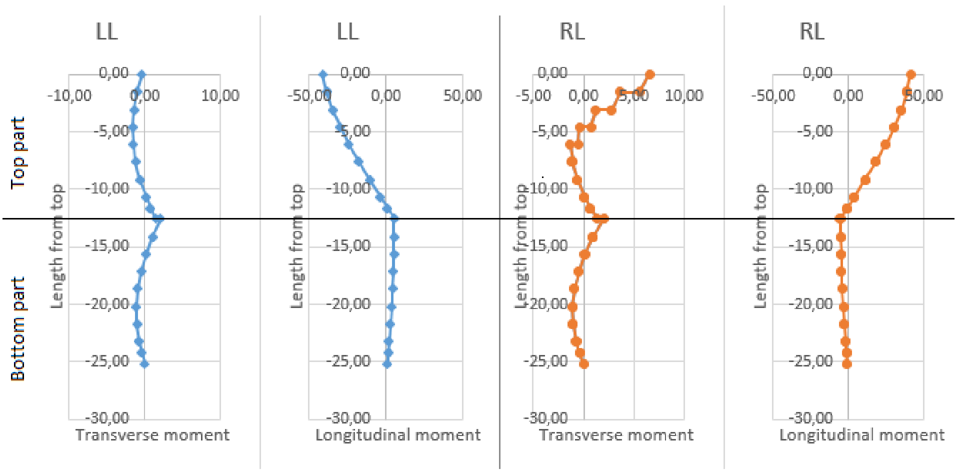

Figure C.2: Moment distribution in steel poles due to load case: Max ice load.

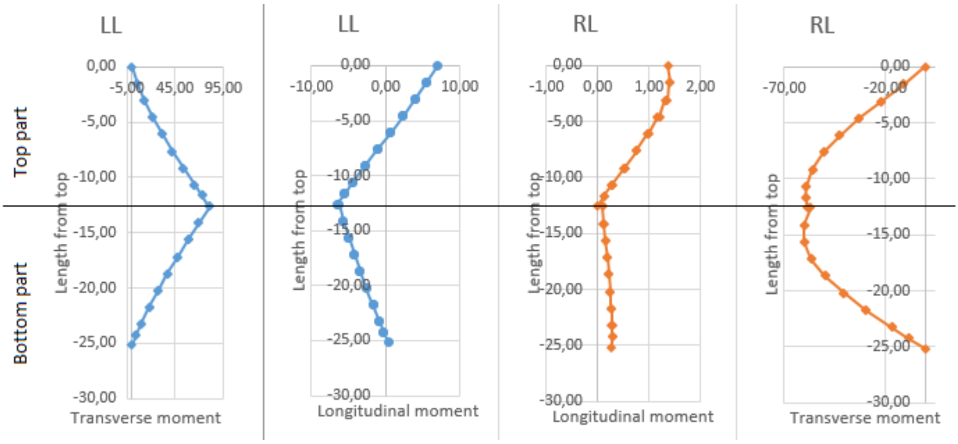

Figure C.3: Moment distribution in steel poles due to load case: Wind on line towards the right.

1 Max ice load

RT=Right leg, Top. LT=Left leg, Top. RB=Right leg, Bottom. LB=Left leg, Bottom

$N_{Ed.RT} := 250.29\ kN$

$M_{y.Ed.RT} := 40.99\ kN \cdot m$

$M_{z.Ed.RT} := 6.56\ kN \cdot m$

$N_{Ed.LT} := 250.04\ kN$

$M_{y.Ed.LT} := 41.46\ kN \cdot m$

$M_{z.Ed.LT} := 1.63\ kN \cdot m$

$N_{Ed.RB} := 272.88\ kN$

$M_{y.Ed.RB} := 5.04\ kN \cdot m$

$M_{z.Ed.RB} := 1.98\ kN \cdot m$

$N_{Ed.LB} := 272.52\ kN$

$M_{y.Ed.LB} := 4.99\ kN \cdot m$

$M_{z.Ed.LB} := 2.08\ kN \cdot m$

Tverrsnittsklasse 1, 250*250*10mm But still check elastic

Assuming guys prevent sideways buckling. So that: $L_{cr.y} = L_{cr.z} = \frac{L}{2}$

$f_y := 355\ MPa$

EN 50341 $\gamma_{M1} := 1.00$

EC3 $\gamma_{M0} := 1.05$

$A := 92.57 \cdot 10^2\ mm^2$

$N_{Rk} := f_y \cdot A = \left(3.286 \cdot 10^3\right)\ kN$

$W_{y.pl} := 822.00 \cdot 10^3\ mm^3$

$M_{y.Rk} := f_y \cdot W_{y.pl} = 291.81\ kN \cdot m$

$W_{y.el} := 696.53 \cdot 10^3 \cdot mm^3$

$M_{y.Rk.el} := f_y \cdot W_{y.el} = 247.268\ kN \cdot m$

$W_{z.pl} := W_{y.pl} = \left(8.22 \cdot 10^5\right)\ mm^3$

$M_{z.Rk} := f_y \cdot W_{z.pl} = 291.81\ kN \cdot m$

$W_{z.el} := W_{y.el} = \left(6.965 \cdot 10^5\right)\ mm^3$

$M_{z.Rk.el} := f_y \cdot W_{z.el} = 247.268\ kN \cdot m$

$\Delta M_{y.Ed} := 0$ $\Delta M_{z.Ed} := 0$

Clause 6.3.1.3:

$E := 210000\ MPa$ $\quad$ $I := 8706.67 \cdot 10^4\ mm^4$

$L := 25.19\ m$ $\quad$ $L_{cr} := \frac{L}{2} = 12.595\ m$

$N_{cr.y} := \frac{\pi^2 \cdot E \cdot I}{L_{cr}^2} = \left(1.138 \cdot 10^3\right)\ kN$ $\quad$ $N_{cr.z} := \frac{\pi^2 \cdot E \cdot I}{L_{cr}^2} = \left(1.138 \cdot 10^3\right)\ kN$

$\lambda_y := \sqrt{\frac{N_{Rk}}{N_{cr.y}}} = 1.7$ $\quad$ $\lambda_z := \sqrt{\frac{N_{Rk}}{N_{cr.z}}} = 1.7$

$\chi_y := 0.3$

Warm formed: Buckling curve a in figure 6.4

$\chi_z := 0.3$

Clause 6.3.2.3:

$M_{c.Rd} := W_{y.el} \cdot \frac{f_y}{\gamma_{M0}} = 235.493\ kN \cdot m$

Other cross section: Buckling curve d $\quad$ $\alpha_{LT} := 0.76$

$\lambda_{LT} := \sqrt{\frac{W_{y.el} \cdot f_y}{M_{c.Rd}}} = 1.025$

$\Phi_{LT} := 0.5 \cdot \left(1 + \alpha_{LT} \cdot \left(\lambda_{LT} - 0.2\right) + \lambda_{LT}^2\right) = 1.338$

$\chi_{LT} := \frac{1}{\Phi_{LT} + \sqrt{\Phi_{LT}^2 - \lambda_{LT}^2}} = 0.455$

Annex B:

1) Top part right leg:

$N_{Ed} := N_{Ed.RT} = 250.29\ kN$

$M_{y.Ed} := M_{y.Ed.RT} = 40.99\ kN \cdot m$

$M_{z.Ed} := M_{z.Ed.RT} = 6.56\ kN \cdot m$

Long.: $\alpha_h := 1$ $\psi := -0.139$

$$C_{my} := 0.95 + 0.05 \cdot \alpha_h = 1$$

Trans.: $\alpha_s := -0.200$ $\psi := 0.204$

$$C_{mz} := 0.1 - 0.8 \cdot \alpha_s = 0.26 \qquad C_{mz} := 0.4$$

Elastic - conservative:

$$k_{yy.1} := C_{my} \cdot \left(1 + 0.6 \cdot \lambda_y \cdot \frac{N_{Ed}}{\chi_y \cdot \frac{N_{Rk}}{\gamma_{M1}}} \right) = 1.259$$

$$k_{yy.2} := C_{my} \cdot \left(1 + 0.6 \cdot \frac{N_{Ed}}{\chi_y \cdot \frac{N_{Rk}}{\gamma_{M1}}} \right) = 1.152 \qquad k_{yy} := k_{yy.2} = 1.152$$

$$k_{zz.1} := C_{mz} \cdot \left(1 + 0.6 \cdot \lambda_z \cdot \frac{N_{Ed}}{\chi_z \cdot \frac{N_{Rk}}{\gamma_{M1}}} \right) = 0.504$$

$$k_{zz.2} := C_{mz} \cdot \left(1 + 0.6 \cdot \frac{N_{Ed}}{\chi_z \cdot \frac{N_{Rk}}{\gamma_{M1}}} \right) = 0.461 \qquad k_{zz} := k_{zz.2} = 0.461$$

$$k_{yz} := k_{zz} = 0.461 \qquad k_{zy} := 0.8 \cdot k_{yy} = 0.922$$

NS-EN 1993-1-1:2005, Equation 6.61:

$$\frac{N_{Ed}}{\frac{\chi_y \cdot N_{Rk}}{\gamma_{M1}}} + k_{yy} \cdot \frac{M_{y.Ed} + \Delta M_{y.Ed}}{\chi_{LT} \cdot \frac{M_{y.Rk.el}}{\gamma_{M1}}} + k_{yz} \cdot \frac{M_{z.Ed} + \Delta M_{z.Ed}}{\frac{M_{z.Rk.el}}{\gamma_{M1}}} = 0.686 \qquad < 1 \qquad OK$$

NS-EN 1993-1-1:2005, Equation 6.62:

$$\frac{N_{Ed}}{\frac{\chi_z \cdot N_{Rk}}{\gamma_{M1}}} + k_{zy} \cdot \frac{M_{y.Ed} + \Delta M_{y.Ed}}{\chi_{LT} \cdot \frac{M_{y.Rk.el}}{\gamma_{M1}}} + k_{zz} \cdot \frac{M_{z.Ed} + \Delta M_{z.Ed}}{\frac{M_{z.Rk.el}}{\gamma_{M1}}} = 0.602 \qquad < 1 \qquad OK$$

2) Bottom part right leg:

$$N_{Ed} := N_{Ed.RB} = 272.88\ \boldsymbol{kN}$$

$$M_{y.Ed} := M_{y.Ed.RB} = 5.04\ \boldsymbol{kN \cdot m}$$

$$M_{z.Ed} := M_{z.Ed.RB} = 1.98\ \boldsymbol{kN \cdot m}$$

Long.: $\alpha_h := 1$ $\psi := 0.165$

$$C_{my} := 0.95 + 0.05 \cdot \alpha_h = 1$$

Trans.: $\alpha_s := -0.561$ $\psi := 0$

$$C_{mz} := 0.1 - 0.8 \cdot \alpha_s = 0.549$$

Elastic - conservative:

$$k_{yy.1} := C_{my} \cdot \left(1 + 0.6 \cdot \lambda_y \cdot \frac{N_{Ed}}{\chi_y \cdot \frac{N_{Rk}}{\gamma_{M1}}}\right) = 1.282$$

$$k_{yy.2} := C_{my} \cdot \left(1 + 0.6 \cdot \frac{N_{Ed}}{\chi_y \cdot \frac{N_{Rk}}{\gamma_{M1}}}\right) = 1.166 \qquad k_{yy} := k_{yy.2} = 1.166$$

$$k_{zz.1} := C_{mz} \cdot \left(1 + 0.6 \cdot \lambda_z \cdot \frac{N_{Ed}}{\chi_z \cdot \frac{N_{Rk}}{\gamma_{M1}}}\right) = 0.704$$

$$k_{zz.2} := C_{mz} \cdot \left(1 + 0.6 \cdot \frac{N_{Ed}}{\chi_z \cdot \frac{N_{Rk}}{\gamma_{M1}}}\right) = 0.64 \qquad k_{zz} := k_{zz.2} = 0.64$$

$$k_{yz} := k_{zz} = 0.64$$

$$k_{zy} := 0.8 \cdot k_{yy} = 0.933$$

NS-EN 1993-1-1:2005, Equation 6.61:

$$\frac{N_{Ed}}{\frac{\chi_y \cdot N_{Rk}}{\gamma_{M1}}} + k_{yy} \cdot \frac{M_{y.Ed} + \Delta M_{y.Ed}}{\chi_{LT} \cdot \frac{M_{y.Rk.el}}{\gamma_{M1}}} + k_{yz} \cdot \frac{M_{z.Ed} + \Delta M_{z.Ed}}{\frac{M_{z.Rk.el}}{\gamma_{M1}}} = 0.334 \qquad < 1 \qquad OK$$

NS-EN 1993-1-1:2005, Equation 6.62:

$$\frac{N_{Ed}}{\frac{\chi_z \cdot N_{Rk}}{\gamma_{M1}}} + k_{zy} \cdot \frac{M_{y.Ed} + \Delta M_{y.Ed}}{\chi_{LT} \cdot \frac{M_{y.Rk.el}}{\gamma_{M1}}} + k_{zz} \cdot \frac{M_{z.Ed} + \Delta M_{z.Ed}}{\frac{M_{z.Rk.el}}{\gamma_{M1}}} = 0.324 \qquad < 1 \qquad OK$$

3) Top part left leg:

$N_{Ed} := N_{Ed.LT} = 250.04\ \boldsymbol{kN}$

$M_{y.Ed} := M_{y.Ed.LT} = 41.46\ \boldsymbol{kN \cdot m}$

$M_{z.Ed} := M_{z.Ed.LT} = 1.63\ \boldsymbol{kN \cdot m}$

Long.: $\alpha_h := 1$ $\qquad \psi := -0.136$

$C_{my} := 0.95 + 0.05 \cdot \alpha_h = 1$

Trans.: $\alpha_h := -0.561$ $\qquad \psi := -0.283$

$C_{mz} := 0.95 + 0.05 \cdot \alpha_h \cdot (1 + 2 \cdot \psi) = 0.938$

Elastic - conservative:

$$k_{yy.1} := C_{my} \cdot \left(1 + 0.6 \cdot \lambda_y \cdot \frac{N_{Ed}}{\chi_y \cdot \frac{N_{Rk}}{\gamma_{M1}}}\right) = 1.259$$

$$k_{yy.2} := C_{my} \cdot \left(1 + 0.6 \cdot \frac{N_{Ed}}{\chi_y \cdot \frac{N_{Rk}}{\gamma_{M1}}}\right) = 1.152 \qquad k_{yy} := k_{yy.2} = 1.152$$

$$k_{zz.1} := C_{mz} \cdot \left(1 + 0.6 \cdot \lambda_z \cdot \frac{N_{Ed}}{\chi_z \cdot \frac{N_{Rk}}{\gamma_{M1}}}\right) = 1.18$$

$$k_{zz.2} := C_{mz} \cdot \left(1 + 0.6 \cdot \frac{N_{Ed}}{\chi_z \cdot \frac{N_{Rk}}{\gamma_{M1}}}\right) = 1.081 \qquad k_{zz} := k_{zz.2} = 1.081$$

$$k_{yz} := k_{zz} = 1.081$$

$$k_{zy} := 0.8 \cdot k_{yy} = 0.922$$

NS-EN 1993-1-1:2005, Equation 6.61:

$$\frac{N_{Ed}}{\frac{\chi_y \cdot N_{Rk}}{\gamma_{M1}}} + k_{yy} \cdot \frac{M_{y.Ed} + \Delta M_{y.Ed}}{\chi_{LT} \cdot \frac{M_{y.Rk.el}}{\gamma_{M1}}} + k_{yz} \cdot \frac{M_{z.Ed} + \Delta M_{z.Ed}}{\frac{M_{z.Rk.el}}{\gamma_{M1}}} = 0.686 \qquad < 1 \qquad OK$$

NS-EN 1993-1-1:2005, Equation 6.62:

$$\frac{N_{Ed}}{\frac{\chi_z \cdot N_{Rk}}{\gamma_{M1}}} + k_{zy} \cdot \frac{M_{y.Ed} + \Delta M_{y.Ed}}{\chi_{LT} \cdot \frac{M_{y.Rk.el}}{\gamma_{M1}}} + k_{zz} \cdot \frac{M_{z.Ed} + \Delta M_{z.Ed}}{\frac{M_{z.Rk.el}}{\gamma_{M1}}} = 0.601 \qquad < 1 \qquad OK$$

4) Bottom part left leg:

$$N_{Ed} := N_{Ed.LB} = 272.52\ \boldsymbol{kN}$$

$$M_{y.Ed} := M_{y.Ed.LB} = 4.99\ \boldsymbol{kN \cdot m}$$

$$M_{z.Ed} := M_{z.Ed.LB} = 2.08\ \boldsymbol{kN \cdot m}$$

Long.: $\alpha_h := 0.998$ $\psi := 0.169$

$$C_{my} := 0.95 + 0.05 \cdot \alpha_h = 1$$

Trans.: $\alpha_s := -0.548$ $\psi := 0$

$$C_{mz} := 0.1 - 0.8 \cdot \alpha_s = 0.538$$

Elastic - conservative:

$$k_{yy.1} := C_{my} \cdot \left(1 + 0.6 \cdot \lambda_y \cdot \frac{N_{Ed}}{\chi_y \cdot \frac{N_{Rk}}{\gamma_{M1}}}\right) = 1.282$$

$$k_{yy.2} := C_{my} \cdot \left(1 + 0.6 \cdot \frac{N_{Ed}}{\chi_y \cdot \frac{N_{Rk}}{\gamma_{M1}}}\right) = 1.166 \qquad k_{yy} := k_{yy.2} = 1.166$$

$$k_{zz.1} := C_{mz} \cdot \left(1 + 0.6 \cdot \lambda_z \cdot \frac{N_{Ed}}{\chi_z \cdot \frac{N_{Rk}}{\gamma_{M1}}}\right) = 0.69$$

$$k_{zz.2} := C_{mz} \cdot \left(1 + 0.6 \cdot \frac{N_{Ed}}{\chi_z \cdot \frac{N_{Rk}}{\gamma_{M1}}}\right) = 0.628 \qquad k_{zz} := k_{zz.2} = 0.628$$

$$k_{yz} := k_{zz} = 0.628$$

$$k_{zy} := 0.8 \cdot k_{yy} = 0.933$$

NS-EN 1993-1-1:2005, Equation 6.61:

$$\frac{N_{Ed}}{\frac{\chi_y \cdot N_{Rk}}{\gamma_{M1}}} + k_{yy} \cdot \frac{M_{y.Ed} + \Delta M_{y.Ed}}{\chi_{LT} \cdot \frac{M_{y.Rk.el}}{\gamma_{M1}}} + k_{yz} \cdot \frac{M_{z.Ed} + \Delta M_{z.Ed}}{\frac{M_{z.Rk.el}}{\gamma_{M1}}} = 0.333 \qquad < 1 \qquad OK$$

NS-EN 1993-1-1:2005, Equation 6.62:

$$\frac{N_{Ed}}{\frac{\chi_z \cdot N_{Rk}}{\gamma_{M1}}} + k_{zy} \cdot \frac{M_{y.Ed} + \Delta M_{y.Ed}}{\chi_{LT} \cdot \frac{M_{y.Rk.el}}{\gamma_{M1}}} + k_{zz} \cdot \frac{M_{z.Ed} + \Delta M_{z.Ed}}{\frac{M_{z.Rk.el}}{\gamma_{M1}}} = 0.323 \qquad < 1 \qquad OK$$

2 Wind on line

RT=Right leg, Top. LT=Left leg, Top. RB=Right leg, Bottom. LB=Left leg, Bottom

$N_{Ed.RT} := 531.97\ kN$

$M_{y.Ed.RT} := 1.41\ kN \cdot m$

$M_{z.Ed.RT} := 59.36\ kN \cdot m$

$N_{Ed.LT} := 120.18\ kN$

$M_{y.Ed.LT} := 6.99\ kN \cdot m$

$M_{z.Ed.LT} := 80.36\ kN \cdot m$

$N_{Ed.RB} := 570.47\ kN$

$M_{y.Ed.RB} := 0.28\ kN \cdot m$

$M_{z.Ed.RB} := 60.20\ kN \cdot m$

$N_{Ed.LB} := 137.87\ kN$

$M_{y.Ed.LB} := 6.32\ kN \cdot m$

$M_{z.Ed.LB} := 80.64\ kN \cdot m$

Tverrsnittsklasse 1, 250*250*10mm

But still check elastic

Assuming guys prevent sideways buckling. So that: $L_{cr.y} = L_{cr.z} = \frac{L}{2}$

$f_y := 355\ MPa$

EN 50341

$\gamma_{M1} := 1.00$

EC3

$\gamma_{M0} := 1.05$

$A := 92.57 \cdot 10^2\ mm^2$

$N_{Rk} := f_y \cdot A = \left(3.286 \cdot 10^3\right)\ kN$

$W_{y.pl} := 822.00 \cdot 10^3\ mm^3$

$M_{y.Rk} := f_y \cdot W_{y.pl} = 291.81\ kN \cdot m$

$W_{y.el} := 696.53 \cdot 10^3 \cdot mm^3$

$M_{y.Rk.el} := f_y \cdot W_{y.el} = 247.268\ kN \cdot m$

$W_{z.pl} := W_{y.pl} = \left(8.22 \cdot 10^5\right)\ mm^3$

$M_{z.Rk} := f_y \cdot W_{z.pl} = 291.81\ kN \cdot m$

$W_{z.el} := W_{y.el} = \left(6.965 \cdot 10^5\right)\ mm^3$

$M_{z.Rk.el} := f_y \cdot W_{z.el} = 247.268\ kN \cdot m$

$\Delta M_{y.Ed} := 0$

$\Delta M_{z.Ed} := 0$

Clause 6.3.1.3:

$E := 210000\ MPa$ $\quad I := 8706.67 \cdot 10^4\ mm^4$

$L := 25.19\ m$ $\quad L_{cr} := \frac{L}{2} = 12.595\ m$

$N_{cr.y} := \frac{\pi^2 \cdot E \cdot I}{L_{cr}^2} = \left(1.138 \cdot 10^3\right)\ kN$ $\quad N_{cr.z} := \frac{\pi^2 \cdot E \cdot I}{L_{cr}^2} = \left(1.138 \cdot 10^3\right)\ kN$

$\lambda_y := \sqrt{\frac{N_{Rk}}{N_{cr.y}}} = 1.7$ $\quad \lambda_z := \sqrt{\frac{N_{Rk}}{N_{cr.z}}} = 1.7$

Warm formed: Buckling curve a in figure 6.4

$\chi_y := 0.3$

$\chi_z := 0.3$

Clause 6.3.2.3:

$$M_{c.Rd} := W_{y.el} \cdot \frac{f_y}{\gamma_{M0}} = 235.493\ kN \cdot m$$

Other cross section: Buckling curve d $\quad \alpha_{LT} := 0.76$

$$\lambda_{LT} := \sqrt{\frac{W_{y.el} \cdot f_y}{M_{c.Rd}}} = 1.025$$

$$\Phi_{LT} := 0.5 \cdot \left(1 + \alpha_{LT} \cdot \left(\lambda_{LT} - 0.2\right) + \lambda_{LT}^2\right) = 1.338$$

$$\chi_{LT} := \frac{1}{\Phi_{LT} + \sqrt{\Phi_{LT}^2 - \lambda_{LT}^2}} = 0.455$$

Annex B:

1) Top part right leg:

$$N_{Ed} := N_{Ed.RT} = 531.97\ kN$$

$$M_{y.Ed} := M_{y.Ed.RT} = 1.41\ kN \cdot m$$

$$M_{z.Ed} := M_{z.Ed.RT} = 59.36\ kN \cdot m$$

Long.: $\alpha_h := 0.972$ $\psi := -0.015$

$$C_{my} := 0.95 + 0.05 \cdot \alpha_h = 0.999$$

Trans.: $\alpha_h := 0.986$ $\psi := 0$

$$C_{mz} := 0.95 + 0.05 \cdot \alpha_h = 0.999$$

Elastic - conservative:

$$k_{yy.1} := C_{my} \cdot \left(1 + 0.6 \cdot \lambda_y \cdot \frac{N_{Ed}}{\chi_y \cdot \frac{N_{Rk}}{\gamma_{M1}}}\right) = 1.548$$

$$k_{yy.2} := C_{my} \cdot \left(1 + 0.6 \cdot \frac{N_{Ed}}{\chi_y \cdot \frac{N_{Rk}}{\gamma_{M1}}}\right) = 1.322 \qquad k_{yy} := k_{yy.2} = 1.322$$

$$k_{zz.1} := C_{mz} \cdot \left(1 + 0.6 \cdot \lambda_z \cdot \frac{N_{Ed}}{\chi_z \cdot \frac{N_{Rk}}{\gamma_{M1}}}\right) = 1.549$$

$$k_{zz.2} := C_{mz} \cdot \left(1 + 0.6 \cdot \frac{N_{Ed}}{\chi_z \cdot \frac{N_{Rk}}{\gamma_{M1}}}\right) = 1.323 \qquad k_{zz} := k_{zz.2} = 1.323$$

$$k_{yz} := k_{zz} = 1.323 \qquad k_{zy} := 0.8 \cdot k_{yy} = 1.058$$

NS-EN 1993-1-1:2005, Equation 6.61:

$$\frac{N_{Ed}}{\frac{\chi_y \cdot N_{Rk}}{\gamma_{M1}}} + k_{yy} \cdot \frac{M_{y.Ed} + \Delta M_{y.Ed}}{\chi_{LT} \cdot \frac{M_{y.Rk.el}}{\gamma_{M1}}} + k_{yz} \cdot \frac{M_{z.Ed} + \Delta M_{z.Ed}}{\frac{M_{z.Rk.el}}{\gamma_{M1}}} = 0.874 \qquad < 1 \qquad OK$$

NS-EN 1993-1-1:2005, Equation 6.62:

$$\frac{N_{Ed}}{\frac{\chi_z \cdot N_{Rk}}{\gamma_{M1}}} + k_{zy} \cdot \frac{M_{y.Ed} + \Delta M_{y.Ed}}{\chi_{LT} \cdot \frac{M_{y.Rk.el}}{\gamma_{M1}}} + k_{zz} \cdot \frac{M_{z.Ed} + \Delta M_{z.Ed}}{\frac{M_{z.Rk.el}}{\gamma_{M1}}} = 0.87 \qquad < 1 \qquad OK$$

2) Bottom part right leg:

$N_{Ed} := N_{Ed.RB} = 570.47 \ \boldsymbol{kN}$

$M_{y.Ed} := M_{y.Ed.RB} = 0.28 \ \boldsymbol{kN \cdot m}$

$M_{z.Ed} := M_{z.Ed.RB} = 60.2 \ \boldsymbol{kN \cdot m}$

Long.: $\alpha_h := 0.964$ $\psi := 0.33$

$C_{my} := 0.95 + 0.05 \cdot \alpha_h = 0.998$

Trans.: $\alpha_h := 0.984$ $\psi := 0$

$C_{mz} := 0.95 + 0.05 \cdot \alpha_h = 0.999$

Elastic - conservative:

$$k_{yy.1} := C_{my} \cdot \left(1 + 0.6 \cdot \lambda_y \cdot \frac{N_{Ed}}{\chi_y \cdot \frac{N_{Rk}}{\gamma_{M1}}} \right) = 1.587$$

$$k_{yy.2} := C_{my} \cdot \left(1 + 0.6 \cdot \frac{N_{Ed}}{\chi_y \cdot \frac{N_{Rk}}{\gamma_{M1}}} \right) = 1.345 \qquad k_{yy} := k_{yy.2} = 1.345$$

$$k_{zz.1} := C_{mz} \cdot \left(1 + 0.6 \cdot \lambda_z \cdot \frac{N_{Ed}}{\chi_z \cdot \frac{N_{Rk}}{\gamma_{M1}}} \right) = 1.589$$

$$k_{zz.2} := C_{mz} \cdot \left(1 + 0.6 \cdot \frac{N_{Ed}}{\chi_z \cdot \frac{N_{Rk}}{\gamma_{M1}}} \right) = 1.346 \qquad k_{zz} := k_{zz.2} = 1.346$$

$k_{yz} := k_{zz} = 1.346$

$k_{zy} := 0.8 \cdot k_{yy} = 1.076$

NS-EN 1993-1-1:2005, Equation 6.61:

$$\frac{N_{Ed}}{\frac{\chi_y \cdot N_{Rk}}{\gamma_{M1}}} + k_{yy} \cdot \frac{M_{y.Ed} + \Delta M_{y.Ed}}{\chi_{LT} \cdot \frac{M_{y.Rk.el}}{\gamma_{M1}}} + k_{yz} \cdot \frac{M_{z.Ed} + \Delta M_{z.Ed}}{\frac{M_{z.Rk.el}}{\gamma_{M1}}} = 0.91 \qquad < 1 \qquad OK$$

NS-EN 1993-1-1:2005, Equation 6.62:

$$\frac{N_{Ed}}{\frac{\chi_z \cdot N_{Rk}}{\gamma_{M1}}} + k_{zy} \cdot \frac{M_{y.Ed} + \Delta M_{y.Ed}}{\chi_{LT} \cdot \frac{M_{y.Rk.el}}{\gamma_{M1}}} + k_{zz} \cdot \frac{M_{z.Ed} + \Delta M_{z.Ed}}{\frac{M_{z.Rk.el}}{\gamma_{M1}}} = 0.909 \qquad < 1 \qquad OK$$

3) Top part left leg:

$N_{Ed} := N_{Ed.LT} = 120.18\ \boldsymbol{kN}$

$M_{y.Ed} := M_{y.Ed.LT} = 6.99\ \boldsymbol{kN \cdot m}$

$M_{z.Ed} := M_{z.Ed.LT} = 80.36\ \boldsymbol{kN \cdot m}$

Long.: $\alpha_s := 1$ $\psi := -0.937$

$C_{my} := 0.2 + 0.8 \cdot \alpha_s = 1$

Trans.: $\alpha_s := 1$ $\psi := 0$

$C_{mz} := 0.2 + 0.8 \cdot \alpha_s = 1$

Elastic - conservative:

$$k_{yy.1} := C_{my} \cdot \left(1 + 0.6 \cdot \lambda_y \cdot \frac{N_{Ed}}{\chi_y \cdot \frac{N_{Rk}}{\gamma_{M1}}}\right) = 1.124$$

$$k_{yy.2} := C_{my} \cdot \left(1 + 0.6 \cdot \frac{N_{Ed}}{\chi_y \cdot \frac{N_{Rk}}{\gamma_{M1}}}\right) = 1.073 \qquad k_{yy} := k_{yy.2} = 1.073$$

$$k_{zz.1} := C_{mz} \cdot \left(1 + 0.6 \cdot \lambda_z \cdot \frac{N_{Ed}}{\chi_z \cdot \frac{N_{Rk}}{\gamma_{M1}}}\right) = 1.124$$

$$k_{zz.2} := C_{mz} \cdot \left(1 + 0.6 \cdot \frac{N_{Ed}}{\chi_z \cdot \frac{N_{Rk}}{\gamma_{M1}}}\right) = 1.073 \qquad k_{zz} := k_{zz.2} = 1.073$$

$$k_{yz} := k_{zz} = 1.073$$

$$k_{zy} := 0.8 \cdot k_{yy} = 0.859$$

NS-EN 1993-1-1:2005, Equation 6.61:

$$\frac{N_{Ed}}{\frac{\chi_y \cdot N_{Rk}}{\gamma_{M1}}} + k_{yy} \cdot \frac{M_{y.Ed} + \Delta M_{y.Ed}}{\chi_{LT} \cdot \frac{M_{y.Rk.el}}{\gamma_{M1}}} + k_{yz} \cdot \frac{M_{z.Ed} + \Delta M_{z.Ed}}{\frac{M_{z.Rk.el}}{\gamma_{M1}}} = 0.537 \qquad < 1 \qquad OK$$

NS-EN 1993-1-1:2005, Equation 6.62:

$$\frac{N_{Ed}}{\frac{\chi_z \cdot N_{Rk}}{\gamma_{M1}}} + k_{zy} \cdot \frac{M_{y.Ed} + \Delta M_{y.Ed}}{\chi_{LT} \cdot \frac{M_{y.Rk.el}}{\gamma_{M1}}} + k_{zz} \cdot \frac{M_{z.Ed} + \Delta M_{z.Ed}}{\frac{M_{z.Rk.el}}{\gamma_{M1}}} = 0.524 \qquad < 1 \qquad OK$$

4) Bottom part left leg:

$$N_{Ed} := N_{Ed.LB} = 137.87 \ \boldsymbol{kN}$$

$$M_{y.Ed} := M_{y.Ed.LB} = 6.32 \ \boldsymbol{kN \cdot m}$$

$$M_{z.Ed} := M_{z.Ed.LB} = 80.64 \ \boldsymbol{kN \cdot m}$$

Long.: $\alpha_h := 1$ $\psi := 0.169 - 0.051$

$$C_{my} := 0.95 + 0.05 \cdot \alpha_h = 1$$

Trans.: $\alpha_s := 1$ $\psi := 0$

$$C_{mz} := 0.2 + 0.8 \cdot \alpha_s = 1$$

Elastic - conservative:

$$k_{yy.1} := C_{my} \cdot \left(1 + 0.6 \cdot \lambda_y \cdot \frac{N_{Ed}}{\chi_y \cdot \frac{N_{Rk}}{\gamma_{M1}}}\right) = 1.143$$

$$k_{yy.2} := C_{my} \cdot \left(1 + 0.6 \cdot \frac{N_{Ed}}{\chi_y \cdot \frac{N_{Rk}}{\gamma_{M1}}}\right) = 1.084 \qquad k_{yy} := k_{yy.2} = 1.084$$

$$k_{zz.1} := C_{mz} \cdot \left(1 + 0.6 \cdot \lambda_z \cdot \frac{N_{Ed}}{\chi_z \cdot \frac{N_{Rk}}{\gamma_{M1}}}\right) = 1.143$$

$$k_{zz.2} := C_{mz} \cdot \left(1 + 0.6 \cdot \frac{N_{Ed}}{\chi_z \cdot \frac{N_{Rk}}{\gamma_{M1}}}\right) = 1.084 \qquad k_{zz} := k_{zz.2} = 1.084$$

$$k_{yz} := k_{zz} = 1.084$$

$$k_{zy} := 0.8 \cdot k_{yy} = 0.867$$

NS-EN 1993-1-1:2005, Equation 6.61:

$$\frac{N_{Ed}}{\frac{\chi_y \cdot N_{Rk}}{\gamma_{M1}}} + k_{yy} \cdot \frac{M_{y.Ed} + \Delta M_{y.Ed}}{\chi_{LT} \cdot \frac{M_{y.Rk.el}}{\gamma_{M1}}} + k_{yz} \cdot \frac{M_{z.Ed} + \Delta M_{z.Ed}}{\frac{M_{z.Rk.el}}{\gamma_{M1}}} = 0.554 \qquad < 1 \qquad OK$$

NS-EN 1993-1-1:2005, Equation 6.62:

$$\frac{N_{Ed}}{\frac{\chi_z \cdot N_{Rk}}{\gamma_{M1}}} + k_{zy} \cdot \frac{M_{y.Ed} + \Delta M_{y.Ed}}{\chi_{LT} \cdot \frac{M_{y.Rk.el}}{\gamma_{M1}}} + k_{zz} \cdot \frac{M_{z.Ed} + \Delta M_{z.Ed}}{\frac{M_{z.Rk.el}}{\gamma_{M1}}} = 0.542 \qquad < 1 \qquad OK$$

D Input from PLS-programs

D.1 Input for Transmission Line from PLS-CADD

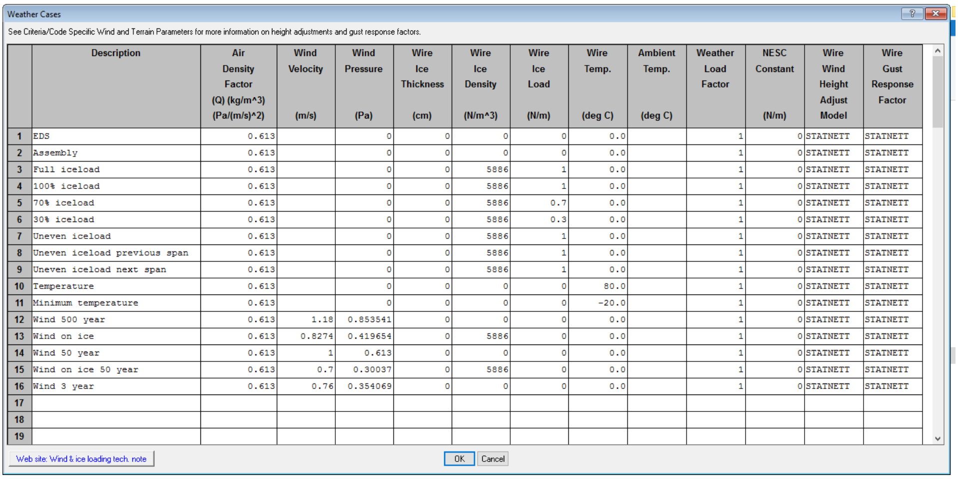

Weather Cases

See Criteria/Code Specific Wind and Terrain Parameters for more information on height adjustments and gust response factors.

	Description	Air Density Factor (Q) (kg/m^3) (Pa/(m/s)^2)	Wind Velocity (m/s)	Wind Pressure (Pa)	Wire Ice Thickness (cm)	Wire Ice Density (N/m^3)	Wire Ice Load (N/m)	Wire Temp. (deg C)	Ambient Temp. (deg C)	Weather Load Factor	NESC Constant (N/m)	Wire Wind Height Adjust Model	Wire Gust Response Factor
1	EDS	0.613		0	0	0	0	0.0		1	0	STATNETT	STATNETT
2	Assembly	0.613		0	0	0	0	0.0		1	0	STATNETT	STATNETT
3	Full iceload	0.613		0	0	5886	1	0.0		1	0	STATNETT	STATNETT
4	100% iceload	0.613		0	0	5886	1	0.0		1	0	STATNETT	STATNETT
5	70% iceload	0.613		0	0	5886	0.7	0.0		1	0	STATNETT	STATNETT
6	30% iceload	0.613		0	0	5886	0.3	0.0		1	0	STATNETT	STATNETT
7	Uneven iceload	0.613		0	0	5886	1	0.0		1	0	STATNETT	STATNETT
8	Uneven iceload previous span	0.613		0	0	5886	1	0.0		1	0	STATNETT	STATNETT
9	Uneven iceload next span	0.613		0	0	5886	1	0.0		1	0	STATNETT	STATNETT
10	Temperature	0.613		0	0	0	0	80.0		1	0	STATNETT	STATNETT
11	Minimum temperature	0.613		0	0	0	0	-20.0		1	0	STATNETT	STATNETT
12	Wind 500 year	0.613	1.18	0.853541	0	0	0	0.0		1	0	STATNETT	STATNETT
13	Wind on ice	0.613	0.8274	0.419654	0	5886	0	0.0		1	0	STATNETT	STATNETT
14	Wind 50 year	0.613	1	0.613	0	0	0	0.0		1	0	STATNETT	STATNETT
15	Wind on ice 50 year	0.613	0.7	0.30037	0	5886	0	0.0		1	0	STATNETT	STATNETT
16	Wind 3 year	0.613	0.76	0.354069	0	0	0	0.0		1	0	STATNETT	STATNETT
17													
18													
19													

Web site: Wind & ice loading tech. note

OK Cancel

Figure D.4: Weather cases from PLS-CADD.

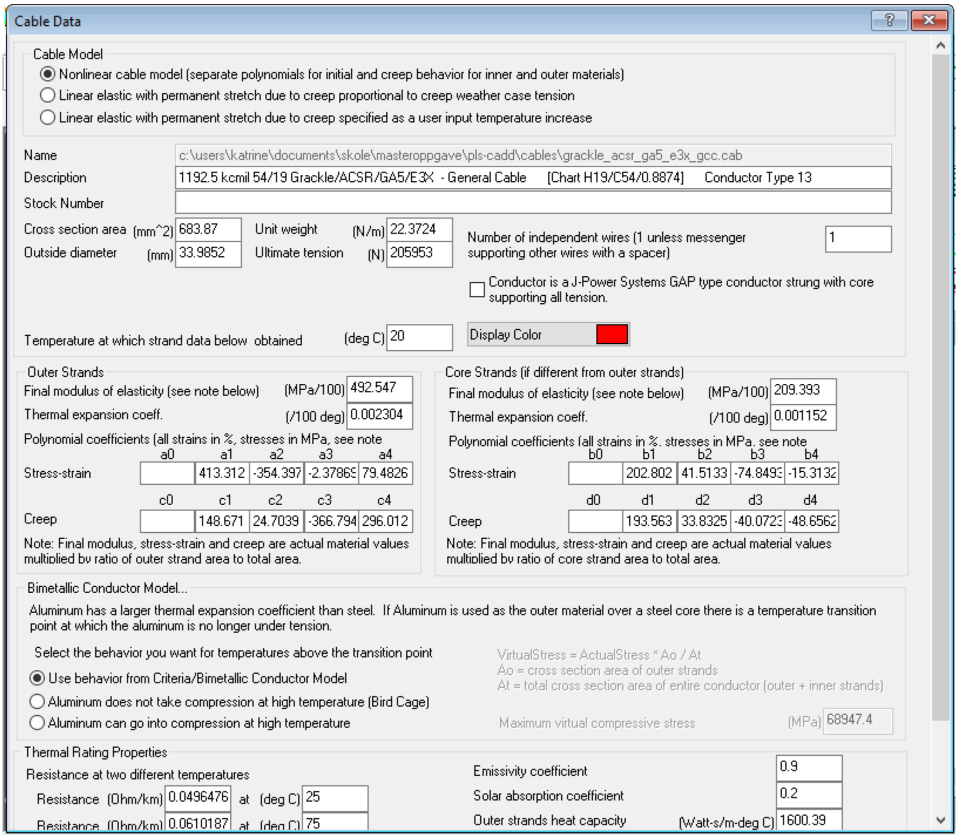

Figure D.5: Triplex Grackle conductor.

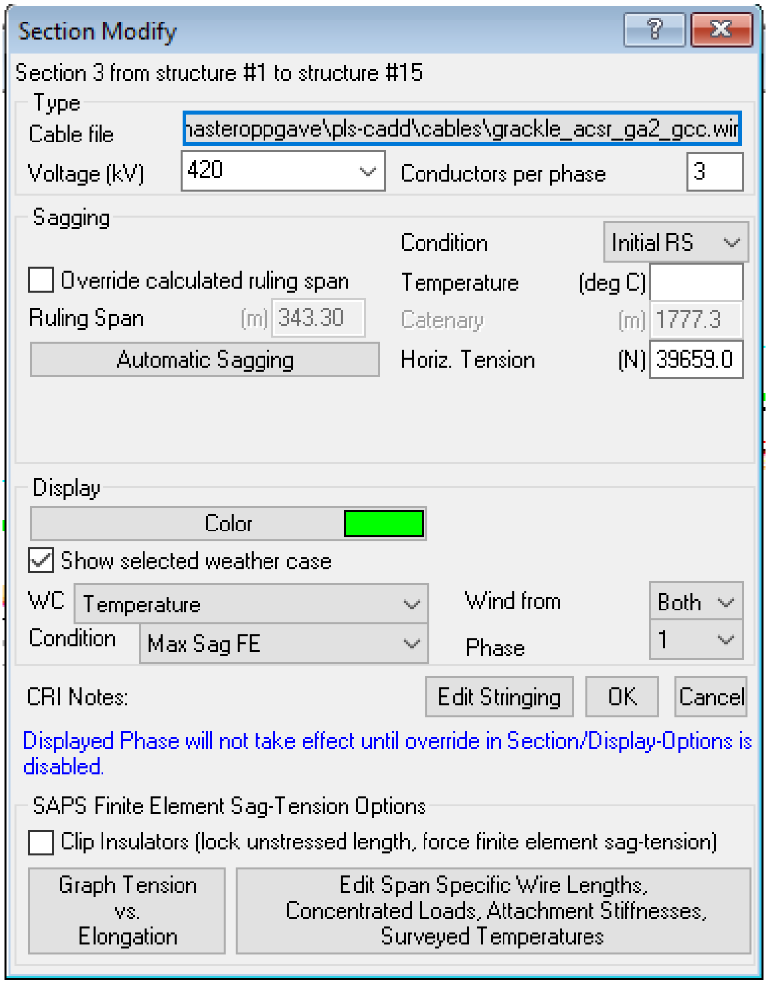

Figure D.6: Triplex Grackle conductor.

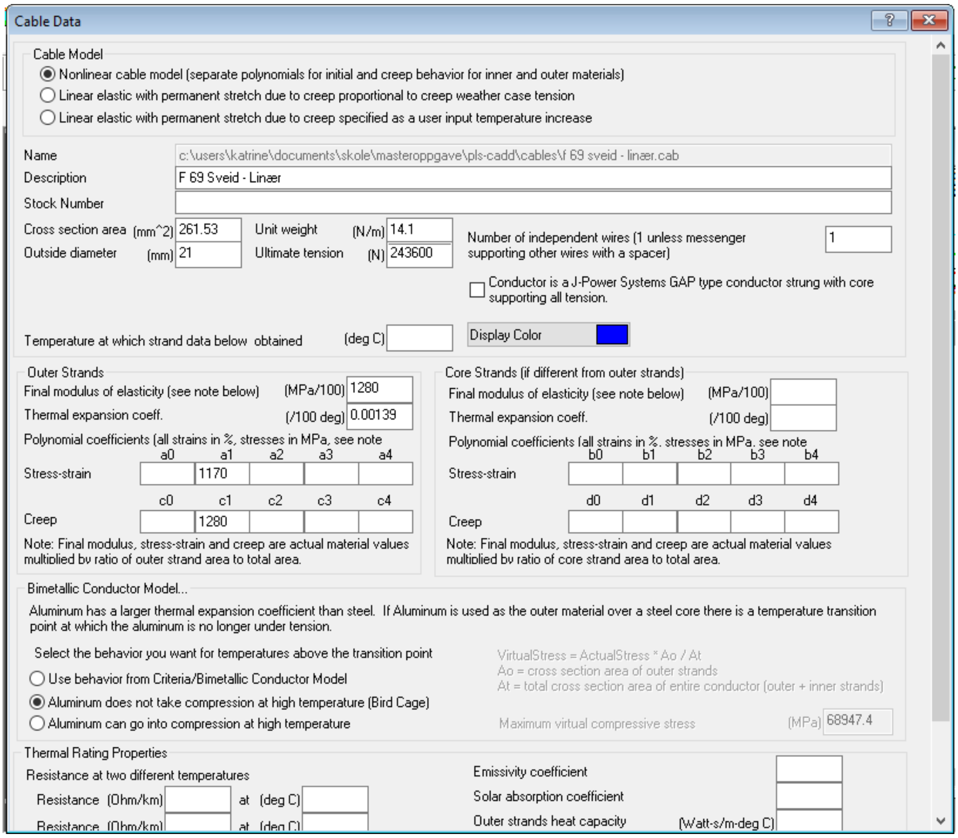

Figure D.7: F 69 Sveid ground wire.

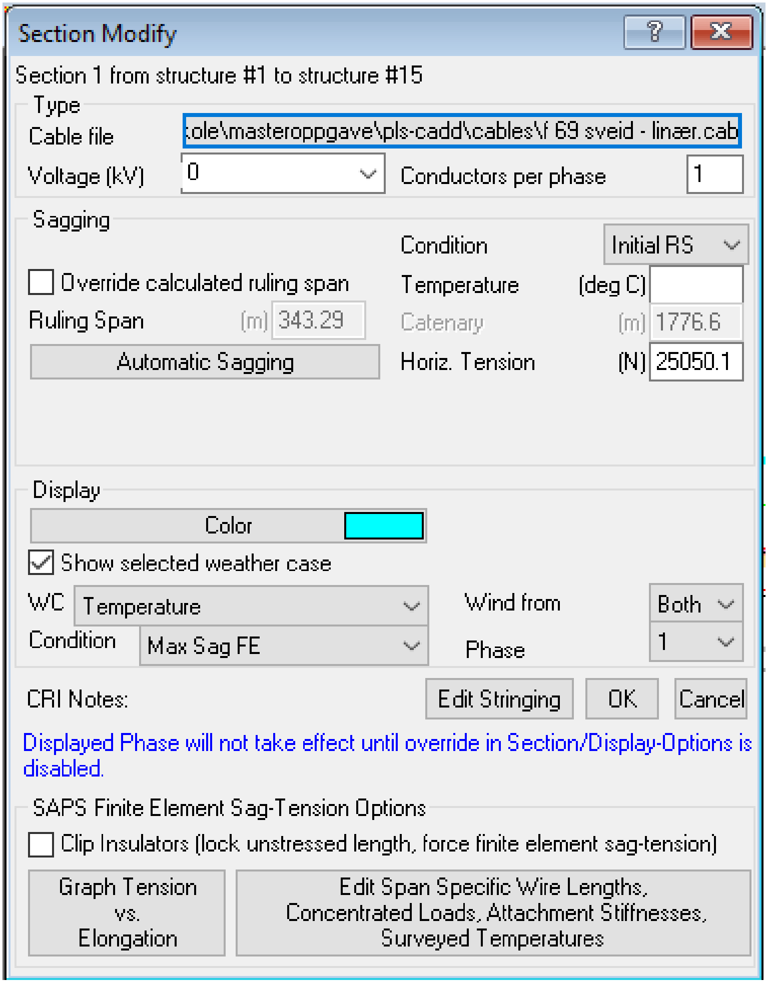

Figure D.8: F 69 Sveid ground wire.

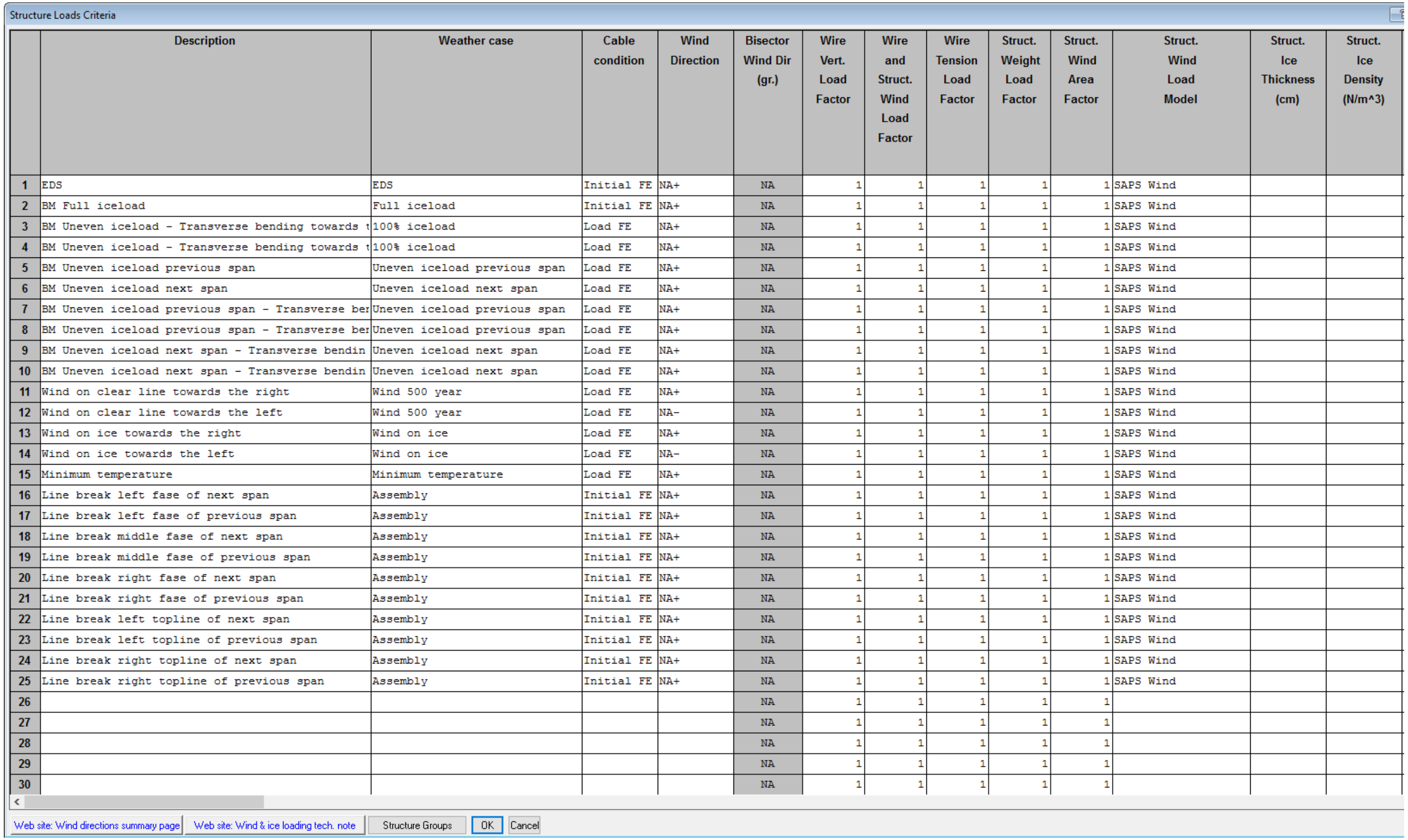

Structure Loads Criteria

	Description	Weather case	Cable condition	Wind Direction	Bisector Wind Dir (gr.)	Wire Vert. Load Factor	Wire and Struct. Wind Load Factor	Wire Tension Load Factor	Struct. Weight Load Factor	Struct. Wind Area Factor	Struct. Wind Load Model	Struct. Ice Thickness (cm)	Struct. Ice Density (N/m^3)
1	EDS	EDS	Initial FE	NA+	NA	1	1	1	1	1	SAPS Wind		
2	BM Full iceload	Full iceload	Initial FE	NA+	NA	1	1	1	1	1	SAPS Wind		
3	BM Uneven iceload - Transverse bending towards t	100% iceload	Load FE	NA+	NA	1	1	1	1	1	SAPS Wind		
4	BM Uneven iceload - Transverse bending towards t	100% iceload	Load FE	NA+	NA	1	1	1	1	1	SAPS Wind		
5	BM Uneven iceload previous span	Uneven iceload previous span	Load FE	NA+	NA	1	1	1	1	1	SAPS Wind		
6	BM Uneven iceload next span	Uneven iceload next span	Load FE	NA+	NA	1	1	1	1	1	SAPS Wind		
7	BM Uneven iceload previous span - Transverse ber	Uneven iceload previous span	Load FE	NA+	NA	1	1	1	1	1	SAPS Wind		
8	BM Uneven iceload previous span - Transverse ber	Uneven iceload previous span	Load FE	NA+	NA	1	1	1	1	1	SAPS Wind		
9	BM Uneven iceload next span - Transverse bendin	Uneven iceload next span	Load FE	NA+	NA	1	1	1	1	1	SAPS Wind		
10	BM Uneven iceload next span - Transverse bendin	Uneven iceload next span	Load FE	NA+	NA	1	1	1	1	1	SAPS Wind		
11	Wind on clear line towards the right	Wind 500 year	Load FE	NA+	NA	1	1	1	1	1	SAPS Wind		
12	Wind on clear line towards the left	Wind 500 year	Load FE	NA-	NA	1	1	1	1	1	SAPS Wind		
13	Wind on ice towards the right	Wind on ice	Load FE	NA+	NA	1	1	1	1	1	SAPS Wind		
14	Wind on ice towards the left	Wind on ice	Load FE	NA-	NA	1	1	1	1	1	SAPS Wind		
15	Minimum temperature	Minimum temperature	Load FE	NA+	NA	1	1	1	1	1	SAPS Wind		
16	Line break left fase of next span	Assembly	Initial FE	NA+	NA	1	1	1	1	1	SAPS Wind		
17	Line break left fase of previous span	Assembly	Initial FE	NA+	NA	1	1	1	1	1	SAPS Wind		
18	Line break middle fase of next span	Assembly	Initial FE	NA+	NA	1	1	1	1	1	SAPS Wind		
19	Line break middle fase of previous span	Assembly	Initial FE	NA+	NA	1	1	1	1	1	SAPS Wind		
20	Line break right fase of next span	Assembly	Initial FE	NA+	NA	1	1	1	1	1	SAPS Wind		
21	Line break right fase of previous span	Assembly	Initial FE	NA+	NA	1	1	1	1	1	SAPS Wind		
22	Line break left topline of next span	Assembly	Initial FE	NA+	NA	1	1	1	1	1	SAPS Wind		
23	Line break left topline of previous span	Assembly	Initial FE	NA+	NA	1	1	1	1	1	SAPS Wind		
24	Line break right topline of next span	Assembly	Initial FE	NA+	NA	1	1	1	1	1	SAPS Wind		
25	Line break right topline of previous span	Assembly	Initial FE	NA+	NA	1	1	1	1	1	SAPS Wind		
26					NA	1	1	1	1	1			
27					NA	1	1	1	1	1			
28					NA	1	1	1	1	1			
29					NA	1	1	1	1	1			
30					NA	1	1	1	1	1			

Web site: Wind directions summary page | Web site: Wind & ice loading tech. note | Structure Groups | OK | Cancel

Figure D.9: Load cases part 1.

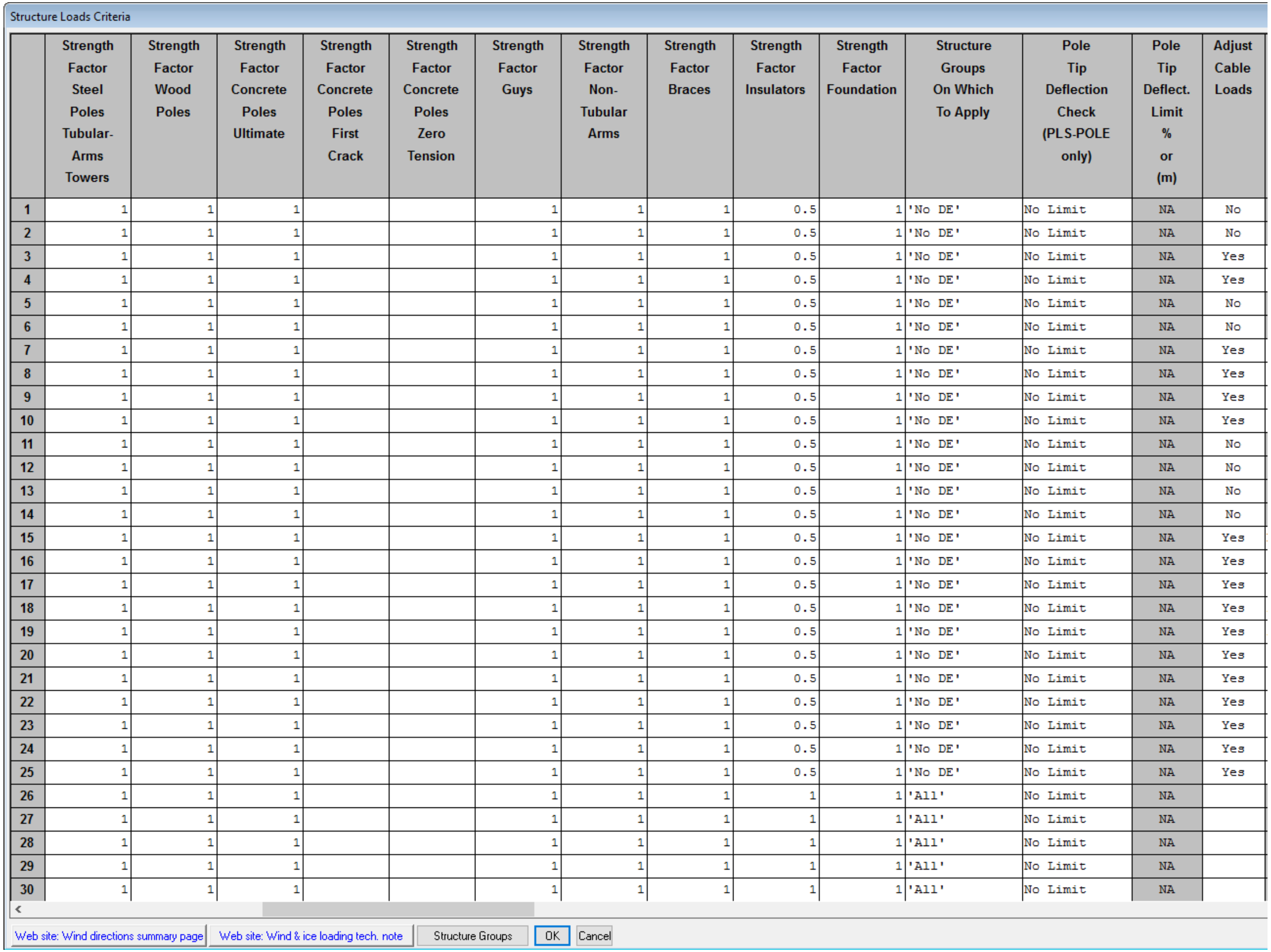

Structure Loads Criteria

	Strength Factor Steel Poles Tubular-Arms Towers	Strength Factor Wood Poles	Strength Factor Concrete Poles Ultimate	Strength Factor Concrete Poles First Crack	Strength Factor Concrete Poles Zero Tension	Strength Factor Guys	Strength Factor Non-Tubular Arms	Strength Factor Braces	Strength Factor Insulators	Strength Factor Foundation	Structure Groups On Which To Apply	Pole Tip Deflection Check (PLS-POLE only)	Pole Tip Deflect. Limit % or (m)	Adjust Cable Loads
1	1	1	1			1	1	1	0.5	1	'No DE'	No Limit	NA	No
2	1	1	1			1	1	1	0.5	1	'No DE'	No Limit	NA	No
3	1	1	1			1	1	1	0.5	1	'No DE'	No Limit	NA	Yes
4	1	1	1			1	1	1	0.5	1	'No DE'	No Limit	NA	Yes
5	1	1	1			1	1	1	0.5	1	'No DE'	No Limit	NA	No
6	1	1	1			1	1	1	0.5	1	'No DE'	No Limit	NA	No
7	1	1	1			1	1	1	0.5	1	'No DE'	No Limit	NA	Yes
8	1	1	1			1	1	1	0.5	1	'No DE'	No Limit	NA	Yes
9	1	1	1			1	1	1	0.5	1	'No DE'	No Limit	NA	Yes
10	1	1	1			1	1	1	0.5	1	'No DE'	No Limit	NA	Yes
11	1	1	1			1	1	1	0.5	1	'No DE'	No Limit	NA	No
12	1	1	1			1	1	1	0.5	1	'No DE'	No Limit	NA	No
13	1	1	1			1	1	1	0.5	1	'No DE'	No Limit	NA	No
14	1	1	1			1	1	1	0.5	1	'No DE'	No Limit	NA	No
15	1	1	1			1	1	1	0.5	1	'No DE'	No Limit	NA	Yes
16	1	1	1			1	1	1	0.5	1	'No DE'	No Limit	NA	Yes
17	1	1	1			1	1	1	0.5	1	'No DE'	No Limit	NA	Yes
18	1	1	1			1	1	1	0.5	1	'No DE'	No Limit	NA	Yes
19	1	1	1			1	1	1	0.5	1	'No DE'	No Limit	NA	Yes
20	1	1	1			1	1	1	0.5	1	'No DE'	No Limit	NA	Yes
21	1	1	1			1	1	1	0.5	1	'No DE'	No Limit	NA	Yes
22	1	1	1			1	1	1	0.5	1	'No DE'	No Limit	NA	Yes
23	1	1	1			1	1	1	0.5	1	'No DE'	No Limit	NA	Yes
24	1	1	1			1	1	1	0.5	1	'No DE'	No Limit	NA	Yes
25	1	1	1			1	1	1	0.5	1	'No DE'	No Limit	NA	Yes
26	1	1	1			1	1	1	1	1	'All'	No Limit	NA	
27	1	1	1			1	1	1	1	1	'All'	No Limit	NA	
28	1	1	1			1	1	1	1	1	'All'	No Limit	NA	
29	1	1	1			1	1	1	1	1	'All'	No Limit	NA	
30	1	1	1			1	1	1	1	1	'All'	No Limit	NA	

Figure D.10: Load cases part 2.

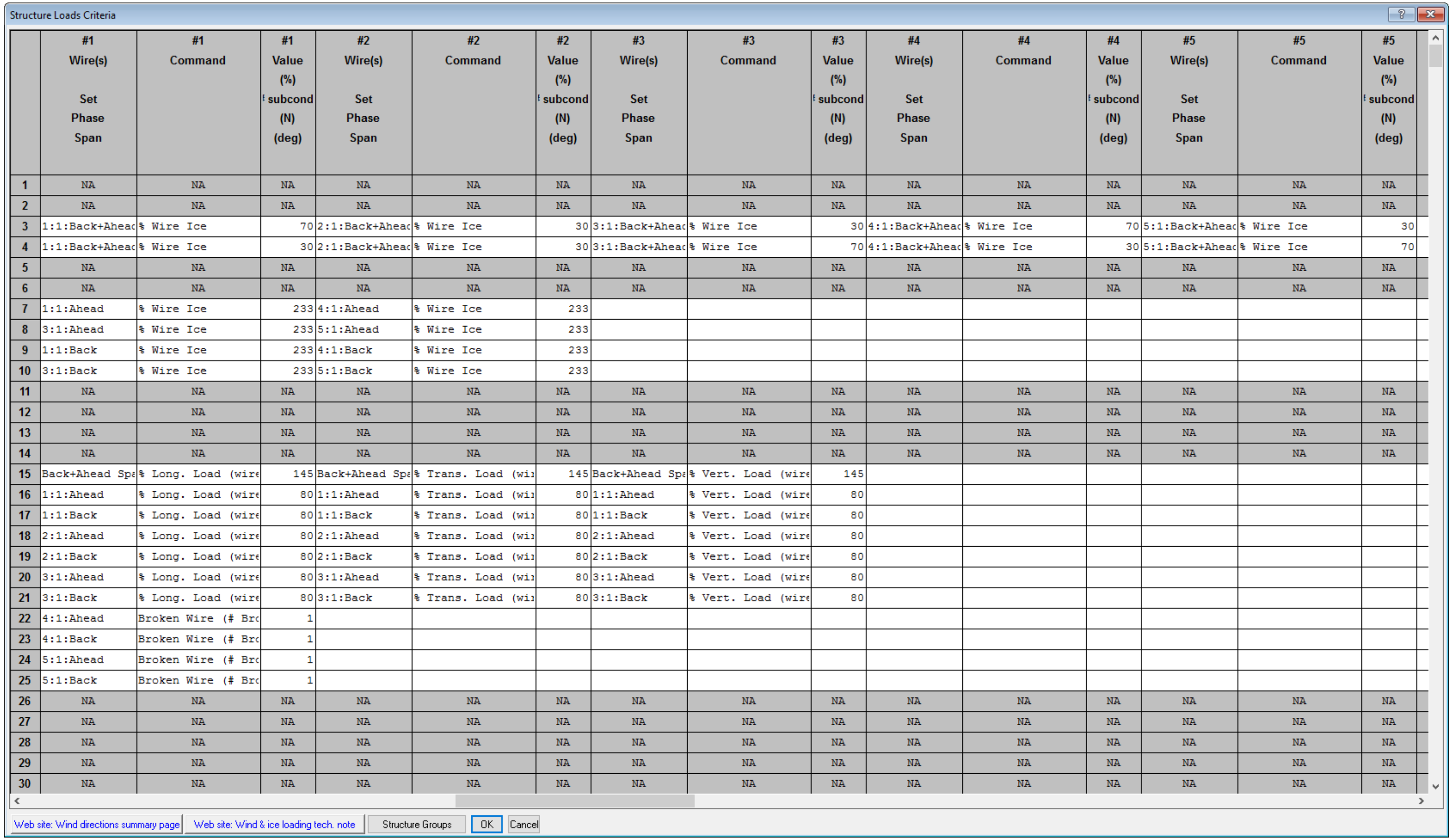

	#1 Wire(s) Set Phase Span	#1 Command	#1 Value (%) subcond (N) (deg)	#2 Wire(s) Set Phase Span	#2 Command	#2 Value (%) subcond (N) (deg)	#3 Wire(s) Set Phase Span	#3 Command	#3 Value (%) subcond (N) (deg)	#4 Wire(s) Set Phase Span	#4 Command	#4 Value (%) subcond (N) (deg)	#5 Wire(s) Set Phase Span	#5 Command	#5 Value (%) subcond (N) (deg)
1	NA	NA	NA	NA	NA	NA	NA	NA	NA	NA	NA	NA	NA	NA	NA
2	NA	NA	NA	NA	NA	NA	NA	NA	NA	NA	NA	NA	NA	NA	NA
3	1:1:Back+Aheac	% Wire Ice	70	2:1:Back+Aheac	% Wire Ice	30	3:1:Back+Aheac	% Wire Ice	30	4:1:Back+Aheac	% Wire Ice	70	5:1:Back+Aheac	% Wire Ice	30
4	1:1:Back+Aheac	% Wire Ice	30	2:1:Back+Aheac	% Wire Ice	30	3:1:Back+Aheac	% Wire Ice	70	4:1:Back+Aheac	% Wire Ice	30	5:1:Back+Aheac	% Wire Ice	70
5	NA	NA	NA	NA	NA	NA	NA	NA	NA	NA	NA	NA	NA	NA	NA
6	NA	NA	NA	NA	NA	NA	NA	NA	NA	NA	NA	NA	NA	NA	NA
7	1:1:Ahead	% Wire Ice	233	4:1:Ahead	% Wire Ice	233									
8	3:1:Ahead	% Wire Ice	233	5:1:Ahead	% Wire Ice	233									
9	1:1:Back	% Wire Ice	233	4:1:Back	% Wire Ice	233									
10	3:1:Back	% Wire Ice	233	5:1:Back	% Wire Ice	233									
11	NA	NA	NA	NA	NA	NA	NA	NA	NA	NA	NA	NA	NA	NA	NA
12	NA	NA	NA	NA	NA	NA	NA	NA	NA	NA	NA	NA	NA	NA	NA
13	NA	NA	NA	NA	NA	NA	NA	NA	NA	NA	NA	NA	NA	NA	NA
14	NA	NA	NA	NA	NA	NA	NA	NA	NA	NA	NA	NA	NA	NA	NA
15	Back+Ahead Spa	% Long. Load (wire	145	Back+Ahead Spa	% Trans. Load (wi	145	Back+Ahead Spa	% Vert. Load (wire	145						
16	1:1:Ahead	% Long. Load (wire	80	1:1:Ahead	% Trans. Load (wi	80	1:1:Ahead	% Vert. Load (wire	80						
17	1:1:Back	% Long. Load (wire	80	1:1:Back	% Trans. Load (wi	80	1:1:Back	% Vert. Load (wire	80						
18	2:1:Ahead	% Long. Load (wire	80	2:1:Ahead	% Trans. Load (wi	80	2:1:Ahead	% Vert. Load (wire	80						
19	2:1:Back	% Long. Load (wire	80	2:1:Back	% Trans. Load (wi	80	2:1:Back	% Vert. Load (wire	80						
20	3:1:Ahead	% Long. Load (wire	80	3:1:Ahead	% Trans. Load (wi	80	3:1:Ahead	% Vert. Load (wire	80						
21	3:1:Back	% Long. Load (wire	80	3:1:Back	% Trans. Load (wi	80	3:1:Back	% Vert. Load (wire	80						
22	4:1:Ahead	Broken Wire (# Brc	1												
23	4:1:Back	Broken Wire (# Brc	1												
24	5:1:Ahead	Broken Wire (# Brc	1												
25	5:1:Back	Broken Wire (# Brc	1												
26	NA	NA	NA	NA	NA	NA	NA	NA	NA	NA	NA	NA	NA	NA	NA
27	NA	NA	NA	NA	NA	NA	NA	NA	NA	NA	NA	NA	NA	NA	NA
28	NA	NA	NA	NA	NA	NA	NA	NA	NA	NA	NA	NA	NA	NA	NA
29	NA	NA	NA	NA	NA	NA	NA	NA	NA	NA	NA	NA	NA	NA	NA
30	NA	NA	NA	NA	NA	NA	NA	NA	NA	NA	NA	NA	NA	NA	NA

Figure D.11: Load cases part 3.

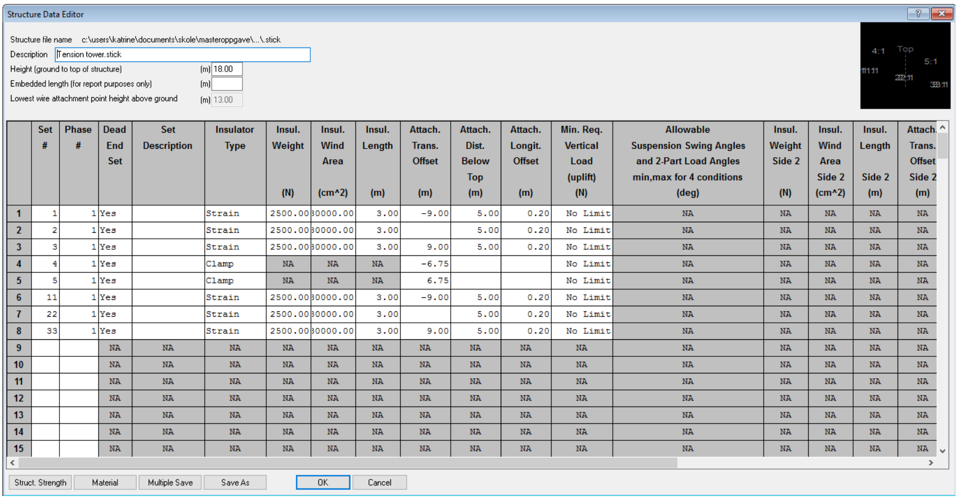

	Set #	Phase #	Dead End Set	Set Description	Insulator Type	Insul. Weight (N)	Insul. Wind Area (cm^2)	Insul. Length (m)	Attach. Trans. Offset (m)	Attach. Dist. Below Top (m)	Attach. Longit. Offset (m)	Min. Req. Vertical Load (uplift) (N)	Allowable Suspension Swing Angles and 2-Part Load Angles min,max for 4 conditions (deg)	Insul. Weight Side 2 (N)	Insul. Wind Area Side 2 (cm^2)	Insul. Length Side 2 (m)	Attach. Trans. Offset Side 2 (m)
1	1	1	Yes		Strain	2500.00	30000.00	3.00	-9.00	5.00	0.20	No Limit	NA	NA	NA	NA	NA
2	2	1	Yes		Strain	2500.00	30000.00	3.00		5.00	0.20	No Limit	NA	NA	NA	NA	NA
3	3	1	Yes		Strain	2500.00	30000.00	3.00	9.00	5.00	0.20	No Limit	NA	NA	NA	NA	NA
4	4	1	Yes		Clamp	NA	NA	NA	-6.75			No Limit	NA	NA	NA	NA	NA
5	5	1	Yes		Clamp	NA	NA	NA	6.75			No Limit	NA	NA	NA	NA	NA
6	11	1	Yes		Strain	2500.00	30000.00	3.00	-9.00	5.00	0.20	No Limit	NA	NA	NA	NA	NA
7	22	1	Yes		Strain	2500.00	30000.00	3.00		5.00	0.20	No Limit	NA	NA	NA	NA	NA
8	33	1	Yes		Strain	2500.00	30000.00	3.00	9.00	5.00	0.20	No Limit	NA	NA	NA	NA	NA
9			NA	NA	NA	NA	NA	NA	NA	NA	NA	NA	NA	NA	NA	NA	NA
10			NA	NA	NA	NA	NA	NA	NA	NA	NA	NA	NA	NA	NA	NA	NA
11			NA	NA	NA	NA	NA	NA	NA	NA	NA	NA	NA	NA	NA	NA	NA
12			NA	NA	NA	NA	NA	NA	NA	NA	NA	NA	NA	NA	NA	NA	NA
13			NA	NA	NA	NA	NA	NA	NA	NA	NA	NA	NA	NA	NA	NA	NA
14			NA	NA	NA	NA	NA	NA	NA	NA	NA	NA	NA	NA	NA	NA	NA
15			NA	NA	NA	NA	NA	NA	NA	NA	NA	NA	NA	NA	NA	NA	NA

Figure D.12: Dead end structures.

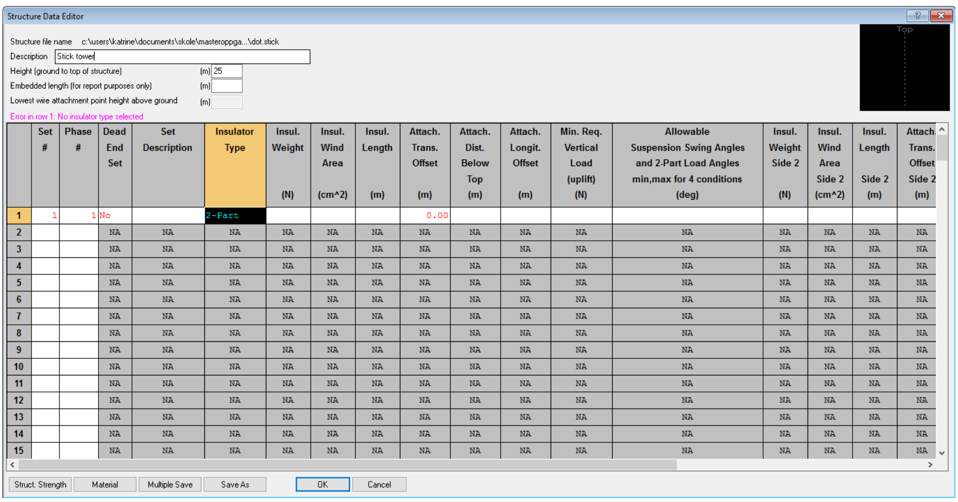

	Set #	Phase #	Dead End Set	Set Description	Insulator Type	Insul. Weight (N)	Insul. Wind Area (cm^2)	Insul. Length (m)	Attach. Trans. Offset (m)	Attach. Dist. Below Top (m)	Attach. Longit. Offset (m)	Min. Req. Vertical Load (uplift) (N)	Allowable Suspension Swing Angles and 2-Part Load Angles min,max for 4 conditions (deg)	Insul. Weight Side 2 (N)	Insul. Wind Area Side 2 (cm^2)	Insul. Length Side 2 (m)	Attach. Trans. Offset Side 2 (m)
1	1	1	No		2-Part				0.00								
2			NA	NA	NA	NA	NA	NA	NA	NA	NA	NA	NA	NA	NA	NA	NA
3			NA	NA	NA	NA	NA	NA	NA	NA	NA	NA	NA	NA	NA	NA	NA
4			NA	NA	NA	NA	NA	NA	NA	NA	NA	NA	NA	NA	NA	NA	NA
5			NA	NA	NA	NA	NA	NA	NA	NA	NA	NA	NA	NA	NA	NA	NA
6			NA	NA	NA	NA	NA	NA	NA	NA	NA	NA	NA	NA	NA	NA	NA
7			NA	NA	NA	NA	NA	NA	NA	NA	NA	NA	NA	NA	NA	NA	NA
8			NA	NA	NA	NA	NA	NA	NA	NA	NA	NA	NA	NA	NA	NA	NA
9			NA	NA	NA	NA	NA	NA	NA	NA	NA	NA	NA	NA	NA	NA	NA
10			NA	NA	NA	NA	NA	NA	NA	NA	NA	NA	NA	NA	NA	NA	NA
11			NA	NA	NA	NA	NA	NA	NA	NA	NA	NA	NA	NA	NA	NA	NA
12			NA	NA	NA	NA	NA	NA	NA	NA	NA	NA	NA	NA	NA	NA	NA
13			NA	NA	NA	NA	NA	NA	NA	NA	NA	NA	NA	NA	NA	NA	NA
14			NA	NA	NA	NA	NA	NA	NA	NA	NA	NA	NA	NA	NA	NA	NA
15			NA	NA	NA	NA	NA	NA	NA	NA	NA	NA	NA	NA	NA	NA	NA

Figure D.13: Stick figures.

D.2 Input for Steel Lattice Tower from PLS-TOWER

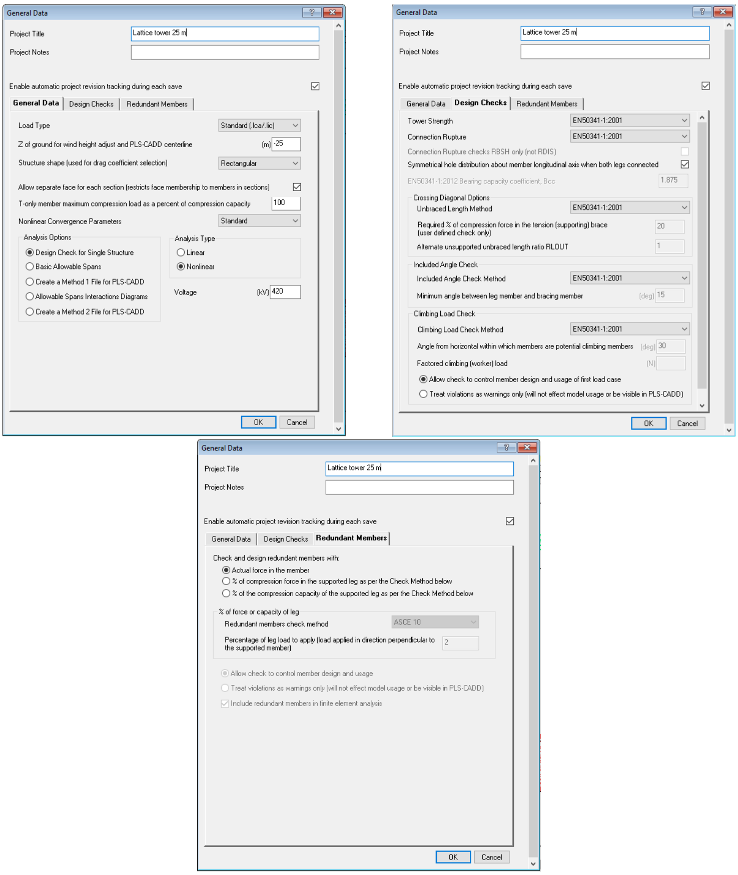

Figure D.14: General data

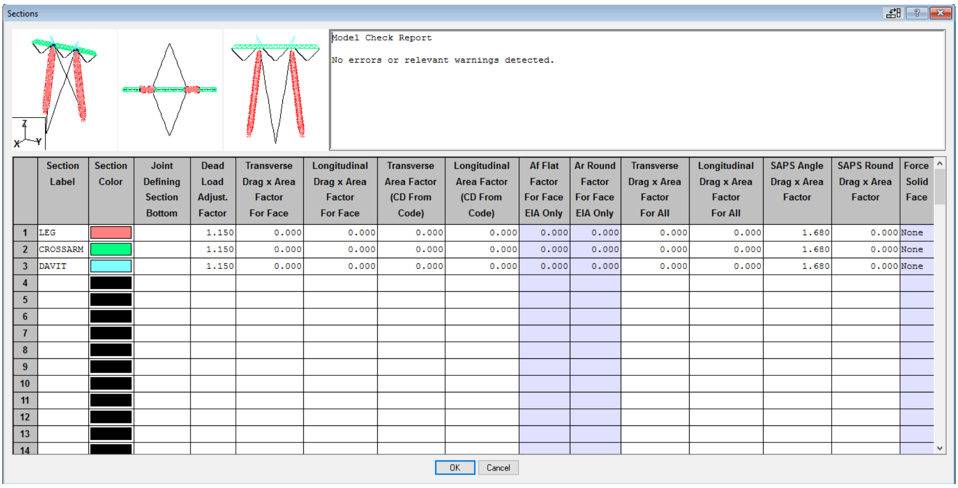

	Section Label	Section Color	Joint Defining Section Bottom	Dead Load Adjust. Factor	Transverse Drag x Area Factor For Face	Longitudinal Drag x Area Factor For Face	Transverse Area Factor (CD From Code)	Longitudinal Area Factor (CD From Code)	Af Flat Factor For Face EIA Only	Ar Round Factor For Face EIA Only	Transverse Drag x Area Factor For All	Longitudinal Drag x Area Factor For All	SAPS Angle Drag x Area Factor	SAPS Round Drag x Area Factor	Force Solid Face
1	LEG			1.150	0.000	0.000	0.000	0.000	0.000	0.000	0.000	0.000	1.680	0.000	None
2	CROSSARM			1.150	0.000	0.000	0.000	0.000	0.000	0.000	0.000	0.000	1.680	0.000	None
3	DAVIT			1.150	0.000	0.000	0.000	0.000	0.000	0.000	0.000	0.000	1.680	0.000	None
4															
5															
6															
7															
8															
9															
10															
11															
12															
13															
14															

Figure D.15: Sections

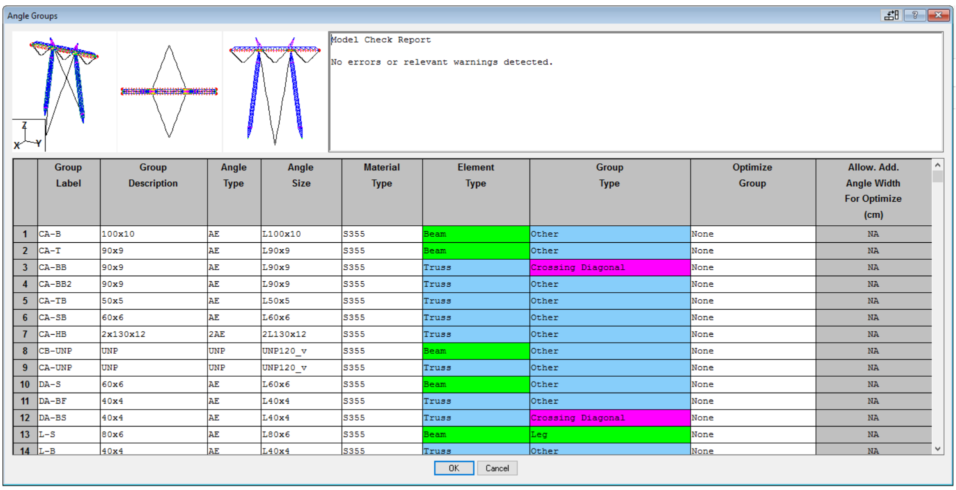

	Group Label	Group Description	Angle Type	Angle Size	Material Type	Element Type	Group Type	Optimize Group	Allow. Add. Angle Width For Optimize (cm)
1	CA-B	100x10	AE	L100x10	S355	Beam	Other	None	NA
2	CA-T	90x9	AE	L90x9	S355	Beam	Other	None	NA
3	CA-BB	90x9	AE	L90x9	S355	Truss	Crossing Diagonal	None	NA
4	CA-BB2	90x9	AE	L90x9	S355	Truss	Other	None	NA
5	CA-TB	50x5	AE	L50x5	S355	Truss	Other	None	NA
6	CA-SB	60x6	AE	L60x6	S355	Truss	Other	None	NA
7	CA-HB	2x130x12	2AE	2L130x12	S355	Truss	Other	None	NA
8	CB-UNP	UNP	UNP	UNP120_v	S355	Beam	Other	None	NA
9	CA-UNP	UNP	UNP	UNP120_v	S355	Truss	Other	None	NA
10	DA-S	60x6	AE	L60x6	S355	Beam	Other	None	NA
11	DA-BF	40x4	AE	L40x4	S355	Truss	Other	None	NA
12	DA-BS	40x4	AE	L40x4	S355	Truss	Crossing Diagonal	None	NA
13	L-S	80x6	AE	L80x6	S355	Beam	Leg	None	NA
14	L-B	40x4	AE	L40x4	S355	Truss	Other	None	NA

Figure D.16: Angle groups

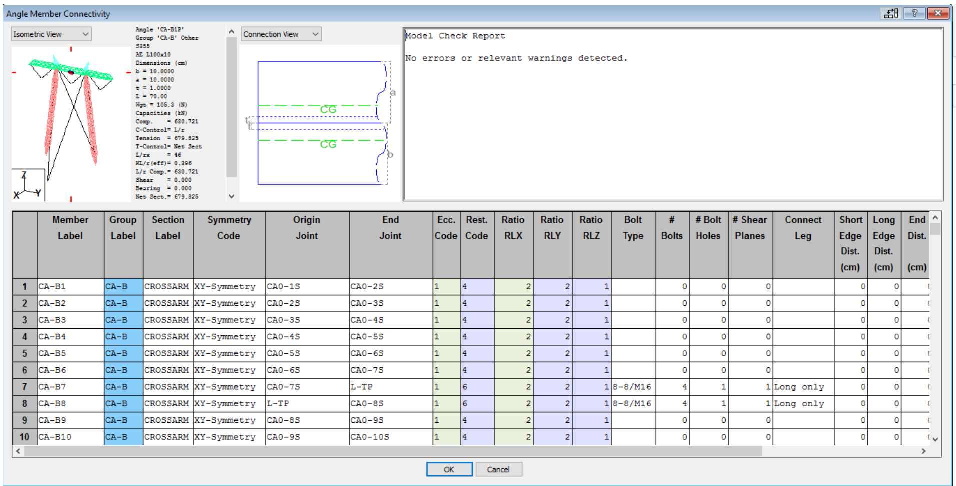

	Member Label	Group Label	Section Label	Symmetry Code	Origin Joint	End Joint	Ecc. Code	Rest. Code	Ratio RLX	Ratio RLY	Ratio RLZ	Bolt Type	# Bolts	# Bolt Holes	# Shear Planes	Connect Leg	Short Edge Dist. (cm)	Long Edge Dist. (cm)	End Dist. (cm)
1	CA-B1	CA-B	CROSSARM	XY-Symmetry	CA0-1S	CA0-2S	1	4	2	2	1		0	0	0		0	0	[illegible]
2	CA-B2	CA-B	CROSSARM	XY-Symmetry	CA0-2S	CA0-3S	1	4	2	2	1		0	0	0		0	0	[illegible]
3	CA-B3	CA-B	CROSSARM	XY-Symmetry	CA0-3S	CA0-4S	1	4	2	2	1		0	0	0		0	0	[illegible]
4	CA-B4	CA-B	CROSSARM	XY-Symmetry	CA0-4S	CA0-5S	1	4	2	2	1		0	0	0		0	0	[illegible]
5	CA-B5	CA-B	CROSSARM	XY-Symmetry	CA0-5S	CA0-6S	1	4	2	2	1		0	0	0		0	0	[illegible]
6	CA-B6	CA-B	CROSSARM	XY-Symmetry	CA0-6S	CA0-7S	1	4	2	2	1		0	0	0		0	0	[illegible]
7	CA-B7	CA-B	CROSSARM	XY-Symmetry	CA0-7S	L-TP	1	6	2	2	1	8-8/M16	4	1	1	Long only	0	0	[illegible]
8	CA-B8	CA-B	CROSSARM	XY-Symmetry	L-TP	CA0-8S	1	6	2	2	1	8-8/M16	4	1	1	Long only	0	0	[illegible]
9	CA-B9	CA-B	CROSSARM	XY-Symmetry	CA0-8S	CA0-9S	1	4	2	2	1		0	0	0		0	0	[illegible]
10	CA-B10	CA-B	CROSSARM	XY-Symmetry	CA0-9S	CA0-10S	1	4	2	2	1		0	0	0		0	0	[illegible]

Figure D.17: Angle members

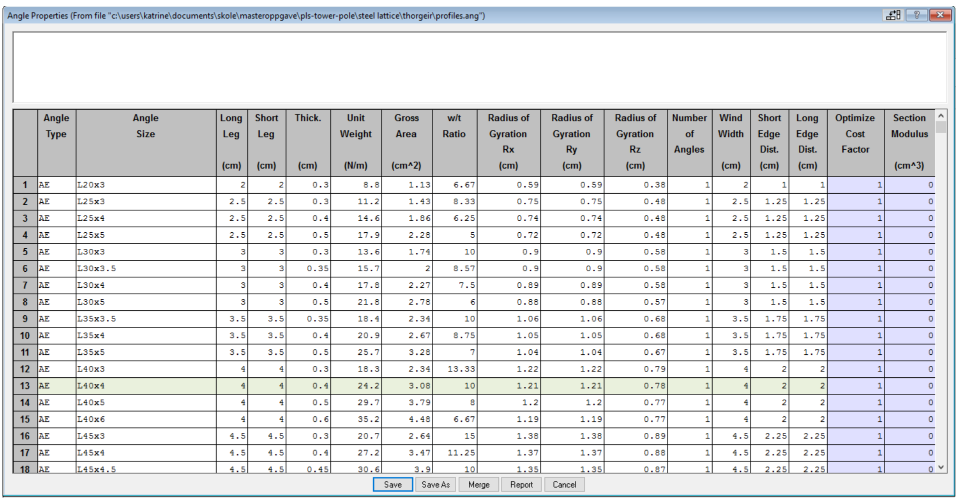

	Angle Type	Angle Size	Long Leg (cm)	Short Leg (cm)	Thick. (cm)	Unit Weight (N/m)	Gross Area (cm^2)	w/t Ratio	Radius of Gyration Rx (cm)	Radius of Gyration Ry (cm)	Radius of Gyration Rz (cm)	Number of Angles	Wind Width (cm)	Short Edge Dist. (cm)	Long Edge Dist. (cm)	Optimize Cost Factor	Section Modulus (cm^3)
1	AE	L20x3	2	2	0.3	8.8	1.13	6.67	0.59	0.59	0.38	1	2	1	1	1	0
2	AE	L25x3	2.5	2.5	0.3	11.2	1.43	8.33	0.75	0.75	0.48	1	2.5	1.25	1.25	1	0
3	AE	L25x4	2.5	2.5	0.4	14.6	1.86	6.25	0.74	0.74	0.48	1	2.5	1.25	1.25	1	0
4	AE	L25x5	2.5	2.5	0.5	17.9	2.28	5	0.72	0.72	0.48	1	2.5	1.25	1.25	1	0
5	AE	L30x3	3	3	0.3	13.6	1.74	10	0.9	0.9	0.58	1	3	1.5	1.5	1	0
6	AE	L30x3.5	3	3	0.35	15.7	2	8.57	0.9	0.9	0.58	1	3	1.5	1.5	1	0
7	AE	L30x4	3	3	0.4	17.8	2.27	7.5	0.89	0.89	0.58	1	3	1.5	1.5	1	0
8	AE	L30x5	3	3	0.5	21.8	2.78	6	0.88	0.88	0.57	1	3	1.5	1.5	1	0
9	AE	L35x3.5	3.5	3.5	0.35	18.4	2.34	10	1.06	1.06	0.68	1	3.5	1.75	1.75	1	0
10	AE	L35x4	3.5	3.5	0.4	20.9	2.67	8.75	1.05	1.05	0.68	1	3.5	1.75	1.75	1	0
11	AE	L35x5	3.5	3.5	0.5	25.7	3.28	7	1.04	1.04	0.67	1	3.5	1.75	1.75	1	0
12	AE	L40x3	4	4	0.3	18.3	2.34	13.33	1.22	1.22	0.79	1	4	2	2	1	0
13	AE	L40x4	4	4	0.4	24.2	3.08	10	1.21	1.21	0.78	1	4	2	2	1	0
14	AE	L40x5	4	4	0.5	29.7	3.79	8	1.2	1.2	0.77	1	4	2	2	1	0
15	AE	L40x6	4	4	0.6	35.2	4.48	6.67	1.19	1.19	0.77	1	4	2	2	1	0
16	AE	L45x3	4.5	4.5	0.3	20.7	2.64	15	1.38	1.38	0.89	1	4.5	2.25	2.25	1	0
17	AE	L45x4	4.5	4.5	0.4	27.2	3.47	11.25	1.37	1.37	0.88	1	4.5	2.25	2.25	1	0
18	AE	L45x4.5	4.5	4.5	0.45	30.6	3.9	10	1.35	1.35	0.87	1	4.5	2.25	2.25	1	0

Figure D.18: Angle member properties

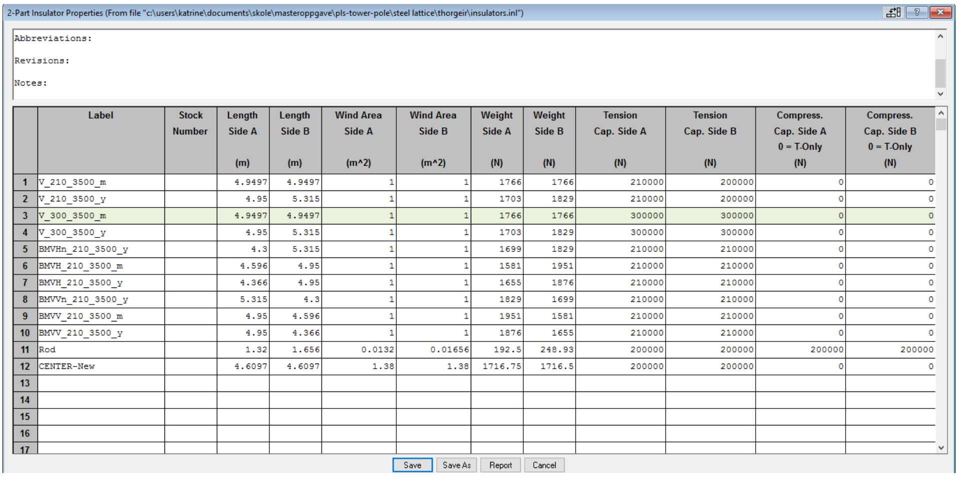

2-Part Insulator Properties (From file "c:\users\katrine\documents\skole\masteroppgave\pls-tower-pole\steel lattice\thorgeir\insulators.inl")

Abbreviations:

Revisions:

Notes:

	Label	Stock Number	Length Side A (m)	Length Side B (m)	Wind Area Side A (m^2)	Wind Area Side B (m^2)	Weight Side A (N)	Weight Side B (N)	Tension Cap. Side A (N)	Tension Cap. Side B (N)	Compress. Cap. Side A 0 = T-Only (N)	Compress. Cap. Side B 0 = T-Only (N)
1	V_210_3500_m		4.9497	4.9497	1	1	1766	1766	210000	200000	0	0
2	V_210_3500_y		4.95	5.315	1	1	1703	1829	210000	200000	0	0
3	V_300_3500_m		4.9497	4.9497	1	1	1766	1766	300000	300000	0	0
4	V_300_3500_y		4.95	5.315	1	1	1703	1829	300000	300000	0	0
5	BMVHn_210_3500_y		4.3	5.315	1	1	1699	1829	210000	210000	0	0
6	BMVH_210_3500_m		4.596	4.95	1	1	1581	1951	210000	210000	0	0
7	BMVH_210_3500_y		4.366	4.95	1	1	1655	1876	210000	210000	0	0
8	BMVVn_210_3500_y		5.315	4.3	1	1	1829	1699	210000	210000	0	0
9	BMVV_210_3500_m		4.95	4.596	1	1	1951	1581	210000	210000	0	0
10	BMVV_210_3500_y		4.95	4.366	1	1	1876	1655	210000	210000	0	0
11	Rod		1.32	1.656	0.0132	0.01656	192.5	248.93	200000	200000	200000	200000
12	CENTER-New		4.6097	4.6097	1.38	1.38	1716.75	1716.5	200000	200000	0	0
13												
14												
15												
16												
17												

Save Save As Report Cancel

Figure D.19: V-insulator chain properties

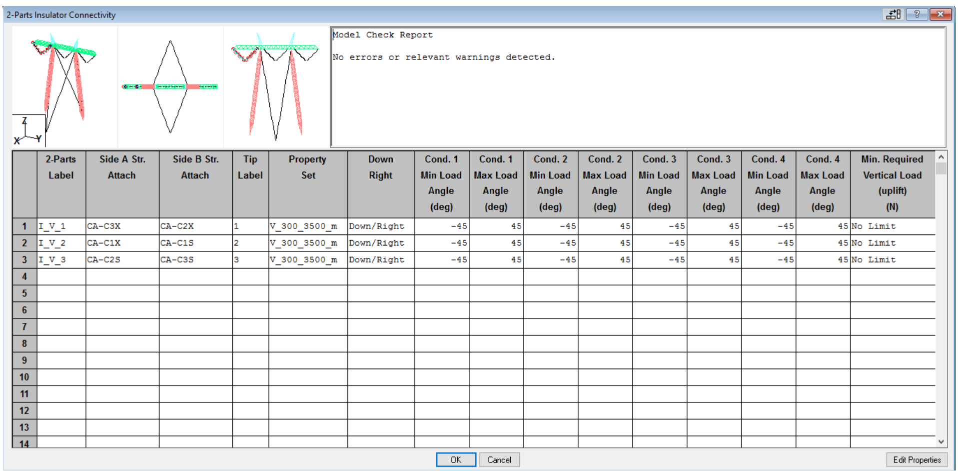

2-Parts Insulator Connectivity

Model Check Report

No errors or relevant warnings detected.

	2-Parts Label	Side A Str. Attach	Side B Str. Attach	Tip Label	Property Set	Down Right	Cond. 1 Min Load Angle (deg)	Cond. 1 Max Load Angle (deg)	Cond. 2 Min Load Angle (deg)	Cond. 2 Max Load Angle (deg)	Cond. 3 Min Load Angle (deg)	Cond. 3 Max Load Angle (deg)	Cond. 4 Min Load Angle (deg)	Cond. 4 Max Load Angle (deg)	Min. Required Vertical Load (uplift) (N)
1	I_V_1	CA-C3X	CA-C2X	1	V_300_3500_m	Down/Right	-45	45	-45	45	-45	45	-45	45	No Limit
2	I_V_2	CA-C1X	CA-C1S	2	V_300_3500_m	Down/Right	-45	45	-45	45	-45	45	-45	45	No Limit
3	I_V_3	CA-C2S	CA-C3S	3	V_300_3500_m	Down/Right	-45	45	-45	45	-45	45	-45	45	No Limit
4															
5															
6															
7															
8															
9															
10															
11															
12															
13															
14															

OK Cancel Edit Properties

Figure D.20: V-insulator chain

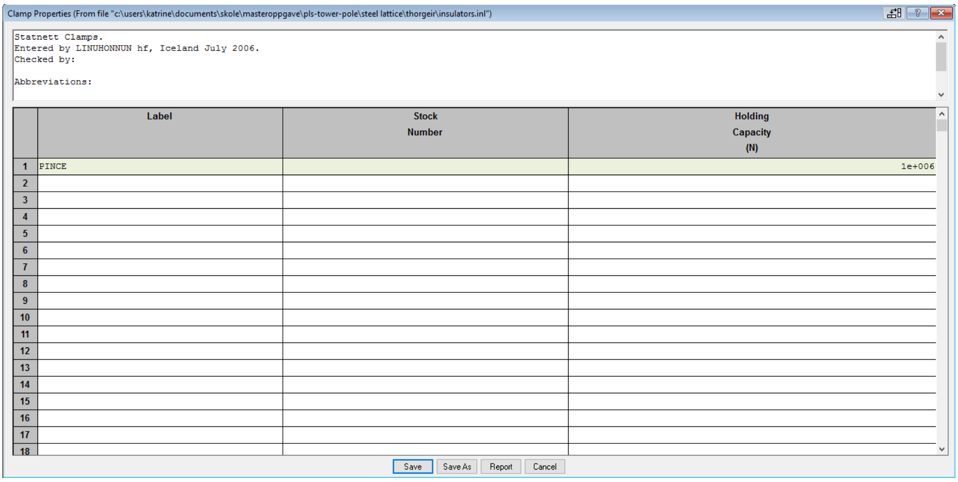

Figure D.21: Clamp insulator properties

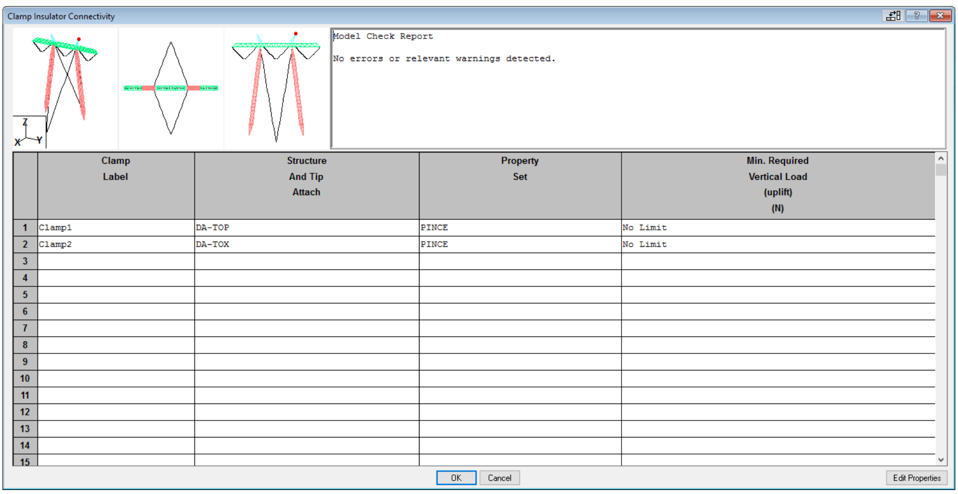

Figure D.22: Clamp insulators

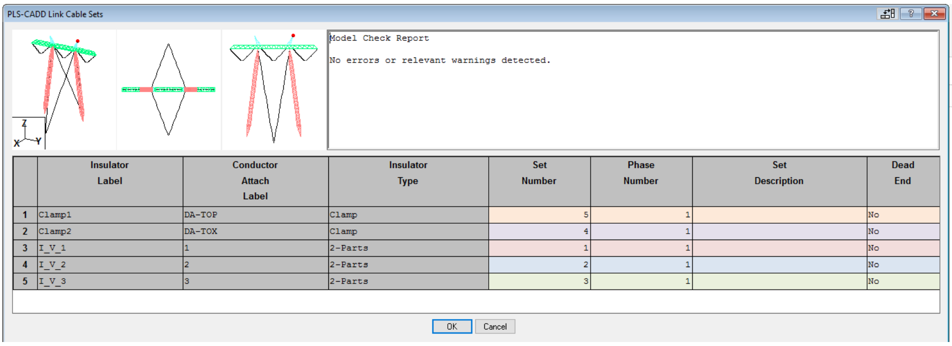

PLS-CADD Link Cable Sets

Model Check Report

No errors or relevant warnings detected.

	Insulator Label	Conductor Attach Label	Insulator Type	Set Number	Phase Number	Set Description	Dead End
1	Clamp1	DA-TOP	Clamp	5	1		No
2	Clamp2	DA-TOX	Clamp	4	1		No
3	I_V_1	1	2-Parts	1	1		No
4	I_V_2	2	2-Parts	2	1		No
5	I_V_3	3	2-Parts	3	1		No

OK Cancel

Figure D.23: Insulator link

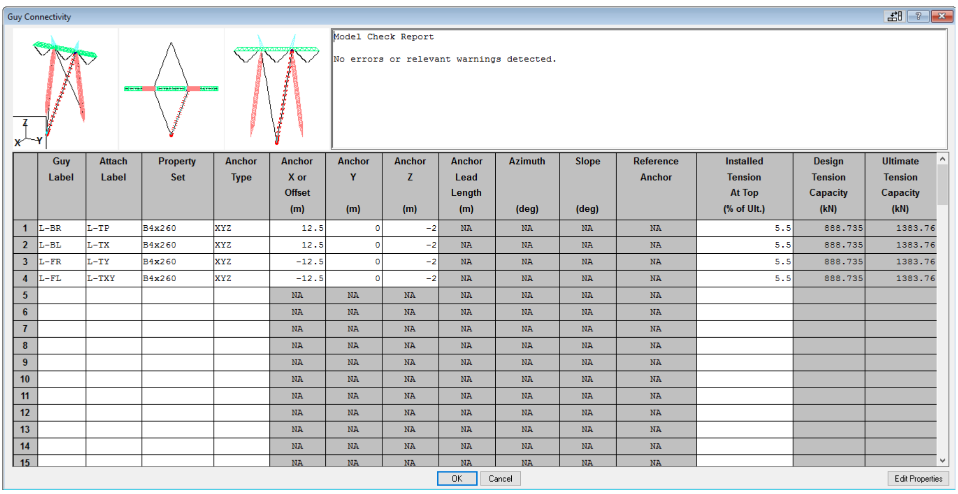

Guy Connectivity

Model Check Report

No errors or relevant warnings detected.

	Guy Label	Attach Label	Property Set	Anchor Type	Anchor X or Offset (m)	Anchor Y (m)	Anchor Z (m)	Anchor Lead Length (m)	Azimuth (deg)	Slope (deg)	Reference Anchor	Installed Tension At Top (% of Ult.)	Design Tension Capacity (kN)	Ultimate Tension Capacity (kN)
1	L-BR	L-TP	B4x260	XYZ	12.5	0	-2	NA	NA	NA	NA	5.5	888.735	1383.76
2	L-BL	L-TX	B4x260	XYZ	12.5	0	-2	NA	NA	NA	NA	5.5	888.735	1383.76
3	L-FR	L-TY	B4x260	XYZ	-12.5	0	-2	NA	NA	NA	NA	5.5	888.735	1383.76
4	L-FL	L-TXY	B4x260	XYZ	-12.5	0	-2	NA	NA	NA	NA	5.5	888.735	1383.76
5					NA	NA	NA	NA	NA	NA	NA			
6					NA	NA	NA	NA	NA	NA	NA			
7					NA	NA	NA	NA	NA	NA	NA			
8					NA	NA	NA	NA	NA	NA	NA			
9					NA	NA	NA	NA	NA	NA	NA			
10					NA	NA	NA	NA	NA	NA	NA			
11					NA	NA	NA	NA	NA	NA	NA			
12					NA	NA	NA	NA	NA	NA	NA			
13					NA	NA	NA	NA	NA	NA	NA			
14					NA	NA	NA	NA	NA	NA	NA			
15					NA	NA	NA	NA	NA	NA	NA			

OK Cancel Edit Properties

Figure D.24: Guy properties

D.3 Input for Steel Tubular Tower from PLS-POLE

The insulators used and insulator links are similar to those in in D.2.

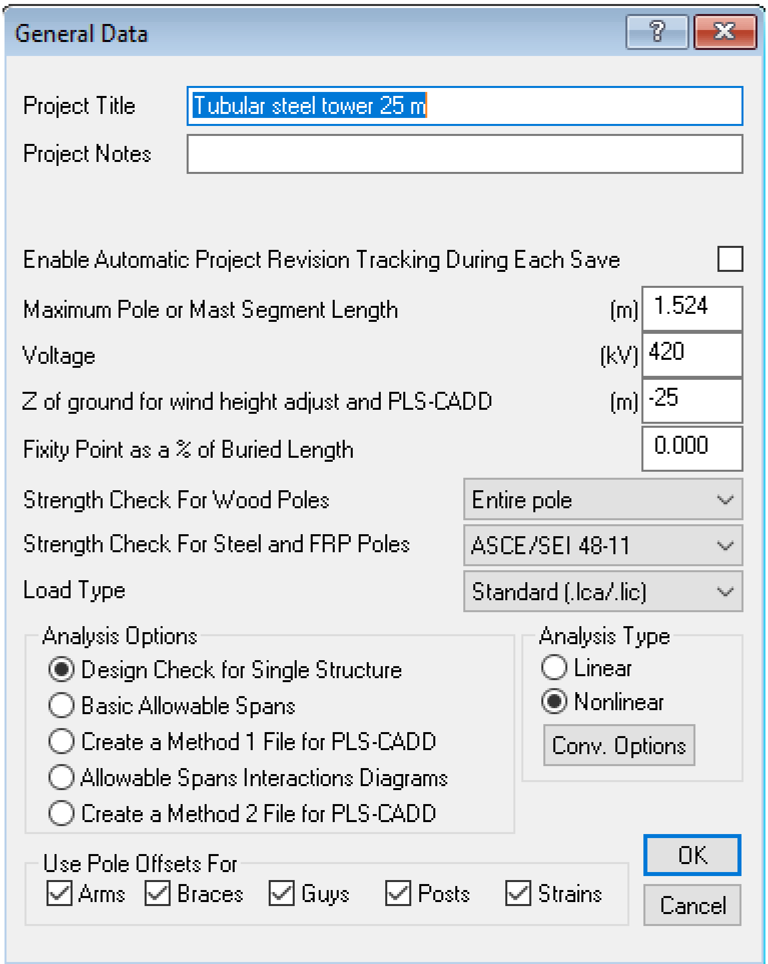

Figure D.25: General data

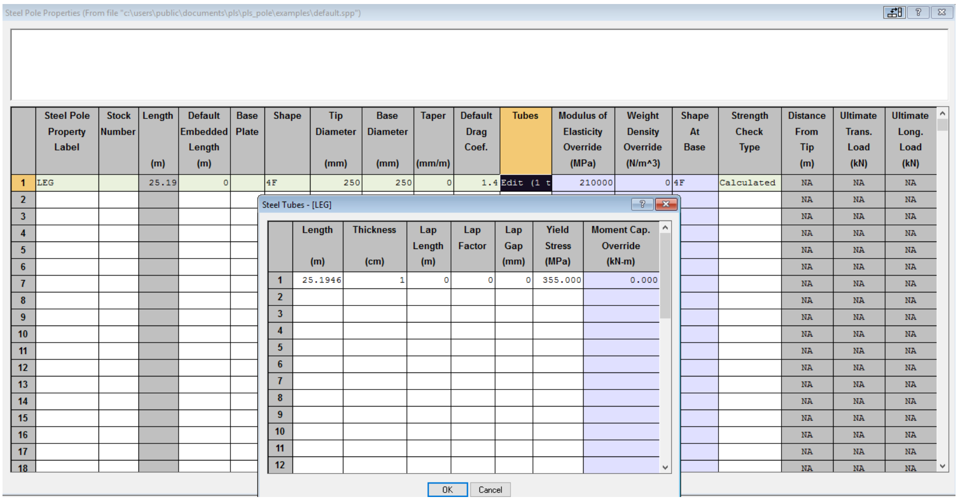

Figure D.26: Steel pole properties

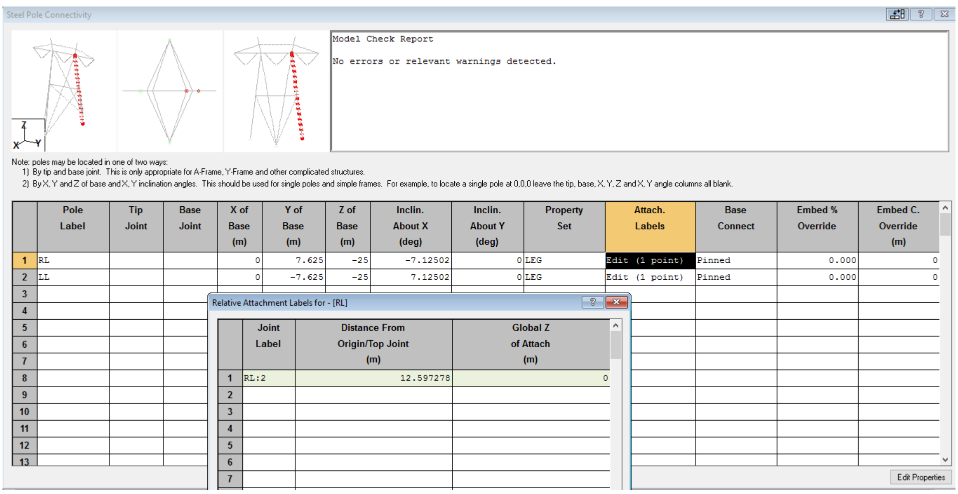

Figure D.27: Steel poles

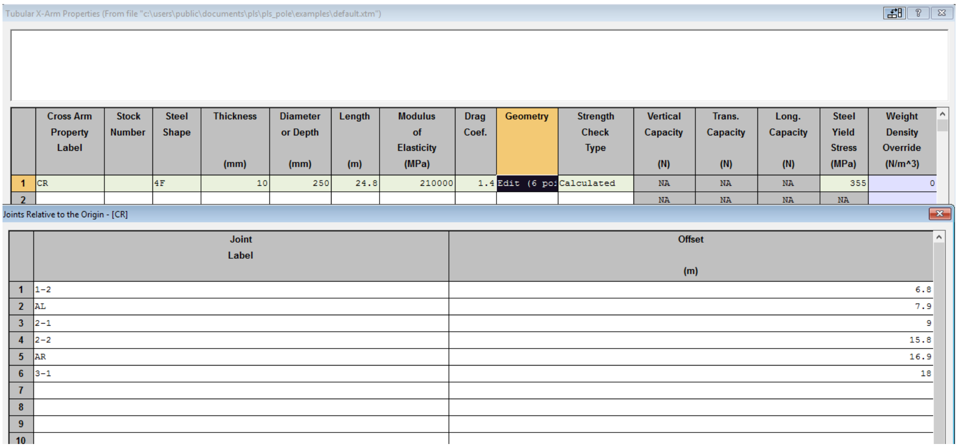
Tubular X-Arm Properties (From file "c:\users\public\documents\pls\pls_pole\examples\default.xtm")

	Cross Arm Property Label	Stock Number	Steel Shape	Thickness (mm)	Diameter or Depth (mm)	Length (m)	Modulus of Elasticity (MPa)	Drag Coef.	Geometry	Strength Check Type	Vertical Capacity (N)	Trans. Capacity (N)	Long. Capacity (N)	Steel Yield Stress (MPa)	Weight Density Override (N/m^3)
1	CR		4F	10	250	24.8	210000	1.4	Edit (6 po:	Calculated	NA	NA	NA	355	0
2											NA	NA	NA	NA	

Joints Relative to the Origin - [CR]

	Joint Label	Offset (m)
1	1-2	6.8
2	AL	7.9
3	2-1	9
4	2-2	15.8
5	AR	16.9
6	3-1	18
7		
8		
9		
10		

Figure D.28: Steel cross arm properties

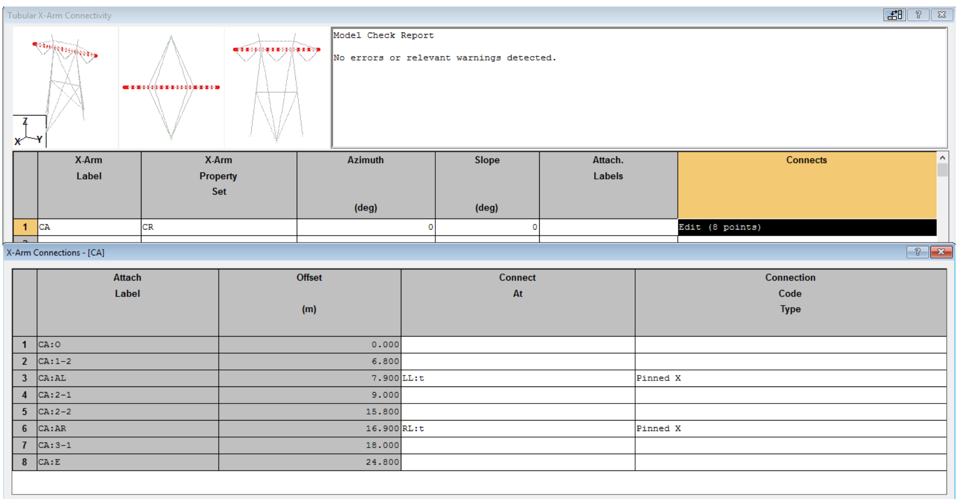
Tubular X-Arm Connectivity

Model Check Report

No errors or relevant warnings detected.

	X-Arm Label	X-Arm Property Set	Azimuth (deg)	Slope (deg)	Attach. Labels	Connects
1	CA	CR	0	0		Edit (8 points)

X-Arm Connections - [CA]

	Attach Label	Offset (m)	Connect At	Connection Code Type
1	CA:O	0.000		
2	CA:1-2	6.800		
3	CA:AL	7.900	LL:t	Pinned X
4	CA:2-1	9.000		
5	CA:2-2	15.800		
6	CA:AR	16.900	RL:t	Pinned X
7	CA:3-1	18.000		
8	CA:E	24.800		

Figure D.29: Steel cross arm

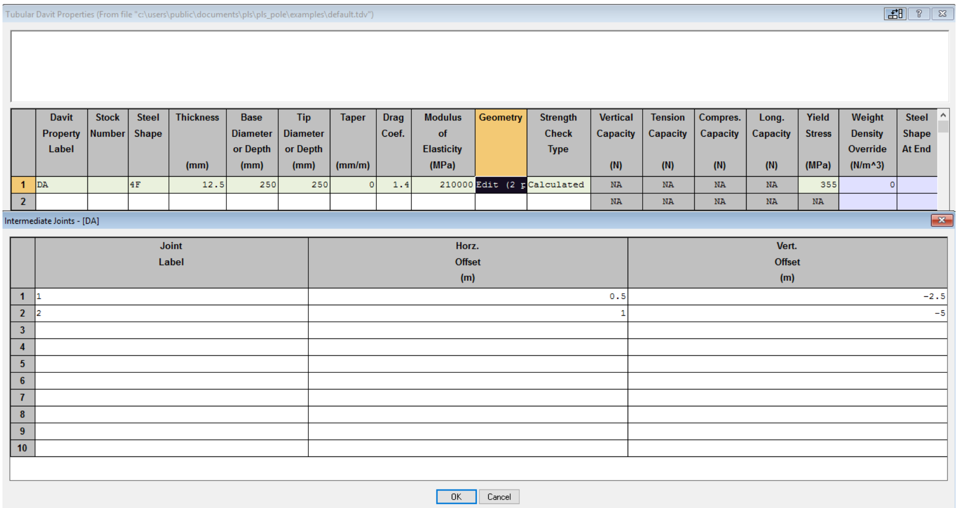

Figure D.30: Steel davit arm properties

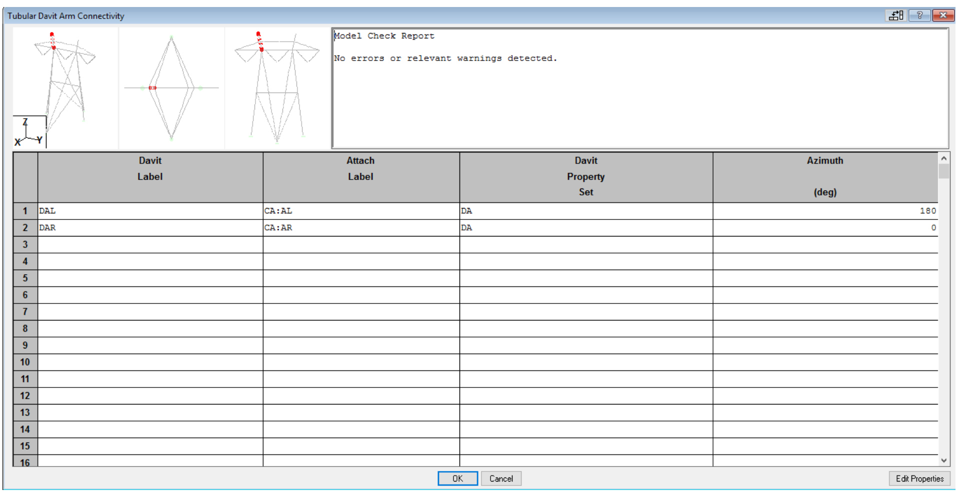

Figure D.31: Steel davit arms

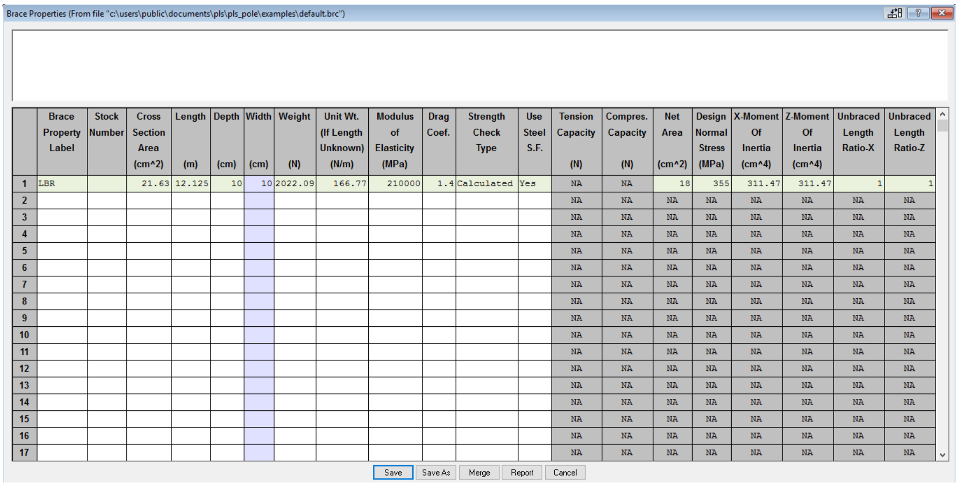

Figure D.32: Steel brace properties

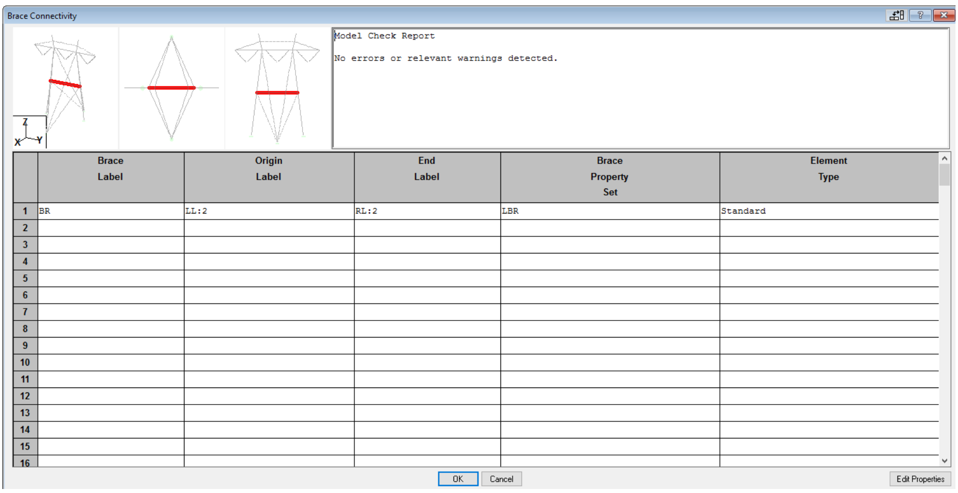

Figure D.33: Steel brace

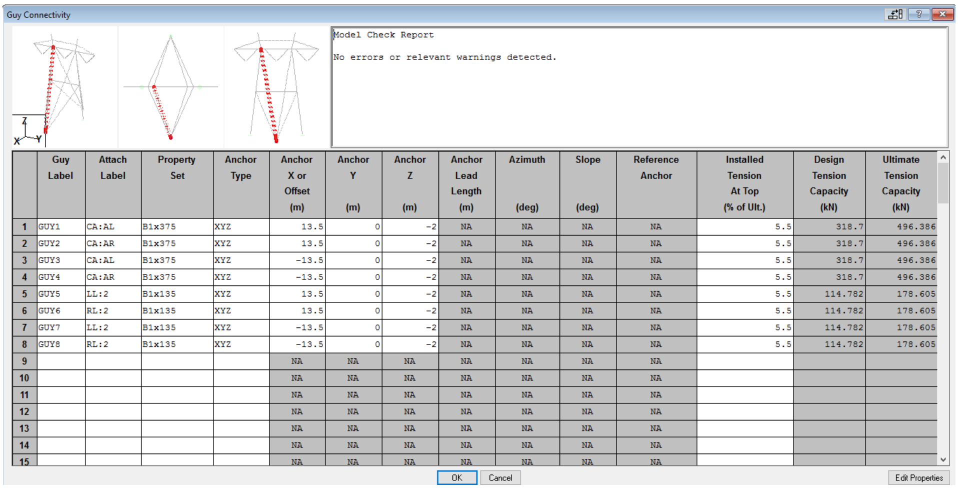

	Guy Label	Attach Label	Property Set	Anchor Type	Anchor X or Offset (m)	Anchor Y (m)	Anchor Z (m)	Anchor Lead Length (m)	Azimuth (deg)	Slope (deg)	Reference Anchor	Installed Tension At Top (% of Ult.)	Design Tension Capacity (kN)	Ultimate Tension Capacity (kN)
1	GUY1	CA:AL	B1x375	XYZ	13.5	0	-2	NA	NA	NA	NA	5.5	318.7	496.386
2	GUY2	CA:AR	B1x375	XYZ	13.5	0	-2	NA	NA	NA	NA	5.5	318.7	496.386
3	GUY3	CA:AL	B1x375	XYZ	-13.5	0	-2	NA	NA	NA	NA	5.5	318.7	496.386
4	GUY4	CA:AR	B1x375	XYZ	-13.5	0	-2	NA	NA	NA	NA	5.5	318.7	496.386
5	GUY5	LL:2	B1x135	XYZ	13.5	0	-2	NA	NA	NA	NA	5.5	114.782	178.605
6	GUY6	RL:2	B1x135	XYZ	13.5	0	-2	NA	NA	NA	NA	5.5	114.782	178.605
7	GUY7	LL:2	B1x135	XYZ	-13.5	0	-2	NA	NA	NA	NA	5.5	114.782	178.605
8	GUY8	RL:2	B1x135	XYZ	-13.5	0	-2	NA	NA	NA	NA	5.5	114.782	178.605
9					NA	NA	NA	NA	NA	NA	NA			
10					NA	NA	NA	NA	NA	NA	NA			
11					NA	NA	NA	NA	NA	NA	NA			
12					NA	NA	NA	NA	NA	NA	NA			
13					NA	NA	NA	NA	NA	NA	NA			
14					NA	NA	NA	NA	NA	NA	NA			
15					NA	NA	NA	NA	NA	NA	NA			

Figure D.34: Guys used in steel tubular model

D.4 Input for FRP Tubular Tower from PLS-POLE

The insulators used and insulator links are similar to those in in D.2.

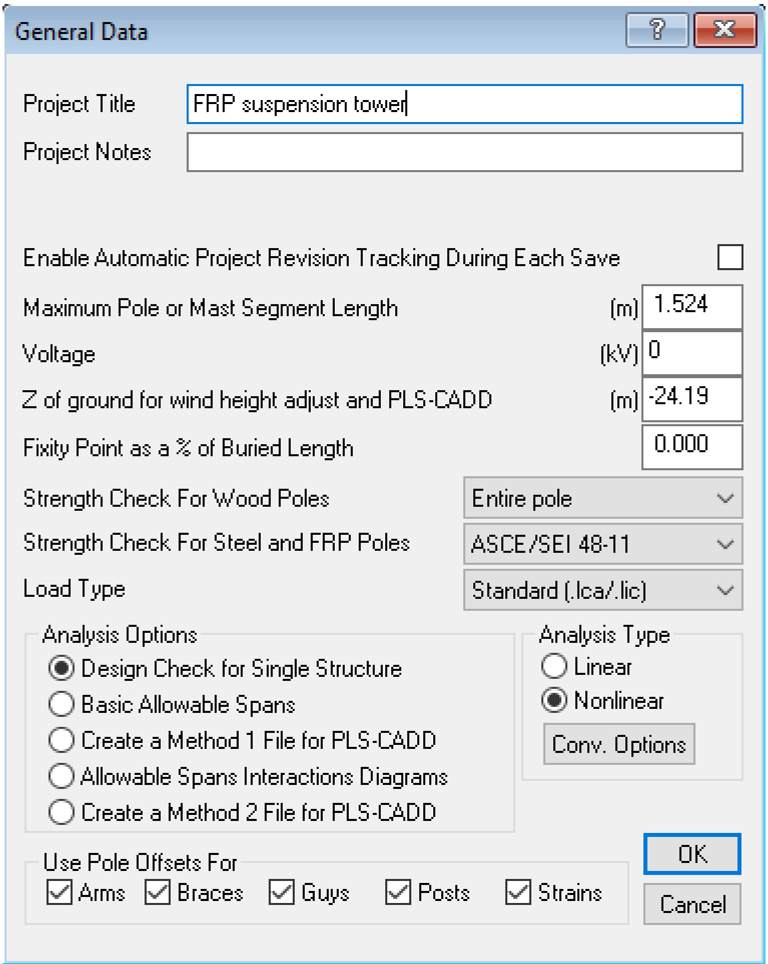

Figure D.35: General data

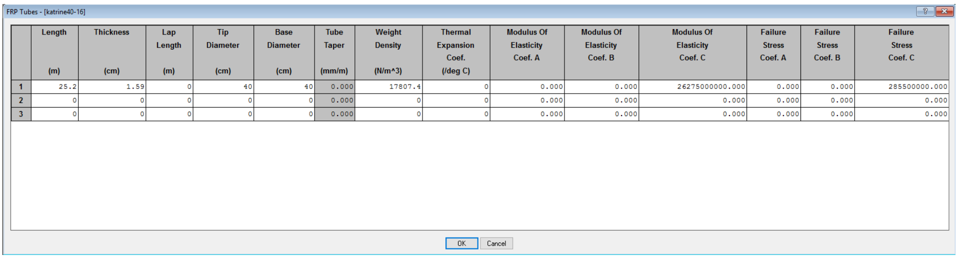

FRP Tubes - [katrine40-16]

	Length (m)	Thickness (cm)	Lap Length (m)	Tip Diameter (cm)	Base Diameter (cm)	Tube Taper (mm/m)	Weight Density (N/m^3)	Thermal Expansion Coef. (/deg C)	Modulus Of Elasticity Coef. A	Modulus Of Elasticity Coef. B	Modulus Of Elasticity Coef. C	Failure Stress Coef. A	Failure Stress Coef. B	Failure Stress Coef. C
1	25.2	1.59	0	40	40	0.000	17807.4	0	0.000	0.000	26275000000.000	0.000	0.000	285500000.000
2	0	0	0	0	0	0.000	0	0	0.000	0.000	0.000	0.000	0.000	0.000
3	0	0	0	0	0	0.000	0	0	0.000	0.000	0.000	0.000	0.000	0.000

OK Cancel

Figure D.36: FRP pole properties

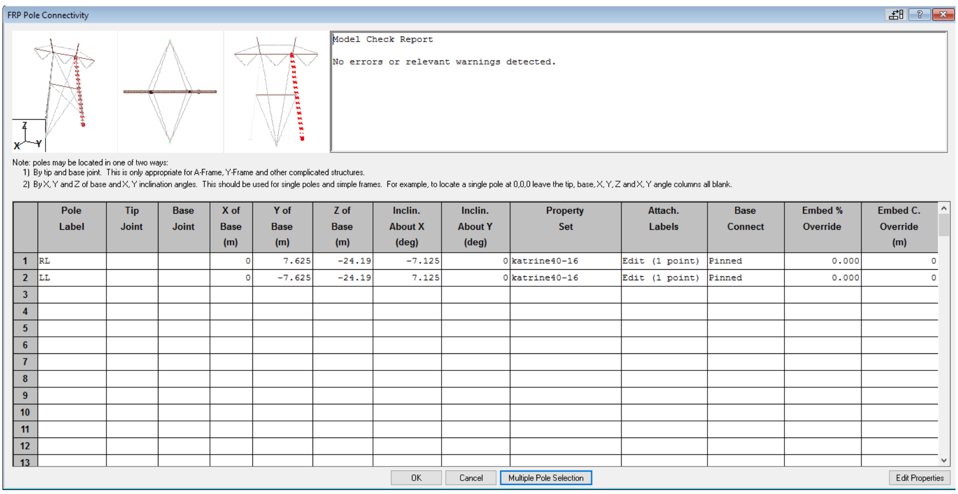

FRP Pole Connectivity

Model Check Report

No errors or relevant warnings detected.

Note: poles may be located in one of two ways:
1) By tip and base joint. This is only appropriate for A-Frame, Y-Frame and other complicated structures.
2) By X, Y and Z of base and X, Y inclination angles. This should be used for single poles and simple frames. For example, to locate a single pole at 0,0,0 leave the tip, base, X, Y, Z and X, Y angle columns all blank.

	Pole Label	Tip Joint	Base Joint	X of Base (m)	Y of Base (m)	Z of Base (m)	Inclin. About X (deg)	Inclin. About Y (deg)	Property Set	Attach. Labels	Base Connect	Embed % Override	Embed C. Override (m)
1	RL			0	7.625	-24.19	-7.125	0	katrine40-16	Edit (1 point)	Pinned	0.000	0
2	LL			0	-7.625	-24.19	7.125	0	katrine40-16	Edit (1 point)	Pinned	0.000	0
3													
4													
5													
6													
7													
8													
9													
10													
11													
12													
13													

OK Cancel Multiple Pole Selection Edit Properties

Figure D.37: FRP poles

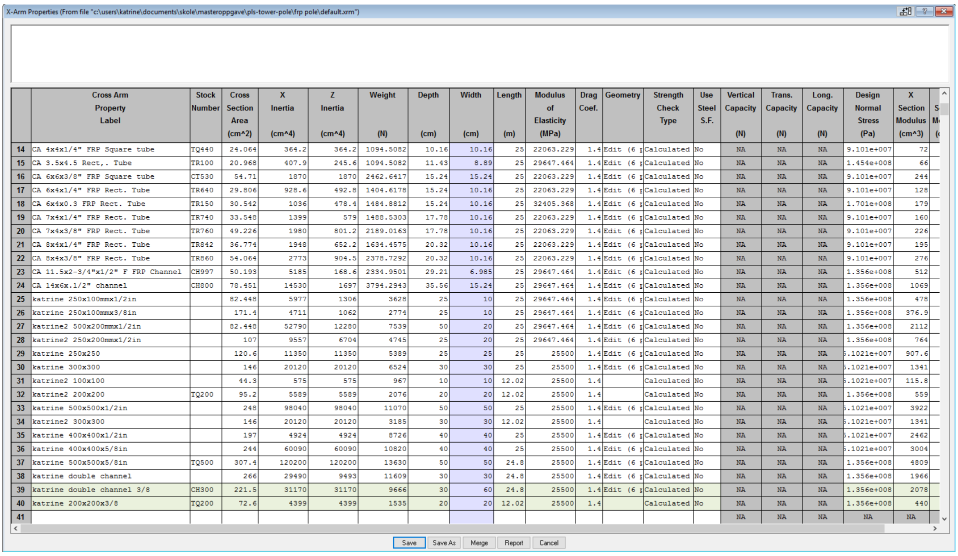

X-Arm Properties (From file "c:\users\katrine\documents\skole\masteroppgave\pls-tower-pole\frp pole\default.xrm")

	Cross Arm Property Label	Stock Number	Cross Section Area (cm^2)	X Inertia (cm^4)	Z Inertia (cm^4)	Weight (N)	Depth (cm)	Width (cm)	Length (m)	Modulus of Elasticity (MPa)	Drag Coef.	Geometry	Strength Check Type	Use Steel S.F.	Vertical Capacity (N)	Trans. Capacity (N)	Long. Capacity (N)	Design Normal Stress (Pa)	X Section Modulus (cm^3)
14	CA 4x4x1/4" FRP Square tube	TQ440	24.064	364.2	364.2	1094.5082	10.16	10.16	25	22063.229	1.4	Edit (6 p	Calculated	No	NA	NA	NA	9.101e+007	72
15	CA 3.5x4.5 Rect,. Tube	TR100	20.968	407.9	245.6	1094.5082	11.43	8.89	25	29647.464	1.4	Edit (6 p	Calculated	No	NA	NA	NA	1.454e+008	66
16	CA 6x6x3/8" FRP Square tube	CT530	54.71	1870	1870	2462.6417	15.24	15.24	25	22063.229	1.4	Edit (6 p	Calculated	No	NA	NA	NA	9.101e+007	244
17	CA 6x4x1/4" FRP Rect. Tube	TR640	29.806	928.6	492.8	1404.6178	15.24	10.16	25	22063.229	1.4	Edit (6 p	Calculated	No	NA	NA	NA	9.101e+007	128
18	CA 6x4x0.3 FRP Rect. Tube	TR150	30.542	1036	478.4	1484.8812	15.24	10.16	25	32405.368	1.4	Edit (6 p	Calculated	No	NA	NA	NA	1.701e+008	179
19	CA 7x4x1/4" FRP Rect. Tube	TR740	33.548	1399	579	1488.5303	17.78	10.16	25	22063.229	1.4	Edit (6 p	Calculated	No	NA	NA	NA	9.101e+007	160
20	CA 7x4x3/8" FRP Rect. Tube	TR760	49.226	1980	801.2	2189.0163	17.78	10.16	25	22063.229	1.4	Edit (6 p	Calculated	No	NA	NA	NA	9.101e+007	226
21	CA 8x4x1/4" FRP Rect. Tube	TR842	36.774	1948	652.2	1634.4575	20.32	10.16	25	22063.229	1.4	Edit (6 p	Calculated	No	NA	NA	NA	9.101e+007	195
22	CA 8x4x3/8" FRP Rect. Tube	TR860	54.064	2773	904.5	2378.7292	20.32	10.16	25	22063.229	1.4	Edit (6 p	Calculated	No	NA	NA	NA	9.101e+007	276
23	CA 11.5x2-3/4"x1/2" F FRP Channel	CH997	50.193	5185	168.6	2334.9501	29.21	6.985	25	29647.464	1.4	Edit (6 p	Calculated	No	NA	NA	NA	1.356e+008	512
24	CA 14x6x.1/2" channel	CH800	78.451	14530	1697	3794.2943	35.56	15.24	25	29647.464	1.4	Edit (6 p	Calculated	No	NA	NA	NA	1.356e+008	1069
25	katrine 250x100mmx1/2in		82.448	5977	1306	3628	25	10	25	29647.464	1.4	Edit (6 p	Calculated	No	NA	NA	NA	1.356e+008	478
26	katrine 250x100mmx3/8in		171.4	4711	1062	2774	25	10	25	29647.464	1.4	Edit (6 p	Calculated	No	NA	NA	NA	1.356e+008	376.9
27	katrine2 500x200mmx1/2in		82.448	52790	12280	7539	50	20	25	29647.464	1.4	Edit (6 p	Calculated	No	NA	NA	NA	1.356e+008	2112
28	katrine2 250x200mmx1/2in		107	9557	6704	4745	25	20	25	29647.464	1.4	Edit (6 p	Calculated	No	NA	NA	NA	1.356e+008	764
29	katrine 250x250		120.6	11350	11350	5389	25	25	25	25500	1.4	Edit (6 p	Calculated	No	NA	NA	NA	5.1021e+007	907.6
30	katrine 300x300		146	20120	20120	6524	30	30	25	25500	1.4	Edit (6 p	Calculated	No	NA	NA	NA	5.1021e+007	1341
31	katrine2 100x100		44.3	575	575	967	10	10	12.02	25500	1.4		Calculated	No	NA	NA	NA	5.1021e+007	115.8
32	katrine2 200x200	TQ200	95.2	5589	5589	2076	20	20	12.02	25500	1.4		Calculated	No	NA	NA	NA	1.356e+008	559
33	katrine 500x500x1/2in		248	98040	98040	11070	50	50	25	25500	1.4	Edit (6 p	Calculated	No	NA	NA	NA	5.1021e+007	3922
34	katrine2 300x300		146	20120	20120	3185	30	30	12.02	25500	1.4		Calculated	No	NA	NA	NA	5.1021e+007	1341
35	katrine 400x400x1/2in		197	4924	4924	8726	40	40	25	25500	1.4	Edit (6 p	Calculated	No	NA	NA	NA	5.1021e+007	2462
36	katrine 400x400x5/8in		244	60090	60090	10820	40	40	25	25500	1.4	Edit (6 p	Calculated	No	NA	NA	NA	5.1021e+007	3004
37	katrine 500x500x5/8in	TQ500	307.4	120200	120200	13630	50	50	24.8	25500	1.4	Edit (6 p	Calculated	No	NA	NA	NA	1.356e+008	4809
38	katrine double channel		266	29490	9493	11609	30	30	24.8	25500	1.4	Edit (6 p	Calculated	No	NA	NA	NA	1.356e+008	1966
39	katrine double channel 3/8	CH300	221.5	31170	31170	9666	30	60	24.8	25500	1.4	Edit (6 p	Calculated	No	NA	NA	NA	1.356e+008	2078
40	katrine 200x200x3/8	TQ200	72.6	4399	4399	1535	20	20	12.02	25500	1.4		Calculated	No	NA	NA	NA	1.356e+008	440
41															NA	NA	NA	NA	NA

Save Save As Merge Report Cancel

Figure D.38: FRP cross arm properties

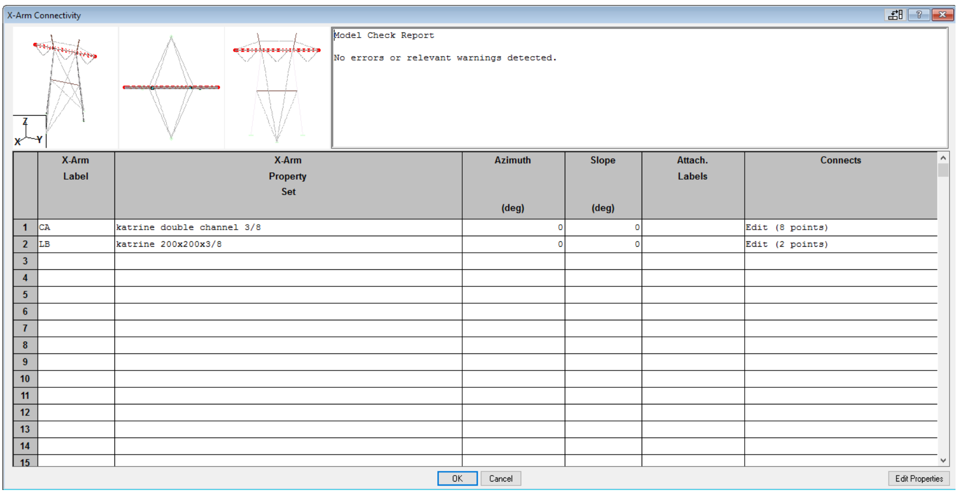

X-Arm Connectivity

Model Check Report

No errors or relevant warnings detected.

	X-Arm Label	X-Arm Property Set	Azimuth (deg)	Slope (deg)	Attach. Labels	Connects
1	CA	katrine double channel 3/8	0	0		Edit (8 points)
2	LB	katrine 200x200x3/8	0	0		Edit (2 points)
3						
4						
5						
6						
7						
8						
9						
10						
11						
12						
13						
14						
15						

OK Cancel Edit Properties

Figure D.39: FRP cross arm

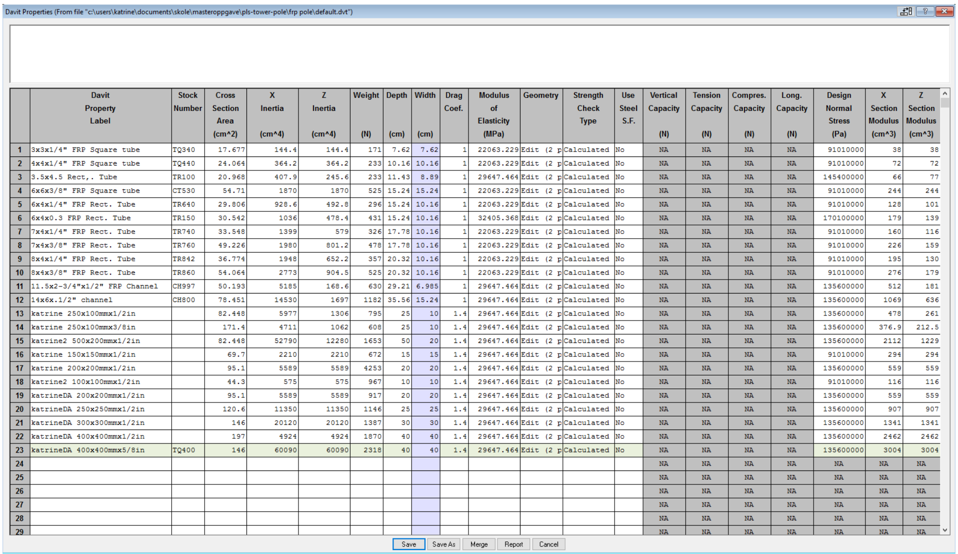

Davit Properties (From file "c:\users\katrine\documents\skole\masteroppgave\pls-tower-pole\frp pole\default.dvt")

	Davit Property Label	Stock Number	Cross Section Area (cm^2)	X Inertia (cm^4)	Z Inertia (cm^4)	Weight (N)	Depth (cm)	Width (cm)	Drag Coef.	Modulus of Elasticity (MPa)	Geometry	Strength Check Type	Use Steel S.F.	Vertical Capacity (N)	Tension Capacity (N)	Compres. Capacity (N)	Long. Capacity (N)	Design Normal Stress (Pa)	X Section Modulus (cm^3)	Z Section Modulus (cm^3)
1	3x3x1/4" FRP Square tube	TQ340	17.677	144.4	144.4	171	7.62	7.62	1	22063.229	Edit (2 p	Calculated	No	NA	NA	NA	NA	91010000	38	38
2	4x4x1/4" FRP Square tube	TQ440	24.064	364.2	364.2	233	10.16	10.16	1	22063.229	Edit (2 p	Calculated	No	NA	NA	NA	NA	91010000	72	72
3	3.5x4.5 Rect,. Tube	TR100	20.968	407.9	245.6	233	11.43	8.89	1	29647.464	Edit (2 p	Calculated	No	NA	NA	NA	NA	145400000	66	77
4	6x6x3/8" FRP Square tube	CT530	54.71	1870	1870	525	15.24	15.24	1	22063.229	Edit (2 p	Calculated	No	NA	NA	NA	NA	91010000	244	244
5	6x4x1/4" FRP Rect. Tube	TR640	29.806	928.6	492.8	296	15.24	10.16	1	22063.229	Edit (2 p	Calculated	No	NA	NA	NA	NA	91010000	128	101
6	6x4x0.3 FRP Rect. Tube	TR150	30.542	1036	478.4	431	15.24	10.16	1	32405.368	Edit (2 p	Calculated	No	NA	NA	NA	NA	170100000	179	139
7	7x4x1/4" FRP Rect. Tube	TR740	33.548	1399	579	326	17.78	10.16	1	22063.229	Edit (2 p	Calculated	No	NA	NA	NA	NA	91010000	160	116
8	7x4x3/8" FRP Rect. Tube	TR760	49.226	1980	801.2	478	17.78	10.16	1	22063.229	Edit (2 p	Calculated	No	NA	NA	NA	NA	91010000	226	159
9	8x4x1/4" FRP Rect. Tube	TR842	36.774	1948	652.2	357	20.32	10.16	1	22063.229	Edit (2 p	Calculated	No	NA	NA	NA	NA	91010000	195	130
10	8x4x3/8" FRP Rect. Tube	TR860	54.064	2773	904.5	525	20.32	10.16	1	22063.229	Edit (2 p	Calculated	No	NA	NA	NA	NA	91010000	276	179
11	11.5x2-3/4"x1/2" FRP Channel	CH997	50.193	5185	168.6	630	29.21	6.985	1	29647.464	Edit (2 p	Calculated	No	NA	NA	NA	NA	135600000	512	181
12	14x6x.1/2" channel	CH800	78.451	14530	1697	1182	35.56	15.24	1	29647.464	Edit (2 p	Calculated	No	NA	NA	NA	NA	135600000	1069	636
13	katrine 250x100mmx1/2in		82.448	5977	1306	795	25	10	1.4	29647.464	Edit (2 p	Calculated	No	NA	NA	NA	NA	135600000	478	261
14	katrine 250x100mmx3/8in		171.4	4711	1062	608	25	10	1.4	29647.464	Edit (2 p	Calculated	No	NA	NA	NA	NA	135600000	376.9	212.5
15	katrine2 500x200mmx1/2in		82.448	52790	12280	1653	50	20	1.4	29647.464	Edit (2 p	Calculated	No	NA	NA	NA	NA	135600000	2112	1229
16	katrine 150x150mmx1/2in		69.7	2210	2210	672	15	15	1.4	29647.464	Edit (2 p	Calculated	No	NA	NA	NA	NA	91010000	294	294
17	katrine 200x200mmx1/2in		95.1	5589	5589	4253	20	20	1.4	29647.464	Edit (2 p	Calculated	No	NA	NA	NA	NA	135600000	559	559
18	katrine2 100x100mmx1/2in		44.3	575	575	967	10	10	1.4	29647.464	Edit (2 p	Calculated	No	NA	NA	NA	NA	91010000	116	116
19	katrineDA 200x200mmx1/2in		95.1	5589	5589	917	20	20	1.4	29647.464	Edit (2 p	Calculated	No	NA	NA	NA	NA	135600000	559	559
20	katrineDA 250x250mmx1/2in		120.6	11350	11350	1146	25	25	1.4	29647.464	Edit (2 p	Calculated	No	NA	NA	NA	NA	135600000	907	907
21	katrineDA 300x300mmx1/2in		146	20120	20120	1387	30	30	1.4	29647.464	Edit (2 p	Calculated	No	NA	NA	NA	NA	135600000	1341	1341
22	katrineDA 400x400mmx1/2in		197	4924	4924	1870	40	40	1.4	29647.464	Edit (2 p	Calculated	No	NA	NA	NA	NA	135600000	2462	2462
23	katrineDA 400x400mmx5/8in	TQ400	146	60090	60090	2318	40	40	1.4	29647.464	Edit (2 p	Calculated	No	NA	NA	NA	NA	135600000	3004	3004
24														NA	NA	NA	NA	NA	NA	NA
25														NA	NA	NA	NA	NA	NA	NA
26														NA	NA	NA	NA	NA	NA	NA
27														NA	NA	NA	NA	NA	NA	NA
28														NA	NA	NA	NA	NA	NA	NA
29														NA	NA	NA	NA	NA	NA	NA

Figure D.40: FRP davit arm properties

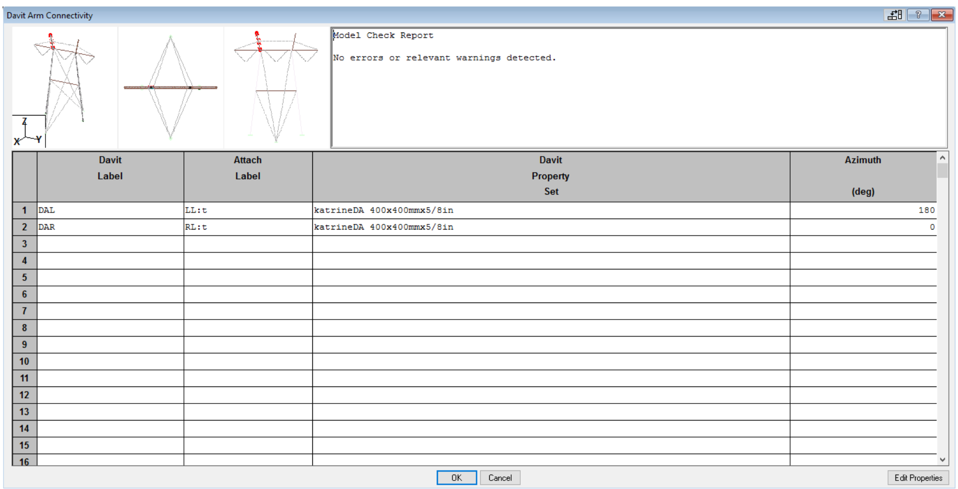

	Davit Label	Attach Label	Davit Property Set	Azimuth (deg)
1	DAL	LL:t	katrineDA 400x400mmx5/8in	180
2	DAR	RL:t	katrineDA 400x400mmx5/8in	0
3				
4				
5				
6				
7				
8				
9				
10				
11				
12				
13				
14				
15				
16				

Figure D.41: FRP davit arms

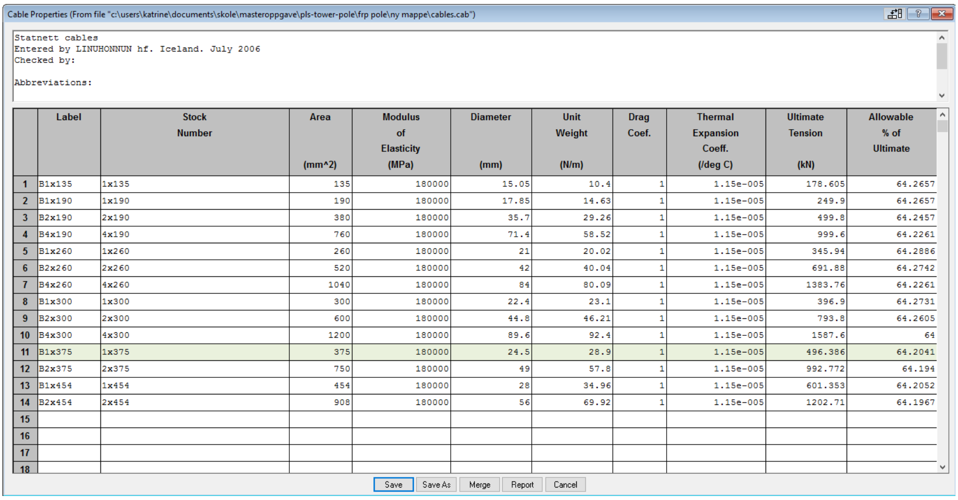

Cable Properties (From file "c:\users\katrine\documents\skole\masteroppgave\pls-tower-pole\frp pole\ny mappe\cables.cab")

Statnett cables
Entered by LINUHONNUN hf. Iceland. July 2006
Checked by:

Abbreviations:

	Label	Stock Number	Area (mm^2)	Modulus of Elasticity (MPa)	Diameter (mm)	Unit Weight (N/m)	Drag Coef.	Thermal Expansion Coeff. (/deg C)	Ultimate Tension (kN)	Allowable % of Ultimate
1	B1x135	1x135	135	180000	15.05	10.4	1	1.15e-005	178.605	64.2657
2	B1x190	1x190	190	180000	17.85	14.63	1	1.15e-005	249.9	64.2657
3	B2x190	2x190	380	180000	35.7	29.26	1	1.15e-005	499.8	64.2457
4	B4x190	4x190	760	180000	71.4	58.52	1	1.15e-005	999.6	64.2261
5	B1x260	1x260	260	180000	21	20.02	1	1.15e-005	345.94	64.2886
6	B2x260	2x260	520	180000	42	40.04	1	1.15e-005	691.88	64.2742
7	B4x260	4x260	1040	180000	84	80.09	1	1.15e-005	1383.76	64.2261
8	B1x300	1x300	300	180000	22.4	23.1	1	1.15e-005	396.9	64.2731
9	B2x300	2x300	600	180000	44.8	46.21	1	1.15e-005	793.8	64.2605
10	B4x300	4x300	1200	180000	89.6	92.4	1	1.15e-005	1587.6	64
11	B1x375	1x375	375	180000	24.5	28.9	1	1.15e-005	496.386	64.2041
12	B2x375	2x375	750	180000	49	57.8	1	1.15e-005	992.772	64.194
13	B1x454	1x454	454	180000	28	34.96	1	1.15e-005	601.353	64.2052
14	B2x454	2x454	908	180000	56	69.92	1	1.15e-005	1202.71	64.1967
15										
16										
17										
18										

Save Save As Merge Report Cancel

Figure D.42: Cable properties

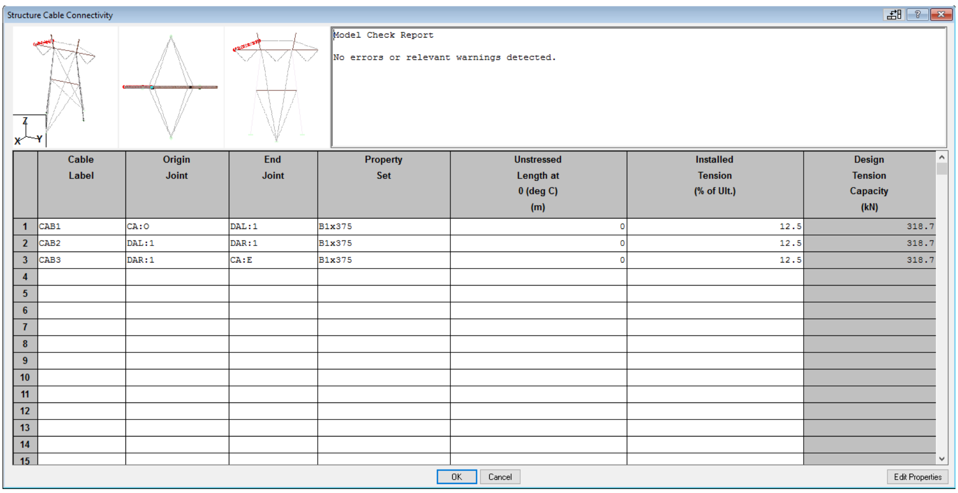

Structure Cable Connectivity

Model Check Report

No errors or relevant warnings detected.

	Cable Label	Origin Joint	End Joint	Property Set	Unstressed Length at 0 (deg C) (m)	Installed Tension (% of Ult.)	Design Tension Capacity (kN)
1	CAB1	CA:O	DAL:1	B1x375	0	12.5	318.7
2	CAB2	DAL:1	DAR:1	B1x375	0	12.5	318.7
3	CAB3	DAR:1	CA:E	B1x375	0	12.5	318.7
4							
5							
6							
7							
8							
9							
10							
11							
12							
13							
14							
15							

OK Cancel Edit Properties

Figure D.43: Cables used in FRP model

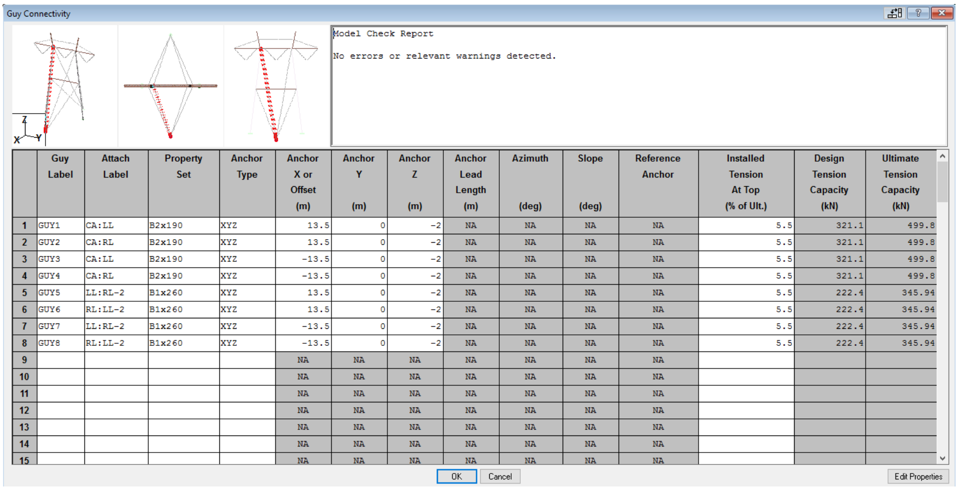

	Guy Label	Attach Label	Property Set	Anchor Type	Anchor X or Offset (m)	Anchor Y (m)	Anchor Z (m)	Anchor Lead Length (m)	Azimuth (deg)	Slope (deg)	Reference Anchor	Installed Tension At Top (% of Ult.)	Design Tension Capacity (kN)	Ultimate Tension Capacity (kN)
1	GUY1	CA:LL	B2x190	XYZ	13.5	0	-2	NA	NA	NA	NA	5.5	321.1	499.8
2	GUY2	CA:RL	B2x190	XYZ	13.5	0	-2	NA	NA	NA	NA	5.5	321.1	499.8
3	GUY3	CA:LL	B2x190	XYZ	-13.5	0	-2	NA	NA	NA	NA	5.5	321.1	499.8
4	GUY4	CA:RL	B2x190	XYZ	-13.5	0	-2	NA	NA	NA	NA	5.5	321.1	499.8
5	GUY5	LL:RL-2	B1x260	XYZ	13.5	0	-2	NA	NA	NA	NA	5.5	222.4	345.94
6	GUY6	RL:LL-2	B1x260	XYZ	13.5	0	-2	NA	NA	NA	NA	5.5	222.4	345.94
7	GUY7	LL:RL-2	B1x260	XYZ	-13.5	0	-2	NA	NA	NA	NA	5.5	222.4	345.94
8	GUY8	RL:LL-2	B1x260	XYZ	-13.5	0	-2	NA	NA	NA	NA	5.5	222.4	345.94
9					NA	NA	NA	NA	NA	NA	NA			
10					NA	NA	NA	NA	NA	NA	NA			
11					NA	NA	NA	NA	NA	NA	NA			
12					NA	NA	NA	NA	NA	NA	NA			
13					NA	NA	NA	NA	NA	NA	NA			
14					NA	NA	NA	NA	NA	NA	NA			
15					NA	NA	NA	NA	NA	NA	NA			

Figure D.44: Guys used in FRP model

E LCC and LCA

E.1 LCC

Steel Lattice Tower

Table E.85: Cost of production phase of steel lattice tower

Production:	kg	NOK/kg	NOK
Manufacturing	8287	20	165740
		TOTAL	165740

Table E.85: Cost of installation phase of steel lattice tower

Installation:	h/ton	h	NOK/h	NOK
Transport - truck		32	1100	35200
Assembly - helicopter		1.336	15000	20040
Assembly - manual labour	20	166	680	112703
			TOTAL	167943

Table E.85: Cost of use phase of steel lattice tower

Use:	NOK/kg	h	NOK/h	NOK
Maintenance - coating	3000			24861
Maintenance - helicopter		0,3	15000	4500
			TOTAL	29361

Table E.85: Cost of end-of-life phase of steel lattice tower

End-of-life:	h/kg	h	NOK/h	NOK/kg	NOK
Deconstruction - manual labour	20	166	680		112703
Deconstruction - helicopter		1.336	15000		20040
Transport - truck		6	1100		6600
Recycling				-1.25	-10359
				TOTAL	128984

Steel Tubular Tower

Table E.86: Cost of production phase of steel tubular tower

Production:	kg	NOK/kg	NOK
Manufacturing	7820	25	195500
		TOTAL	195500

Table E.86: Cost of installation phase of steel tubular tower

Installation:	h/ton	h	NOK/h	NOK
Transport - truck		32	1100	35200
Assembly - helicopter		1.336	15000	20040
Assembly - manual labour	10	78.2	680	53176
			TOTAL	108416

Table E.86: Cost of use phase of steel tubular tower

Use:	NOK/kg	h	NOK/h	NOK
Maintenance - coating	3000			23460
Maintenance - helicopter		0.3	15000	4500
			TOTAL	27960

Table E.86: Cost of end-of-life phase of steel tubular tower

End-of-life:	h/kg	h	NOK/h	NOK/kg	NOK
Deconstruction - manual labour	10	78.2	680		53176
Deconstruction - helicopter		1.336	15000		20040
Transport - truck		6	1100		6600
Recycling				-1.25	-9775
				TOTAL	70041

FRP Tubular Tower

Table E.87: Cost of production phase of FRP tubular tower

Production:	kg	m	NOK/unit	NOK
Manufacturing FRP		87	2500	217500
Manufacturing steel	815		20	16300
			TOTAL	233800

Table E.87: Cost of installation phase of FRP tubular tower

Installation:	h/ton	h	NOK/h	NOK
Transport - ship				60000
Transport - truck		20	1100	22000
Assembly - helicopter		0.835	15000	12525
Assembly - manual labour	9	44.172	680	30037
			TOTAL	124562

Table E.87: Cost of use phase of FRP tubular tower

Use:	kg	NOK/kg	NOK
Maintenance - coating	5482	0	0
		TOTAL	0

Table E.87: Cost of end-of-life phase of FRP tubular tower

End-of-life:	h/kg	h	NOK/h	NOK/kg	NOK
De-construction - manual labour	9	44.172	680		30037
De-construction - helicopter		0.835	15000		12525
Transport - truck		6	1100		6600
Landfill FRP				1.567	8590
Recycle steel				-1.25	-1019
				TOTAL	55834

E.2 LCA

Steel Lattice Tower

Table E.88: Emission from production phase of steel lattice tower

Production:	kg	kg CO2/kg	kg CO2
Raw materials	8287	2,44	20220
Manufacturing	8287	0,26	2155
		TOTAL	22375

Table E.88: Emission from installation phase of steel lattice tower

Installation:	km	g/t km	h	L/h	kg CO2/L	kg CO2
Transport - truck	2200	159.95				2916
Assembly - helicopter			1.336	200	3	802
					TOTAL	3718

Table E.88: Emission from use phase of steel lattice tower

Use:	h	L/h	kg CO2/L	kg CO2
Refurbishment	0.3	200	3	180
			TOTAL	180

Table E.88: Emission from end-of-life phase of steel lattice tower

End-of-life:	h	L/h	kg CO2/L	km	g/t km	CO2/kg	kg CO2
Deconstruction -helicopter	1.336	200	3				802
Transport - truck				360	159.95		477
Recycling						-1.3	-10773
						TOTAL	-9494

Steel Tubular Tower

Table E.89: Emission from production phase of steel tubular tower

Production:	kg	kg CO2/kg	kg CO2
Raw materials	7820	2,44	19081
Manufacturing	7820	0,26	2033
		TOTAL	21114

Table E.89: Emission from installation phase of steel tubular tower

Installation:	km	g/t km	h	L/h	kg CO2/L	kg CO2
Transport - truck	2200	159,95				2752
Assembly - helicopter			1.336	200	3	802
					TOTAL	3553

Table E.89: Emission from use phase of steel tubular tower

Use:	h	L/h	kg CO2/L	kg CO2
Refurbishment	0.3	200	3	180
			TOTAL	180

Table E.89: Emission from end-of-life phase of steel tubular tower

End-of-life:	h	L/h	kg CO2/L	km	g/t km	CO2/kg	kg CO2
Deconstruction - helicopter	1.336	200	3				802
Transport - truck				360	159.95		450
Recycling						-1.3	-10166
						TOTAL	-8914

FRP Tubular Tower

Table E.90: Emission from production phase of FRP tubular tower

Production:	kg	kg CO2/kg	kg CO2
Raw materials FRP	5482	6,73	33031
Manufacturing FRP	5482	0,00	0
Materials and manufacturing steel	815	2,7	2201
		TOTAL	35231

Table E.90: Emission from installation phase of FRP tubular tower

Installation:	km	g/t km	h	L/h	kg CO2/L	kg CO2
Transport - ship	6300	31.99				989
Transport - truck	1500	159.95				1178
Assembly - helicopter			0.835	200	3	501
					TOTAL	1679

Table E.90: Emission from use phase of FRP tubular tower

Use:	h	L/h	kg CO2/L	kg CO2
Refurbishment	0	200	3	0
			TOTAL	0

Table E.90: Emission from end-of-life phase of FRP tubular tower

End-of-life:	h	L/h	kg CO2/L	km	g/t km	CO2/kg	kg CO2
Deconstruction - helicopter	0.835	200	3				501
Transport - truck				360	159.95		330
Landfill						0	0
Recycling						-1.3	-1060
						TOTAL	-229

E.3 Sensitivity Analysis

Table E.91: Steel lattice tower, 120 year life span, steel replaced

Lattice, steel replaced after 80 years				
Year	Event	Cost	Inflated cost	NPV
0	Manufacture	165740	165740	165740
0	Import tax	0	0	0
0	Transport	35200	35200	35200
0	Installation	132743	132743	132743
20	Refurbishment	29361	43629	16443
40	Refurbishment	29361	64830	9209
60	Refurbishment	29361	96334	5157
80	Deconstruction	132743	647180	13058
80	Transport	6600	32178	649
80	Recycle	-10359	-50505	-1019
80	Manufacture	165740	808055	16304
80	Import tax	0	0	0
80	Transport	35200	171615	3463
80	Installation	132743	647180	13058
100	Refurbishment	29361	212710	1618
120	Refurbishment	29361	316076	906
	TOTAL	943155	3322967	412529

Table E.91: Steel tubular tower, 120 year life span, steel replaced

Tubular, steel replaced after 80 years				
Year	Event	Cost	Inflated cost	NPV
0	Manufacture	195500	195500	195500
0	Import tax	0	0	0
0	Transport	35200	35200	35200
0	Installation	73216	73216	73216
20	Refurbishment	27960	41547	15659
40	Refurbishment	27960	61737	8769
60	Refurbishment	27960	91738	4911
80	Deconstruction	73216	356960	7202
80	Transport	6600	32178	649
80	Recycle	-9775	-47657	-962
80	Manufacture	195500	953148	19232
80	Import tax	0	0	0
80	Transport	35200	171615	3463
80	Installation	73216	356960	7202
100	Refurbishment	27960	202560	1540
120	Refurbishment	27960	300994	863
	TOTAL	817673	2825696	372445

Table E.91: FRP tubular tower, 120 year life span

FRP				
Year	Event	Cost	Inflated cost	NPV
0	Manufacture	233800	233800	233800
0	Import tax	0	0	0
0	Transport	82000	82000	82000
0	Installation	42562	42562	42562
20	Refurbishment	NA	NA	NA
40	Refurbishment	NA	NA	NA
60	Refurbishment	NA	NA	NA
80	Refurbishment	NA	NA	NA
60	Refurbishment	NA	NA	NA
120	Deconstruction	42562	458178	1313
120	Transport	6600	71050	204
120	Landfill and recycle	6672	71825	206
	TOTAL	414196	959424	360085

Table E.91: Steel lattice tower, 120 year life span, steel maintained

Lattice, steel maintained				
Year	Event	Cost	Inflated cost	NPV
0	Manufacture	165740	165740	165740
0	Import tax	0	0	0
0	Transport	35200	35200	35200
0	Installation	132743	132743	132743
20	Refurbishment	29361	43629	16443
40	Refurbishment	29361	64830	9209
60	Refurbishment	29361	96334	5157
80	Refurbishment	29361	143148	2888
100	Refurbishment	29361	212710	1618
120	Deconstruction	132743	1429000	4096
120	Transport	6600	71050	204
120	Recycle	-10359	-111516	-320
	TOTAL	609472	2282868	372978

Table E.91: Steel lattice tower, 120 year life span, steel maintained

Tubular, steel maintained				
Year	Event	Cost	Inflated cost	NPV
0	Manufacture	195500	195500	195500
0	Import tax	0	0	0
0	Transport	35200	35200	35200
0	Installation	73216	73216	73216
20	Refurbishment	27960	41547	15659
40	Refurbishment	27960	61737	8769
60	Refurbishment	27960	91738	4911
80	Refurbishment	27960	136317	2750
100	Refurbishment	27960	202560	1540
120	Deconstruction	73216	788182	2259
120	Transport	6600	71050	204
120	Recycle	-9775	-105229	-302
	TOTAL	513757	1591818	339707

Table E.91: Lattice, Discount rate raised to 7 %

Lattice				
Year	Event	Cost	Inflated cost	NPV
0	Manufacture	165740	165740	165740
0	Import tax	0	0	0
0	Transport	35200	35200	35200
0	Installation	132743	132743	132743
20	Refurbishment	29361	43629	11275
40	Refurbishment	29361	64830	4327
60	Refurbishment	29361	96334	1662
80	Deconstruction	132743	647180	2886
80	Transport	6600	32178	144
80	Recycle	-10359	-50505	-225
	TOTAL	550750	1167330	353754

Tubular				
Year	Event	Cost	Inflated cost	NPV
0	Manufacture	195500	195500	195500
0	Import tax	0	0	0
0	Transport	35200	35200	35200
0	Installation	73216	73216	73216
20	Refurbishment	27960	41547	10737
40	Refurbishment	27960	61737	4123
60	Refurbishment	27960	91738	1583
80	Deconstruction	73216	356960	1592
80	Transport	6600	32178	144
80	Recycle	-9775	-47657	-213
	TOTAL	457837	840418	321881

FRP				
Year	Event	Cost	Inflated cost	NPV
0	Manufacture	217500	217500	217500
0	Import tax	0	0	0
0	Transport	82000	82000	82000
0	Installation	42562	42562	42562
20	Refurbishment	NA	NA	NA
40	Refurbishment	NA	NA	NA
60	Refurbishment	NA	NA	NA
80	Deconstruction	42562	207508	925
80	Transport	6600	32178	144
80	Landfill and recycle	6672	14732	145
	TOTAL	414196	630577	359576

Table E.91: Discount rate lowered to 3 %

Lattice				
Year	Event	Cost	Inflated cost	NPV
0	Manufacture	165740	165740	165740
0	Import tax	0	0	0
0	Transport	35200	35200	35200
0	Installation	132743	132743	132743
20	Refurbishment	29361	43629	24156
40	Refurbishment	29361	64830	19874
60	Refurbishment	29361	96334	16351
80	Deconstruction	132743	647180	60820
80	Transport	6600	32178	3024
80	Recycle	-10359	-50505	-4746
	TOTAL	550750	1167330	453162

Tubular				
Year	Event	Cost	Inflated cost	NPV
0	Manufacture	195500	195500	195500
0	Import tax	0	0	0
0	Transport	35200	35200	35200
0	Installation	73216	73216	73216
20	Refurbishment	27960	41547	23004
40	Refurbishment	27960	61737	18926
60	Refurbishment	27960	91738	15571
80	Deconstruction	73216	356960	33546
80	Transport	6600	32178	3024
80	Recycle	-9775	-47657	-4479
	TOTAL	457837	840418	393508

FRP				
Year	Event	Cost	Inflated cost	NPV
0	Manufacture	233800	233800	233800
0	Import tax	0	0	0
0	Transport	82000	82000	82000
0	Installation	42562	42562	42562
20	Refurbishment	0	0	0
40	Refurbishment	0	0	0
60	Refurbishment	0	0	0
80	Deconstruction	42562	207508	19501
80	Transport	6600	32178	3024
80	Landfill and recycle	6672	32529	3057
	TOTAL	414196	630577	383944

Table E.91: Inflation rate raised to 3 %

Lattice				
Year	Event	Cost	Inflated cost	NPV
0	Manufacture	165740	165740	165740
0	Import tax	0	0	0
0	Transport	35200	35200	35200
0	Installation	132743	132743	132743
20	Refurbishment	29361	53029	19986
40	Refurbishment	29361	95777	13605
60	Refurbishment	29361	172983	9261
80	Deconstruction	132743	1412504	28500
80	Transport	6600	70230	1417
80	Recycle	-10359	-110229	-2224
	TOTAL	550750	2027977	404228

Tubular				
Year	Event	Cost	Inflated cost	NPV
0	Manufacture	195500	195500	195500
0	Import tax	0	0	0
0	Transport	35200	35200	35200
0	Installation	73216	73216	73216
20	Refurbishment	27960	50499	19032
40	Refurbishment	27960	91207	12956
60	Refurbishment	27960	164729	8819
80	Deconstruction	73216	779083	15720
80	Transport	6600	70230	1417
80	Recycle	-9775	-104015	-2099
	TOTAL	457837	1355649	359761

FRP				
Year	Event	Cost	Inflated cost	NPV
0	Manufacture	233800	233800	233800
0	Import tax	0	0	0
0	Transport	82000	82000	82000
0	Installation	42562	42562	42562
20	Refurbishment	0	0	0
40	Refurbishment	0	0	0
60	Refurbishment	0	0	0
80	Deconstruction	42562	452898	9138
80	Transport	6600	70230	1417
80	Landfill and recycle	6672	70996	1432
	TOTAL	414196	952485	370350

Table E.91: Inflation rate lowered to 1 %

Lattice				
Year	Event	Cost	Inflated cost	NPV
0	Manufacture	165740	165740	165740
0	Import tax	0	0	0
0	Transport	35200	35200	35200
0	Installation	132743	132743	132743
20	Refurbishment	29361	35826	13502
40	Refurbishment	29361	43715	6209
60	Refurbishment	29361	53340	2856
80	Deconstruction	132743	294253	5937
80	Transport	6600	14630	295
80	Recycle	-10359	-22963	-463
	TOTAL	550750	752484	362020

Tubular				
Year	Event	Cost	Inflated cost	NPV
0	Manufacture	195500	195500	195500
0	Import tax	0	0	0
0	Transport	35200	35200	35200
0	Installation	73216	73216	73216
20	Refurbishment	27960	34117	12858
40	Refurbishment	27960	41629	5913
60	Refurbishment	27960	50795	2719
80	Deconstruction	73216	162299	3275
80	Transport	6600	14630	295
80	Recycle	-9775	-21668	-437
	TOTAL	457837	585717	328539

FRP				
Year	Event	Cost	Inflated cost	NPV
0	Manufacture	233800	233800	233800
0	Import tax	0	0	0
0	Transport	82000	82000	82000
0	Installation	42562	42562	42562
20	Refurbishment	0	0	0
40	Refurbishment	0	0	0
60	Refurbishment	0	0	0
80	Deconstruction	42562	94348	1904
80	Transport	6600	14630	295
80	Landfill and recycle	6672	14790	298
	TOTAL	414196	482130	360859